Investigations into the Determination of Hydride-Forming Elements

By

Xiao-chun Le

A Thesis

Presented to the Department of Chemistry in partial fulfilment of the requirements for the degree of Master of Science

December, 1988

Brock University

St. Catharines, Ontario

Canada

Abstract

Analytical methods for the determination of trace amounts of germanium, tin and arsenic were established using hydride generation coupled with direct current plasma atomic emission spectrometry. A continuous gas flowing batch system for the hydride generation was investigated and was applied to the determination of germanium(Ge), tin(Sn), antimony(Sb) and lead(Pb) (Preliminary results suggest that it is also applicable to arsenic)As)). With this system, the reproducibility of signals was improved and the determination was speeded up, compared with the conventional batch type hydride generation system. Each determination was complete within one minute. Interferences from a number of transition metal ions, especially from Pd(II), Pt(IV), Ni(II), Cu(II), Co(II), and Fe(II, III), have proven to be very serious under normal conditions, in the determination of germanium, tin, and arsenic. These interference effects were eliminated or significantly reduced in the presence of L-cystine or L-cysteine. Thus, a 10-1000 fold excess of Ni(II), Cu(II), Co(II), Fe(II), Pt(IV), Pd(II), etc. can be tolerated without interference, in the presence of L-cystine or L-cysteine, compared with absence of interference reducing agent. The methods for the determination of Ge, Sn, and As were examined by the analyses of standard reference materials. Interference effects from the sample matrix, for example, in transition metal-rich samples, copper, iron and steel, were eliminated by L-cystine (for As and Sn) and by L-

cysteine (for Ge). The analysis of a number of standard reference materials gave excellent results of As and Sn contents in agreement with the certified values, showing there was no systematic interference. The detection limits for both germanium and tin were 20 pg ml^{-1}.

Preliminary studies were carried out for the determination of antimony and lead. Antimony was found to react with $NaBH_4$, remaining from the previous determinations, giving an analytical signal. A reversed injection manner, i.e., injection of the $NaBH_4$ solution prior to the analyte solution was used to avoid uncertainty caused by residual $NaBH_4$ present and to ensure that an excess of $NaBH_4$ was available. A solution of 0.4% L-cysteine was found to reduce the interference from selected transition metal ions, Co(II), Cu(II), Ni(II) and Pt(IV). Hydrochloric acid - hydrogen peroxide, nitric acid - ammonium persulphate, and potassium dichromate - malic acid reaction systems for lead hydride generation were compared. The potassium dichromate - malic acid reaction medium proved to be the best with respect to reproducibility and minimal interference. Cu(II), Ni(II), and Fe(II) caused strong interference in lead determinations, which was not reduced by L-cysteine or L-cystine. Sodium citrate, ascorbic acid, dithizone, thiosemicarbazide and penicillamine reduced interferences to some extent.

Further interference reduction studies were carried out using a number of amino acids, glycine, alanine, valine, leucine and histidine, as possible interference reducing agents in the determination of germanium. From glycine, alanine, valine to leucine, the interference reduction effect in germanium determinations decreased. Histidine

was found to be very promising in the reduction of interference. In fact, histidine proved more efficient than L-cystine and L-cysteine in the reduction of interference from Ni(II) in the determination of germanium.

Signal enhancement by easily ionized elements (EIEs), usually regarded as an interference effect in analysis by DCP-AES, was studied and successfully applied to advantage in improving the sensitivity and detection limit in the determination of As, Ge, Sn, Sb, and Pb. The effect of alkali and alkaline-earth elements on the determination of the above five hydride forming elements was studied. With the appropriate EIE, a signal enhancement of 40-115% was achieved. Linear calibration and good reproducibility were also obtained in the presence of EIEs.

Acknowledgements

I would like specially to thank Professor Ian D. Brindle for his encouragement, direction and correction of my English throughout this work and also for his help both academically and personally.

The author also thank Dr. H. L. Holland and Dr. S. M. Rothstein for their advice.

I would like to express my special gratitude to my dearest wife for her help and support, and to my families for their understanding and support.

Thanks also go to Lev Pidwerbesky, Barbara Buchanan, and Nicole Kushner for their cooperation.

The author is grateful to the Air Resources Branch of the Ontario Ministry of the Environment for funding this research (project 360 G). The author also acknowledges receipt of a grant from the Ontario Government BILD program for the purchase of the Spectraspan V d.c. plasma atomic emission spectrometer.

I would also like to thank the Chemistry Department of Brock University and Canada for giving me this wonderful opportunity to study and work here, and to the people who have helped me during these two years at Brock University.

Table of Contents

List of Figures

List of Tables

Chapter 1. Literature Review and Introduction

I. Development of direct current plasma

Atomic emission spectrometry (AES) is a useful tool for analytical chemistry. Initially, arc and spark excitation sources in various forms were used (1). Although both arc (2) and spark (3) have some desirable characteristics for AES, they also have deficiencies. The arc is sensitive but is difficult to stabilize, while the sensitivity of the spark is low. Therefore, a search for an improved excitation sources was initiated and soon centered on plasmas as discussed in a number of review papers (4-6). A plasma can be defined as a gaseous assembly of atoms, ions, molecules, and electrons, with a high percentage of ions. Interactions in a plasma occur primarily between ions, or ions and neutral species. High temperature can be readily achieved with a plasma (6). Well developed plasmas nowadays include the inductively-coupled plasma (ICP), the direct current plasma (DCP), the microwave-induced plasma (MIP), and the capacitively-coupled microwave plasma (CMP) (7). Only the DCP source will be discussed in detail in this paper.

The first DCP devices intended for spectrochemical analysis were independently developed by Margoshes and Scribner (8) and Korolev and Vainshtein (9) in 1959. The basic design for the flame-like "plasmajet" developed by Margoshes and Scribner (8) is shown in Figure 1. Graphite disk electrodes are used for both anode (lower electrode) and cathode (upper electrode). A d.c. plasma is ignited between the electrodes. A tangential stream of inert gas (helium)

entering the chamber blows the plasma through an opening in the cathode. A direct injection nebulizer using argon as the spraying gas was used to spray 0.5 to 1 ml min^{-1} of the sample solution into the plasma. A standard d.c. arc power supply was used with currents of about 15 to 20 amps. Thus a simple DCP source for spectrochemical analysis was achieved. The major shortcoming of this device, however, was the tendency of the cathode spot to wander slowly and erratically around the surface of the cathode disk.

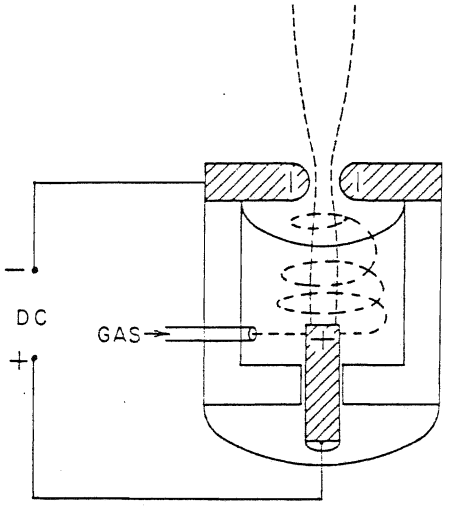

Figure 1. Basic diagram of a d. c. plasma excitation unit

In 1961, Owen (10) showed that a considerable improvement in plasma stability was achieved by using a third electrode maintained at the same potential as the cathode ring. Following Owen's work, Margoshes and Scribner (11,12) modified their original design to include a third electrode mounted vertically above the orifice of the cathode disk and to use water to cool the electrodes. The ring electrode which originally served as the cathode was used as the control ring. Further modifications and applications of this and closely related devices have been the subject of a number of subsequent papers (13-20).

Based on these plasma designs and investigations, Spex Industries (Metuchen, New Jersey, USA) introduced the first commercially available DCP in mid 1960's, similar in design to the modified Scribner and Margoshes (12) system. Helium was normally used as the tangential gas and argon served as the nebulizing gas for the introduction of sample solutions.

Other major modifications on DCP devices investigated in 1960's include those designed by McGinn (21), Dranz (22,23), Jahn (24), Yamamoto (25,26), and Goto and Atsuya (27,28).

In 1970, Valente and Schrenk (29) described another design of DCP source. This has an inverted "V" flame-like configuration when operating. The plasma is ignited with the cathode vertically aligned with the anode. The cathode is then rotated to form a 30^{o} angle with the anode. A relatively stable, sensitive plasma resulted. Sample, along with argon, was transported to the anode chamber tangentially just below the control orifice and thence to the plasma. Temperatures in the

plasma were about 6000 K with a d.c. source operating at 300 V and 10 A and required less than 2.5 L min^{-1} of argon. Elliott(30) placed a second tungsten cathode along and slightly to the side of the plasma plume from the graphite ring cathode. This arrangement helped to stabilize a zone in the plume in which the excitation process occurred and resulted in some increase in stability.

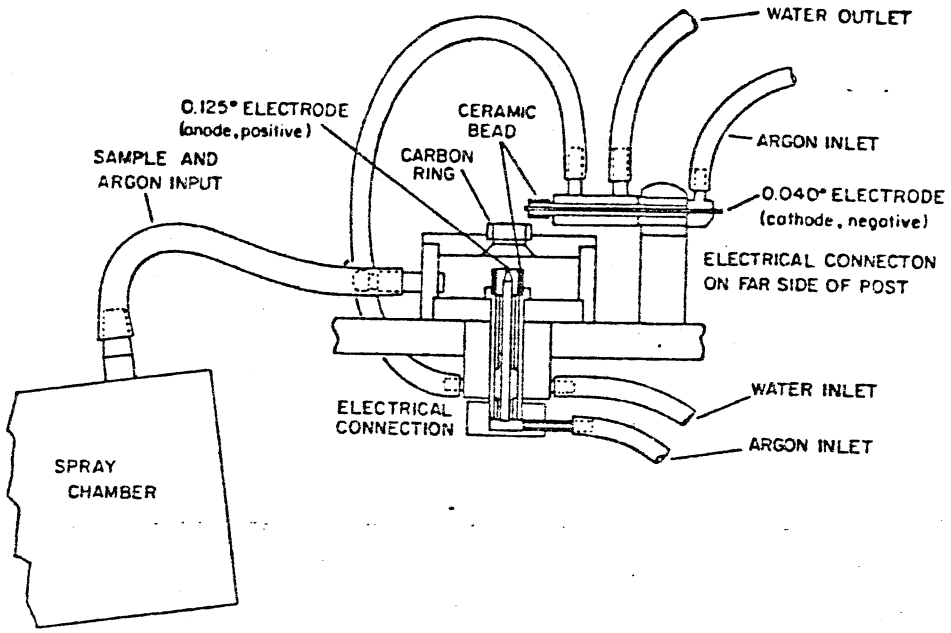

Figure 2. Schematic representation of Spectrametrics SpectraJet DCP

Ten years after Owen's work (10), a similar gas-stabilized arc device was described by Elliott (31) and offered commercially as the SpectraJet by SpectraMetrics, Inc. (Andover, Massachusetts, USA). As shown in Figure 2, the tungsten rod cathode was positioned off the central arc column axis, producing a nearly right-angle bend in the column. A "flame-like" plasma was formed above the bent primary arc. The argon flow that carried the sample into the plasma jet chamber was introduced tangentially. The sample aerosol particles generated by a pneumatic nebulizer were desolvated during their passage through a heated spray chamber prior to the jet mixing chamber. The SpectraJet required 5 liters per minute of argon and operated from a specially designed power supply requiring only 500 W of input power. A core plasma temperature of about 10,000 K with temperatures in the plume ranging from 4000 K to 8000 K were estimated (31).

In 1974, Elliott (32) described a new version of his right-angle plasma. This was subsequently introduced by SpectraMetrics and called a "Spectrajet II". As shown in Figure 3, the plasma formed between thoriated tungsten electrodes partially withdrawn into ceramic tubes through which argon flowed as the coolant gas. The flow of argon from the anode and cathode intersect to form a continuous plasma shaped like an inverted letter "V". Sample aerosol generated in a chamber type pneumatic nebulizer was directed toward the top of the inverted "V" by a third argon stream through a sample introduction tube under the plasma. Unlike all the previous plasma devices described, the optimum region of observation with this device was at the crook position of the "V", which was below the current-carrying arc column. This results in a

noticeable reduction of emission background intercepted by the entrance slit of the spectrometer.

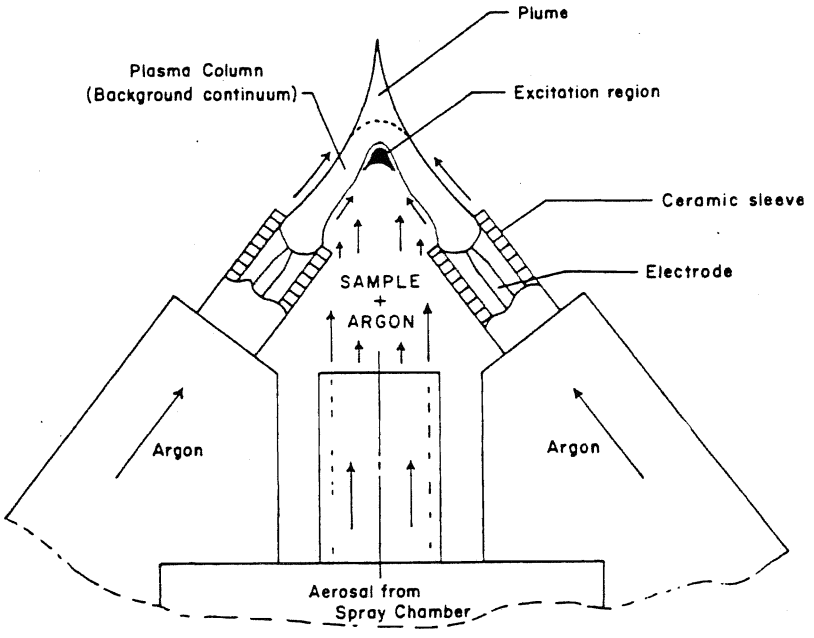

Figure 3. Schematic representation of Spectrametrics SpectraJet II DCP

In 1978 , SpectraMetrics introduced the SpectraJet III, shown in Figure 4. This is a three-electrode d.c. plasma. The three electrodes consist of a front and a rear graphite anode and a top tungsten cathode, forming an inverted "Y" plasma when operating, the cathode forms the "leg" of the "Y". The electrodes are located inside water-cooled blocks and can be moved relative to each other via argon-activated pistons. This design results in improved stability and better detection limits than previously reported for the DCP. Of particular importance is the stability of the plasma in the presence of varying solvent types such as those containing large amounts of salts, organics, high acid or alkaline concentrations. The sample excitation region and photometric observation area of the SpectraJet III is centered uniquely in the crook of the Y where spectral contribution from the plasma continuum is minimal. The plasma requires less than 1000 W of power and is sustained by a low voltage of approximately 40 V and a current of 7.5 A after ignition. Approximately 8 L min^{-1} of commercial grade (99.5%) inert argon is used as the plasma support gas. The argon performs three functions in the SpectraJet III; (i) it is used as the support gas through each electrode to form the plasma and to sustain thermal pinch effect of the plasma (33,34); (ii) it is used as the nebulizer and aerosol carrier gas; (iii) it actuates the piston used to move the electrodes into position for ignition.

Compared with two-electrode plasma (Spectrajet II), the three-electrode plasma (SpectraJet III) has proved to be superior in terms of improved stability and lower background (35-37). The SpectraJet III is

the presently available DCP source from Applied Research Laboratories (ARL) (Sunland, California, USA.)

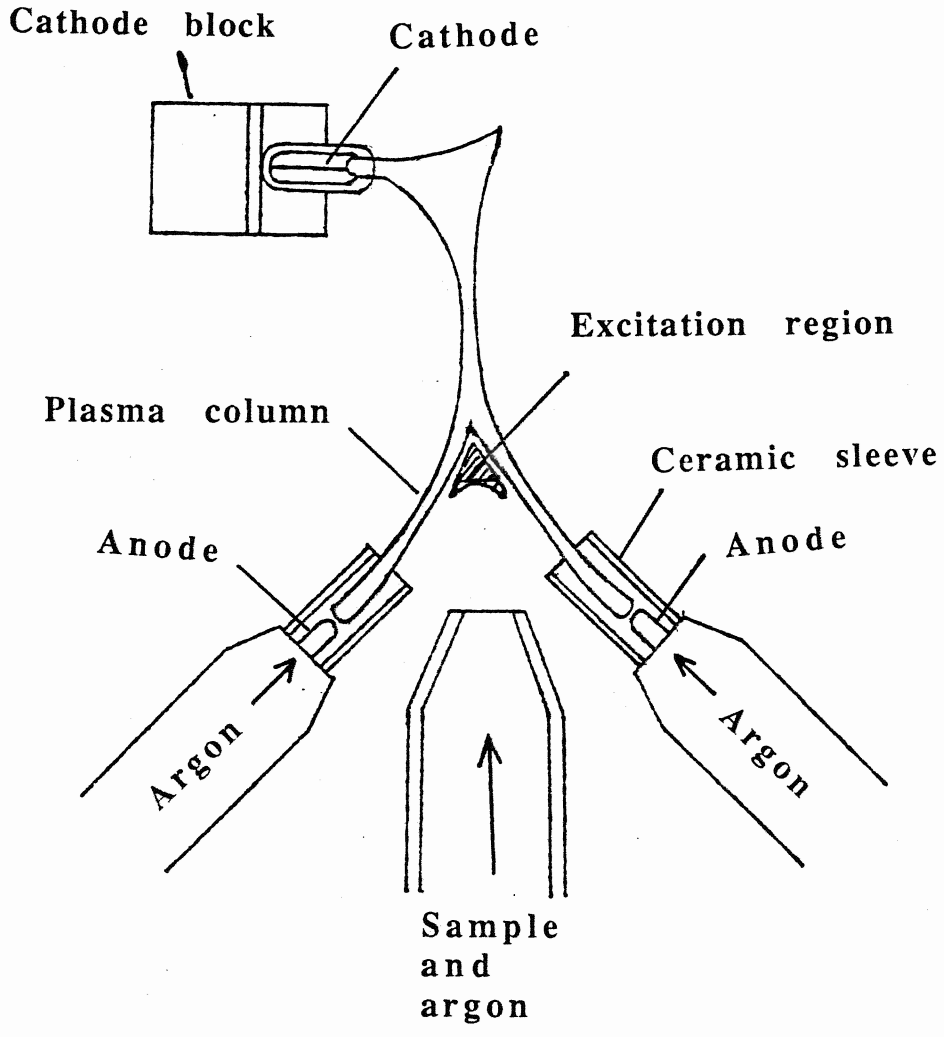

Figure 4. Three-electrode d. c. plasma (Spectrametrics Spectra Jet III)

Other interesting designs include three phase DCP (38, 39), rotating arc DCP (40, 41), and conical DCP (42). In these designs, the aerosol sample is introduced into the DCP concentrically. They result in an extended interaction between the sample aerosol and arc discharge. For example, a conical DCP has recently been described a design based on the three-electrode DCP (42). Orientation of three electrodes symmetrically about a flat-topped 30° cone with a centrally located aerosol injection tube is employed to increase aerosol transfer into the conical DCP. Interaction by the aerosol yields distinct regions of sample decomposition and excitation visible in the axial region of the plasma. This facilitates separation of atomic from ionic emission zones in the discharge similar to those displayed by an ICP. The linear dynamic range and detection limits for six elements studied, according to the reports (42), were improved compared to the commercial DCP source.

The DCP has been applied as an excitation source for atomic fluorescence spectrometry (AFS) (43,44), as a primary pseudocontinuum radiation source for wavelength-modulated atomic absorption spectrometry (45), as an atomizer for a Zeeman AAS system (46), and as an ionization source for mass spectrometry (MS) (47-50), it has often been utilized as an effective excitation source for AES.

II. Detection System

With temperatures as high as 10,000 K, the DCP sources provide an extremely rich spectrum. One is not limited to ground state transition lines, but can choose from first or even second ionization state lines for detection. This provides an opportunity to determine a wide variety of elements. On the other hand, it also creates a problem which is an increased occurrence of spectral interferences. To solve this problem, a resolving device capable of reliably isolating the line of interest is required.

The combination of a DCP and an echelle grating spectrometer for AES has shown a rational match (51, 52). With extremely high resolution, an echelle spectrometer limits spectral interferences from a DCP source. An echelle grating spectrometer mainly consists of an echelle grating, a prism and other optical elements for the light dispersion of spectra at different wavelength, and a photomultiplier (PMT) as a detector of line intensity. The principles of the echelle grating were first described by Harrison (53) in 1949. An echelle grating is a special type of diffraction grating having broad flat grooves ruled with extremely high optical precision. The angle at which the grooves are ruled such that the width of each step is several times its height, and the spacing from one step to the next is many times greater than the wavelength of the light being dispersed.

An echelle grating spectrometer typically has a resolution and dispersion an order of magnitude better than normal spectrometers of the same focal length (54-57). Because of the improved resolution and

dispersion, the first commercial echelle spectrograph (that is , photographic readout only) was introduced by Bausch and Lomb in 1953 (58) and immediately applied to the quantitative analysis of boron in steel (59). Prior to this application, the determination of boron was severely limited by spectral interference using normal spectrometers. In 1969, a commercial echelle atomic emission spectrometer, SpectraSpan, was introduced by SpectraMetrics and was described by Elliot (30) and Matz (60). The subsequent new version of the echelle grating spectrometer system have shown vastly improved capability of resolution and dispersion and light throughput. Therefore, the echelle grating spectrometer has the resolution needed to perform even the most complex emission experiment (61).

III. Sample Introduction System

Browner and Boorn (62, 63) have discussed factors associated with sample introduction and summarized a number of sample introduction techniques for atomic spectrometry. Because of inherent problems that often restrict detection limits and produce interference effects, the authors called sample introduction the Achilles' heel of atomic spectroscopy. A number of papers (40, 64-67) have also specifically addressed sample introduction as a key problem for DCP techniques. Therefore, a variety of sample introduction techniques have been developed and evaluated for the introduction of gaseous, liquid, and solid samples to a DCP jet.

Liquid sample introduction has the advantages of relative simplicity and reliability. The conventional DCP sample introduction for liquid samples consists of a two-channel peristaltic pump, a ceramic crossflow nebulizer, a spray chamber, and a sample tube through which the aerosol is directed to the plasma. Approximately 1-2 ml min^{-1} of sample solution is taken with transport efficiency of approximately 15% (37, 66, 68) and droplet size of aerosol between 3-10 μm reported by Zander(33) and 1-20 μm reported by Mohamed *et al.* (69). This overall sample loading is relatively higher than both ICP and flame AAS (62).

Not only the analyte, but also the accompanying solvent are introduced into the plasma. Large amounts of solvent may have a significant effect in lowering the temperature or even extinguishing the plasma discharge. The solvent effect becomes particularly significant when volatile organic solvents are used. The effect of organic solvents on the DCP has been described by Gilbert and Penney (70). With a slight modification of the sample introduction system to avoid carbon deposit on the ceramic sleeves formed from organic vapor and aerosol, hexane, dichloro-, trichloro-, and tetrachloromethane, and 4-methyl-2-pentanone as sample solvents were introduced to the DCP. Because these solvents were extensively vaporized in the nebulization system, the transport efficiencies of analyte were improved, resulting in an enhanced sensitivity. Background emission, principally from C_2 and CN bands and incandescent carbonaceous aerosol was reduced by the addition of 0.1 L min^{-1} of oxygen to the sample aerosol-nebulizer gas flow. The nebulizer gas flow rates at 4-6 L min^{-1} were optimal. Above

this level, the plasma became unstable and even extinguished at gas flow rate greater that 8 L min^{-1}. The technique has been applied to determine silicone fluid in bond paper and trace metals in coastal seawater following solvent extraction (70).

To improve the transport efficiency of analyte to the plasma, electrothermal vaporization (ETV) techniques were studied (71-76). Transport mechanisms with electrothermal vaporization are much simpler than those involving liquid sampling. A microliter amount ($\geq$ 5 µl) of the sample is introduced into a vaporization cell, usually made from graphite or metallic (W, Ta, Pt) materials. Samples undergo drying and ashing cycles as in GFAAS prior to vaporizing. During a high temperature vaporization step, the sample vapor is formed and transported by carrier gas from the ETV to the DCP. A transient signal is thus obtained since the sample is vaporized in one pulse under optimal conditions. Because of the desolvation by the ETV, more efficient introduction of analyte directly into the excitation region of the DCP was achieved, resulting in higher sensitivities, especially for volatile materials (elements or compounds). Relatively low transport efficiencies of less volatile and carbide-forming species were improved by the addition of volatilizing gases, such as freons, halocarbon, and volatile halides, to the argon carrier gas (77,78). On the other hand, to prevent some very volatile elements or compounds from vaporization during sample drying stage, sodium sulfide (72), nickel salts (78), and iodine (79) were added to stabilize mercury (72), arsenic and selenium (78), and volatile alkyl lead compounds (79), respectively. This sample introduction method complements the conventional pneumatic

nebulizer for micro amount, high-salt-content samples, and viscous solutions, and may be applied to solutions consisting of suspended particles and solid samples (80).

Slurry sample introduction to the plasma for direct analysis of solid samples with no need for sample digestion procedure has recently brought great attention because it reduces sample preparation time and minimizes contamination and analyte losses. A DCP, having high excitation temperature, showed advantages for atomization and excitation of slurry samples. Particle size dependent effects was observed in the case of slurry introduction (69, 81, 82). Therefore, fine particle size for slurry was suggested in order to reach adequate precision (69, 81-83). Ideally, a sample should be readily reduced in particle size to less than 10 μm and dispersed to form a homogeneous suspension in order to prepare for a slurry sample introduction to a DCP. Slurry methods for DCP-AES have been applied to the analysis of coal (83), kaolin (81), soil (81), minerals (84), food (85, 86), biological materials (85), plant material (86), turkey bones (87), refractory carbides (88), and lubricating oil (89-91).

Hydride generation (HG) has proved to be an effective sample introduction method for atomic spectrometry (92-94). This technique was first combined with AAS in 1969 (95) and then with ICP-AES (96) and DCP-AES (97-98). For DCP-AES, hydrides produced in a reaction vessel, called the hydride generator, due to the reaction between the hydride-forming elements and reducing agent (sodium tetrahydroborate(III)), are carried by a stream of argon and introduced through a modified sample tube to the DCP (99). Through the hydride

generation process, the analytes were preconcentrated and separated from the sample matrix. Therefore, spectral interferences were eliminated or reduced and the sensitivity was improved by a factor of approximately 20 over the direct aqueous nebulization (67, 92). Applications of hydride generation coupled with DCP-AES have been found in the determination of arsenic (98-101), selenium (100-102), germanium (103), tellurium (102), and tin (104).

Similar methods investigated for gaseous sample introduction to the DCP include cold vapor (105) for mercury determinations, and chloride formation for arsenic determinations (106). For more information on hydride generation techniques, please refer to section VI of this paper.

Another interesting sample introduction technique is chromatography. By coupling a chromatograph directly to DCP-AES instrument, the latter functions as a multielement detector. Van Loon (107) has reviewed the combination of chromatography and atomic spectrometry, while Carnahan *et al.* (108) summarized the application of plasma emission spectrometry in chromatography. This application can be carried out by two approaches: (i) independent collection of chromatographic fractions followed by analysis, in which the chromatography is similar to a preconcentration/separation step of sample preparation; and (ii) direct introduction of the column effluent into the analytical instrument. The DCP is tolerant of a wide range of gas flow rates, gas and solvent types. This indicates that the DCP has the versatility to interface with chromatographic techniques. Gas chromatography (GC) (109-115), high performance liquid

chromatography (HPLC) (68, 116-125), gel filtration chromatography (126, 127), and ion exchange chromatography (128) have been reported coupled with DCP-AES.

In GC-DCP-AES combination, a heated interface to prevent sample condensation around the injector nozzle, serving as a transfer line, has shown advantages (109, 110). The applications of GC-DCP-AES found in literature include the determination of organomanganese compounds in gasoline (110), iron in ferrocene and haloderivatives (111), organometallic compounds of Cr, Cu, Ni, and Pd (109), various alkyl derivatives of Si, Ge, Sn, and Pb (112), silicon in a silicone polymer (113), and methylmercury in fish and other food samples (115). The application of a DCP coupled with a vacuum U.V. spectrometer as a sulfur specific detector for GC has also been illustrated (114).

An HPLC system can be easily coupled to a DCP system because the flow rates can be adjusted to those required by the nebulizer and samples can be separated in a relatively short time. Uden *et al.* (117-119) have found that the standard nebulization system was sufficient for eluents used in ion-exchange and reversed-phase chromatography, but a novel nebulizer has been designed to avoid forming carbon deposits when organic solvents used for adsorption chromatography. Mazzo *et al.* (68) have also described an interface for HPLC-DCP-AES. Normal phase HPLC has been used to separate various transition metal complexes (117, 118) with detection limits using DCP-AES in the sub-ng range, while reversed phase HPLC with DCP-AES has been used to determine Cr(VI), and Cr(III) species (122). Also, a combination of

HPLC-hydride-generation-DCP has been described for determination of total tin and organotin species (123).

A DCP-AES has also been interfaced with a gel filtration chromatography column (126, 127) because it can tolerate a larger sample load compared to an analytical HPLC column where the amount of sample used is limited by the column size. With simultaneous detection of protein bound copper, iron and zinc, speciations in serum and intravenous infusion fluids was studied (126).

In addition to the above common sample introduction techniques, a new technique by using laser, laser ablation DCP-AES, has been reported (129-133) for the direct determination of metals in solid samples. These preliminary studies have shown potential of excellent selectivity and sensitivity, low detection limits, and little interference.

IV. Comparison of DCP with Other Plasma Sources

Among all plasma sources developed, the ICP has been extensively studied and shown extremely useful for inorganic major, minor, and trace analysis (134-137). Thus ICP-AES has been applied to the analysis of "almost every material under the sun" as stated by Greenfield (1), one of the fathers of the ICP for spectrochemistry. In order to assess the DCP, a number of papers (33, 52, 61, 138) have compared DCP with ICP with all aspects. For AES, the DCP source has been found to be superior to the ICP source in terms of instrumental and operational costs, and versatility for organic, high-salt content and slurry sample introduction, whereas ICP is less prone to matrix effects and has slightly better or similar precision than DCP (52). ICP is more developed than DCP from both a theoretical and practical point of view, partly due to its widely commercial availability. This leaves more potential for the development of the DCP source.

The basic characteristics, capabilities and limitations of commercial DCP, both two-electrode and three-electrode DCP, have been discussed in a number of publications (31, 33, 35, 37, 51, 139-140). They may be summarized as follows.

(i) low detection limits -- usually comparable with those of ICP. This characteristic allows DCP-AES to determine directly trace elements in samples.

(ii) wide linear dynamic range -- at least three orders of magnitude. With simple sample dilution procedure, the simultaneous determinations of major, minor, and trace elements are possible.

(iii) relatively high precision -- relative standard deviations of about 1.5% for most elements in aqueous solutions at concentrations well above the detection limits.

(iv) acceptable both long-term and short-term stabilities.

(v) high versatility -- It can tolerate certain amounts of organic solvents and also accept solutions which contain more than 10% dissolved solids.

(vi) extremely small excitation region -- This makes its use with conventional spectrographic and spectrometric equipment difficult. However, with an echelle grating spectrometer as a detector, this is no longer a problem. This is again why the combination of a DCP with an echelle grating spectrometer is a rational and ideal one.

(vii) Excitation processes are greatly affected by elements with low ionization potentials (141-144), for example, alkali and alkaline earth metals.

V. Applications of DCP-AES

Because of the above characteristics, the DCP-AES has been applied to determine a variety of elements in environmental, geological, metallurgical, clinical, biological, industrial, and other samples (145).

The presence of easily ionized elements (EIEs) has been found to enhance the emission signals (29, 37, 71, 144, 146-152). Although emission line to background ratios are often improved, this enhancement effect has been generally regarded as a nuisance due to

its unpredictability (139, 143, 146, 147, 153-160). For DCP-AES determinations, variable EIE concentrations in different sample matrices make accurate determinations difficult. Even for fixed EIE concentrations, emission line enhancements differ between wavelengths of the same element, and between different elements (144, 161).

Through the study of characteristics and possible mechanism, a number of papers have ascribed the signal enhancement effect by EIEs to suppression of populations of ionized analyte by EIE-donated electrons (35, 164-165). Later research, however, showed that intensities of both atomic and ionic emission lines were enhanced and that the addition of EIE appeared to have little influence on electron densities measured in the analytical zone (161, 166, 167). With more detail study, a number of mechanistic models have suggested possible explanations of this complex phenomenon(141-142, 168-169). An important paper by Miller *et al.* (168), proposes a radiative transfer-collisional redistribution of energy model for analyte excitation.

To minimize the interference caused by EIE, a number of possible approaches for elemental analyses have been suggested. These have included matrix matching of samples, blanks, and standards (4, 147, 154, 162), standard additions or internal standards (141, 146), EIE buffers (139, 143, 155-169), and removing EIEs by ion exchange (163). Among these approaches, EIE buffering has been most often applied, where samples and standards are typically spiked with excess amounts of EIEs, such as salts of lithium (139, 157), sodium (158), potassium (155), cesium (156), and lithium-lanthanum mixture (143, 170) to minimize signal

differences due to EIEs present in samples with unknown matrices. However, these compensations and matrix matches have not always been successful since enhancement effects due to EIEs are very complicated (144).

The selective applications of DCP-AES are tabulated below with a description of element(s) determined, sample matrix, and comments including the method for reduction of matrix interferences.

Table 1. Applications of DCP-AES to Various Matrices

1. Geological Samples

Elements Determined	Sample Analyzed	Comments	Reference
Ten oxides and 7 trace elements	Silicate rocks	Lithium metaborate fusion of samples and cesium buffering to reduce interference	156
Be, Al, Si, Fe Zn, Nb, Sn, Ta, W	Minerals	Introduction of suspensions of finely powdered samples (10μm diameter) to the DCP	84
Nb	Ores Steels	Good agreement between this work and certified values. Background shifts and spectral interference studied	171
U	Phosphatic materials	A 2% oxalic acid adjusted to pH 4.5 with triethanolamine was used quantitatively to back-extract U from trioctylphosphine oxide in cyclohexane. This sample pretreatment method overcame matrix interferences	172
Si, Fe, Al	Soil	Li or Na buffering was suggested. The results for the 10	

Ca, Mg, Mn Ti, K, Na, P		elements were satisfactory for routine analysis when compared with those obtained by chemical methods	173
20 elements	Rocks	Lab-made "two-jet plasmatron" was used. Matrix interferences were the same order as the random error of analysis.	174
Cu	Ores	Laser ablation technique was used for solid sample direct introduction.	129
10 elements	Geological materials	A 2-electrode DCP was used. Samples analyzed included Lunar rocks and soils.	155
Major and trace elements	Geological materials	A review on geochemical analysis and geostandards	175
Major, minor, and REEs	Ore concentrates	Simple calibration	176
La	Geological samples	A review of methods for the determination of La in geological samples with 128 references	177
B	Rocks	Matrix interferences were minimized by carefully selecting the most suitable line for each samples	163

		and/or by cation excange. The results were compared with those obtained by azomethine H method (178).	

2. Environmental Samples

Ba, Sr	Sediments	Li, Na, K, or Cs alone did not completely eliminate matrix interferences. Lithium, from preliminary fusion, and lanthanum together removed interferences	179
18 elements	Estuarine sediments	Lithium metaborate fusion of samples. Lithium also served as EIE buffer.	154, 180
Au	Solid algal cells	ETV introduction of 0.2-0.6 mg of samples to DCP.	181
Various	Sediments Waters Marine organisms	Stray light and spectral interferences from Ca and Mg were observed. Compensation for the interferences using simple linear correction or matrix matching was reported.	182
Trace heavy metals	Seawater Ocean sediments	Na, Ca, and Mg in seawater increased both background and signal. EIE buffering minimizes the matrix effects	149

14 elements	Saline waters	Enhancement effects were studied by using an empirical approach combined with statistical analysis.	150
Several transition metals	Saline matrices	Sodium-induced emission enhancement was studied. A partial thermodynamic equilibrium (PTE) instead of a local thermodynamic equilibrium (LTE) was suggested.	161
18 trace elements	Natural waters	Interferences from stray light due to the presence of Ca and/or Mg can be compensated by using a simple linear correction. Two- and three-electrode DCP systems were compared and the latter offered advantaged of improved stability and lower background.	35
As, B, C P, Se, Si	Natural waters	No significant interference from natural water and waste water sample matrix.	158
Various trace elements	Coastal seawater	Non-aqueous sample introduction to the DCP. Effects of organic solvents were studied	70
U	Ground and mine waters	Standard addition and matrix matching methods were recommended for reducing the enhancement effects due to Na and Ca.	183

Ba, B, Fe Mn, Sr	Oilfield water	Enhancement effects due to EIEs were encountered on original plasma arc.	146
Hg	Solid algal cells	ETV introduction of 0.6-0.9 mg of solid sample to DCP. The addition of sulphur-containing alga or cysteine modified the sample and allowed a reproducible mercury signal to be obtained.	80
V	Workplace air	The results obtained by DCP-AES, flame AAS, and electrothermal AAS were compared.	184
Be	Industrial aerosol	Iron did not interfere with Be determinations at levels < 2.0 mg Fe/sample. Linear dynamic range 0.001-5 μg ml^{-1} of Be.	185
Mo	Plant tissue	Solvent extraction followed by organic phase introduction to a DCP. Due to low Mo content in plant samples, Mo was not detected by flame AAS, but was determined by DCP-AES and graphite furnace AAS with good agreement.	186
B, P, Zn, Mn Mg, Mo, Al, Fe, Cu, Ca, K	Plant tissue	Analysis was fast, requiring 1.25 min/sample. Results and RSDs compared favorably with NBS certified values.	187
B	Fertilizers	Rapid, precise, and accurate determination of B in	188

		fertilizers at levels > 0.002% at wavelength 249.773 nm. Lithium buffer was used to mask enhancement by other alkali metals.	
B	Fertilizers	A much faster and equally accurate method was described for determining B in fertilizers at B wavelength 249.67 nm. No significant difference in results were found among DCP-AES, metaborate distillation, and a modified azo-methine H spectrometric methods.	189

3. Biological and Clinical Samples

Cu, Mn, Cd Pb, Ca, Mg	Diet, Stool Urine	Results obtained by DCP-AES and electrothermal AAS were compared and used for human metabolic studies.	190
Al, Pb, Zn	Biological matrices	The advantages of the method, speed, minimal sample preparation, and multielement determination, were discussed. Results were compared with literature data.	191
Si	Urine	LiCl buffering was used to reduce interferences.	159
Li, Na, K, Mg Ca, Fe, Cu, Zn	Human serum	Simultaneous determination of the eight elements with RSD of 1-3%.	192

Li	Serum	A correlation was observed between the values obtained by DCP-AES and AAS.	193
V	Urine, Blood Serum	Detection limits for V were 2 and 10 μg L^{-1} for pyrolytic graphite furnace AAS and DCP-AES, respectively.	194
Cu, Fe, Zn	Biological fluids	DCP-AES was interfaced with a gel filtration chromatography column. Detection limits were 3.2, 3.9, and 9.3 μg L^{-1} for Cu, Fe, and Zn, respectively.	126
Al, Ba, Si, Sr, Zn, Fe, K, Cu, Ca	Amniotic fluids	The detection limits for Al, Ba, Si, and Sr were 2, 2, 15, and 2 μg L^{-1}, respectively.	195
Ca, Cu, P, and Zn	Bovine liver (NBS SRM)	Due to slurry sample introduction, an analysis was done within 10 min. from the time the unprepared solid bovine liver sample was received. DCP showed remarkably wide range of gas flow rates acceptable for nebulizer operation. Laser diffraction was used to detect droplet size distribution.	69
15 elements	Horse hair	Simultaneous determination of 15 trace elements.	196

14 metals	Animal tissue	0.25 M $LiNO_3$ was used as EIE buffer to minimize matrix interferences.	157

4. Metallurgical Samples

16 elements	Steels, Irons	Background shifts and enhancement effects were overcome by using an iron matrix synthetic standard.	197
10 major and minor elements	Steels	High pressure sample decomposition with HNO_3-HCl-HF in teflon container-metal bomb apparatus for DCP-AES analysis.	198
21 minor and trace elements	Lead, Pb alloys	Automated DCP-AES analysis	199
20 trace metals	99.95% Pd	Enhancement effects were reduced by using matched matrix standards or aqueous standards with Li buffer.	200
W	Steels, Alloys	Because of high resolution of echelle monochromator, there was little or no spectral interference. DCP provide approximately the same power of detection as the more expensive ICP.	201

P	Steels, Cu-based alloys	Emission lines, spectral interference effects of Cu and Fe, and matrix effects of Na, K, Ca, Mg, Al, and Si were studied.	202
B, Nd	Alloys	Li buffer was added to minimize interferences. RSD was 1% and accuracies were comparable to those obtained by gravimetric and spectrophotometric methods.	203
10 elements	Steel	Closed-vessel microwave sample dissolution for DCP-AES analysis.	204
P	Cu-based alloys	The interference of Cu and Fe on P was eliminated by ion-exchange separation.	128
Pt, Pd, Rh	Alumina-based matrices	Non-alkali metal interferences were not fully controlled by only Li buffer, but eliminated by Li-La mixture buffering.	143, 170

5. Industrial Materials

Cr, Cu, Mg, Mn, Ni, Pb	Coal	Slurry introduction with extremely small (less than 20μm) coal particle size. Quantitative agreement between experimental and certified values	83

B, Cr, Cu, Fe, Mn, Mo, Ni, W	Industrial products	Alkaline fusion for sample dissolution. Matrix matching to eliminate interferences.	205
12 wear metals	Aircraft lubricating oils	Direct analysis. DCP-AES and AAS methods were compared and results were in agreement. Recoveries were 89-102% and RSDs were 2-12%.	206, 207
Hg	ICl	The wide linear range (0.50-130 μg ml^{-1}) negated the necessity of diluting samples, resulting in the DCP-AES procedure ten times faster than the standard electrothermal AAS.	208
B	Glass	Spectral and matrix interferences were studied. Lines of B at 249.773 nm and Fe at 249.782 nm were easily resolved by the echelle spectrometer.	209
Al, Fe, Ca, Mg	Wet process phosphoric acid	DCP-AES and AAS methods were compared and the former showed advantages. The suppression of Ca and Mg emission by phosphate encountered in flame AAS was nonexistent in DCP-AES.	210
B, Fe, Cr,	Industrial	Matrix matching for obtaining accurate results.	211

Cu, Mn, Mo, Ni, W	products		
Al, B, Ca, Cr, Fe, Mg, M, W	Silicon nitride (Si_3N_4)	samples were dissolved by alkali fusion method. The suppressing effects of Si on the determination of Ca and Mg were discussed.	212
As(III), As(V)	Nitrate	DCP-AES and ion chromatography were combined and the advantages of this combination were demonstrated.	213
Silicon compounds	Sodium silicate derivatives	Gradient liquid chromatography with DCP-AES.	162

6. Food

10 trace metals	Orange juice	Flame AAS, flame AES/AFS, DCP-AES, and ICP-AES methods were compared. They gave reasonable agreement in the values obtained.	214
Trace alkali and alkaline earth metals	Orange juice	DCP-AES and ICP-AES methods were compared. Matrix interferences were present in both cases but more pronounced in DCP-AES.	138

Various	Foods	Slurry introduction-DCP-AES. Results were compared with the certified values.	86

VI. Hydride Generation

Elements of groups IVA, VA and VIA in the periodic table form covalent hydrogen compounds, usually called hydrides. Among them, germane (GeH_4), stannane (SnH_4), plumbane (PbH_4), arsine (AsH_3), stibine (SbH_3), bismuthine (BiH_3), hydrogen selenide (H_2Se), and hydrogen telluride (H_2Te) have been occasionally used for trace analyses of these eight elements. The technique for producing the hydrides, often called hydride generation, is readily combined with detection systems, especially to atomic spectrometers.

The generation of arsine and stibine by the reduction of arsenic and antimony compounds with zinc in acidic solutions has been well-known over a century as the Marsh reaction and Guzeit test. The Marsh reaction has been utilized for qualitative analysis of arsenic and antimony, in which AsH_3 and SbH_3 are decomposed by heat to a metallic mirror. Subsequently, arsenic, but not antimony, is oxidized by NaOCl. The Guzeit test has been applied to quantitative analysis of As and Sb. Arsine and stibine are absorbed on a paper impregnated with $AgNO_3$ or $HgCl_2$. This test can be made quantitative by comparison with standard stains for known samples. The application of hydride generation in spectroscopic analysis initiated with the spectrophotometric determination of arsenic in 1951 (215), with d.c. arc emission spectrometry in 1955 (216), and with atomic absorption spectrometry in 1969 (95). Since then, numerous publications have appeared in literature dealing with hydride generation for atomic spectrometric analysis (92-94). By coupling hydride generation with

spectrometric techniques, detection limits of 2 to 3 orders of magnitude better than conventional nebulization methods have been achieved (92-93, 217-218). Although only a few elements can be determined with hydride generation, most of them are of great importance and have to be determined frequently at low levels in a variety of sample matrices. Therefore, hydride generation technique has shown to be promising for trace analysis.

Reaction for Hydride Generation

Metal-acid reaction was first used to generate covalent hydrides (215-216, 219-223). Zinc-hydrochloric acid system has been often used (219-221). In addition to the Zn-HCl reaction system, other metal-acid reactions investigated include mixtures of Mg and $TiCl_3$ with HCl and H_2SO_4 to generate AsH_3, SeH_2, SbH_3 and BiH_3 (222), and aqueous slurry of Al-HCl reaction to produce AsH_3, SeH_2, and SbH_3 (223).

Metal-acid reaction systems have been found capable of generating only AsH_3, SeH_2, SbH_3, and BiH_3, with need for a reaction time generally over 20 minutes in order to react quantitatively with trace amounts of analytes. For arsenic determinations, As(V) has to be prereduced to As(III) prior to the formation of arsine with metal-acid reaction. A combination of $SnCl_2$ and KI has been often used for this reason (224-226). However, the prereduction and the actural hydride generation procedures make the determination time-consuming. Furthermore, the metal-acid reaction system is not readily automated.

Therefore, a more homogeneous and powerful reaction system, $NaBH_4$ reduction system, has been studied.

Sodium tetrahydroborate(III) reduction to form elemental hydrides for synthetic purposes has proved extremely useful (227-228). The use of $NaBH_4$ to form hydrides for spectrometric analysis was first described in 1972 by Braman *et al.* (229), who used 1% aqueous $NaBH_4$ to generate arsine and stibine and swept the hydrides, with helium carrier gas, to a d.c. discharge detector. With this system, they were able to achieve detection limits of 1 ng and 0.5 ng for arsenic and antimony, respectively.

Initially, $NaBH_4$ pellets (230) were used in a similar manner as the metal-acid reaction. In order to obtain a better homogeneous reaction solution, greater control, and potential for automation, $NaBH_4$ pellets were replaced by its aqueous solution with concentrations of 0.1% to 12% (W/V). With $NaBH_4$, eight elements, Ge, Sn, Pb, As, Sb, Bi, Se, and Te were able to form their related hydrides. This reaction system also overcame the drawbacks apparent in the metal-acid reaction system. Thus there is no need for long reaction time under the optimum conditions. The fast reaction rate results in more rapid determination of hydrides. It is also ease of automation. Therefore, the $NaBH_4$ reaction has virturally replaced the metal-acid reaction system for analytical methods of hydride generation.

Manipulation

Two basic hydride generation - transportation systems, batch system and continuous flow system, have been widely used. In a batch system, an accurate volume of analyte solution is placed in a reaction vessel followed by the addition of reducing agent, e.g. $NaBH_4$ solution. The hydrides and hydrogen produced in the reaction vessel are then swept with carrier gas either directly to a detector or into a collector/condenser prior to the detection system. The collectors/condensers used included a balloon (221, 224, 230-231), a collection tank under the pressure (225-226, 232-233) and a cold trap, such as a liquid nitrogen trap (95, 234-237). In the former two cases, hydrides along with hydrogen were collected together and then introduced as a discrete plug of vapor into a detection system. Under the condition of liquid nitrogen trap, only hydrides were collected and excess amounts of hydrogen were released due to its lower boiling point (-252.8 ^oC) than that of liquid nitrogen (-195.8 ^oC). The separation of hydrogen from hydrides has some advantages. The sensitivity is increased due to the elimination of dilution factor by hydrogen. Instability of a plasma or a flame caused by large amounts of flammable hydrogen (229, 238-240) is also overcome. After the hydrides are completely trapped in a U-shape tube, liquid nitrogen is removed and the U-tube is electrically heated. The hydrides are then evaporated upon heating, and transported to a detection system. Through this cold trapping-evaporating process, different species of hydride, inorganic and organic, can be determined separately (241-

244). All hydride species, trapped in the U-tube, are eluted sequentially upon heating and detected sequentially. This serves as a fractionation based on the boiling points of different hydride species.

The batch type hydride generation system serves as a preconcentration and separation procedure. Large amounts of sample containing trace concentration of analyte can be used. The analyte is separated from the sample matrix through the hydride generation process and is simultaneously concentrated. Because the hydride is introduced to the detection system as one pulse, a transient signal is obtained.

A continuous flow hydride generation system, on the other hand, gives a continuous signal. Sample/standard solutions, acid solution, and $NaBH_4$ solution are continuously taken by a proportioning peristaltic pump (244-246) or a pressurized reagent pump (247) and react in a mixing coil. The generated hydride is then separated from the waste solution in a gas/liquid separator. Hydride is continuously introduced into an atomizer or a plasma for detection. Since it requires fast reaction only $NaBH_4$, but not the metal-acid reduction system, can be used. Compared with a batch system, the continuous flow system is easier for automation, more suitable for ICP-AES detection system, where the stability of the ICP suffers from the single shot introduction manner of the batch system. However, the sensitivity for the continuous flow system is relatively lower than that for the batch system.

Detection System

A variety of spectroscopic detection systems have been coupled with hydride generation technique. Most often used have been atomic absorption spectrometry and plasma emission spectrometry.

Atomic absorption spectrometry was first coupled with hydride generation in 1969 (95). Since then, the major detection system for hydride generation has been the AAS since the instrumentation has been readily available in most laboratories. A number of different flames were studied for AAS detection of hydrides (225-226, 231, 248-254). Argon/hydrogen flame AAS combined with hydride generation has shown relatively lower background absorption and improved detection limits (248) compared to direct solution nebulization AAS (92). Apart from the flame AAS, two common flameless (or electrothermal) AAS devices, electrically heated quartz (244, 246, 255-257) and graphite furnace (223, 258-259) have been used as atomizers for hydride generation AAS. Due to the increased residence time that the atoms spend in the optical path, elimination of the dilution of hydride by flame gases, and the much reduced noise levels, the flameless AAS has been shown to be more sensitive than the argon hydrogen flame AAS (224). Therefore, a number of works (260-268) have adopted the flameless AAS as the detection system for hydride generation.

Lee (265) and Sturgeon *et al.* (268-270) have used a graphite furnace as both trapping medium and atomization cell for hydride generation. Hydrides, generated with $NaBH_4$, were trapped in a

graphite furnace at lower temperature (e.g. 600 °C), subsequently atomized at higher temperature (e.g. 2600 °C), and detected by AAS. As a result of the in-situ preconcentration, this combination of hydride generation with subsequent trapping in the graphite furnace provided increased sensitivity. This method has been applied for the determination of Bi (265), As, Se, and Sb (269), and Sn (268) in environmental samples.

Plasma AES coupled with hydride generation is becoming widespread due to the increasing availability of commercial plasma instrument. In 1978, Thompson *et al.* (240, 271) first reported the simultaneous determination of trace amounts of As, Bi, Sb, Se, and Te by hydride generation in conjunction with ICP-AES. The hydrides, formed in a continuous flow hydride generator system, were directly introduced into the ICP and simultaneously detected by a multichannel atomic emission spectrometer. With this system, the sensitivities and detection limits were improved by an order of magnitude over conventional ICP-AES methods. Up to now, the hydride generation ICP-AES method has been applied for the determination of all eight hydride forming elements. However, one commonly encountered difficulty in the combination of ICP and hydride generation is the instability of the ICP with the large quantity of hydrogen produced during the generation reaction. This is overcome by using a liquid nitrogen trap to separate the hydrides from the hydrogen (217, 272-273), which otherwise normally extinguished a medium power plasma discharge (274), or using low acid concentration and continuous flow system to

maintain a constant flow of the mixture gas of hydrides and hydrogen (274-277) and using relatively high power RF input (271, 278-279).

Miyazaki *et al.* (97) has coupled hydride generation with DCP-AES for the determination of submicrogram amounts of As and Sb. The excess amounts of hydrogen, produced in the Zn-HCl reduction batch system, were separated from hydrides through a liquid nitrogen trap. Detection limits of 8 ng for As and 40 ng for Sb in a 20 ml sample were achieved. Panaro and Krull (98) used a more stable three-electrode DCP-AES system as a detector for the determination of arsenic through hydride generation by using $NaBH_4$ as reducing agent. A continuous flow hydride generator system was used and the DCP-AES was compared with flame AAS. The designs of hydride introduction sample tube for a three-electrode DCP have also been described in a number of papers (99-101).

ICP-MS has shown great promise for elemental analysis (280-284). It combines the advantages of high energy ionization of the ICP and sensitive detection of the MS. This technique has also been combined with hydride generation for the determination of As, Se, Hg, Sb, Bi, and Te (285) and Pb (286). With hydride generation, two orders of magnitude greater sensitivity were obtained on ICP-MS. Multielement and isotope ratio analyses can be made by ICP-MS system with its additional advantage of fast scanning ability.

MIP-AES has also been utilized as a detector for hydride generation (220, 238, 287-288). Non-dispersive atomic fluorescence spectrometry (AFS) with both flame (289-291) and plasma (292) has been shown to be very sensitive for hydride detection. Thermal

conductivity (293), flame ionization (293), photoionization (294), mass spectrometry (295-296), and molecular emission cavity analysis (297-299) have also been utilized as detection system for hydride generation with the combination of preliminary chromatographic separation.

Interference

Advantages of hydride generation have usually been stressed because of its high sensitivity and relative simplicity. The desirable analyte elements can be separated from almost all other accompanying materials through hydride generation processes. Thus spectral interferences, such as background attenuation by matrix elements, and chemical interferences encountered in the detection system are essentially eliminated. However, hydride generation itself is not free from interference. The interferences can stem from both the hydride production and transport processed (300).

Since Smith (301) carried out, in 1975, a general survey of interference by 48 elements on the determination of antimony, arsenic, bismuth, germanium, selenium, and tin, a number of papers (271, 302-306) have been published on interference effects. Quantitative data were determined by Pierce and Brown (304) for various concentrations of several anions, cations, and acids on arsenic and selenium hydride formation. In a later paper, these authors discussed the radical differences in the interfering effects which derived from the method of generation of the hydride and the mode of production of the atomized arsenic in the beam of the atomic absorption spectrometer (305).

Manual hydride generation with argon-hydrogen flame atomization, automated hydride generation with heated quartz tube atomization, and graphite furnace atomization were employed in their studies. Thompson *et al.* (271) studied the effects of the valence states of the potentially interfering elements in hydride generation by ICP-AES.

In a study of interference, Hershey and Keliher (306) extensively investigated the interference effect in the determination of arsenic, antimony, bismuth, and selenium by continuous flow and batch hydride generation AAS and continuous hydride generation ICP-AES systems. They observed that nineteen from a total of fifty elements produced an interference effect greater than 10%. Cobalt, copper, nickel, palladium, and platinum reduced the signal severely. It appeared that transition metal ions caused the strongest interferences. Many other papers have also reported interferences in the determination of hydride forming elements (307, 309-315).

The mechanism of interference has been the subject of considerable discussion. It was first thought that the interferences of transition metal ions on hydride forming elements were due to their competition for sodium tetrahydroborate(III). The reducing agent was preferentially consumed by the interfering metals so that not enough was available to convert the analyte elements into their hydrides (235, 248, 308). McDaniel *et al.* (235) suggested that interference effects decrease with increasing concentrations of $NaBH_4$. However, later research (309-310) has proved this assumption was wrong. Welz and Schubert-Jacobs (310) and Dittrich *et al.* (309) have found that less

than 0.1% of the $NaBH_4$ was normally consumed to generate the hydride and the interference was actually less with lower $NaBH_4$ concentration. Similar results were obtained by Astrom (311), who stated that the interference could be reduced by using a concentration of $NaBH_4$ as low as 0.1%.

Welz and Melcher (310, 312-314) have proposed that interference was related to the precipitation of the interfering element. Thus the precipitation of a transition element prior to complete reduction of analytes is described as producing a gas-solid reaction in which the hydrides are decomposed following adsorption onto the finely divided metal. This was confirmed by using fine copper powder instead of Cu^{2+} solution, where similar interference effects were observed.

Brown *et al.* (307), Yamamoto *et al.* (315) and Bye (316) suggested that interfering metal ions react with $NaBH_4$ to produce metal borides, not elemental metals. The metal borides then cause capture and decomposition of hydrides (e.g SeH_2) due to the high reactivity of metal borides (316). Bye also noted that in the case of reaction between $NaBH_4$ and Co^{2+}, the precipitate was analyzed and found consisting of cobalt boride with apparent stoichiometry of Co_2B (317).

On the other hand, Aggett and Hayashi (318) suggested that interference occurs in solution via the formation of a soluble species formed between the interferant in a low oxidation state, stabilized by

the tetrahydroborate(III), and the hydrides, for example arsine. In the paper, the authors support this conclusion with semi-quantitative results for the analysis of arsenic and nickel in the spent solution and solid material formed during reaction with sodium tetrahydroborate(III) solution. In a 10 ml solution containing 0.2 μg ml^{-1} As(V) and 10 μg ml^{-1} of Ni(II) in 0.5 M HCl, 78% loss in arsenic signal on AAS was observed after treated with 2.5 ml of 5% $NaBH_4$, compared with that in the absence of Ni(II). After the filtration of the above mixing reduction solution, arsenic and nickel were analyzed by GFAAS. Only 6% of arsenic and < 0.04% of nickel were found on the filter. With differential-pulse polarogram analysis of the filtrate, nickel was completely recovered.

The mechanism of interferences is still not completely clear. Research on hydride generation is certainly important to establish the mechanism of interference effects and that responsible for the interference reduction.

In order to reduce the interference effect, a number of papers (319-325) have described the separation of analyte from sample matrix prior to the determination by hydride generation. The separation techniques applied include coprecipitation with manganese dioxide (319), iron(III) (320) and $La(OH)_3$ (321), liquid extraction (322), electrodeposition, ion exchange chromatography, and chelating resin (323-325).

Various reagents have been used to reduce or eliminate interferences in hydride generation. Belcher *et al.* (326) reported that ethylenediaminetetraacetic acid (EDTA) reduced the interference from Co, Fe, Ni, Zn, etc. in the determination of arsenic. EDTA has also been used to reduce interference in the determination of other hydride forming elements by hydride generation (327-328). Aggett and Aspell (329) reported that acetate and citrate ions behave in a similar fashion to EDTA. Guimont *et al.* (330) observed that thiocynate ion was better able to reduce interference than either cyanide ion or EDTA. However, with nickel contents over 100 μg, signal reduction was observed that required a mathematical correction based on a linear relationship between nickel concentration and arsenic recovery. Dornemann and Kleist (331) investigated a number of chelating agents with a view to eliminating the interfering effects of cobalt, copper, and nickel. They reported that pyridine-2-aldoxime was more efficient than EDTA or 2,2'-dipyridyl. Peacock and Singh (332) reported that thiourea is extremely effective in reducing interferences from a wide range of elements. Unfortunately, high blank readings make the method unreliable for the determination of trace concentrations of arsenic.

Iron(III) has been used as a releasing agent for the determination of arsenic (313) and selenium (333). In both cases, the authors suggest that iron behaves as an oxidizing agent and the reduction of iron(III) to iron(II) is kinetically favored over the reduction of nickel(II) to nickel(0) (313) or nickel boride (316, 333). Thus the formation of the hydride is essentially complete before the

strongly interfering, low oxidation state nickel has had an opportunity to form and interact with the arsine. Similar logic has been used in rationalizing the partial reduction of interferences by use of mercury(II) in the generation of germane from a solution containing 1000 $\mu g\ ml^{-1}$ of cadmium(II) (334). It is clear that these experimental results would support both the interelement compound formation mechanism and the finely divided precipitation adsorption mechanism.

Other interference reducing agents include iodide (271), 1,10-phenanthroline (335), thiosemicarbazide (335), tartaric acid (336), ascorbic acid (337). The efficiency of interference reduction by masking agents was found to depend on the reaction medium (338). In many cases, especially if trace concentrations of the analyte exists in large amounts of complicated matrix, the interference reducing agent is inadequate.

Application of Hydride Generation Technique to Analysis

The selective application of hydride generation is summarized in Table 2 with a description of sample matrix, interferences and methods for their reduction, detection technique for hydrides, and other comments. In addition to the eight elements being occasionally

determined, phosphorus (339-342), indium (343-344), Tl (344), chlorine (345-346) and bromine (346-347) have also been determined by their hydrides.

Other gaseous sample introduction techniques for spectroscopic instrument include cold vapor for mercury determinations (348-350), chloride volatilization for arsenic (351), tetramethyl lead by AAS (352), formation of carbonyl compounds for nickel (353) and osmium (354) determinations.

Table 2. Selected Applications of Hydride Generation Techniques

1. Germanium Determination

Sample Matrix	Comment	Reference
Silicate rocks Sulphide ores	Germanium was extracted into a mixture of CCl_4 and 9 M HCl and back-extracted into distilled water. Ge was determined by HG-AAS with N_2O-acetylene flame.	355
GaAs Semiconductor, Polyethylene tetraphthalate	HG-ICP-AES was combined with flow injection and a membrane gas/liquid separator. $NaBH_4$ and phosphate buffer (at pH 6.5) solutions were used as reductants. Interferences from other hydride forming elements were negligible, and those from transition metal ions were reduced with EDTA, but Au and Pd still interfered severely.	356
Natural waters	Inorganic and methylgermanium species were reduced by $NaBH_4$ to the corresponding hydrides, stripped from solution by helium gas stream, and collected in a liquid N_2 cold trap. The hydrides were released upon heating, and measured by graphite furnace AAS. 25 min. of reduction and stripping time was required for a 100-ml^{-1} sample.	357
Natural waters	HG-graphite furnace AAS. Same system as above. Detection	358

limit was 140 pg or 0.56 ng L^{-1} of Ge for a 250-ml sample.

2. Tin Determination

Marine biological tissue and sediments	Stannane, generated with $NaBH_4$, was subsequently trapped and atomized in a graphite furnace for AAS detection. 2000 ppm Fe^{3+}, 2 ppm As^{3+}, 1 ppm Ni^{2+}, 0.1 ppm Cu^{2+}, and 0.1 ppm Se^{4+} in solution did not interfere with tin determinations.	268
Atmospheric particulates	Atmospheric particulate samples, collected on Whatman 41 cellulose filters, were decomposed with H_2SO_4-HNO_3, followed by HF to dissolve residual silicates. Stannane was detected by AAS with detection limit of 2 ng mL^{-1} of Sn.	359
Suspended air particulate	A semiautomated continuous flow hydride generation system for AAS with quartz atomizer. The interferences from 20-fold excess of Cu, Ni, Sb, and As were eliminated by the addition of sodium oxalate to the sample solution or by precoprecipitation with heated manganese dioxide.	319
Waters	Total tin and organotin species were determined by U-tube collection-batch hydride generation system coupled with graphite furnace AAS, quartz atomizer AAS,	241

	and flame AAS. Interferences from germanium, especially from methylgermanium compounds, were eliminated with a dual-channel detection system. The inorganic tin blank in $NaBH_4$ was reduced by adding 1 ml of 2 M NaOH to 100 ml of $NaBH_4$ and standing overnight to allow the tin to adsorb to the container walls.	
Waters	Volatile speciation of inorganic tin, methyl- and n-butyltin compounds were formed through hydride generation, trapped and separated on a chromatographic packing material, and detected by AAS with an quartz tube atomizer. Detection limits of 50 pg.	360
Natural waters, Human urine	SnH_4, CH_3SnH_3, $(CH_3)_2SnH_2$, and $(CH_3)SnH$ were formed by reaction of analyte with $NaBH_4$. They were then scrubbed with He carrier gas, trapped in a U-tube, cooled with a liquid N_2 bath, and separated upon heating. The Sn-H bond emission was detected with a H_2-air flame emission detector. This method achieved high sensitivity but had a narrow calibration range and was time consuming, with 6-8 min. for process required.	243
Waters, Sediments, Macro algae	Hydrides of inorganic tin and organotin compounds were trapped in a liquid N_2 cooled V-tube packed with glass and separated based on their boiling points as the V-tube	361

	was heated. Detection limits of 0.4 ng for inorganic tin(IV) and 2 ng for tri-n-butyltin chloride were achieved.	
Seawater	Hydride derivatives, formed by the reaction with $NaBH_4$, were cryogenically trapped in a silanized glass wool U-tube, eluted to a quartz cuvette atomizer, and detected by AAS.	362
Marine and estuarine waters	Inter-laboratory comparison of results of di- and tributyltin obtained by (i) hydride generation-dichloromethane extraction followed by GC separation and flame photometric detection; and (ii) hydride generation followed by cold trapping with boiling point separation and flame AAS mesurement. Good agreement obtained.	363
Salmon tissue	Tri-n-butyltin (TBT) and di-n-butyltin (DBT) were determined as hydride derivatives by GC. Organotins in fish were extracted with a methanol/methylene chloride mixture and the extracts were cleaned up on a small silica gel column. Hydride derivatives of TBT and DBT were formed in a packed reactor inside the injection port of a GC. Following hydride generation, the hydrides were separated on a wide bore capillary column and detected with a flame photometric detector.	364
Oysters	Inorganic tin, methyl- and butyltin compounds were determined	365

	by HG-AAS. A method for simultaneous extraction of the above three species from oyster tissue without breaking the carbon-tin bond was described.	
Foods	HG-AAS. The tin signals were suppressed by 100 μg of Co, Cu, Fe, and Ni without changing peak symmetry. As, Sb, and Se reduced tin signals with peak distortion and imprecision.	366
Wines, Sugar beets	HG-AAS. Reaction time of 25 seconds. and pH values between 0.90-1.25 were recommended. Four buffers, potassium acetate, potassium phthalate, KCl, and sodium hydrogen tartrate were compared for hydride reaction.	367
Foods, Alloys	Tin was extracted into chloroform with ammonium N-nitrosophenylhydroxamate prior to the determination by HG-AAS with an acetylene-air flame.	322
Foods, Steels, Alloys	A continuous flow HG system coupled with ICP-AES was used to determine tin with detection limit of 50 pg ml^{-1}. Mixtures of HNO_3-succinic acid and of HNO_3-malic acid were found suitable reaction media. Thiourea reduced interferences. Standard addition method was used for accurate determination.	274
Low alloy steel	HG was coupled with AFS and a small Ar-H_2-entrained air flame. Cr, Mn, and Mo did not interfere, but Ni and Cu significantly	368

	decreased tin signal. To eliminate the error caused by the interferences, a standard addition method was employed.	
Low alloy steels	Non-dispersive AFS was used for HG detection with detection limit of 1.2 ng or 0.6 ng ml^{-1} of tin. At levels 1000-fold in excess of tin, 29 elements studied caused tin signal change less than 10% while 17 elements, with most of which being transition elements, suppressed tin signal more than 10%.	292

3. Lead Determination

Water, Galena	A combination of continuous flow hydride generation, isotope dilution, and ICP-MS was studied and applied for lead determination. Sulphosalicylic acid (0.4%) and NaCN (0.02%), dissolved in $NaBH_4$ solution, were used to reduce the serious interferences from iron and copper, respectively. The detection limit was restricted to 0.01-0.05 ng ml^{-1} by the reagent blanks.	286
Water, Oyster tissue	Malic acid-$K_2Cr_2O_7$, HNO_3-H_2O_2, and HNO_3-$(NH_4)_2S_2O_8$ reaction matrices were compared for the determination of lead by continuous flow HG-AAS with a quartz tube atomizer. Ag, Au, Cu and Cd interfered severely in all reaction systems. A dithizone-chloroform extraction and back-extraction method was applied to eliminate interfering ions.	260

Aqueous solution	Three reaction media, 0.25 M malic acid (or tartaric acid)/ 0.025 M $K_2Cr_2O_7$, 0.5 M HNO_3 (or HCl, $HClO_4$, or 0.25M H_2SO_4)/ 1.3 M H_2O_2, and 0.3 M HNO_3 (or HCCl, $HClO_4$)/0.12 M $K_2S_2O_8$, were used to enhance Pb sensitivity by HG-flame AAS. Pd(II), Cu(II), Te(IV,VI), and EDTA interfered severely.	369
Drinking waters	Lead in water samples was co-precipitated with manganese to eliminate interferences from Cu and Ni. The precipitate was then dissolved in 0.85% HNO_3, and lead was determined by HG-flame AAS. The results were compared with those obtained by graphite furnace AAS, flame AAS, and differential pulse anodic-stripping voltammetry.	370
Aqueous solution	Plumbane was continuously generated and carried directly into a low-power (100W) Ar or He MIP by the HG by-products, predominantly being H_2. Detection limit was 0.3 ppm with HG-helium MIP-AES.	371
Aqueous solution	The Pb^{2+} was oxidized to Pb^{4+} with 0.2 M $KBrO_3$ in acidic solution followed by addition of $NaBH_4$. The gaseous PbH_4 formed was introduced into a premixed Ar-H_2 flame and detected by non-dispersive AFS. Detection limit was 20 ng or 2 $\mu g\ ml^{-1}$.	372
Drinking	HG-AAS. Copper interference was reduced by addition of KCN	373

water	and the pH of the sample solution was controlled between 1.5 and 2.2.	
Aqueous solution	Plumbane was generated with efficiency of 64% in 0.5M-0.8M H_2O_2 solution with addition of 5% $NaBH_4$, and was carried by argon to an ICP for AES detection.	374
Air, Water, Vegetable	Analyte solutions were made in 0.7% (V) HNO_3 or 1.0% $HClO_4$ with 12% H_2O_2. Hydrides were produced by reacting with 4% $NaBH_4$, and were detected by AAS with a quartz tube atomizer.	375
Aqueous solution	$Cr_2O_7^{2+}$, MnO_4^-, Ce^{4+}, $S_2O_8^{2-}$, and H_2O_2 as oxidizing agents in determination of lead as hydride using $NaBH_4$ were studied and showed necessary. The effect of an oxidizing agent on the plumbane formation was attributed to the oxidation of lead to a metastable tetravalent state before conversion into plumbane.	376
Aqueous solution	Hydride generation efficiency using $NaBH_4$ was found to be 90% for trimethyl-, triethyl-, and diethyl-lead, 59% for dimethyl-lead, and 27% for inorganic lead. Hydrides were measured by a non-dispersive AFS with a small Ar-H_2 flame. Cu, Se, Te, and EDTA suppressed severely the lead signals.	377 378
Urine	Triethyllead (Et_3PbCl), diethyllead (Et_2PbCl_2) and inorganic lead were determined by HG-AAS with detection limits of	379

	0.005 μg Pb for Et_3Pb^+ and Et_2Pb^{2+} and 0.1 μg for Pb^{2+}. Urine samples were prepared by the use of 0.5 M malic acid for the generation of Et_3Pb^+, 0.75 M H_2O_2-0.004 M $HClO_4$ for Et_2Pb^{2+}, and 1.6 M malic acid-0.05 M $K_2Cr_2O_7$ for Pb^{2+}; and $NaBH_4$ was used to generate hydrides. The hydrides were condensed in a U-trap cooled with liquid N_2, fractionated upon heating, and atomized in a quartz tube heated to 1000 °C for AAS detection.	
Steels, Air particulates	The lead hydride generation was carried out on an aliquot of Pb pyrrolidine-1-carbodithioate extract in chloroform by the addition of $NaBH_4$ solution in DMF.	380
Biological materials, Foods	Oxidizing agents HNO_3-H_2O_2 were used to improve the efficiency of plumbane generation by reduction with $NaBH_4$. The presence of transition metals, Ni, Co, and Mn, considerably increased the lead signal, with the enhancement depending on the concentration of $NaBH_4$.	381
Gasoline	With $NaBH_4$, no plumbane was generated in organic medium. Lead was introduced into a silica tube atomizer for AAS detection in the form of a volatile organometallic compound, PbR_4, rather than PbH_4. $NaHCO_3$ was used to improve the efficiency of the volatilization.	382

4. Arsenic Determination

Mineral water, Plant, Soil digests	Hydrides of inorganic and methylated arsenic species were trapped in a small volume of absorping solution containing 1000 μg ml^{-1} of Ce(IV) as $Ce(NH_4)_2(NO_3)_6$ and 800 μg ml^{-1} of iodide as KI, and determined by graphite furnace AAS.	383
Natural waters	Selective determination of As(V), As(III), monomethylarsonic acid (MMAA) and dimethylarsinic acid (DMAA) by using continuous HG and AAS detection. Citric acid-citrate, KI, 1,10-phenanthroline, EDTA, thiourea, and thiosemicarbazide were used to minimize interferences in different reaction media.	384
Cocoa beans	HG with ICP-AES. Detection limit of arsenic in dry ashed cocoa beans was 0.004 μg g^{-1}.	385
Seeweed (hijiki) Mouse liver	Four arsenic species were determined by HPLC-HG-flame AAS system equipped with either an anion exchange column or a gel permeation column.	386
Seawater	A membrane gas-liquid separator was used for flow injection HG-AAS determination of arsenic. Ni and Pt interfered with arsenic determination.	387

Waters	As(V), As(III), methylarsonic acid and dimethlarsinic acid were reduced to their corresponding hydrides at pH 1-2 by $NaBH_4$. The hydrides were collected and separated on a liquid N_2 cold trap, and then introduced into a d.c. discharge detector.	388
Seawater	HG-AAS. As(III), As(V) and organoarsenic species determined.	389
Marine materials	Arsine was trapped in a graphite furnace at 600 °C prior to the atomization and detection by AAS.	390
Copper	HG-AAS with air-C_2H_2 flame. Interferences studied.	253
Glycerine	HG was combined with ICP-AES and flow injection with a vapor-liquid separation cell. Peak area were used to measure arsenic in the concentration range 0.12-3.0 $\mu g\ ml^{-1}$.	391
Orchard leaves Bovine liver	HG-AAS with a long absorption cell. Arsine was collected in a liquid N_2 cooled trap and then carried with He into a heated Al_2O_3 tube (19 cm long) placed within the graphite furnace for AA detection.	392
Soils	HG-AAS. Ten sample digestion methods were compared.	393
Steel Cast iron	HG-AAS. Samples were decomposed with HNO_3-$HClO_4$.	394

5. Antimony Determination

Natural waters	Differentiation of Sb(III) and Sb(V) species was achieved by pH dependent selective reduction with $NaBH_4$; i.e., pH at 2.2 for the formation of stibine from Sb(III) only, and in 1 M HCl for total Sb. Stibine was preconcentrated in a cold trap and atomized in a quartz tube atomizer for AAS detection.	395
Geological samples	A DCP-AES system was coupled with a batch-type hydride generator.	396
PVC	Stibine was measured by a UV-Visible molecular absorption spectrometer with diode-arry detection.	397
River water	HG-AAS. Water sample was preconcentrated and separated with chelating resin.	323
Wastewaters	Continuous HG system with ICP-AES detection. Differentiation of Sb(III) and Sb(V) was performed according to the pH dependence of the $NaBH_4$ reduction step.	239
Plastics	The samples were dissolved in HCl-DMF solution without destruction of the organic material. Stibine was formed in nonaqueous medium, DMF, and determined by AAS with quartz	398

tube atomizer.

6. Bismuth Determination

Wastewaters, Copper, Alloys, Geological samples	HG-ICP-AES. KI and either $K_2Cr_2O_7$ or H_2O_2 improved bismuthine generation in HCl (1.0 M) with $NaBH_4$. Thiourea minimized some of interference effects. Standard addition method was recommended for accurate determination. Sensitivity was increased of a factor of three orders of magnitude compared with a conventional nebulization ICP-AES.	399
Environmental samples	HG-AAS with argon-hydrogen flame. Detection limit was 1 ng of bismuth.	400
Aqueous solution	A flow injection technique was applied for semiautomatic sample introduction for bismuth determinations by HG-AAS. Nickel and copper were found to cause interferences.	311
Geological materials	Automated HG-AAS with a quartz tube atomizer.	401

7. Selenium Determination

Lyophilized human serum,	Interlaboratory trial on the determination of Se by HG-AAS. Thirty laboratories from different countries obtained results	402

Blood, Urine	in good agreement.	
Bovine liver	Continuous HG-AAS with quartz tube atomizer. Standard addition method was used. Results were compared with those obtained by NAA.	403
Coal	HG-AAS with quartz atomizer. Interference caused by NO_x formed during sample digestion was eliminated by sulphamic acid. The efficiency of the Se(IV) reduction with $NaBH_4$ was increased in the presence of halide anion. (KI was used)	404
Marine materials	HG-AAS. in-situ concentration of selenium hydride in a graphite furnace.	405
Geological samples	Selenium in 32 geological reference materials were determined by continuous flow HG-AAS. Samples were decomposed with a mixture of HNO_3, $HClO_4$ and HF.	406
Zinc ore	Thiourea was used to minimize the interference from copper in the determination of Se by HG-AAS. The results agreed well with those obtained by NAA.	407
Natural waters	The hydrides of Se(IV) and Se(VI) were condensed and revolatilized in a cryogenic trap, atomized in a quartz atomizer and measured by AAS.	408

Wastewater, Soil, Plants	Flow injection with HG-AAS.	409
NBS SRM's	HG with flame-in-tube AAS.	254
Biotic materials	H_2Se was preconcentrated on a Chromosorb W column at -150 °C prior to its atomization in a quartz tube for AA detection.	410
Cu alloys, Ni sponge	A minicolumn of a chelating resin with iminodiacetate groups was used for on-line removal of transition metal interferences in microscale suction-flow HG-AAS	411
Biological materials	HG-AAS with quartz cell atomizer. A miniaturized suction-flow on-line prereduction of Se(VI) to Se(IV) technique was described.	412

8. Tellurium Determination

Steel and Commercial sulfur	Te(IV) and Te(VI) were determined by HG-AAS. $NaBH_4$ solution alone was used as reducing agent to generate Te(IV) hydride. $TiCl_3$ solution was used as prereductant before the addition of $NaBH_4$ solution to obtain signal from total tellurium.	413
High-purity	HG-nondispersive-AFS with premixed argon-entrained air-	325

coppers	hydrogen flame. Zinc and $NaBH_4$ reduction methods were compared. Interferences were reduced by passing sample solution through a Chelex-100 resin.	

9. Multielements

Elements	Sample Matrix	Comment	Reference
As,Bi,Pb, Sb,Se,Sn, Te	Steels	The seven elements were determined by HG-AAS in an Ar-H_2-entrained air flame with detection limits in steel of 1 ppm for As, Sb, B, Se, and Te, and 2 ppm for Sn and Pb. Interferences from Cu, Co and Ni were partially reduced by Fe(III), iodide, and tartaric acid.	414
Ge, Sn	Aqueous solution	A continuous flow HG system coupled with ICP-AES was applied for determination of Ge and Sn with detection limits of approximately 0.2 ng ml^{-1}. Intererences from a wide range of metals were found and considerably decreased by addition of tartaric acid to the HCl reaction media.	336
As, Bi, Sb, Se, Te	Steels, Coal fly ash, Flour	Hydride gerneration technique was coupled with flow injection and AAS.	415

As, Sb	Seawater	Differential determination of As(III) and As(V), and Sb(III) and Sb(V) was made by using HG-AAS with H_2-N_2 flame. Ag^{+}, Cu^{2+}, Sn^{2+}, Se^{4+}, and Te^{4+} interferences were encountered.	416
As, Bi, Sb	Low alloy steels	HG in conjunction with sequential ICP-AES.	417
As, Sb, Se, Te	Silicate rocks and Sulphide ores	Simultaneous determination by continuous HG-ICP-AES. The interference effects caused by lead, gold and the platinum-group metals were extremely serious. Analytes were separated from sample matrix by coprecipitation with iron(III) at pH 2.4. A standard addition method was used.	320
As, Se	Coal	Continuous flow HG coupled with AAS or AFS. Arsenic and selenium were separated from potentially interfering metal ions by coprecipitation with $La(OH)_3$.	321
As, Bi, Sb, Se, Sn, Te	Mineral water, Soil	HG-graphite furnace AAS. Hydrides were subsequently trapped into a small volume of absorbing solution containing 500 $\mu g\ ml^{-1}$ of Ce(IV) as $Ce(NH_4)_2(NO_3)_6$ and 500 $\mu g\ ml^{-1}$ of iodide as KI. Ce served as an efficient matrix modifier in graphite furnace AAS.	418

Bi, Pb	Steel, Cast iron	A Na_2O_2 flux in Zr crucibles and a HNO_3-$HClO_4$ mixture in a Bethge digestion apparatus were used for sample dissolution. BiH_3 was measured by graphite furnace AAS with Zeeman background correction. Calibration was done by standard addition.	419 420
As, Bi, Pb, Sb, Se, Sn	Aqueous solution	A modified technique with a simple T-tube for atomization held above conventional AAS burners was described. Prior oxidation of Pb markedly increased the sensitivity for Pb.	421
As, Pb, Sn	Aqueous solution	Hydride generation and flameless AAS.	422
As, Se	Environmental samples	DCP-AES with continuous hydride introduction was applied for As and Se determinations with detection limits of 4 ng ml^{-1}.	100
As, Se	Biological samples	A DCP-AES system was coupled with a continuous hydride generator. Detection limits were 0.3 and 0.5 ng ml^{-1} for As and Se, respectively. 1,10-phenanthroline was used as masking agent to minimize interferences from copper and nickel.	101

As, Bi, Hg, Sb, Se, Te	Environmental samples	An ICP-MS system was used with hydride introduction. Hydride generation gave 2 orders of magnitude greater sensitivity. Memory effects were pronounced for Hg.	285
Ge, Sb	Natural waters, Air particulates	Antimony, germanium and methylgermanium compounds in aqueous solution at pH 1.5 were converted to their corresponding hydrides with $NaBH_4$ reduction. The hydrides were collected in a liquid N_2 cold trap prior to the detection by a d.c. discharge AES. Spectral interferences from CO_2, N_2 and H_2O and chemical interferences form Ag, Cu, Co, and Ni were encountered.	423
As, Ge, Sb	EPA water samples	HG-ICP-AES with a sequential slew scan monochromator. Hydrides of As, Ge and Sb were separated on a column of Chromosorb 102, and introduced in the ICP.	273
Bi, Sb, Sn	Pollution aerosols	Atmospheric particulates were collected on cellulose filters, digested with H_2SO_4-H_2O_2 for Sb and Bi, and with H_2SO_4-HNO_3 for Sn determinations by HG-AAS.	424
As, Sb	Geological samples	Automated HG-AAS with a quartz cell atomizer. Samples were decomposed with a mixture of $HClO_4$-HNO_3-HF-$KMnO_4$ solution. Interferences were reduced by KI, $AlCl_3$ and ascorbic acid. 85 samples were analyzed.	425

As, Se	Copper, Nickel	As and Se in Cu and Ni powder were separated with Chelex 100 resin prior to the determination by HG-AAS.	324
As, Sb	Steels, Orchard leaves	A glass vial with internal volume of 8.6 ml, served as a small hydride generator, was coupled with AAS. Interferences were reduced by a mixture solution of thiourea and ascorbic acid.	426
Bi, Sb	Aqueous solution	HG-AAS. 1,10-phenanthroline was used to reduce the interference from nickel. In the presence of this masking agent, 10,000-fold Ni^{2+} did not interfere Sb and Bi determinations.	427

10. Other Hydrides

P	Phosphate	Calcium phosphate was reduced to calcium phosphide with aluminum powder at about 1100 °C, followed by reaction with 2.7 N HCl to generate phosphine gas in a graphite furnace atomizer as a reaction vessel. PH_3 gas was then introduced into an ICP-AES. Detection limit was 20 ng or 2 μg ml^{-1} of P, which was one order of magnitude lower than that obtained by direct nebulization ICP-AES.	339

P	Commercial reagents	Phosphine was formed by passing the sample mist containing phosphate ion, produced by a ultrasonic nebulizer, through an incandescent carbon tube. Phosphine gas was then detected by gas phase chemiluminescence with ozone oxidation.	340
P	Natural water	Hydride generation combined with GC.	342
In	Aqueous solution	Indium hydride, produced by addition of 2% $NaBH_4$ to a solution of indium in 3 M HCl, was flushed with argon into an electrically heated silica tube and detected by AAS. The sensitivity of 0.3 μg of In for 1% absorption was obtained.	343
In, Tl	Aqueous solution	The hydrides were formed in 1 M HCl (for In) and 1-1.5 M HCl or HNO_3 (for Tl) with 1% $NaBH_4$ solution, flushed with argon into an electrically heated silica tube, and detected by AAS. Effects of HCl concentration and interferences from As, Te, Pb, and In on Tl were reported.	344

VII. Research Goals

Interference effects cause the accurate and rapid analysis difficult or even impossible (301, 306, 319-325, 336). The search for the approaches for the interference reduction appears to be of importance. The purpose of this research was to attempt to find effective interference reducing agents and to apply them to the determination of hydride forming elements. In addition, the benefits of signal enhancement by easily ionized elements could provide some advantages for analysis. If the analyte is introduced to the DCP while a solution of EIE of fixed concentration is separately nebulized and transported to the plasma jet, it should be possible to convert the enhancement effect to an advantage in improving the sensitivity and detection limit which is beneficial to trace analysis. Hydride generation technique coupled with DCP-AES exactly offers this opportunity. Through a modified DCP sample tube, hydrides and EIE solution can be separately introduced into the DCP. The EIE buffering effect is thus achieved with no need of time-consuming procedures for preparing sample solutions with EIE doping. Therefore, a series of investigations of the effects of EIEs on the determination of antimony, arsenic, germanium, lead, and tin by hydride generation coupled with direct current plasma atomic emission spectrometry also form part of this research work.

Chapter 2. Experimental Section

Instrumentation

The equipment used included a Beckman Spectraspan V d.c. plasma atomic emission spectrometer with a modified sample tube (99), a Dataspan data storage system, a Sargent-Welch XKR chart recorder and a modified Beckman hydride generator as shown in Figure 5. In the determination of arsenic with a gas-interrupted batch system, two columns, M and N in Figure 5, were packed with a calcium sulphate column (M) and Porapak Q (N). The Porapak Q column originally served as a delay column in the gas-interrupted system to prevent the escape of hydrides from the reaction vessel prior to recording signals and possibly to separate large amounts of hydrogen. In the determination of tin by a gas flow system, this column was replaced by a calcium chloride drying column since the presence of Porapak Q did not improve the tin signal and since it was expensive and needed to be replaced frequently because of wetting. Therefore, two drying columns in series, packed with calcium sulphate (M) and calcium chloride (N), respectively, were used in tin determinations. Only one drying column, packed with calcium sulphate was applied in the determination of germanium. By using calcium sulphate (indicating Drierite) as the drying material, lead signals were severely reduced due possibly to the interference of cobalt, used as an indicator in the drying agent. To overcome this problem, a U-shape water trap, shown in Figure 6, was used instead of any drying column, in the determination of lead. The water trap was also used in antimony

determinations, and was later found also applicable to tin and germanium determinations.

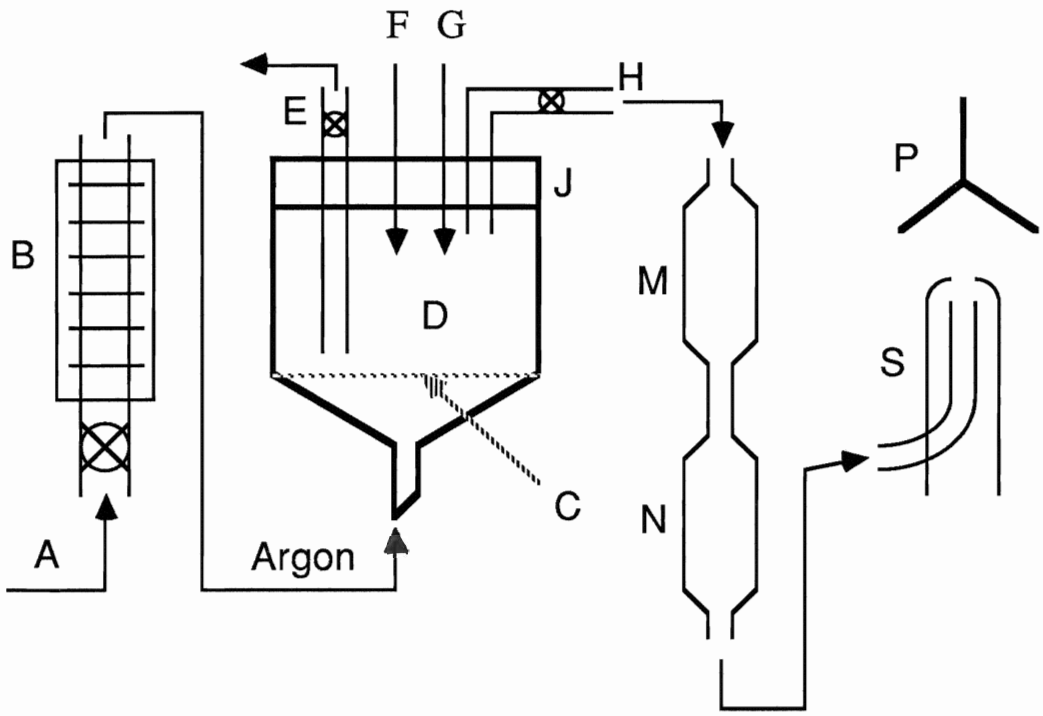

Figure 5. Schematic presentation of hydride generation system

A - Argon supply, B - Flowmeter, C - Sintered glass,

D - Buchner funnel (reaction vessel), E - to waste line,

F - Sample injection port, H - Hydride carried by argon,

G - $NaBH_4$ solution (reducing agent) injection port,

J - Rubber stopper, M and N - Drying columns,

S - DCP sample introduction tube, P - DCP jet

A Brinckman variable-volume Macro-Transferpettor was used for all analyte injections with the volume fixed at 5.0 or 9.0 ml. A disposable syringe was used for the injection of 1.0-2.0 ml of sodium tetrahydroborate(III) solution. A variable-volume Eppendorf pipette fitted with disposable polypropylene tips was used to introduce the interfering solutions for the interference studies.

An entrance slit of 50 μm (horizontal) and 300 μm (vertical) and an exit slit of 100 μm (horizontal) and 300 μm (vertical) were used for all five elements as recommended in the instrument instruction manual (428). Wavelengths chosen were: arsenic at 193.696 nm, tin at 283.999 nm, germanium at 303.906 nm, lead at 283.306 nm, and antimony at 259.805 nm. Photomultiplier voltage and amplifier gain settings were used appropriately to provide convenient signals and to minimize noise.

Other instruments used include a pH Meter (Model 810, Fisher Scientific) and a DMS-100 UV-Visible Spectrophotometer (Varian).

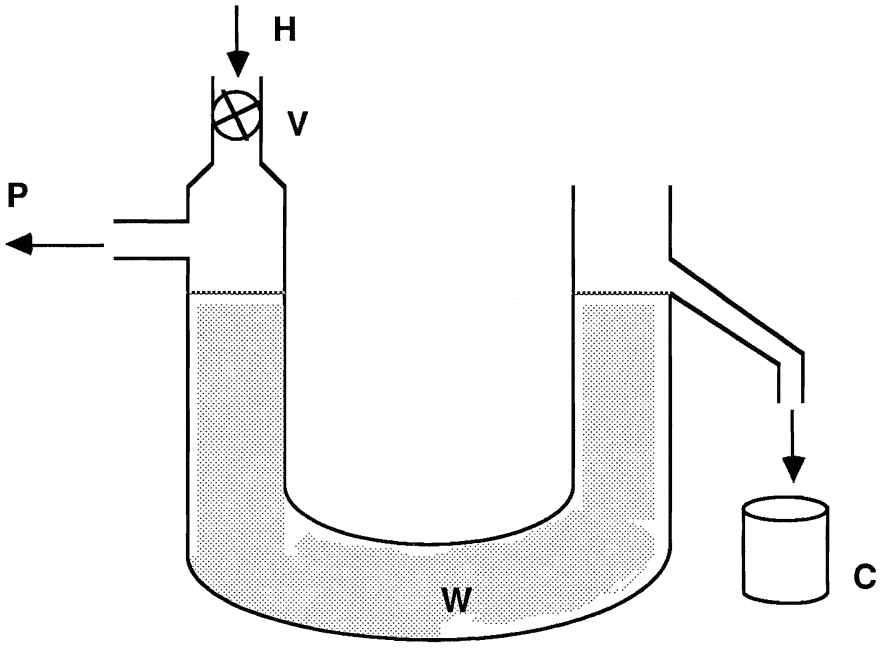

Figure 6. Schematic representation of the U-shape water trap

H - From the hydride generator, (mixture of hydride, argon, hydrogen, and water)

V - Stopcock valve

P - To the DC plasma

W - Distilled water

C - Container for collecting water

Reagents

1. Stock solutions and standard solutions

Arsenic(V) solution (1000 μg ml^{-1}) and arsenic(III) solution (1000 μg ml^{-1}) were prepared from $Na_2HAsO_4 \cdot 7H_2O$ (BDH, AnalaR, 98.5%) and As_2O_3 (Thorn Smith, 100.00%) respectively. Since the As(V) solution was

prepared from a non-standard reagent, the concentration was verified by comparison with the As(III) solution, prepared from standard arsenic(III) oxide, in the d.c. plasma spectrometer. Solutions for the determinations were subsequently prepared by dilution with 5 M hydrochloric acid solution with or without 3% L-cystine.

Germanium stock solution (1000 μg ml^{-1}) was prepared by dissolving the appropriate amount of ammonium germanium(V) oxalate hydrate (Aldrich Chemical Co. Inc., 99.998%, containing 14.5% of germanium) in deionized water and making up to 500.0 ml. The standard solutions of germanium were obtained by serial dilution from this stock solution with 0.04 M HNO_3 or 0.015 M HNO_3 and 0.4 % L-cysteine solution.

Tin stock solution (1000 μg ml^{-1}) was prepared by dissolving 1 g tin shot weighed accurately (J. T. Baker, "Baker Analyzed" Reagent, 100.0%) in concentrated HCl acid (100 ml). The solution was diluted with deionized water to 1000.0 ml. Standard solutions of tin were made by serial dilution from this stock solution with 0.05 M HNO_3 unless stated.

Lead stock solution (1000 μg ml^{-1}) was prepared by dissolving an appropriate amount of accurately weighed $Pb(NO_3)_2$ (AESAR, 99.999%) in 2.0 N HNO_3 and diluted to 1000.0 ml with deionized water. Standard lead solution was made in 0.30% (m/V) potassium dichromate and 0.060 M malic acid.

Antimony stock solution (1000 μg ml^{-1}) was prepared by dissolving 0.6 g of Sb_2O_3 (J. T. Baker Chemical Co., 99.7%), weighed accurately, in 2.0 N HCl and diluting with deionized water to 500.0 ml. Standard solutions of antimony were prepared by serial dilutions of this stock solution with 0.050 M HNO_3.

2. Sodium tetrahydroborate(III) solution

In the determination of tin, the tin blank from sodium tetrahydroborate(III) ($NaBH_4$) was a problem. $NaBH_4$ from Anachemia was used as the reducing agent since it had a very low tin blank. However, later lots were found to have higher concentrations of tin. Thus there is an obvious need to check on each batch of reagent before it is used. In order to decrease the tin blank in the $NaBH_4$ reagent, a 4% (m/V) $NaBH_4$ aqueous solution was treated by sparging. An appropriate amount of $NaBH_4$ was dissolved in deionized water. This solution was sparged with argon for 30 minutes. To minimize decomposition, sufficient solid sodium hydroxide was then added to the solution to make it 0.1 M with respect to NaOH. This solution was filtered prior to use. Solutions of $NaBH_4$ were prepared fresh every three days and kept in polyethylene bottles prior to use. In the determination of arsenic, germanium, lead and antimony, $NaBH_4$ from BDH and from AESAR was also used and was prepared similarly to the above without sparging by argon.

3. Other Reagents

Argon of welding grade (Union Carbide, Canada) proved to be sufficiently pure for use without further treatment. L-cystine and L-cysteine (free base) were obtained from Sigma Chemical Co. (Sigma grade). The blanks, from L-cystine and L-cysteine, of all five hydride forming elements in this study were very low. BDH AnalaR nitric acid was found to have high tin blank and so E. Merck Suprapur nitric acid was used, which was found to have a low tin blank. In the determination of other elements,

BDH AnalaR nitric acid was also used. All other chemicals were analytical reagent grade or better. All reagent blanks were subtracted from the signal of the analyte.

Sample Dissolution

Copper "Benchmark": A sample of the SRM (1.0-1.5 g) was weighed accurately and transferred to a beaker. A solution of 1:1 V/V nitric acid (20 ml) was added and the solution was allowed to stand or was gently heated until all of the sample had dissolved. The solution was transferred to a 100 ml volumetric flask and made up to the mark with deionized water. For the determination of germanium, a 2.0 ml aliquot was taken and diluted to approximately 85 ml with a solution of 0.4 % m/V L-cysteine. The pH was adjusted to 2.3-2.5 with a 1:1 V/V solution of ammonia before the solution was transferred to a 100 ml volumetric flask and made up to the mark with 0.4% m/V L-cysteine. For the determination of tin, a 10-ml aliquot of the sample solution was transferred into a 100-ml volumetric flask and diluted to the mark with 0.04 M HNO_3. The final concentration of nitric acid in the analyte solution was approximately 0.05 M.

Open Hearth Iron 55E: A sample of the SRM (1-1.5 g) was weighed accurately and transferred to a beaker. A solution of 1:1 aqua regia V/V (20 ml) was added and the mixture was allowed to stand, with gentle warming, for one hour. The solution was then transferred to a 500 ml volumetric flask. After the solution was made up to the mark with deionized water, a 5.0 ml aliquot was taken and diluted to 100 ml

with a 0.4 % (m/V) solution of L-cysteine for germanium determinations. Adjustment of the pH to 2.3-2.5 was made with 0.5 M nitric acid prior to the solution being made up to the mark in the volumetric flask. For the determination of tin, a 10-ml aliquot of the sample solution was taken and diluted to 100 ml with 0.04 M HNO_3. A 10-ml aliquot of the sample solution was diluted to 100 ml with a solution of 3% L-cystine in 5 M hydrochloric acid for the determination of arsenic.

Low Alloy Steel 363: Approximately 0.2-0.5 g of the sample was weighed accurately. The sample was dissolved in 20 ml or 1:1 nitric acid-water solution and then transferred to a 500-ml volumetric flask. The solution was diluted to the mark with deionized water. For tin determinations, a 10-ml aliquot of this solution was diluted to 100 ml with 0.04 M HNO_3. For the determination of arsenic, a 10-ml aliquot was diluted to 100 ml with a solution of 3% L-cystine and 5 M hydrochloric acid.

Duplicate samples of the two SRMs were spiked with germanium to determine recoveries. Thus, 0.5 μg germanium was added to one gram of Copper I and 20 μg germanium was added to one gram of the Open Hearth Iron 55E.

Procedure

Arsenic:

The arsenic solution (5.0 ml, 50 ng ml^{-1}) was added to the reaction vessel. Interferent solution (1.0 ml) was added in the case of interference studies. Sodium tetrahydroborate(III) solution (1.0 ml) was added and the reaction was allowed to proceed for 30 seconds before argon was passed through the solution to strip the arsine from the vessel and pass it to the plasma. After the determination was complete, the reduced solution was drained from the reaction vessel. The signals were measured as peak heights.

Tin:

Argon was allowed to flow continuously through the reaction vessel during the entire working time. Solid L-cystine (0.4 g) was added to the reaction vessel. The analyte solution (5.0 ml) (plus 1.0 ml of interferent solutio, in the case of interference studies), was added, followed by 1.0 ml of 4% sodium tetrahydroborate(III) solution. Since argon was kept flowing through the vessel while the analyte solution and the reductant were added, argon stripped the stannane from the reaction vessel and immediately passed it to the plasma. The signals were measured as peak heights. After the determination was complete, the reduced solution was drained from the reaction vessel to waste. The reaction vessel was washed three times with deionized water before the next determination was performed. The peristaltic pump was used to pump distilled water into the nebulizer and thence around the outer tube of the DCP torch

head. Although this did not affect the sensitivity, better stability and baseline were achieved when water was nebulized.

Germanium:

A gas flowing batch system was used for hydride generation similar to that used for the tin determinations. The analyte solutions (5.0 or 9.0 ml) made in 0.015 M HNO_3 and 0.4% L-cysteine were added, followed by sodium tetrahydroborate(III) solution.

Lead:

A gas flow system was also used in the determination of lead. Three reaction media, $(NH_4)_2S_2O_8$ - HNO_3, H_2O_2 - HCl, and $K_2Cr_2O_7$ - malic acid, were studied and the details appear in the discussion section.

Antimony:

A gas flowing batch system was also used for antimony determination. 0.050M nitric acid was used for the preparation of the antimony solutions. It appeared that even a very little $NaBH_4$, remaining in the reaction vessel left from a previous determination, can reduce antimony to its hydride. In order to avoid the uncertainty caused by the adsorbed $NaBH_4$ on the reaction vessel, a reversed order for injection of sample and sodium tetrahydroborate(III) solutions was used, i.e., injection of sodium tetrahydroborate(III) prior to the sample solution to ensure that an excess of $NaBH_4$ was available. The antimony signal was observed immediately after the antimony solution was injected.

Application of signal enhancement by EIEs:

In the study of signal enhancement by EIEs, a gas flow system was employed in the determination of all the five elements. The basic parameters of hydride generation procedures for As, Sb, Ge, Sn, and Pb

are summarized in Table 3. The method of introduction of hydrides and EIEs is illustrated in Figure 7. A modified sample tube (B), discussed elsewhere (97), was used to introduce hydride, carried by argon from the hydride generator, to the d.c. plasma. The inner tube of the modified sample tube was designed for introduction of gaseous hydrides (A), while the outer tube was designed for the introduction of analyte solution by conventional nebulization. In this work, the latter was used for the introduction of distilled water and EIE solutions. The SpectraSpan peristaltic pump (E) was used to pump distilled water into the nebulizer (D and C) and thence around the outer tube of the sample tube. Therefore, a simultaneous but separate introduction of gaseous hydrides and EIE solutions was achieved. Distilled water and EIE solutions were pumped at a rate of 1.9 ml min^{-1}.

Table 3. Experimental parameters for hydride generation

Element	Wavelength (nm)	Carrier Gas Flow Rate ($L\ min.^{-1}$)	Amount of Analyte (1)	Analyte Medium	Amount of $NaBH_4$
As (2)	193.696	0.97	5 ml 20.0 ppb	0.1 M $HN0_3$ or 0.1 M $HN0_3$ & 1% L-cysteine	1.5 ml 6%
Sb	259.805	0.97	5 ml 20.0 ppb	0.05M $HN0_3$	1.0 ml 6%
Ge	303.906	0.74	9 ml 2.0 ppb	0.015M HNO_3 & 0.4% L-Cysteine	1.5 ml 6%
Sn (3)	283.999	1.21	5 ml 2.0 ppb	0.05M HNO_3 + 0.4g solid L-Cystine	1.5 ml 6%
Pb	283.306	0.93	5 ml 20.0 ppb	0.3% $K_2Cr_20_7$ & 0.06 M malic acid	1.5 ml 10%

(1). Analyte concentration may vary.

(2). Analyte medium and $NaBH_4$ for "Determination of Arsenic" in section I were 5M HCl & 3% L-cystine and 1.0 ml of 4%, respectively.

(3). Amount of $NaBH_4$ for "Determination of Tin" in section II was 1.0 ml of 4% (m/V).

A -- Introduction of Hydrides
B -- Modified Sample Tube
C -- Nebulizer Chamber
D -- Pneumatic Nebulizer
E -- Peristaltic Pump
S -- Introduction of Distilled Water or EIEs
W -- To Waste

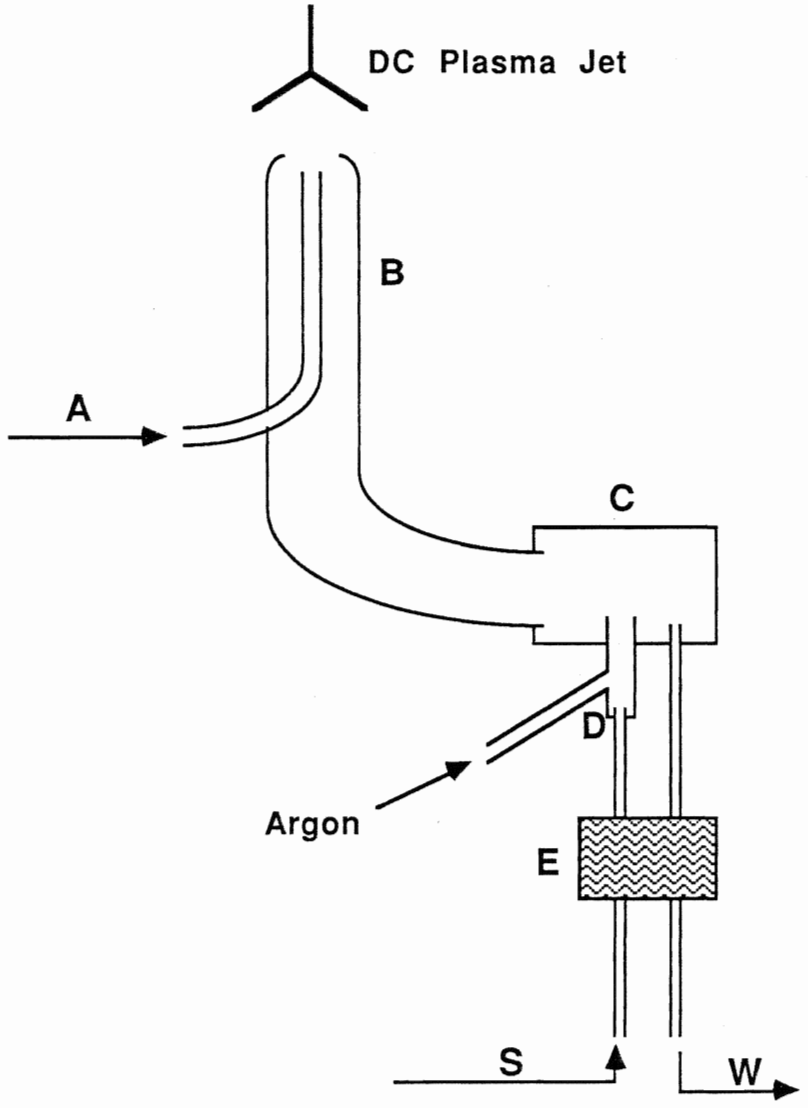

Figure 7. Schematic representation of the introduction of hydrides and EIEs to the d.c. plasma

Chapter 3. Results and Discussion

I. Determination of Arsenic

Acid concentration

Hydrochloric acid at high concentration reduces interference for some elements. Thus, 5 M hydrochloric acid has a negligible effect on the arsenic signal but improves the recovery of arsenic in the presence of iron and copper compared with similar determinations in 1.4 M HCl. These results are in good agreement with the results of Aggett and Aspell (329) and Hershey and Keliher (306). In addition, interference from cadmium was reduced (429). Although high levels of hydrochloric acid in the solution may produce instability in ICP systems, no such problems were encountered in this work.

Effect of L-Cystine

The effectiveness of a solution of 3% L-cystine in 5M HCl on the reduction of interferences is clearly demonstrated in Figures 8-10. 5.0 ml of 50.0 ng ml^{-1} As(III) in 5 M HCl and 5 M HCl-3% L-cystine solution and 1.0 ml of interfering solution were used to perform these experiments. In the absence of L-cystine, 1000 μg ml^{-1} of Co(II), 100 μg ml^{-1} of Ni(II), or 10 μg ml^{-1} of Pt(IV) suppress arsenic(III) signal over 10%. However, with 3% L-cystine, these interferences were eliminated. Recovery of arsenic in the presence of transition elements is summarized in Table 4.

As we can see, interferences from cobalt(II), copper(II), iron(II), nickel(II), and zinc(II) at concentrations of up to 10,000 μg ml^{-1} are effectively eliminated. Thus, a 10-100 fold excess of transition metals can be tolerated, in the presence of 3% L-cystine, compared with solutions containing no L-cystine. Particularly noteworthy is the almost complete elimination of interference from nickel(II).

Very poor recoveries of the arsenic signal were obtained in the cases of gold(III) and palladium(II). Thus, in the absence of L-cystine, a poor (16%) recovery of the arsenic signal was achieved in the presence of only 1 μg ml^{-1} of palladium(II). Although interference was reduced by L-cystine, and a recovery of 76% was achieved at this level, the recovery was only 21% at 10μg ml^{-1} Pd(II).

For comparison, the recoveries of As(V) in the presence of transition metals were also listed in Table 4. Results for arsenic(V) closely followed those for arsenic(III) for the selected examples.

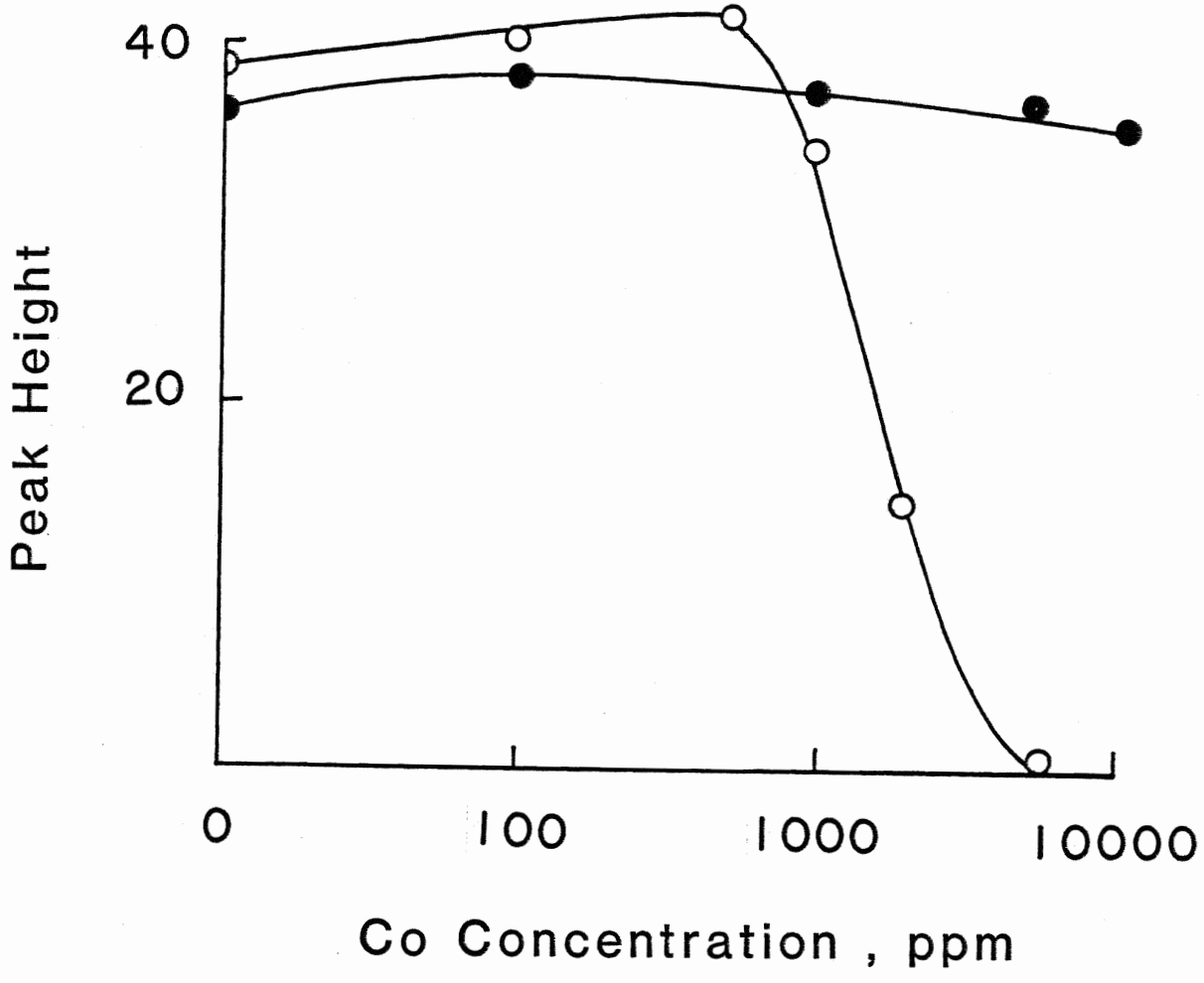

Figure 8. Co(II) interference reduction by L-cystine in the determination of 5.0 ml 50.0 ng ml^{-1} As(III)

○ - in 5 M HCl

● - in 5 M HCl and 3% L-cystine

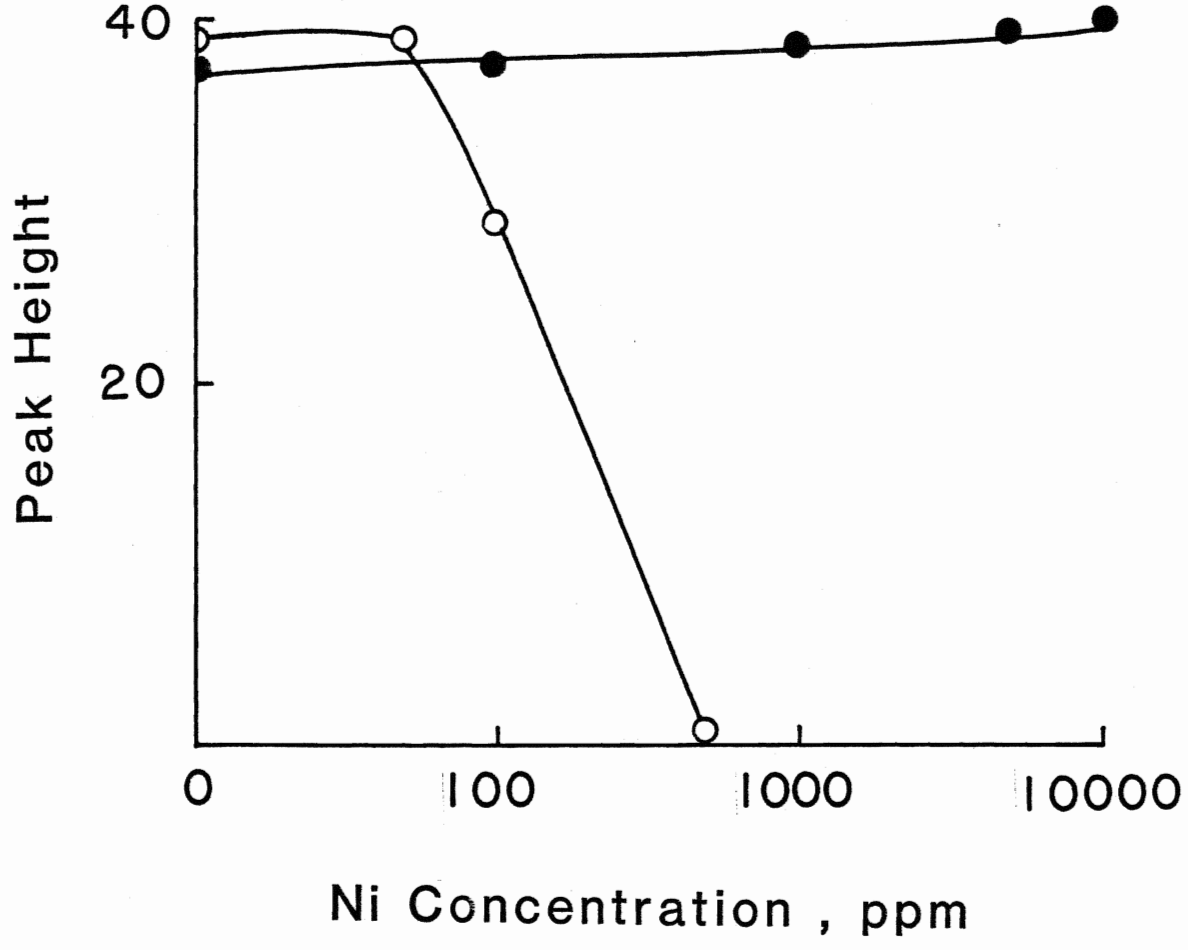

Figure 9. **Ni(II) interference reduction by L-cystine in the determination of 5.0 ml 50.0 ng ml^{-1} As(III)**

○ - in 5 M HCl

● - in 5 M HCl and 3% L-cystine

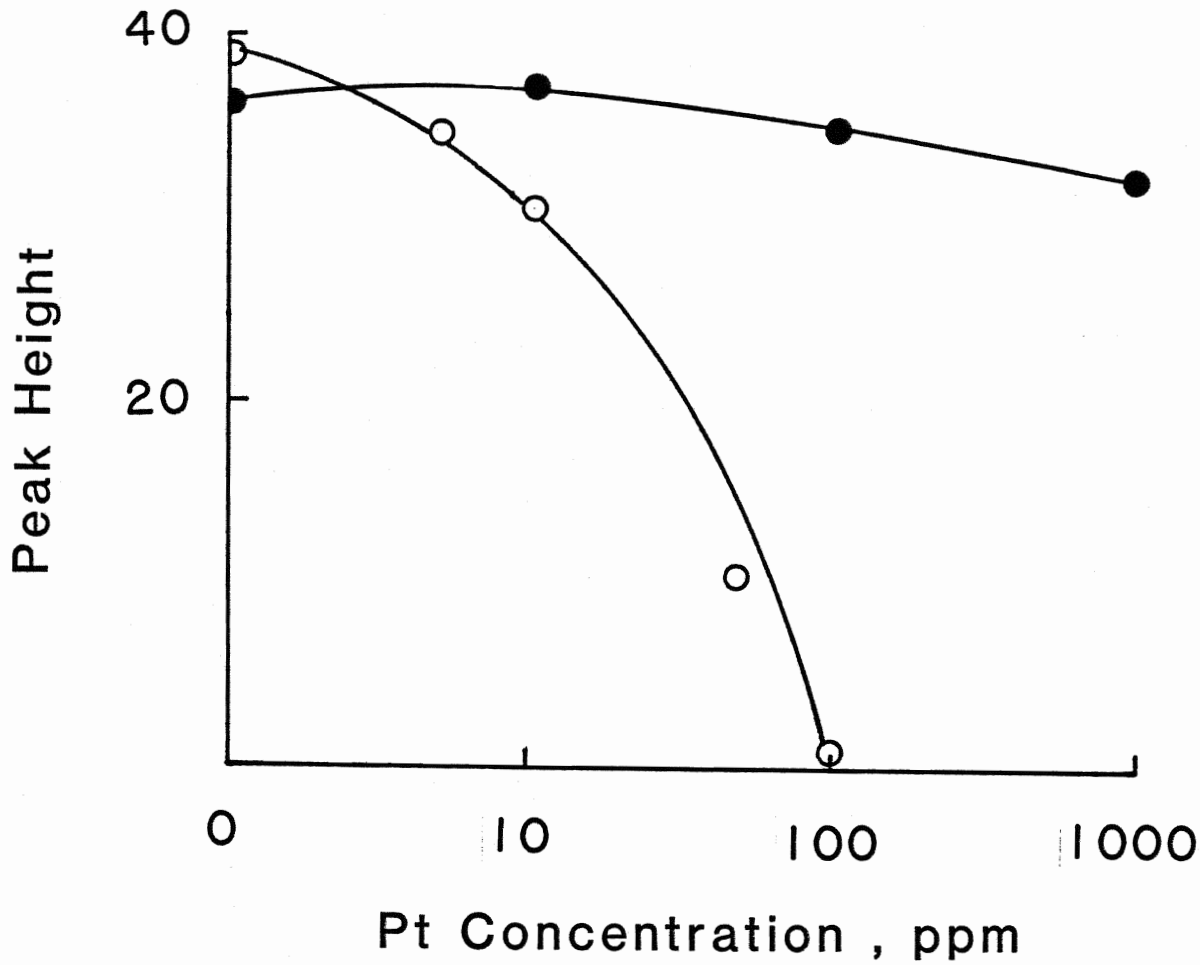

Figure 10. Pt(IV) interference reduction by L-cystine in the determination of 5.0 ml 50.0 ng ml^{-1} As(III)

○ - in 5 M HCl

● - in 5 M HCl and 3% L-cystine

Table 4. Recovery of 50.0 ng ml^{-1} of As(III) and As(V) from Solutions of Transition Metals

Metal Ions	Amount Added 1.0 ml ($\mu g\ ml^{-1}$)	Recovery of As(III) (%) without L-cystine	Recovery of As(III) (%) with 3% L-cystine	Recovery of As(V) (%) * without L-cystine	Recovery of As(V) (%) * with 3% L-cystine
Fe(II)	1000	95	100	108±4 (3)	97±4 (4)
	10000	100	98	106±4 (3)	96±6 (3)
Fe(III)	1000	-	-	108±1 (3)	103±2 (5)
	10000	-	-	61±8 (8)	105±6 (5)
Co(II)	1000	80	100	81±1 (3)	100±1 (3)
	10000	n.d.	86	n.d.	91±1 (3)
Ni(II)	100	75	100	-	-
	1000	n.d.	105	2.8±0.8 (3)	99±2 (3)
	10000	n.d.	112	n.d.	95±1 (3)
Cu(II)	1000	87	100	100±6 (3)	102±3 (3)
	10000	80	87	82±5 (3)	91±3 (3)
Zn(II)	1000	100	99	107±4 (3)	101±3 (3)
	10000	98	96	108±1 (3)	93±2 (3)
Pd(II)	1	16	76	13±1 (3)	82±4 (3)
	10	n.d.	21	n.d.	20±1 (3)
	100	n.d.	n.d.	n.d.	n.d.
Ag(I)	10	100	100	98±5 (3)	103±6 (3)

	100	100	100	91±1 (3)	101±7 (3)
	1000	63	76	92±1 (3)	95±1 (3)
Cd(II)	1000	105	-	92±8 (3)	99±6 (3)
	10000	95	-	80±3 (3)	68±3 (3)
Pt(IV)	10	80	100	87±2 (3)	101±5 (3)
	100	5	92	6±1 (3)	89±1 (3)
	1000	n.d.	89	n.d.	92±2 (3)
Au(III)	10	72	52	74±1 (3)	69±2 (3)
	100	n.d.	n.d.	n.d.	5.9±0.8 (3)
	1000	n.d.	n.d.	n.d.	n.d.
Hg(II)	10	89	110	80	92±2 (3)
	100	79	109	76	89±5 (3)
	1000	55	61	88	100±2 (3)
	10000	-	-	62	64±3 (3)

* See reference 430

† n.d. - not detected

\- - not determined

Determination of Arsenic in Iron and Steel

Determination of arsenic in NBS Standard Reference Material Open Hearth Iron 55E and Low Alloy Steel 363 gave excellent results. Standard additions technique was used to determine if there were any systematic interferences with the method. Final concentrations and standard deviations were determined from the standard addition line by the method outlined in Miller and Miller (431) and adapted for use in the EXCEL database program. In the case of the Open Hearth Iron 55E, two replicate determinations were carried out to verify the methodology; in the case of the Low Alloy Steel 363, a duplicate standard addition was performed. The data for the determinations are summarized in Table 5. The slopes of the calibration lines and standard addition lines gave recoveries between 94 and 107%. This indicates that there are no systematic interferences in these determinations. Under normal circumstances, there would be no need to carry out the standard addition method for this type of analysis.

Table 5

Calibration and Standard Addition for Arsenic Determination

NBS Low Alloy Steel 363 (duplicate)

Correlation Coefficient: 0.996 (calibration (4 points))

Correlation Coefficient: 0.999 (standard addition (6 points))

Calculated Concentration: 101±7 $\mu g\ g^{-1}$

NBS Certified Concentration: 100 $\mu g\ g^{-1}$

NBS Open Hearth Iron 55E (2 replicates)

Correlation Coefficient: 0.999 (calibration (4 points))

Correlation Coefficient (1): 0.999 (standard addition (6 points))

Correlation Coefficient (2): 0.998 (standard addition (6 points))

Calculated Concentration (see reference 431): 72±4 $\mu g\ g^{-1}$ (1), 70±6 $\mu g\ g^{-1}$(2).

Group mean 71±7 $\mu g\ g^{-1}$

NBS Certified Concentration: 70 $\mu g\ g^{-1}$

Preliminary study with gas flowing batch system

Later research showed that the determinations of tin (432) and germanium (433) were speeded up by using a gas flowing system. L-Cysteine was also found to be effective in improving germanium signal and in speeding up the reactions. Therefore, a preliminary study on a gas-flowing batch system for the determination of arsenic and the effect of L-cysteine was carried out. Figure 11 shows the effect of nitric acid concentration on arsenic(V) signal. As the nitric acid concentration increases from 0.02 M to 0.20 M, the peak height of arsenic signals increases. Since high acid concentration caused a distortion of the plasma, due to the large amounts of hydrogen produced, a nitric acid concentration of 0.10 M was chosen, which gave adequate arsenic signals without plasma distortion. Further, the addition of L-cysteine was found to speed the reaction and increase peak height of arsenic signal. The addition of L-cysteine and L-cystine was also found to reduce the interference in the gas flowing system as shown in Table 6.

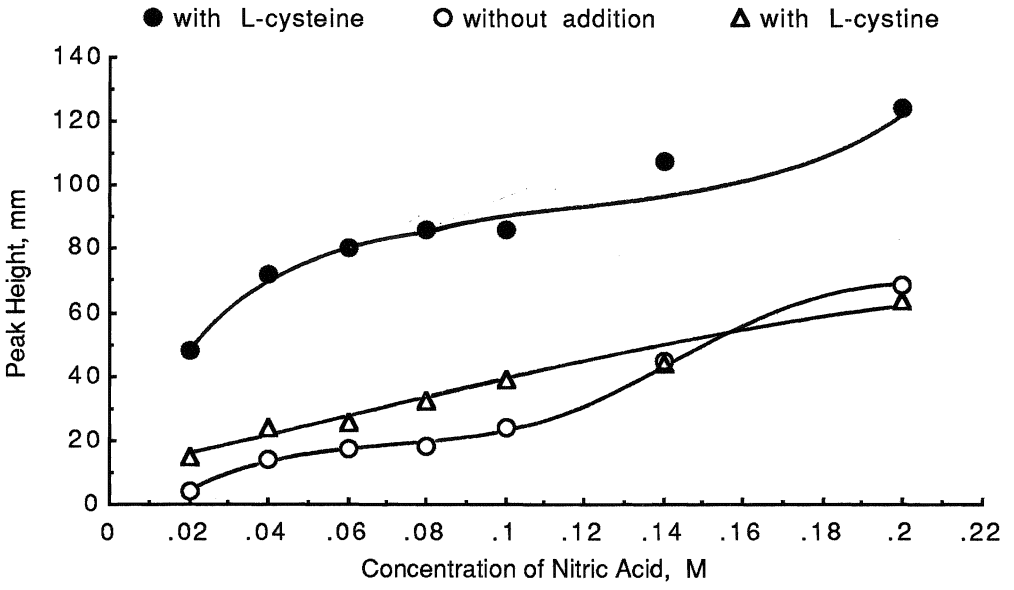

Figure 11. Effect of nitric acid concentration on arsenic signal with gas flowing batch system.

Table 6. Recovery of 5.0 ml 100 ng ml^{-1} As(V) in the presence of Cu(II) and Ni(II)

Metal Ions	Amount Added	Recovery of As(V) (%) Without addition	With 0.3 g solid L-cystine	With 0.3 g solid L-cysteine
Cu(II)	0.1 ml 1000 μg ml^{-1}	39	108	86
Ni(II)	0.1 ml 10 μg ml^{-1}	5	95	90

II. Determination of Tin

Optimization of Instrument Parameters

The detection wavelength is an important factor that influences the sensitivity and detection limit of tin determination. Even at the same wavelength, tin sensitivity is reported to be different using different detection methods (360, 434). Therefore, it was necessary to choose an appropriate wavelength for tin determination by DCP-AES. A 30 $\mu g\ ml^{-1}$ tin solution was nebulized directly into the D.C. plasma by conventional DCP-AES method(428). Wavelength scans of the emission signals at the tin resonance and non-resonance wavelengths: 224.60 nm, 284.00 nm and 286.33 nm, were obtained. Figure 12 shows the tin peak scans obtained with 30 $\mu g\ ml^{-1}$ tin at the given wavelengths with the background signal subtracted. As can be seen, the highest sensitivity of the tin signal was obtained at the wavelength of 284.00 nm, which is approximately nine times higher than that at the 224.60 nm resonance line. Therefore, 284.00 nm was chosen as the tin wavelength. The difference between the sensitivities obtained in this work and the literature reports (360, 434) is probably due to the different detection techniques between DCP-AES and AAS.

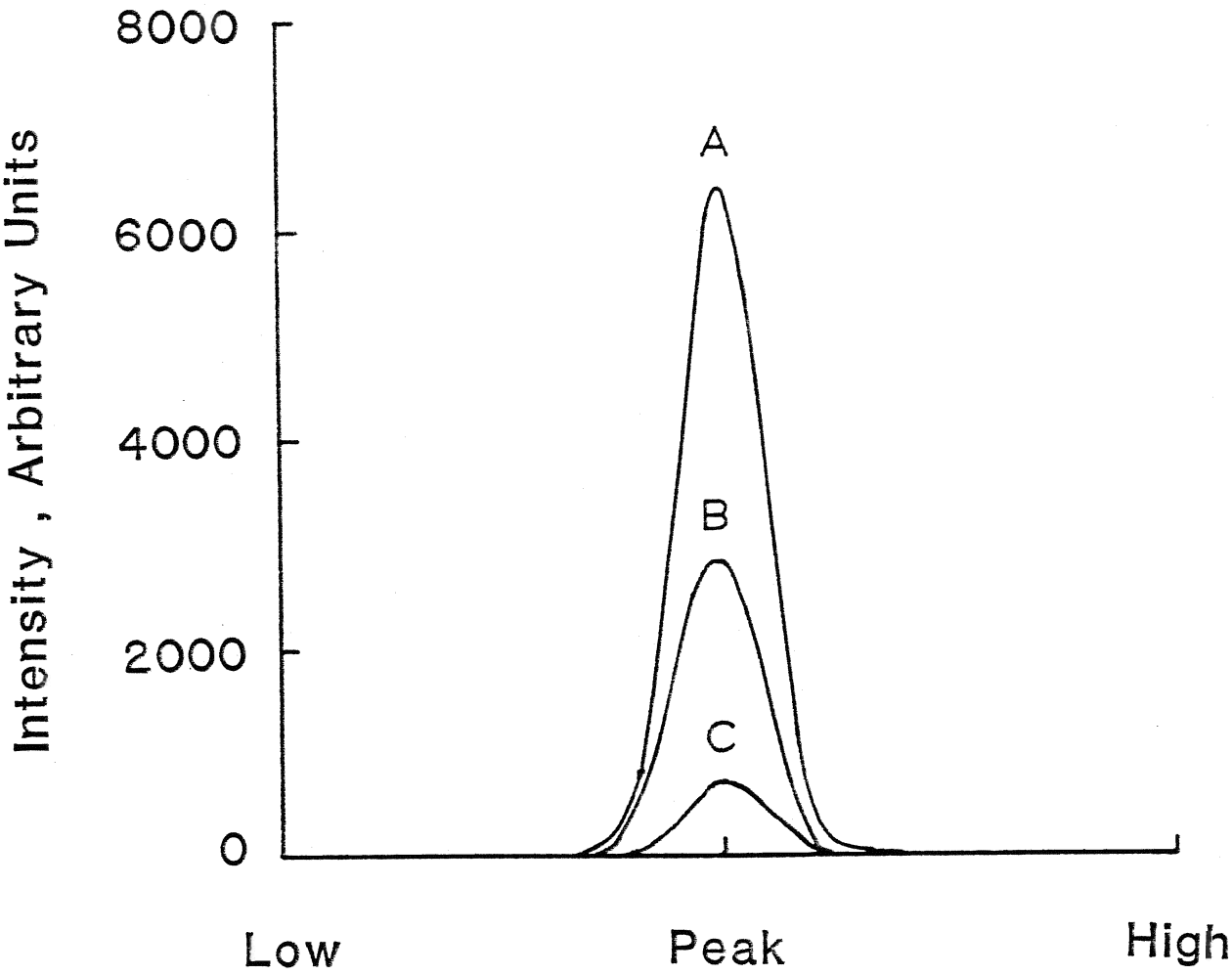

Figure 12. Superimposed scans of the analytical wavelengths recommended for the analysis of tin by d. c. plasma atomic emission spectrometry. A at 284.00 nm, B at 286.33 nm and C at 224.60 nm. Scans were obtained using the Spectraspan Dynamic Background Compensator.

The relative position of plasma and slit (observation height) also affect the tin signal and the background. So the optimium position of plasma jet and slit should be matched in order to give the highest tin sensitivity with low background. Unlike the conventional DCP-AES method in which the relative position of plasma and slit can be optimized by the instrument peaking procedure (428), with the combination of DCP-AES and hydride generation system, the observation height is also affected by the sudden surge of gas as $NaBH_4$ is added to an acidic analyte solution. To find the optimum observation height, a primary requirement is to have an indication or a scale for measuring the observation height. The baseline digital readout was thus chosen as a (non-linear) function of the observation height at a particular PMT voltage and amplifier gain setting. As the observation height is increased the baseline signal increases, since the entrance slit of the spectrometer intercepts more plasma image. At different observation heights, the atomic emission signals of 1 ng ml^{-1} Sn were obtained and are shown in Figure 13. At a PMT setting of 5 and a gain setting of 46, for this instrument, the optimum observation height corresponds to a baseline signal between 250 and 400 in the presence or absence of L-cystine. Therefore, the observation height corresponding to a baseline signal of 300 was chosen for all determinations.

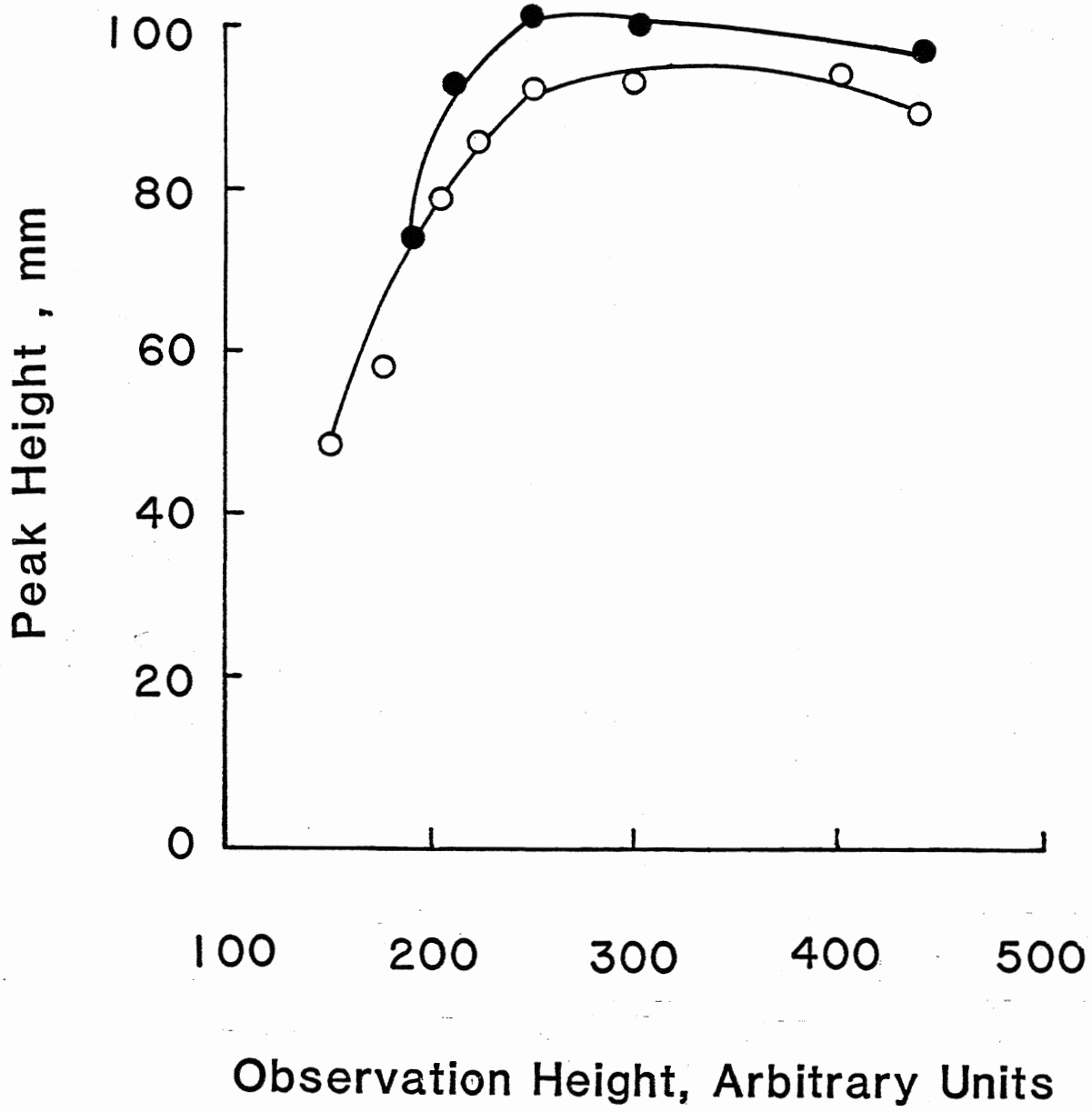

Figure 13. Response as a function of observation height.
● - with L-cystine, ○ - without L-cystine

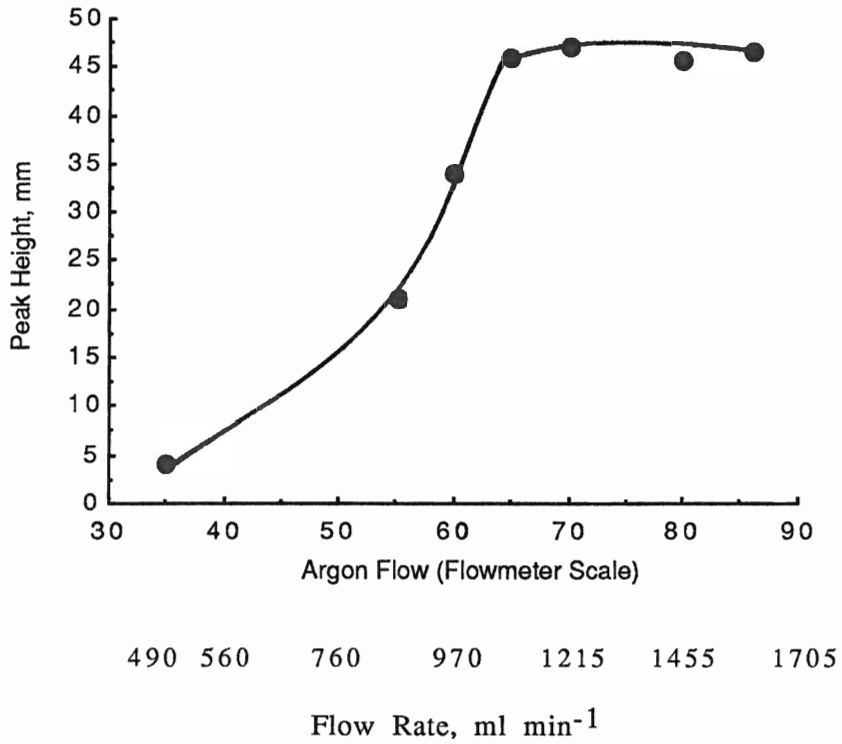

Figure 14. Effect of argon flow rate on tin signal

Argon was used as carrier gas to strip the hydride from the reaction vessel into the plasma. The gas flow rate is also a factor that influences the peak heights of tin signals. Figure 14 shows the effect of gas flow rate on the tin signals. The upper row of numbers on the horizontal axis are the scales shown on the flow meter, and the lower row numbers are the calibrated argon flow rates corresponding to the flow meter scales. As shown in Figure 14, the peak heights of tin signals increased with increasing argon flow rate from 488 to 1045 ml min^{-1}. The optimum argon flow rate was found to be at 1215 ml min^{-1}. Therefore, the argon flow rate to the hydride reaction vessel was adjusted to 1215 ml min^{-1}, which corresponds to the flow meter scale number 70.

Hydride Generation

In order to be sure that the maximum amount of tin in the analyte solution is reduced to stannane, the effect of reaction time on the tin response was investigated. The reaction time here was the period of time between the addition of the sodium tetrahydroborate(III) solution to the analyte in the reaction vessel and the stripping of the hydride by argon. From Figure 15, it is clear that reaction times from 5 to 60 seconds give identical signals for tin. If the reaction time is longer than 60 seconds, the peak heights decrease gradually, due possibly to the diffusion of stannane from the reaction vessel into the tubing or into the

plasma, before the signal is recorded. These results suggest that the reaction between tin species and $NaBH_4$ to form SnH_4 is very fast under the given conditions. Thus, assuming that the reaction was essentially instantaneous, argon was allowed to flow continuously through the reaction vessel while the analyte solution and the reductant were added. Argon stripped the stannane from the reaction vessel and immediately passed it to the plasma. With this modification, the analysis speed is improved dramatically. Thus in one minute a whole determination can be performed, including injection of sample and $NaBH_4$, recording the signal, draining of the reduced sample to waste, and washing. By maintaining the carrier gas flow through the system, the change of plasma position, and the background noise are significantly decreased.

Figure 16 shows the results from the analysis of 2 ng ml^{-1} tin. Figure 16 A shows the signals obtained by the interrupted gas flow system and Figure 16 B shows the signals from the continuous gas flow system. The reproducibility of peak heights, shown in Figure 16 B, is much improved compared to those in Figure 16 A. This improvement in reproducibility is perhaps due to a reduction in the number and timing of the manual operations on the system, such as turning stopcocks, and may also be due to the elimination of the sudden increase in the gas flow.

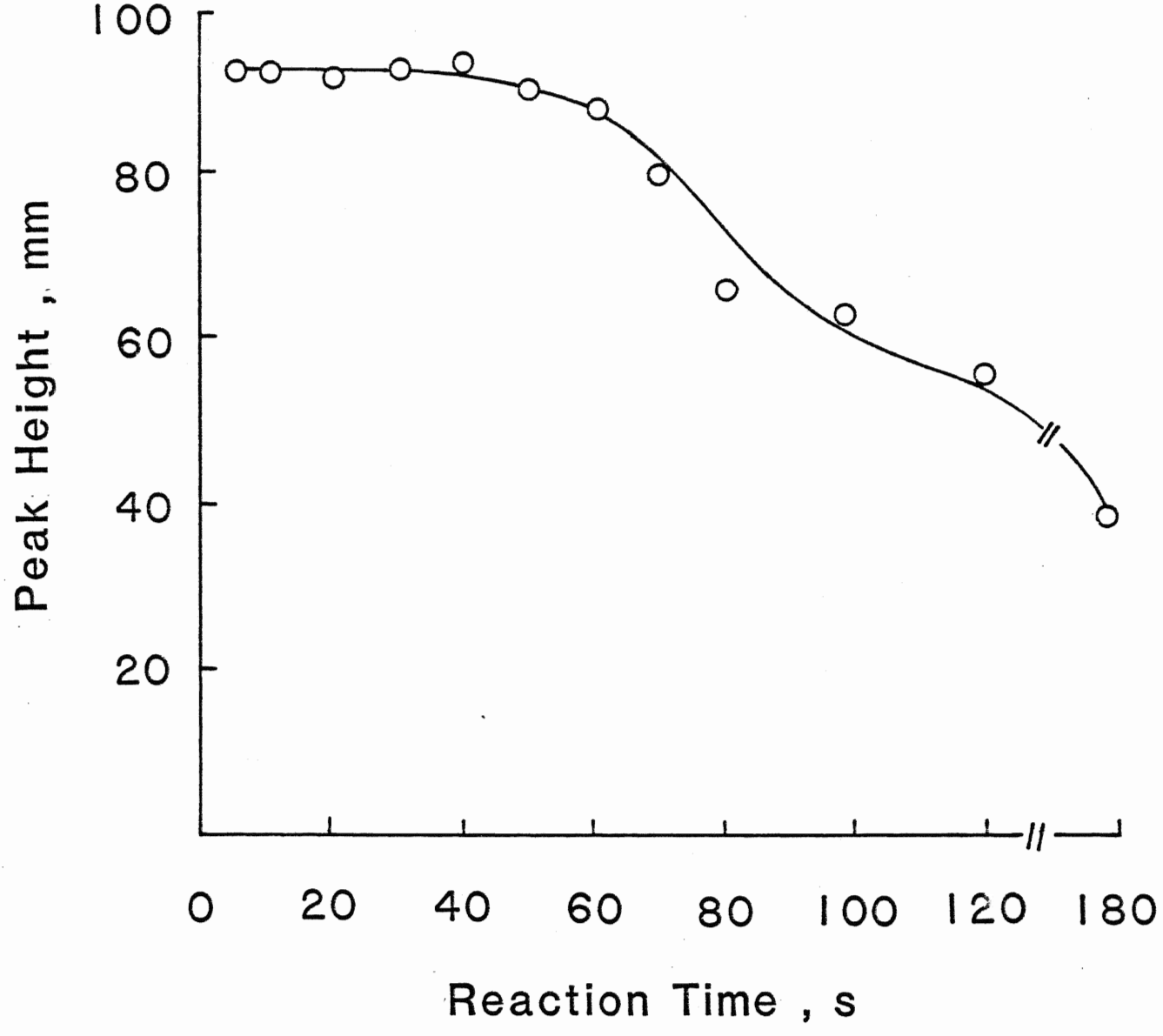

Figure 15. Tin response as a function of reaction time

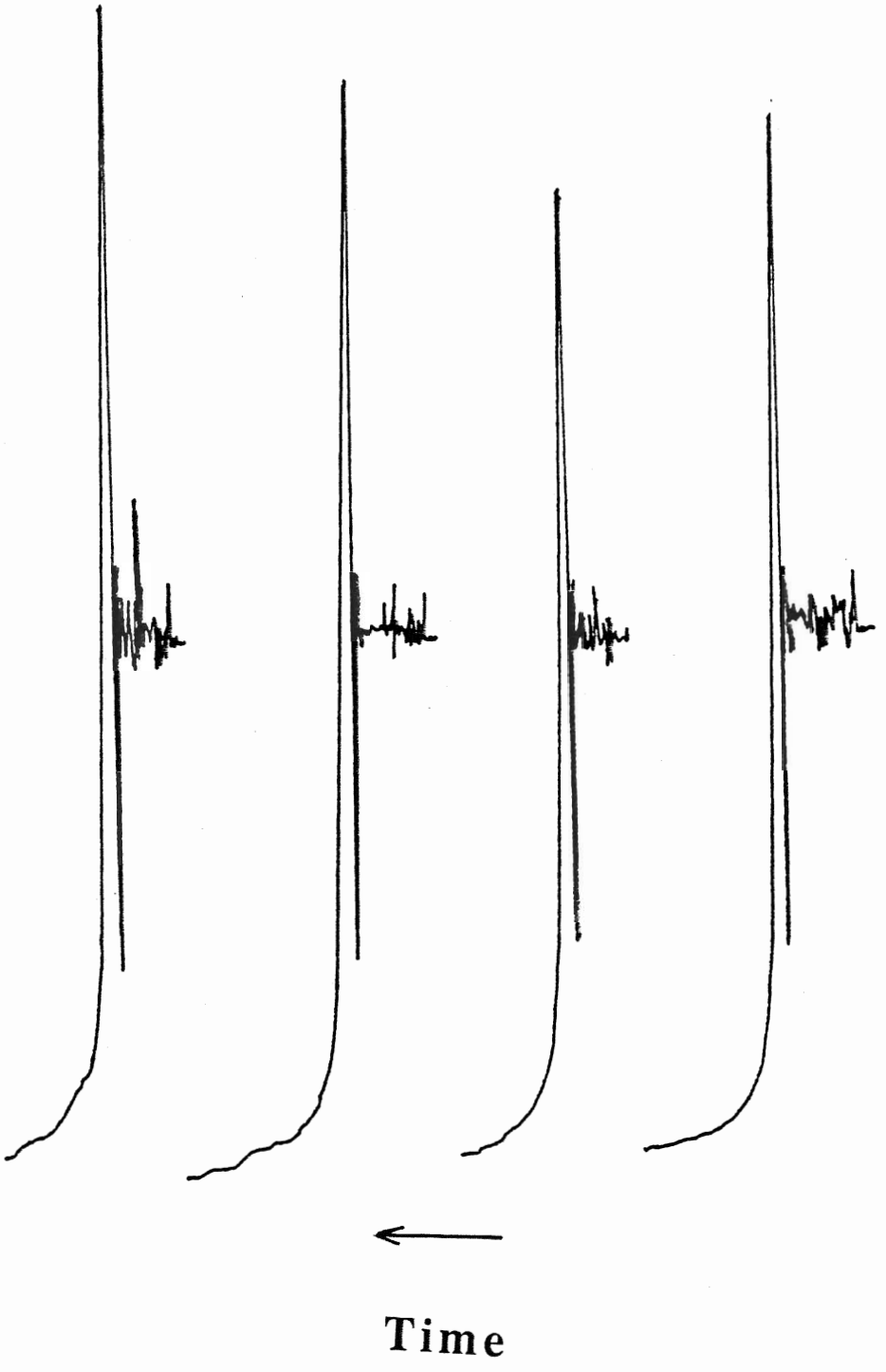

Figure 16A. Tin response after 30 seconds reaction time. Note the high background prior to the analytical determination

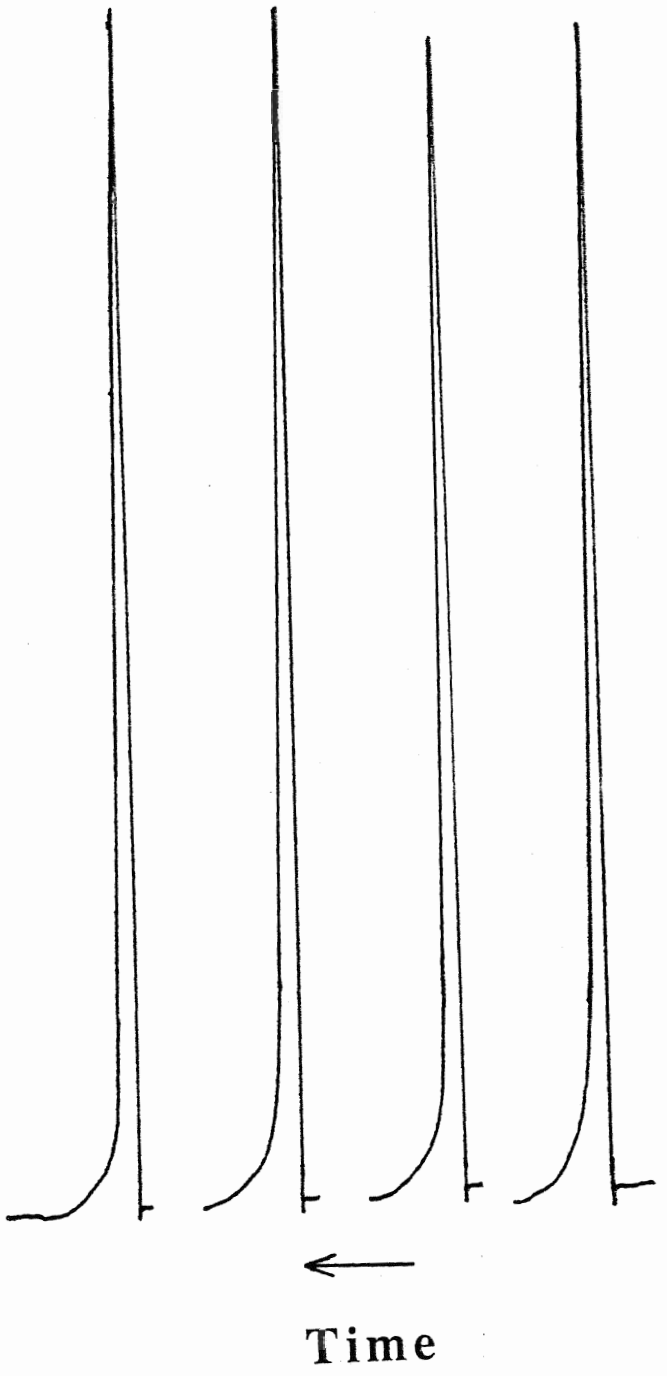

Figure 16B. Response from a solution of 2.0 ng ml^{-1} when argon was allowed to flow through the system continuously. Note improved reproducibility.

In agreement with the literature (274, 336), the acid concentration of the solution is a critical factor which affects stannane formation. Nitric acid and hydrochloric acid were chosen as the media for tin solutions to investigate their effects on the tin hydride generation. As can be seen from Figures 17 and 18, the best tin signals are obtained with either 0.05 M HCl or 0.05 M HNO_3 solutions. The acid concentration is clearly quite critical in the generation of the maximum quantity of SnH_4. However, the addition of 0.4 g L-cystine to the system extends the acceptable range of nitric acid concentration to between 0.04 and 0.06 M. Since HNO_3 gives a relatively wider concentration range for stannane formation, has a lower tin blank, and is often used for sample dissolution, 0.05 M HNO_3 was chosen as the medium for the tin standards and for sample solutions.

In order to know the acidity of reaction solution, the pH values of the reaction solution were determined and shown in Table 7. A 5.0-ml aliquot of 0.50 ng ml^{-1} tin in different concentrations of HNO_3 or HCl was taken and placed in a beaker. Then 1 ml of 4% $NaBH_4$ in 0.1 M NaOH solution was added and the pH value of this reaction solution was measured by using a pH meter. For comparison, the pH determinations of solutions both with and without addition of 0.4 g L-cystine prior to the addition of $NaBH_4$ were performed. As shown in Table 1, under the optimum conditions, the reaction solution, after the hydride reduction is complete, is still slightly basic. This is slightly different from the result reported by Thompson and Pahlavanpour (336), who indicated that a neutral solution was obtained.

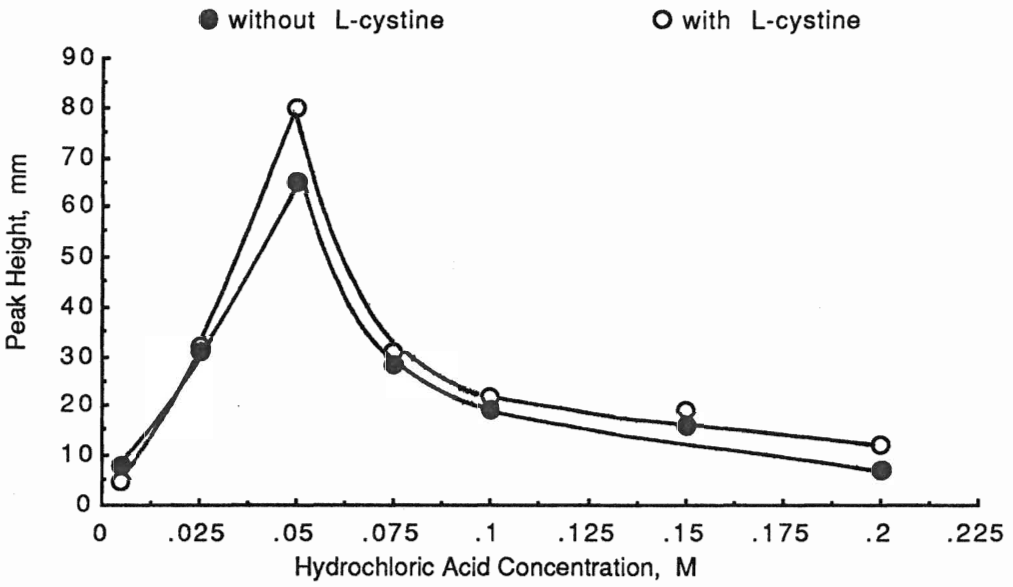

Figure 17. Effect of hydrochloric acid concentration on tin signal.

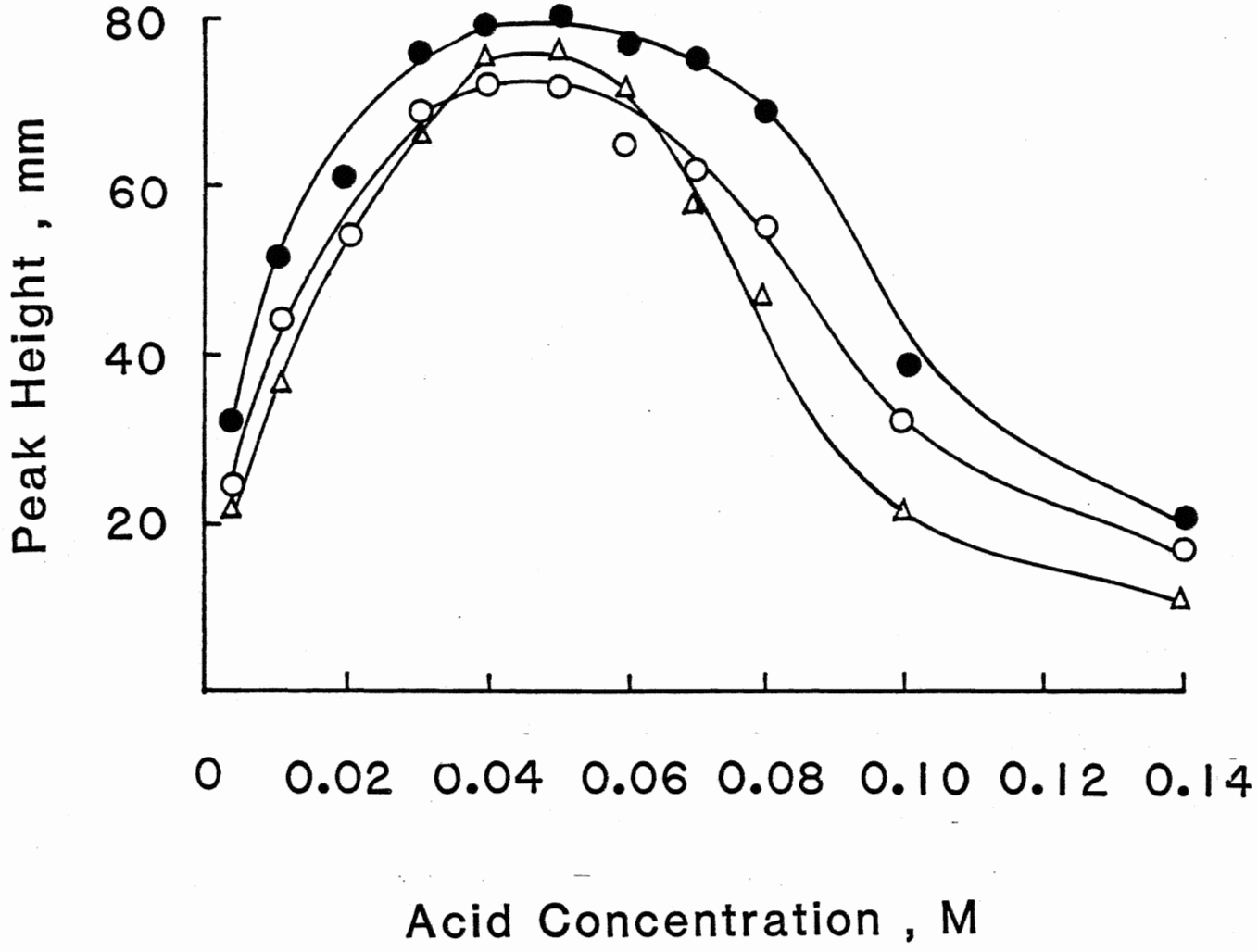

Figure 18. Effect of acid type and concentration on tin response

Δ - 0.40 ng ml^{-1} Sn in HCl, ○ - 0.40 ng ml^{-1} Sn in HNO_3, ● - 0.40 ng ml^{-1} Sn in HNO_3 with 0.4 g L-cystine added.

Table 7. The pH values of reaction solution after hydride reduction is complete.

HCl or HNO_3 Conc. (M)	pH Values of Reaction Solution			
	$\underline{HCl\ Medium}$		$\underline{HNO_3\ Medium}$	
	Without L-cystine	With L-cystine	Without L-cystine	With L-cystine
0.010	9.92	9.46	10.20	9.36
0.020	9.75	9.34	9.76	9.28
0.030	9.58	9.28	9.48	9.18
0.040	9.43	9.13	9.28	9.03
0.050	9.31	9.03	9.14	8.99
0.060	9.22	8.93	8.98	8.87
0.070	9.05	8.84	8.89	8.82
0.080	-	-	8.83	8.78
0.10	-	-	8.63	8.60

Interference Study

The work on the determination of arsenic, as discussed in the previous section, showed that a solution of 3% L-cystine in 5 M HCl played an efficient role in reducing interferences from transition metal ions in the determination of arsenic. L-cystine dissolves in 5 M hydrochloric acid but is poorly soluble in distilled water. Clearly a strongly acidic solution would suppress the production of SnH_4, as indicated in Figures 17 and 18. To solve this problem, solid L-cystine was added directly to the reaction vessel for each determination prior to the addition of analyte and $NaBH_4$ solutions. It became clear that L-cystine was an efficient reagent for transition element interference reduction.

Preliminary studies were carried out to choose the appropriate amount of L-cystine to be added to the reaction vessel. As shown in Figure 19, in the case of the tin standard solution, the tin signal increases with the increase of L-cystine added until 0.07 g had been added. At this point, the tin signal is approximately 10% greater than the signal in the absence of L-cystine and remains at this level as increasing amounts of L-cystine are added. In the presence of interfering ions, a greater amount of L-cystine is required. Thus in the presence of 10 $\mu g\ ml^{-1}$ or 100 $\mu g\ ml^{-1}$ Ni(II), the tin response increases until it reaches a maximum when 0.3 g of L-cystine is added. Although satisfactory recovery of tin is achieved at the level of 10 $\mu g\ ml^{-1}$ Ni(II), the recovery is only 60% and stays at this level over the addition of 0.3 g to 0.9 g L-cystine in the presence of 100 $\mu g\ ml^{-1}$

nickel. Therefore, 0.4 g of solid L-cystine was chosen as the amount to add to the reaction vessel for each determination.

The efficiency of L-cystine on transition metal ion interference reduction can be seen in Figures 20 to 23. At the optimized conditions, signals from 5.0 ml aliquots of a 0.40 ng ml^{-1} tin standard were obtained with the addition of 1.0 ml of interfering ions at a series of concentrations. Figures 20 to 23 compare the interference effects of Ni(II), Co(II), Cu(II), and Fe(II) in the determination of tin with and without the addition of L-cystine as an interference reducing agent. In the absence of modifier, 0.10 μg ml^{-1} Ni(II), 0.50 μg ml^{-1} Co(II), 5.0 μg ml^{-1} Cu(II) or 5.0 μg ml^{-1} Fe(II) suppress the tin signal severely. These results are in agreement with reports in the literature (274, 336, 368). However, with the addition of solid L-cystine, solutions of 10 μg ml^{-1} Ni(II), 100 μg ml^{-1} Co(II), 1000 μg ml^{-1} Cu(II) or 10000 μg ml^{-1} Fe(II) do not interfere significantly with the tin signal. Thus, with L-cystine, a 10^3 to 10^7 fold excess of transition metal ions can be tolerated without interference in the determination of tin by stannane generation. Compared with other interference reducing agents, such as thiourea, sodium oxalate and iodide, L-cystine is the most efficient in reducing tin interferences from transition metal ions. Thiourea, for example, can overcome the interference from a 10^3 fold excess of Ni(II) or a 10^4 fold excess of Cu(II) in the determination of 10 ng ml^{-1} Sn (274). In addition, thiourea was found to have high tin blank. Table 8 summarizes the recoveries of 0.40 ng ml^{-1} tin in the presence of other interfering ions with and without the addition of L-cystine.

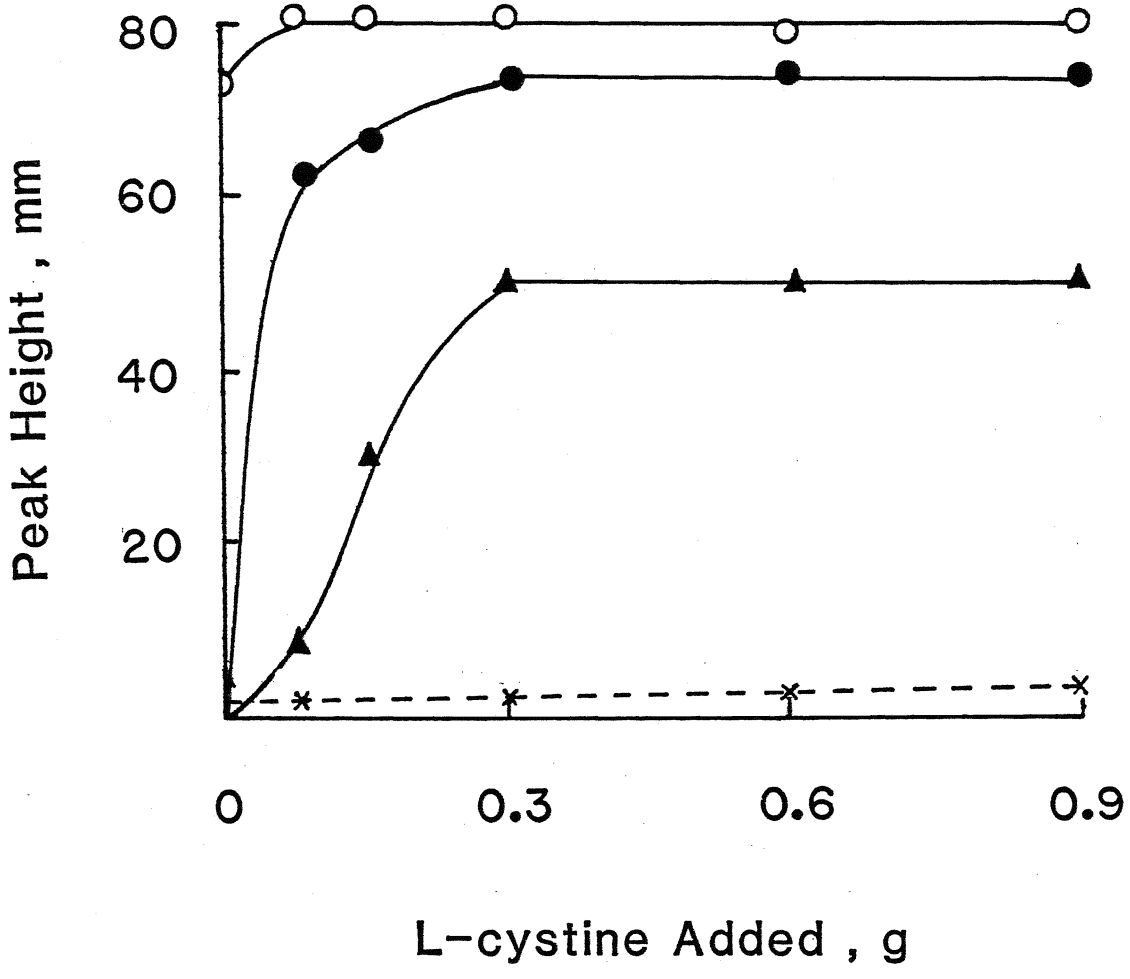

Figure 19. Effect of added L-cystine on tin signal.
○ - 5 ml of 1.0 ng ml^{-1} Sn,
● - 5 ml of 1.0 ng ml^{-1} Sn + 1.0 ml of 10 μg ml^{-1} Ni(II), ▲ - 5 ml of 1.0 ng ml^{-1} Sn + 1.0 ml of 100 μg ml^{-1} Ni(II), X - 5 ml of 0.05 M HNO_3

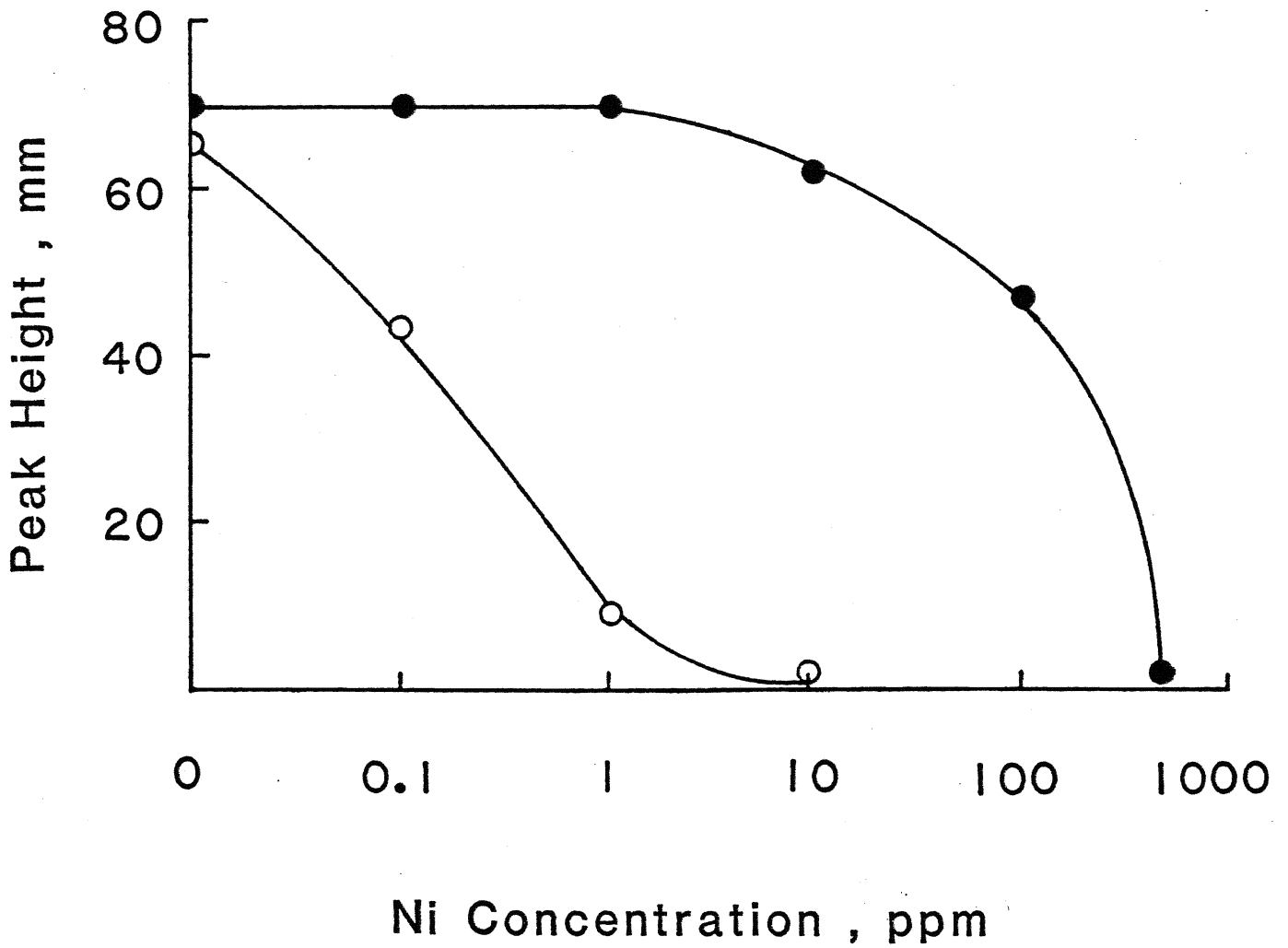

Figure 20. Ni(II) interference reduction by L-cystine in the determination of tin.
○ - 5.0 ml of 0.40 ng ml^{-1} Sn,
● - 5.0 ml of 0.40 ng ml^{-1} Sn + 0.4 g L-cystine.

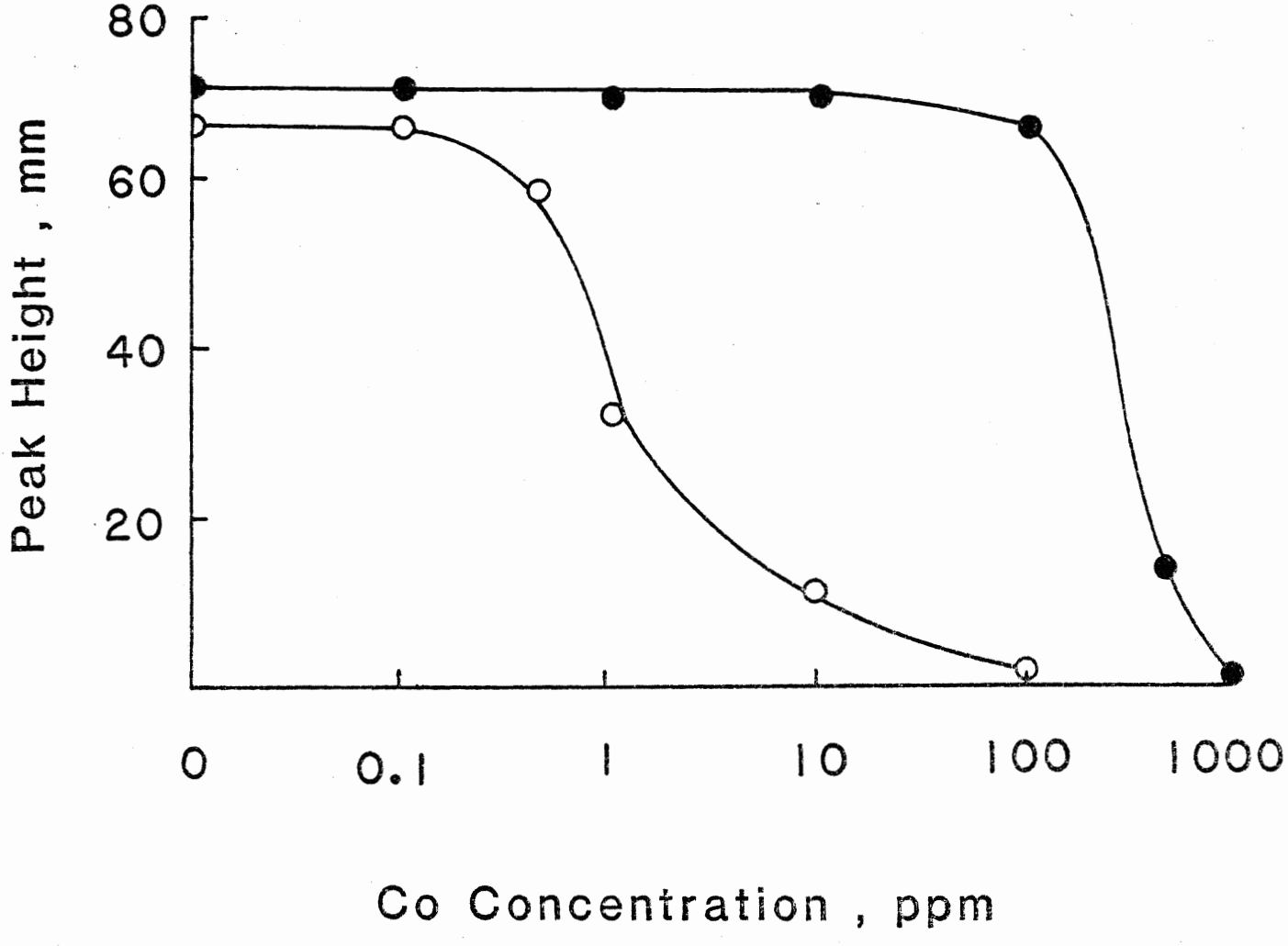

Figure 21. **Co(II) interference reduction by L-cystine in the determination of tin.**
○ - 5.0 ml of 0.40 ng ml^{-1} Sn,
● - 5.0 ml of 0.40 ng ml^{-1} Sn + 0.4 g L-cystine

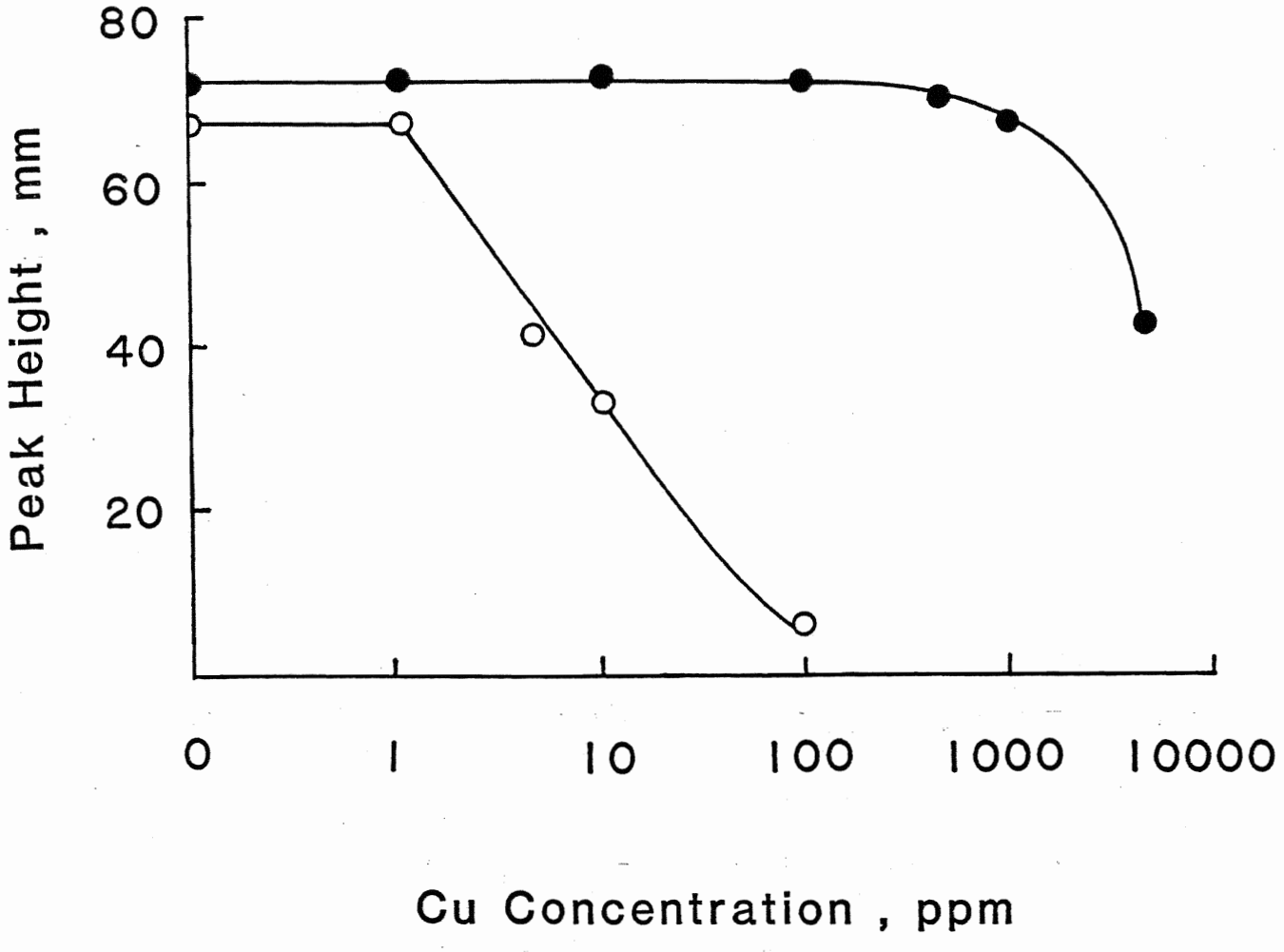

Figure 22. Cu(II) interference reduction by L-cystine in the determination of tin,
○ - 5.0 ml of 0.40 ng ml^{-1} Sn,
● - 5.0 ml of 0.40 ng ml^{-1} Sn + 0.4 g L-cystine.

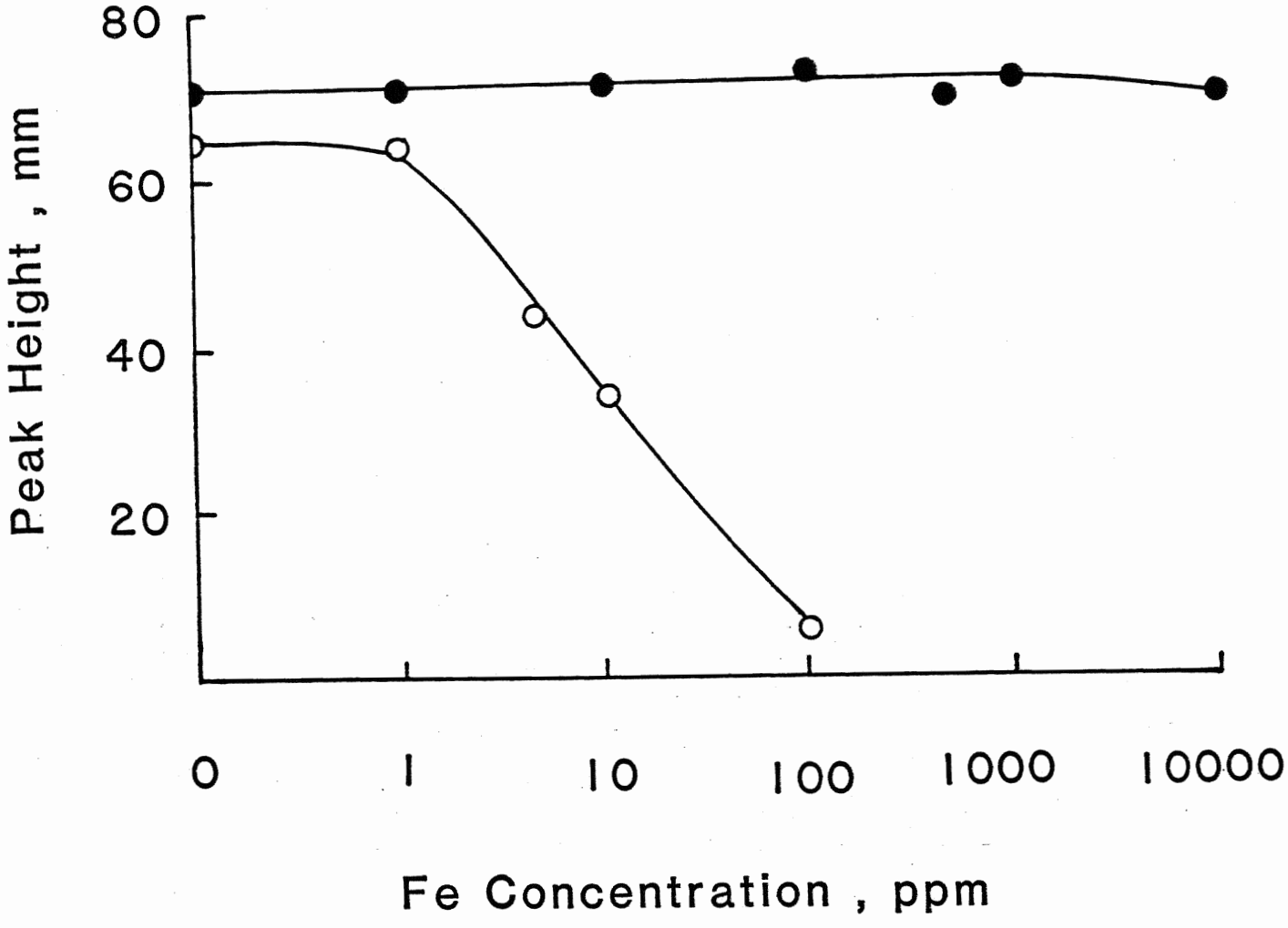

Figure 23. **Fe(II) interference reduction by L-cystine in the determination of tin.**
○ - 5.0 ml of 0.40 ng ml^{-1} Sn,
● - 5.0 ml of 0.40 ng ml^{-1} Sn + 0.4 g L-cystine.

Table 8. Recovery of 0.40 ng ml^{-1} tin in the presence of interfering ions

Interferent	Form of Interferent	Interferent Concentration ($\mu g\ ml^{-1}$)	Recoveries of Sn (%) without L-Cystine	Recoveries of Sn (%) with L-Cystine
Ag(I)	$AgNO_3$	10	96	98
		100	24	82
		1000	11	50
Au(III)	$AuCl_3$	1	100	100
		10	87	77
		100	17	46
Cd(II)	$Cd(NO_3)_2$	100	71	100
		1000	83	74
Cr(VI)	$K_2Cr_2O_7$	100	102	100
		1000	76	82
Hg(II)	$HgCl_2$	10	98	100
		100	91	102
		1000	80	96
Mn(II)	$MnSO_4$	1000	97	100
		10000	100	100

Mo(VI)	$(NH_4)_6Mo_7O_{24}$	100	81	98
		1000	42	67
		10000	22	36
Pb(II)	$Pb(NO_3)_2$	100	100	-
		1000	103	105
Pd(II)	$PdCl_2$	1	65	58
		10	48	21
		100	6	11
Pt(IV)	H_2PtCl_6	1	89	63
		10	46	37
		100	7	26
V(V)	NH_4VO_3	200	100	100
		2000	53	72
Zn(II)	$Zn(NO_3)_2$	100	69	-
		1000	71	87

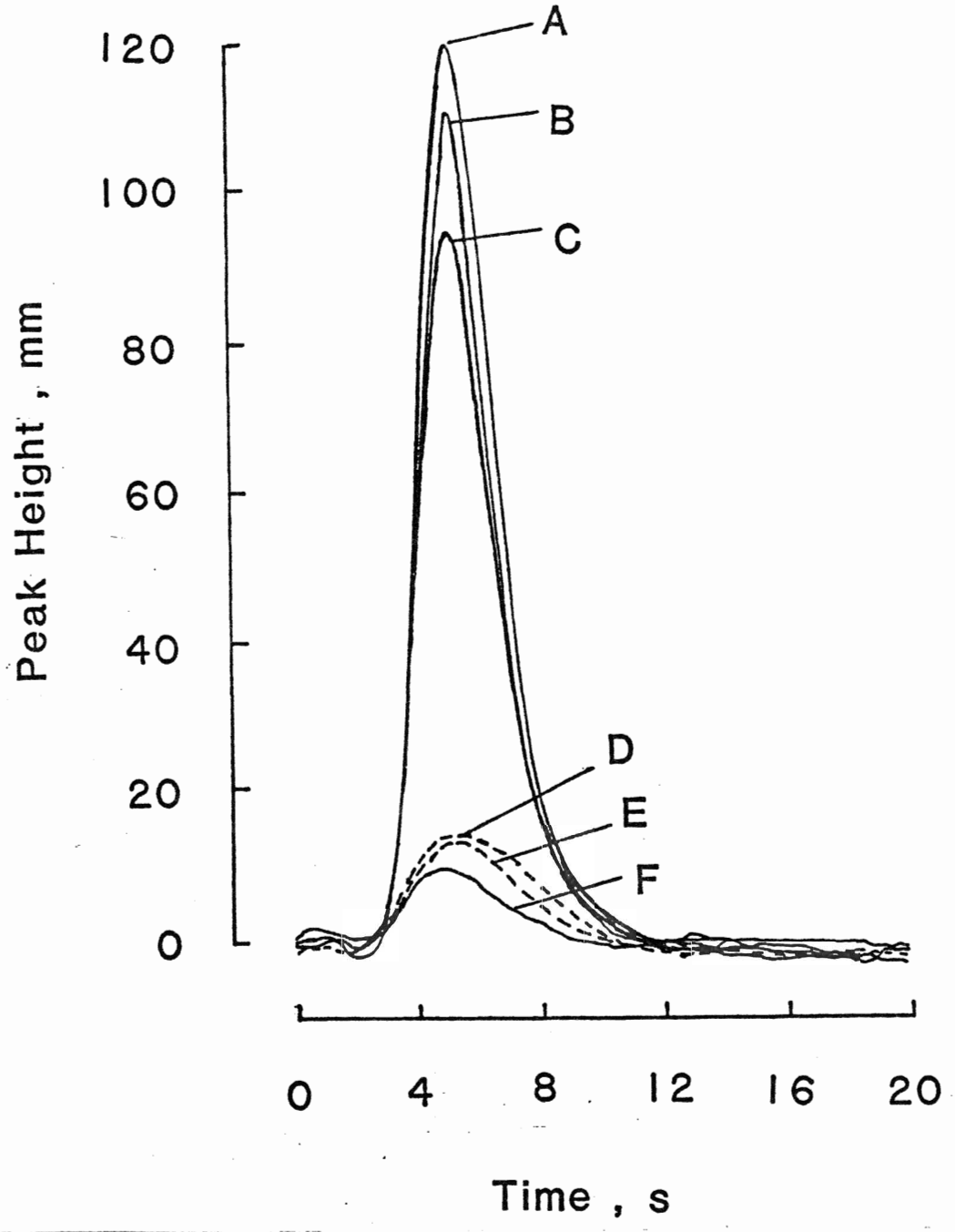

Figure 24. Blank determinations and synthetic mixtures showing their relationship to the determination of tin in Cu Benchmark III. A - 0.20 ng ml^{-1} Sn in 0.050M HNO_3 + 0.4 g L- cystine, B - 0.20 ng ml^{-1} Sn in 0.05 M HNO_3 , C - 0.16 ng ml^{-1} Sn in Copper Benchmark III sample +0.4 g L-cystine, D - tin blank + 0.4 g L-cystine, E - tin blank, F - 0.16 ng ml^{-1} Sn in a solution of Copper Benchmark III.

Determination of Tin in NBS Standard Reference Material Benchmark Copper, Open Hearth Iron and Low Alloy Steel

Without modification, the determination of trace amounts of tin in copper and steel samples by hydride generation is very difficult because of severe interference. It is clear from Figure 24 that, under normal conditions (F), the signal from tin in the copper sample is suppressed completely due to matrix interference. However, this interference is eliminated by the addition of L-cystine. Thus, 0.16 ng ml^{-1} tin in a solution of copper sample is quantitatively recovered (C). The effect of L-cystine on a standard 0.2 ng ml^{-1} Sn solution can also be seen in the figure (A and B). Thus, in the presence of L-cystine (A), the signal from tin is approximately 10% higher than that in the absence of L-cystine (B). Only minor effects are observed in the blank. Thus, in the absence of L-cystine (E), the blank is slightly lower than in the presence of L-cystine.

To demonstrate the utility and accuracy of the present method of sample analysis, this method was applied to the determination of tin in the NBS Standard Reference Copper Benchmark Standards II and III, Open Hearth Iron 55E and Low Alloy Steel 363. Although no matrix interferences were anticipated on the basis of previous experiments, the method of standard additions was used to improve the accuracy of the determination and to see if there were any systematic errors associated with the determination. Three replicate, standard addition determinations were made for each standard, except for the Low Alloy Steel 363. The results are shown in Table 9. Paired t-tests and non-

parametric ranked t-tests (431) showed that there were no significant differences between the results obtained by the present method and certified values.

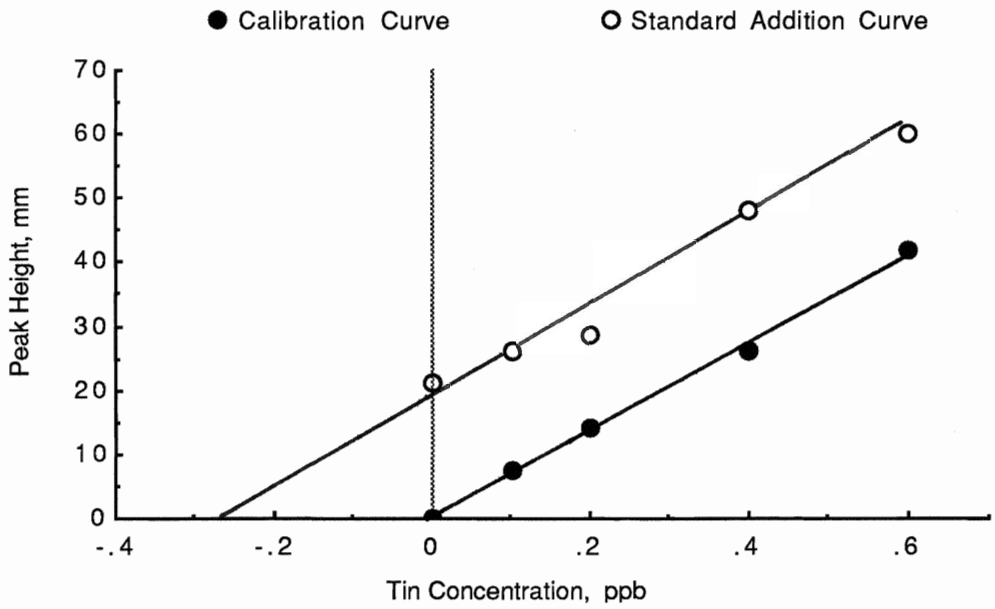

Figure 25. Comparison of calibration curve and standard addition curve in the determination of tin in Copper " Benchmark " II

Table 9. Concentrations of Tin in NBS Standard Reference Materials ($\mu g\ g^{-1}$)

Sample	This work mean ± s.d. (n) from standard addition curve (431); n = number of points on the line	Mean ±Pooled s.d.	Certified Value
Benchmark	1.4 ±0.1 (7)		
Copper II	1.6 ± 0.1 (4)	1.5 ± 0.1	1.5
Benchmark	0.82 ± 0.05 (6)		
Copper III	0.76 ± 0.03 (5)		
	0.77 ± 0.11 (6)	0.78 ± 0.07	0.8
Open Hearth	69 ± 2 (7)		
Iron 55E	68 ± 1 (7)		
	68 ± 3 (7)	68 ± 2	70
Low Alloy			
Steel 363	(9.7 ± 0.4)	(9.7 ± 0.4)	
	x 10^2 (5)	x 10^2	1.0_4 x 10^3

The calibration curve and the standard addition curve of tin in the sample Copper "Benchmark" II are shown in Figure 25. The slopes of the calibration curve and standard addition curve were parallel and that the correlation coefficient factors of these regression lines were better than 0.99. The intercepts and standard deviations were calculated from the standard addition line by the method outlined by Miller and Miller (431) and adapted for use on the Macintosh SE StatView program.

RSD

Figure 26 shows the peaks of eight replicate determinations of 0.40 ng ml^{-1} tin in the presence of L-cystine. Very reproducible tin signals were obtained and the relative standard deviation based on these peak heights was calculated to be 2.0%.

Reagent Blank

High inorganic tin blank from reagents has been considered as a problem which limited the detection limit for tin determinations (241). Therefore, to reduce the blank appears very important for analysis of trace amounts of tin. A series of simple experiments were performed to find the main sources of the tin blank. The tin blank from L-cystine (Sigma grade) was insignificant. BDH AnalaR HNO_3 was found to have a high tin blank, and so E. Merck Suprapur HNO_3 was used, which was found to have a low tin blank. The main source of tin blank was found to be from $NaBH_4$. With an increase of $NaBH_4$ volume or concentration,

the tin blank value increased. Even with $NaBH_4$ pellets instead of $NaBH_4$ in 0.1 M NaOH solution, tin blank was observed. This confirmed that $NaBH_4$ is the main source of high tin blank. Sodium tetrahydroborate(III) ($NaBH_4$) from Anachemia was used as the reducing agent since it had much lower tin blank than others. However, later lots were found to have higher concentrations of tin. Thus there is an obvious need to check on each batch of reagent before it is used. Relatively higher tin blanks were found in 98% $NaBH_4$ from Aesar and Aldrich corresponding to 0.1 $\mu g\ g^{-1}$. In order further to decrease the tin blank in the $NaBH_4$ reagent, a 4% (w/v) $NaBH_4$ aqueous solution was treated by sparging with argon for 30 minutes. As shown in Figure 27, the tin blank was decreased (A) to approximately half of its original value (B) by this procedure due probably to the release of the tin hydride from the $NaBH_4$ solution. To stabilize the solution, sodium hydroxide was added to the solution to make it 0.1 M with respect to NaOH. It is worth noting that to reduce the tin blank in $NaBH_4$ efficiently, the sparging process was undertaken prior to the addition of NaOH. Tin blanks in the reagents were subtracted from tin signals.

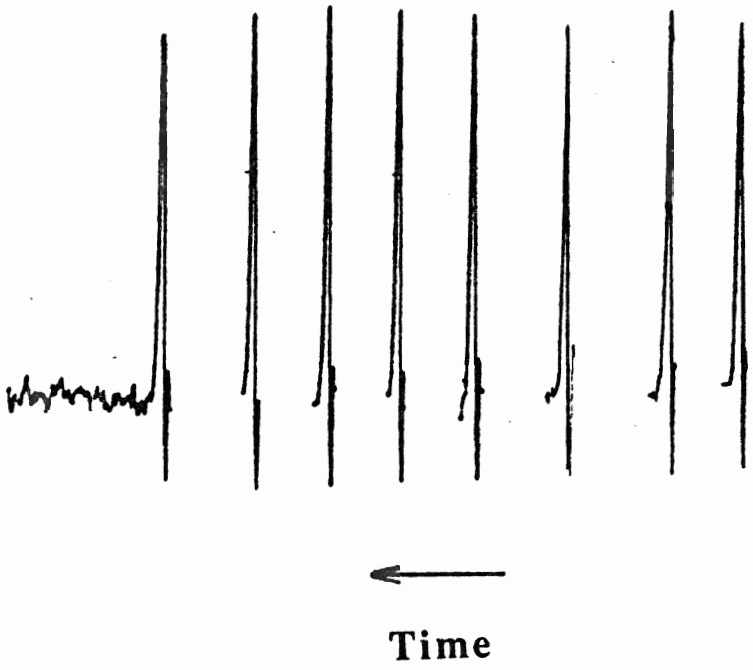

Figure 26. Recorded peaks of eight replicate determinations of 5.0 ml 0.40 ng ml^{-1} Sn in the presence of L-cystine.

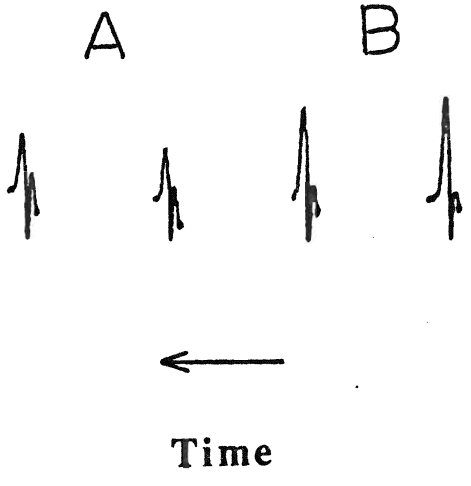

Figure 27. Tin blank and its reduction.
5.0 ml of 0.05. M HNO_3 + 1.0 ml of 4% $NaBH_4$ in 0.1 M NaOH
A - $NaBH_4$ solution with argon sparging treatment
B - $NaBH_4$ solution without argon sparging treatment

Detection Limit

The detection limit, defined as three times the noise, was found to be 20 pg ml^{-1} (or 100 pg for a 5 ml sample) under the optimum conditions.

Effect of L-cysteine

Because L-cysteine is more soluble than L-cystine in aqueous solution, and later work indicated that L-cysteine was as effective as L-cystine in reducing the interference in the determination of germanium(432), the effect of L-cysteine on tin determination was studied. Because of the shortage of time, the optimum condition for this system was not investigated and replicate experiments were not performed. However, the experimental results showed promising features. Thus, in the presence of 0.4% L-cysteine in 2.0 ng ml^{-1} tin solution, the peak heights of tin signals were approximately 120% greater than those in the absence of L-cysteine. The interferences were also reduced by using L-cysteine. With 0.4% L-cysteine, recoveries of 2.0 ng ml^{-1} tin in the presence of 100 μg ml^{-1} Ni(II), 100 μg ml^{-1} Pt(IV), or 1000 μg ml^{-1} Cu(II) were approximately 40%, 40% and 110%, respectively, while they were 0%, 7% and 0%, respectively, in the absence of matrix modifier as shown in Figure 20, Table 8 and Figure 22.

III. Determination of Germanium

Instrumental Parameters

Selection of wavelength was based upon trials using direct aspiration of a solution of 20 $\mu g\ ml^{-1}$ germanium. The wavelengths tried were 303.906, 275.459, and 265.118 nm. Wavelength scans of the atomic emission signals at each of the above three lines were obtained. Among them, the sensitivities of the signals were 303.906 nm $\simeq$ 265.118 nm > 275.459 nm, while the background was 265.118 nm > 303.906 nm > 275.459 nm. The 303.906 nm wavelength was chosen because it gave the best signal-to-background ratio and was used for all determinations.

As indicated in the previous section on tin determination, the relative position of the plasma and the slit is an extremely important factor for the response of the instrument. This is supported by the work of Ebdon *et al.* (435), who, after performing a simplex optimization procedure on the d.c. plasma atomic emission spectrometer in the normal aspiration mode, observed that the "vertical viewing point" (i.e. the observation height) is critical and depends on the element being determined. Unlike the normal aspiration/nebulization mode, the carrier gas flow through the hydride generator influences the determination due to the effect of hydride reduction and transportation processes. Varying the carrier gas flow rates causes the optimum observation height to change. This implies a possible interaction between the carrier gas flow rate and the observation height. Therefore, a simplex

optimization was performed on the system using the hydride generation process in order to find the best conditions for the determination. Since sleeve gas pressure and horizontal position of the plasma were considered by Ebdon *et al.* (435) to be least significant, only two factors, the carrier gas flow rate and the background signal (a non- linear function of observation height), were used for the simplex optimization. The signal to background ratio was taken as the response. Using 1.0 ng ml^{-1} germanium in 0.04 M HNO_3 and 1.0 ng ml^{-1} Ge with 0.4% (m/V) L-cysteine, similar optimum conditions were obtained as shown in Table 10. With eleven experiment units, the optimum conditions for the determination were found to have a flow meter scale of 47 (arbitrary units), which corresponds to an argon flow rate of 730 ml min^{-1}, and a background signal of 6800 (with no gas flowing). After the simplex was performed, the two factors were varied one at a time to find the range of the optimum signal. While keeping background digital signal at 6800, the gas flow rate was varied from 490 ml min^{-1} to 970 ml min^{-1} and germanium signals were obtained as shown in Figure 28. Within the range of gas flow of 630-730 ml min^{-1} in the absence of L-cysteine and 560-730 ml min^{-1} in the presence of L-cysteine, maximum and identical signals of germanium emission were obtained. At the constant argon flow rate of 730 ml min^{-1}, the effect of observation height on Ge signals is shown in Figure 29. The optimum plasma position was found to correspond to

Table 10. Simplex Optimization Results for Germanium Determination

Experiment Number (Vertex)	Simplex Formed by Vertex	Carrier Gas Flow (Arbit. Units)	Background Digital	Signal/Background Ratio	
				Without L-cysteine	With L-cysteine
1		47	6800	49, 48	90, 90
2		43	6100	50, 46	87, 83
3		54	8100	33, 32	58, 60
	1, 2, 3				
4		36	4800	26, 25	68, 70
	1, 2, 4				
5		40	5500	46, 45	83, 85
	1, 4, 5				
6		51	7500	42, 41	82, 75
	1, 5, 6				
7		58	8800	30, 29	43
	1, 6, 7				
8		65	8100	15	13
	1, 7, 8				
9		54	6100	29, 29	48
	1, 8, 9				
10		36	4800	25	68
11	confirm 1	47	6800	48	90

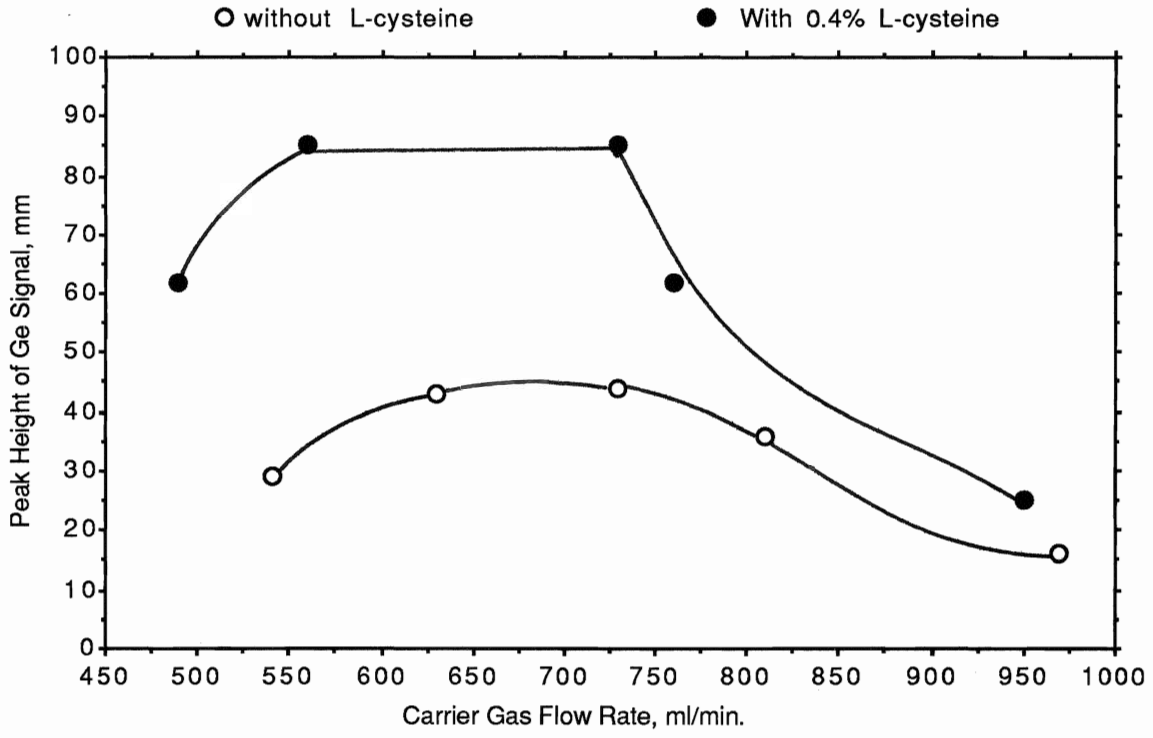

Figure 28. Effect of carrier gas flow on germanium signals.

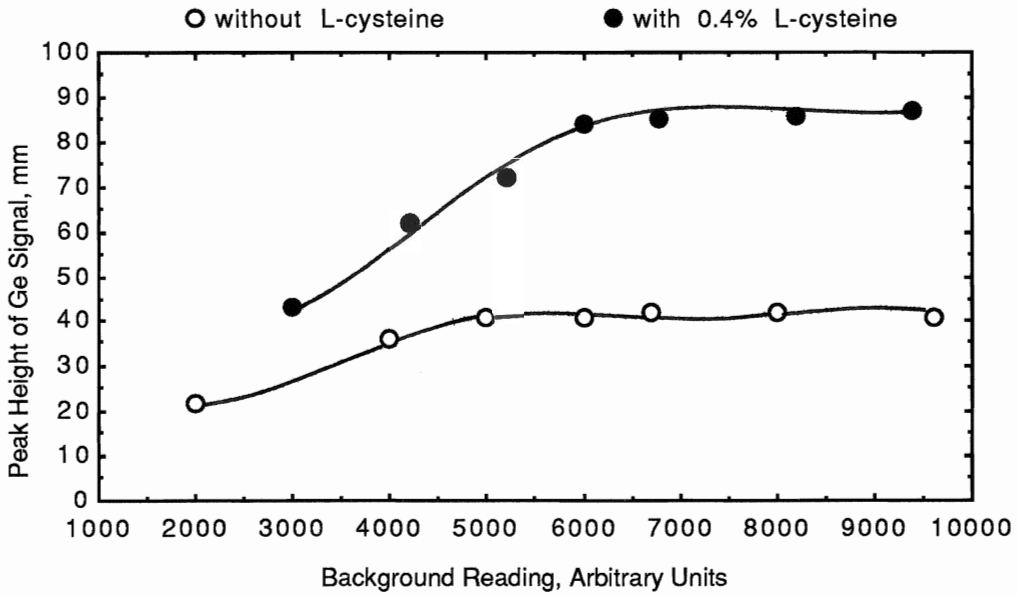

Figure 29. Effect of observation height on germanium signals.

the background reading over a range of 6000 to 9000. Thus the argon flow rate of 730 ml min^{-1} and the background signal of 6800 were used for the entire study. It should be noted that the background fell to between 400 and 600 during the determination as the argon flow changed the shape of the plasma so that less of the plasma image was intercepted by the slit of the spectrometer. The reason for the choice of the background signal with no argon flowing was because the background signal changes very little when the gas is flowing this not be a good indicator of observation height.

The Hydride Generation Process

The speed of evolution of stannane from solution during reduction of solutions of tin by tetrahydroborate(III) ($NaBH_4$) suggested the generation of germane may be similar. Preliminary experiments on the effect of reaction time between germanium and $NaBH_4$ showed that this was indeed the case and so all further determinations were performed with argon flowing continuously through the hydride generator. Addition of solid L-cystine to the reaction vessel before reduction increased the signal from tin and so addition of solid L-cystine was also considered to be important for the determination of germanium. In addition, it was felt that the soluble L-cysteine might be more easily handled and thus provide convenient interference reduction similar to the rather insoluble L-cystine, which created a foaming problem when large amounts of solution and solid L-cystine were used.

Sodium tetrahydroborate(III) solutions, with concentrations from 1 to 10% (m/V), were used to identify the best concentration. Figure 30 demonstrates the effect of $NaBH_4$ concentration on the peak heights of germanium signals. Within the range of 4 to 10%, results were virtually identical. Below these values, the signals of germanium were reduced. A solution of 6% sodium tetrahydroborate(III) stabilized with sodium hydroxide (0.1M) was chosen for all determinations.

Nitric acid and hydrochloric acid were investigated as media for germanium solutions. The effect of their concentrations was found to be rather similar on the signals from germanium as indicated in Figure 31. With either HCl or HNO_3, concentration had a critical effect on the signals from germanium, but a relatively wider range of HNO_3 concentration was tolerated. In the presence of L-cystine, germanium signals were enhanced by approximately 60% over solutions without L-cystine under the optimum HCl or HNO_3 concentrations. Nitric acid was chosen as the medium of germanium solutions for hydride generation since germanium can easily be lost from hydrochloric acid via its volatile tetrachloride and since most samples of metals etc. are dissolved in nitric acid prior to analysis.

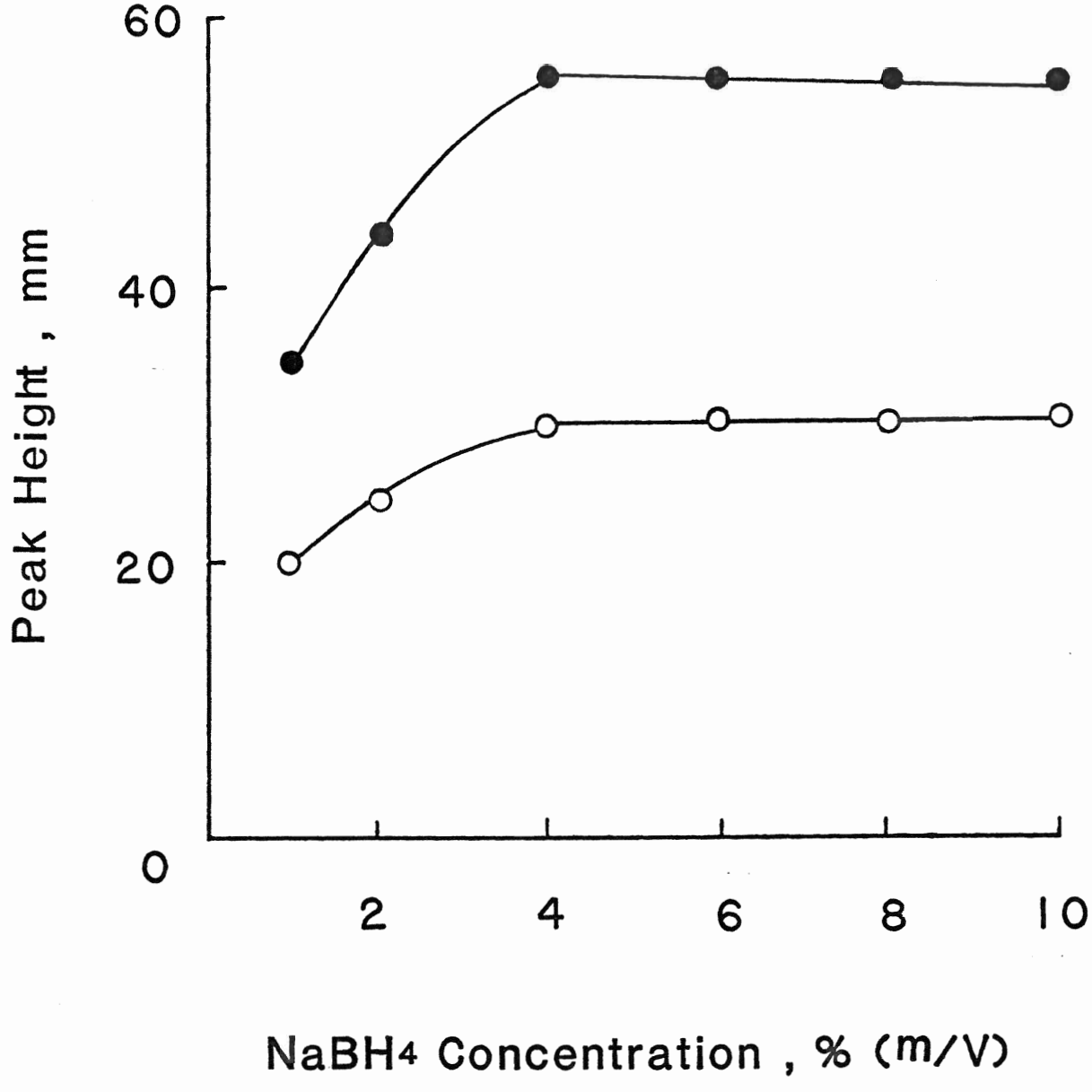

Figure 30. Effect of $NaBH_4$ concentration on germanium signal
○ - 1.0 ng ml^{-1} Ge in 0.04 M HNO_3
● - 1.0 ng ml^{-1} Ge in 0.04 M HNO_3 and 0.4% L-cysteine

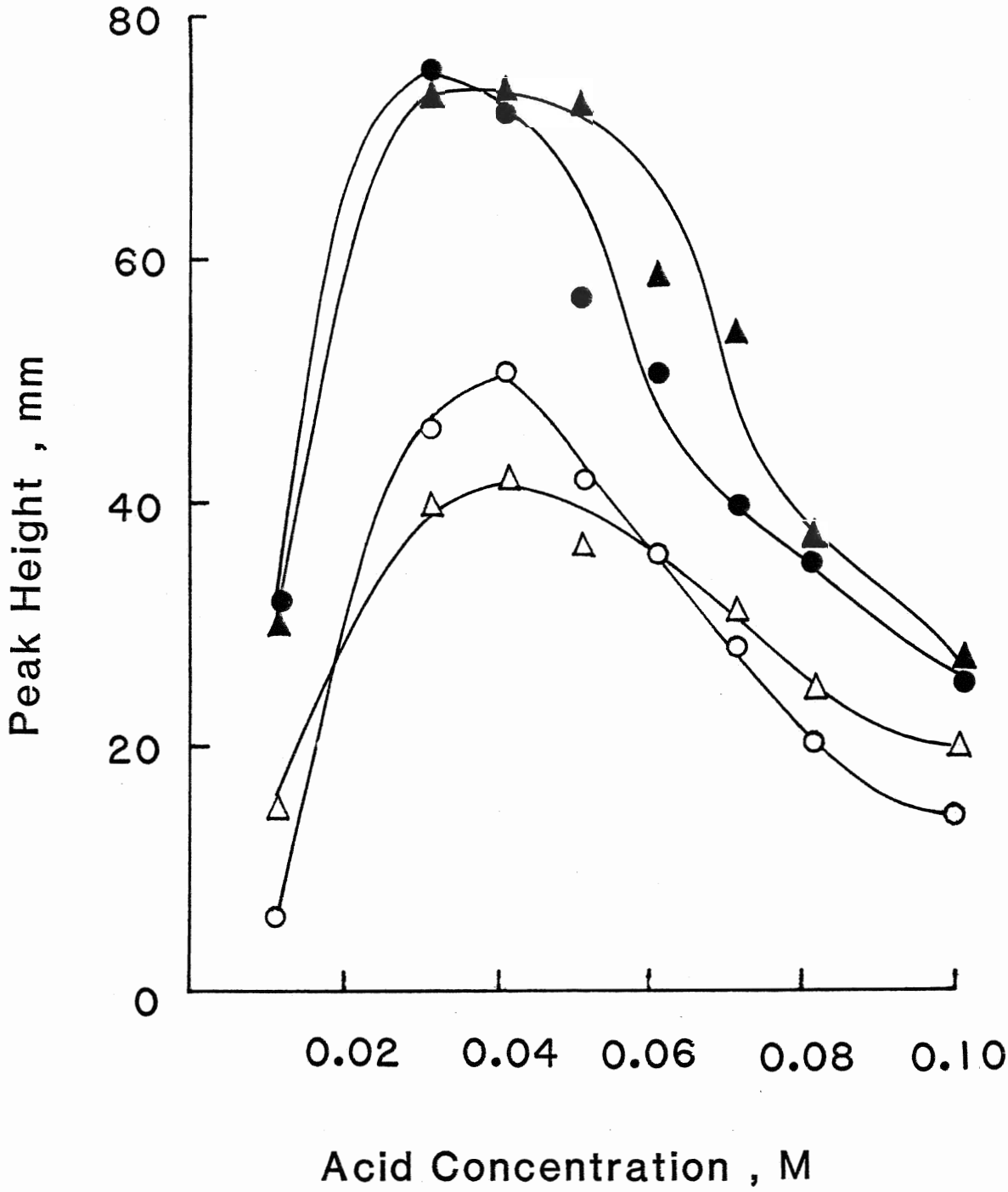

Figure 31. Effect of acid concentration on germanium signals

○ - Hydrochloric acid (HCl)
● - HCl with 0.4 g L-cystine
△ - Nitric acid (HNO_3)
▲ - HNO_3 with 0.4 g L-cystine

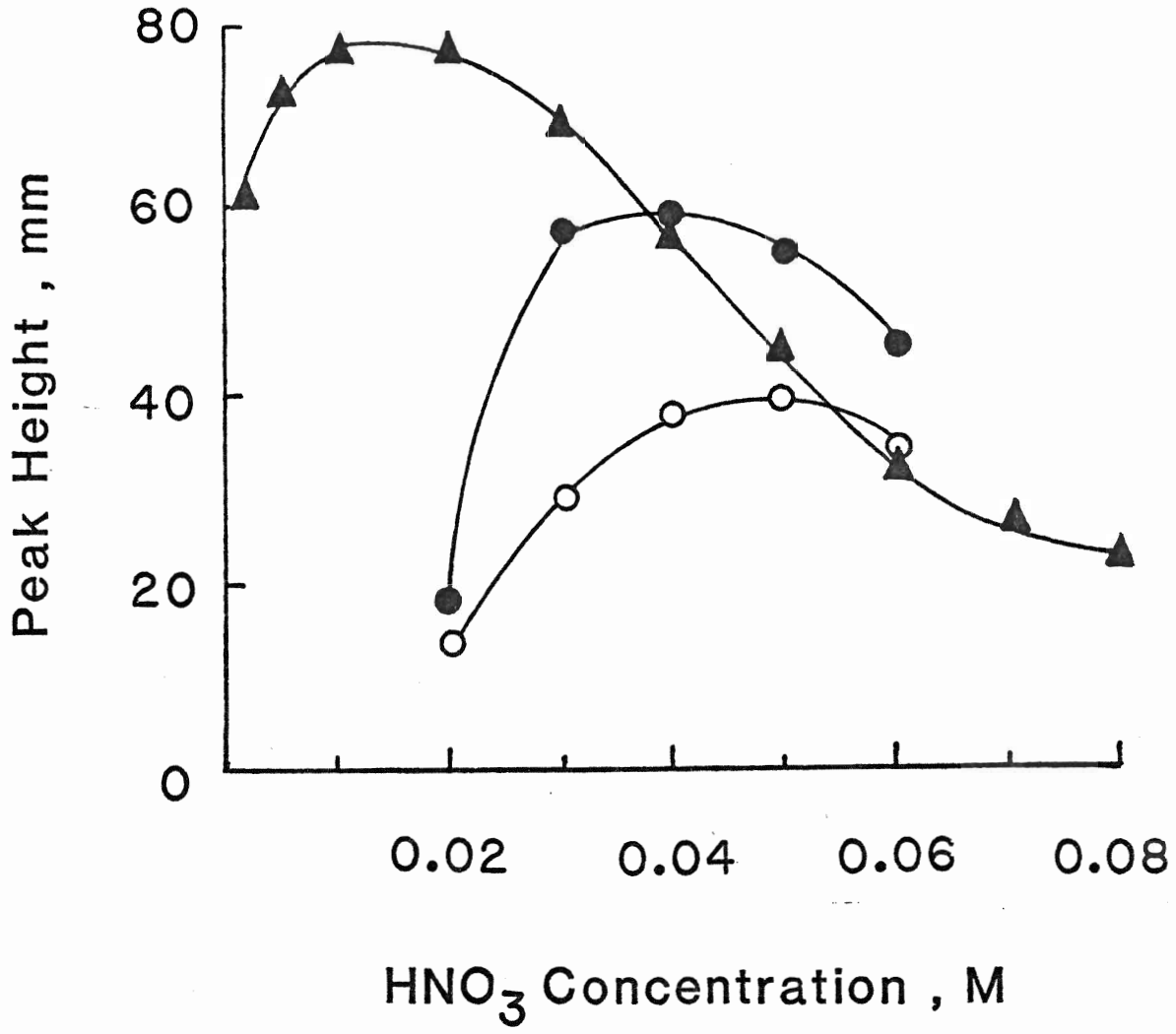

Figure 32. Effect of nitric acid concentration of germanium signal (9.0 ml of 1.0 ng ml^{-1} Ge)
○ - in nitric acid (HNO_3)
● - in HNO_3 with addition of 0.4 g L-cystine
▲ - in HNO_3 and 0.4% (m/V) L-cysteine

Figure 32 illustrates the variation in germanium signal at various nitric acid concentrations and in different media. Solutions of 9.0 ml of 1.0 ng ml^{-1} Ge and 2.0 ml 6% (m/V) $NaBH_4$ in 0.1 M NaOH were used to carry out this experiment. It is clear from the figure that the signals from germanium are considerably enhanced by the presence of L-cysteine and L-cystine. In addition, the best signal from germanium was achieved in the presence of 0.4% L-cysteine and at a lower acid concentration (0.01-0.02M HNO_3). Compared with the signal in the presence of only nitric acid, the signal of germanium was increased by approximately 100% in the presence of 0.4 % L-cysteine.

Since the optimum acid concentration for germane formation depended on the reaction medium, as indicated in Figure 32, it was worthwhile comparing the pH values of the reaction solutions, before and after the hydride reactions were complete. A series of solutions were prepared where the reaction conditions were similar to those used in performing the hydride generation for the determination of germanium. Thus, each aliquot of 9.0 ml of 1.0 ng ml^{-1} Ge solution in HNO_3 (0.001-0.10M) was taken and placed in a beaker. The pH value of this solution was determined as shown in Table 11 (initial pH). Then, a 2.0 ml solution of 6% $NaBH_4$ in 0.1 M NaOH (pH=12.5) was added to the beaker containing the Ge solution. After 10 sec., 40 sec., 80 sec., etc. following the addition of $NaBH_4$, the pH values were determined. Three different media, HNO_3 alone, HNO_3 with addition of 0.4 g solid L-cystine, and HNO_3 with 0.4% (m/V) L-cysteine, were investigated. The pH values are summarized in Table 11. Although the optimum initial pH values for the three media were significantly different, the pH of the reaction

solutions, after the $NaBH_4$ was added, were very close, i.e., 8.4-9.0. This is probably due to the buffering effects of L-cysteine and L-cystine in the aqueous solution. The dissociation constants for L-cysteine, for example, were pK_{a1}= 1.71, pK_{a2}= 8.33.

L-Cystine created a foam during the determination which limited the volume of solution that could be used for the analysis to approximately 5.0 ml. This foaming was considerably less when the solution was made up to 0.4% (m/V) with L-cysteine instead and allowed a larger volume of the analyte solution to be used. The best volume for this system was found to be 9.0 ml. The time for a complete determination typically was less than one minute.

Table 11. pH values of the reaction solutions for germane generation

HNO_3 Conc. (M)	pH Values Determined										
	No Additional reagents			With L-cystine			With L-cysteine				
	Initial	Add $NaBH_4$ and wait for		Initial	Add $NaBH_4$ and wait for		Initial	Add $NaBH_4$ and wait for			
		10 s	40 s		10 s	40 s		10 s	40 s	80 s	180 s
0.001	-	-	-	-	-	-	3.23	8.65	9.00	9.15	-
0.002	-	-	-	-	-	-	3.01	8.75	8.93	9.10	-
0.005	-	-	-	-	-	-	2.70	8.70	8.84	9.03	-
0.01	-	-	-	-	-	-	2.53	8.40	8.79	9.01	-
0.02	1.77	10.11	10.23	1.81	9.15	9.09	2.20	8.36	8.73	8.93	-
0.03	1.60	9.36	9.57	1.65	8.80	8.95	1.96	8.34	8.71	8.91	-
0.04	1.48	8.80	9.10	1.53	8.72	8.92	1.76	8.27	8.69	8.84	9.07
0.05	1.39	8.48	8.86	1.44	8.52	8.83	1.66	8.26	8.69	8.85	9.05
0.06*	1.31	8.50	8.91	1.35	8.47	8.85	1.53	8.22	8.66	8.83	9.00
0.07	-	-	-	-	-	-	1.46	8.20	-	-	-
0.08	-	-	-	-	-	-	1.38	8.17	-	-	-
0.10	-	-	-	-	-	-	1.24	8.15	-	-	-

* In 0.06 M HNO_3 and in the presence of L-cysteine, the pH values were 9.10 and 9.20 after 5 minutes and 12 minutes, respectively.

Interference Study

Both L-cystine and L-cysteine were studied with the objective of reducing interferences. If L-cystine was used, approximately 0.4 g solid reagent was directly added into the reaction vessel for each determination. L-cysteine, on the other hand, was dissolved in the analyte solution since it is water soluble. Preliminary studies were carried out to investigate the optimum concentration of L-cysteine to use in order to reduce interferences. As can be seen from Figure 33, the enhancement of the signals of germanium standard solution reach a maximum when the concentration of L-cysteine is 0.02 % (m/V). At this concentration, interference from 1000 $\mu g\ ml^{-1}$ of copper was also eliminated. For nickel, however, the interference from 10 $\mu g\ ml^{-1}$ of nickel required a minimum concentration of 0.2% (m/V) L-cysteine. Signals from germanium were reduced at a L-cysteine concentration of 1.0 % (m/V). The decrease of germanium signals at high L-cysteine concentration may be due to the change of acidity caused by the large amount of L-cysteine. Thus the concentration of L-cysteine chosen for interference reduction was 0.4 % (m/V).

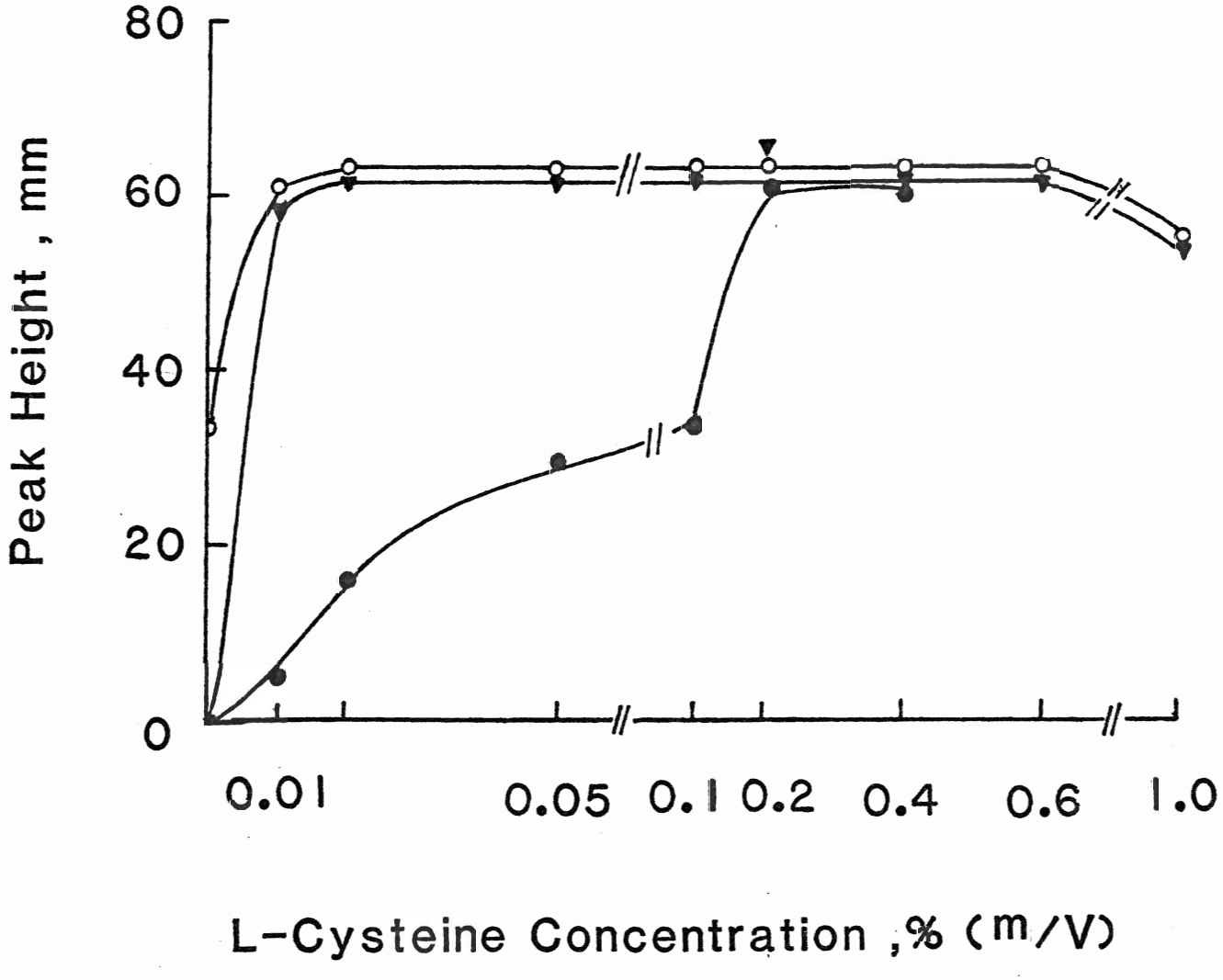

Figure 33. Response of germanium (5.0 ml 1.0 ng ml^{-1}) with increasing L-cysteine concentration
○ - in 0.02 M HNO_3
▼ - in 0.02 M HNO_3 + 0.5 ml 1000 µg ml^{-1} Cu^{2+}
● - in 0.02 M HNO_3 + 0.5 ml 10 µg ml^{-1} Ni^{2+}

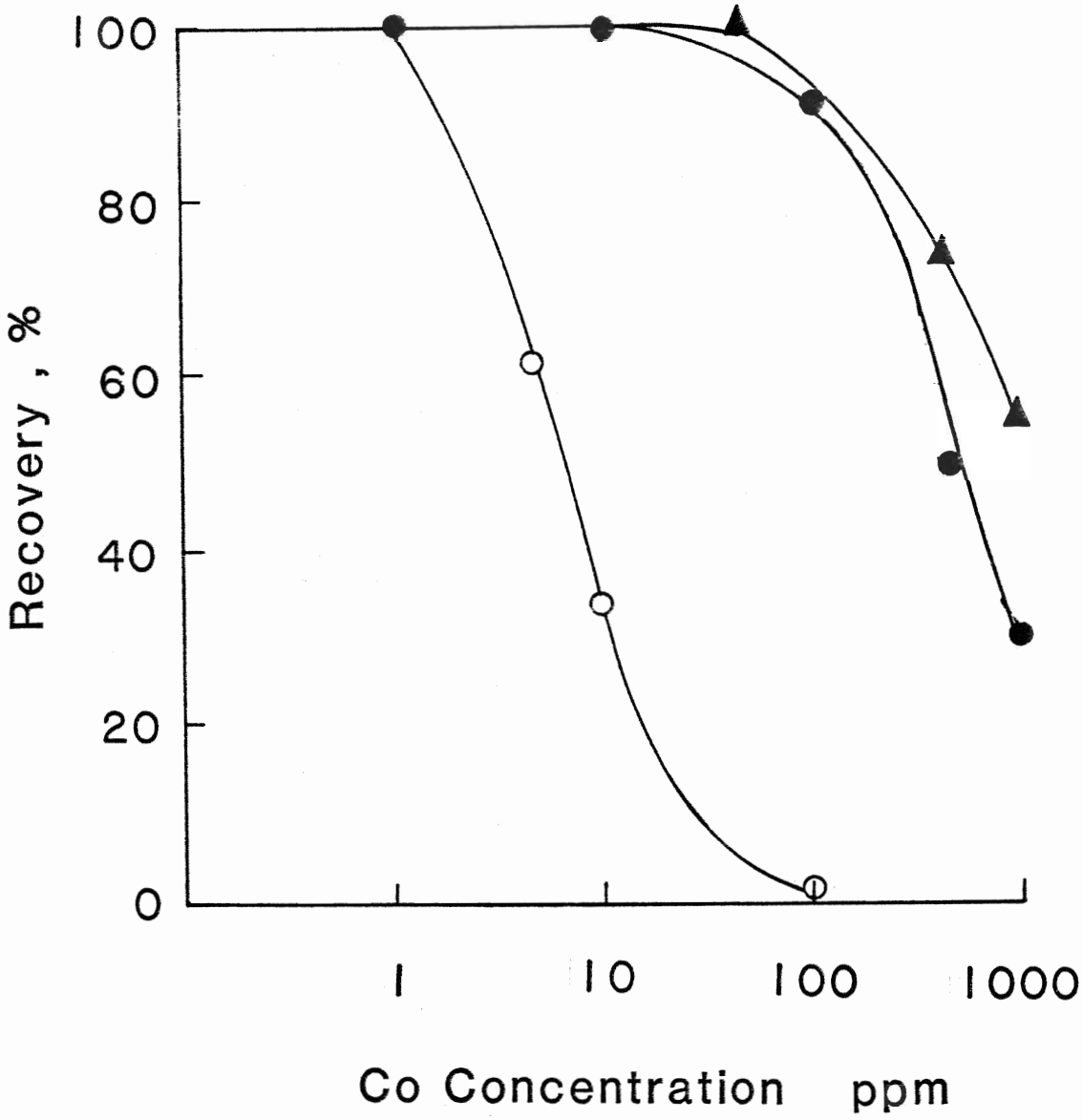

Figure 34. Co(II) interference reduction by L-cystine and L-cysteine in Ge determinations
○ - 5.0 ml of 1.0 ng ml^{-1} Ge in 0.04 M HNO_3
● - 5.0 ml of 1.0 ng ml^{-1} Ge in 0.04 M HNO_3 + 0.4 g L-cystine
▲ - 9.0 ml of 0.50 ng ml^{-1} Ge in 0.04 M HNO_3 and 0.4% L-cysteine

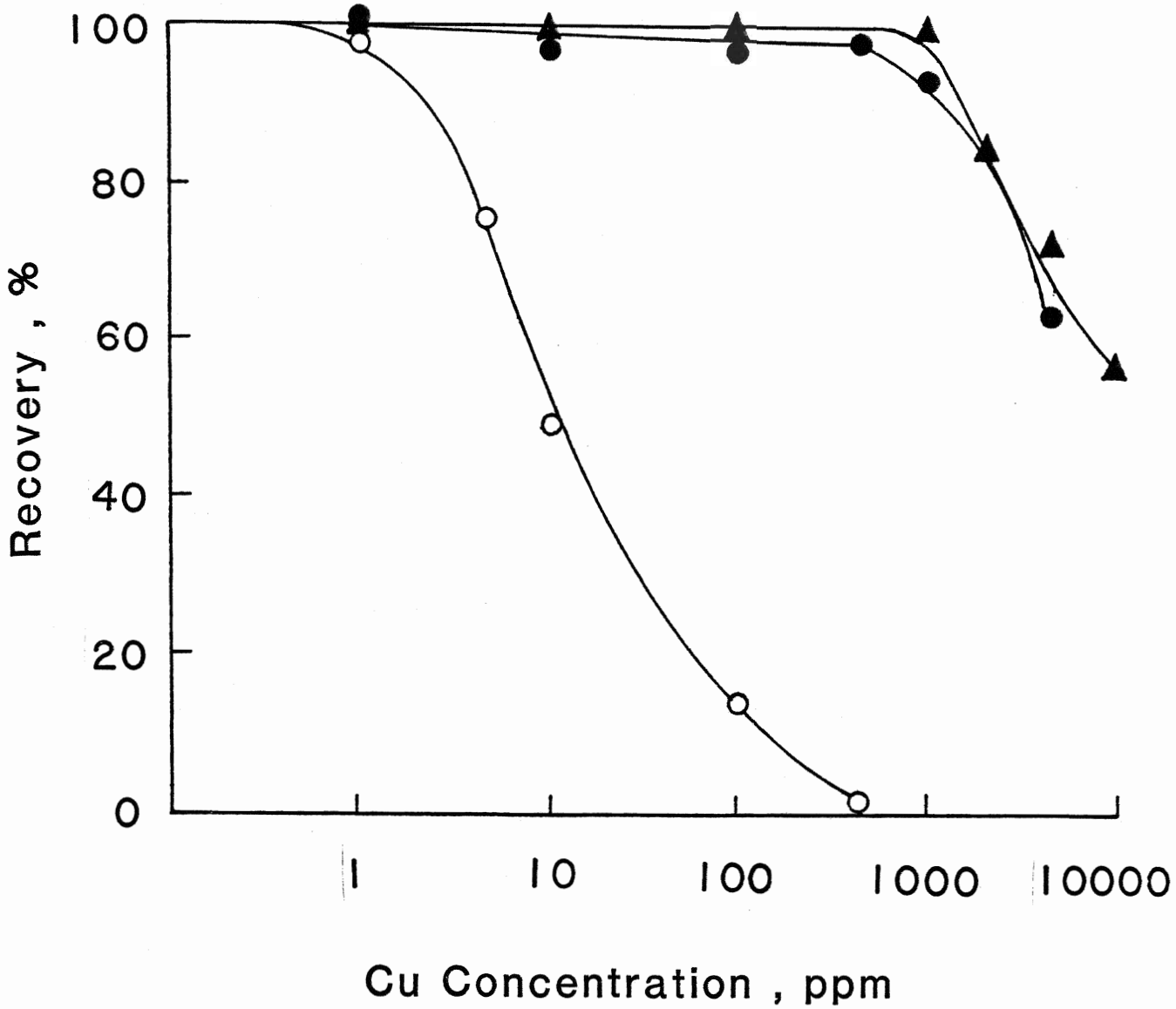

Figure 35. Cu(II) interference reduction by L-cystine and L-cysteine in Ge determinations
○ - 5.0 ml of 1.0 ng ml^{-1} Ge in 0.04 M HNO_3
● - 5.0 ml of 1.0 ng ml^{-1} Ge in 0.04 M HNO_3 + 0.4 g L-cystine
▲ - 9.0 ml of 0.50 ng ml^{-1} Ge in 0.04 M HNO_3 and 0.4% L-cysteine

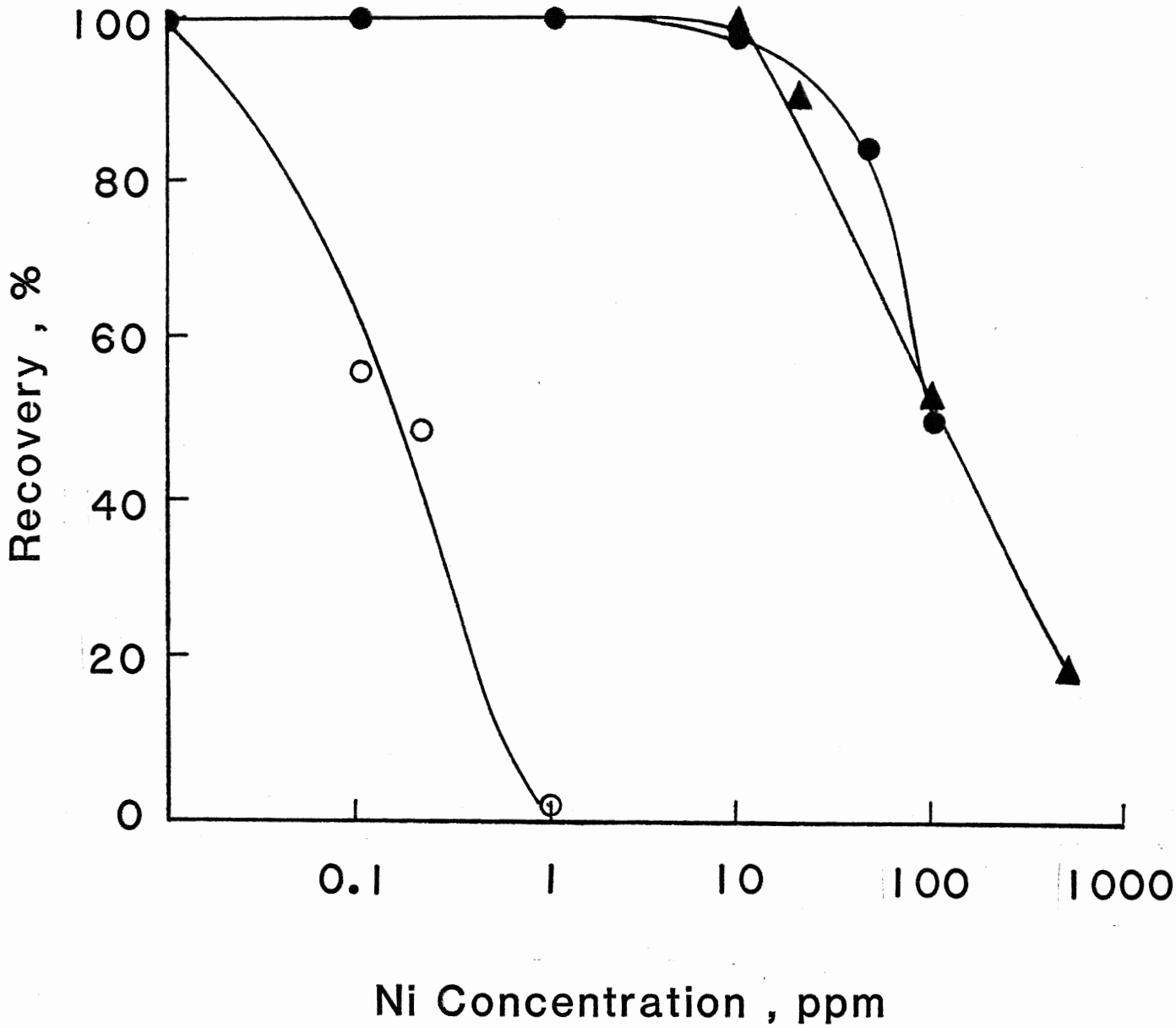

Figure 36. Ni(II) interference reduction by L-cystine and L-cysteine in Ge determinations
○ - 5.0 ml of 1.0 ng ml^{-1} Ge in 0.04 M HNO_3
● - 5.0 ml of 1.0 ng ml^{-1} Ge in 0.04 M HNO_3 + 0.4 g L-cystine
▲ - 9.0 ml of 0.50 ng ml^{-1} Ge in 0.04 M HNO_3 and 0.4% L-cysteine

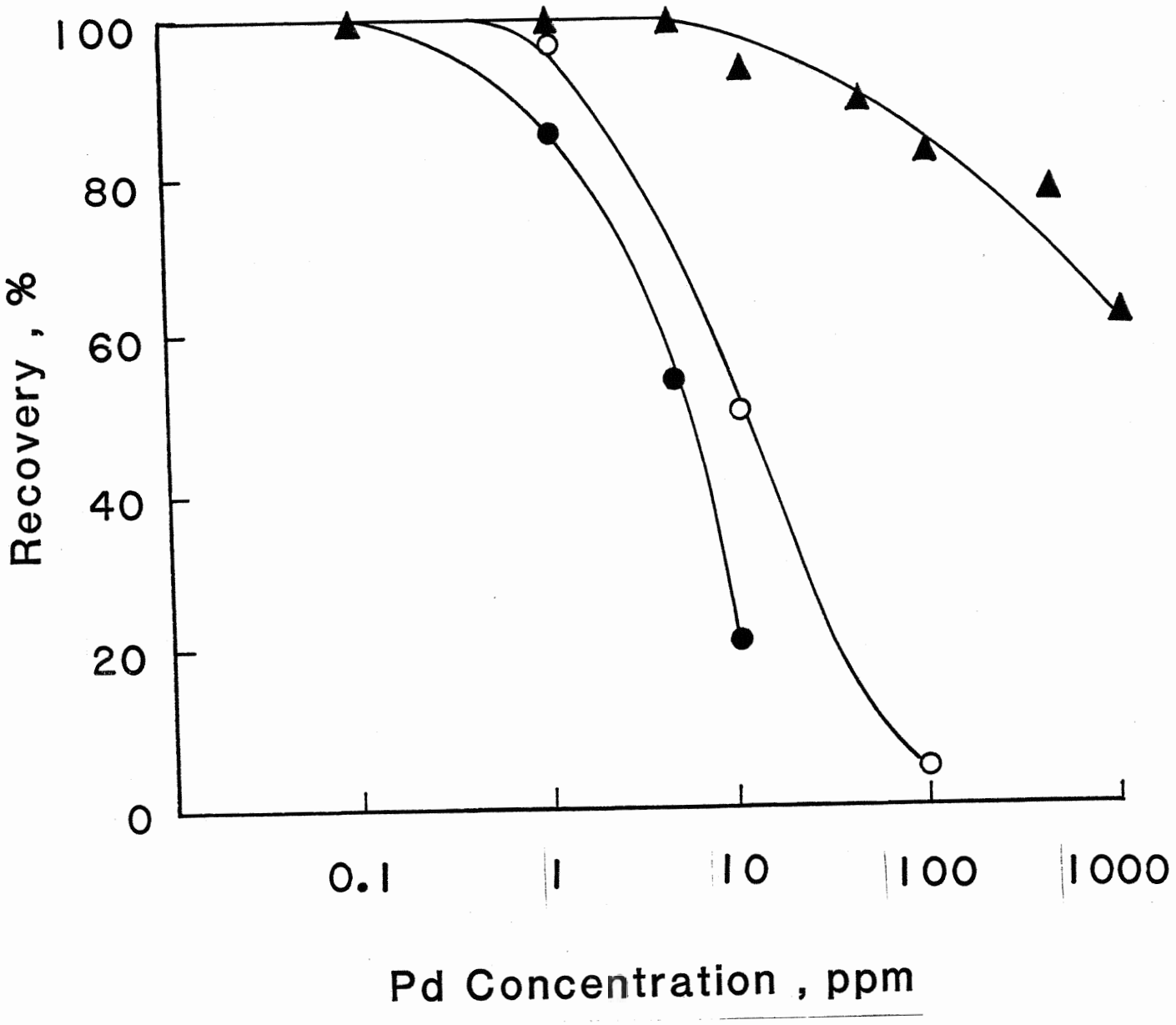

Figure 37. Pd(II) interference reduction by L-cystine and L-cysteine in Ge determinations
○ - 5.0 ml of 1.0 ng ml^{-1} Ge in 0.04 M HNO_3
● - 5.0 ml of 1.0 ng ml^{-1} Ge in 0.04 M HNO_3 + 0.4 g L-cystine
▲ - 9.0 ml of 0.50 ng ml^{-1} Ge in 0.04 M HNO_3 and 0.4% L-cysteine

Figures 34-37 compare the interference effects from typical interfering elements, Co(II), Cu(II), Ni(II), and Pd(II). The figures show the recoveries of germanium in acid solution alone, in the presence of 0.4 g of solid L-cystine, and in the presence of 0.4 % m/V L-cysteine. Signals from 9.0 ml of a solution containing 0.5 ng ml^{-1} germanium or 5.0 ml of 1.0 ng ml^{-1} germanium solution were obtained in the presence of interfering ions at a series of concentrations. Recoveries were calculated by comparison with the germanium standard in the absence of the interfering ion.

It is clear that both solid L-cystine and 0.4 % (m/V) L-cysteine reduce interferences substantially and to a similar degree in most cases. Thus concentrations of interfering ions can be tolerated at 100 to 1000 times the levels without the interference reducing agent. Palladium strongly interfered in the production of GeH_4 both with and without interference reducing agent and this was the only case where addition of solid L-cystine to the Pd(II) containing germanium solution actually causes a reduction in the signal from germanium. With a solution of L-cysteine, however, the interference is reduced and solutions containing up to 10 μg ml^{-1} of palladium can be tolerated without a substantial loss in the signal from germanium.

Table 12. Interference studies in the determination of germanium

Metal Ion Added	Amount Added	Germanium Recovery (%)		
		No interference-reducing agent (5 ml 1.0 ppb Ge)	L-cysteine 0.4% (m/V) (9.0 ml 0.5 ppb Ge)	L-cystine 0.4 g (5.0 ml 1.0 ppb Ge)
V (V)	0.5 ml 200 ppm	-	106	-
	1.0 ml 200 ppm	97	-	100
	0.5 ml 2000 ppm	-	97	-
	1.0 ml 2000 ppm	98	-	97
Cr (VI)	0.5 ml 100 ppm	-	100	-
	1.0 ml 100 ppm	102	-	100
	0.5 ml 1000 ppm	-	97	-
	1.0 ml 1000 ppm	92	-	94
	0.5 ml10000 ppm	-	72	-
	1.0 ml10000 ppm	0	-	40
Mn(II)	0.5 ml 1000 ppm	-	97	-
	1.0 ml 1000 ppm	94	-	97
	0.5 ml10000 ppm	-	100	-
	1.0 ml10000 ppm	86	-	93
Fe(III)	1.0 ml 10.0 ppm	95	100	100
	1.0 ml 100 ppm	83	100	-
	1.0 ml 500 ppm	-	100	-
	1.0 ml 1000 ppm	28	97	96
	2.0 ml 1000 ppm	-	77	-
Zn (II)	0.5 ml 100 ppm	92	100	-
	1.0 ml 100 ppm	74	94	100
	0.5 ml 1000 ppm	-	100	-
	1.0 ml 1000 ppm	-	93	-
Mo(VI)	0.5 ml 100 ppm	-	100	-
	1.0 ml 100 ppm	100	-	100
	0.5 ml 1000 ppm	-	100	-

	1.0 ml 1000 ppm	78	100	96
	0.5 ml10000 ppm	-	50	-
	1.0 ml10000 ppm	0	-	20
Ag(I)	0.5 ml 22.6 ppm	-	94	-
	1.0 ml 22.6 ppm	92	91	100
Cd(II)	0.5 ml 100 ppm	-	100	-
	1.0 ml 100 ppm	87	86	100
	0.5 ml 1000 ppm	-	73	-
	1.0 ml 1000 ppm	56	-	70
Pt(IV)	1.0 ml 0.10 ppm	100	100	100
	1.0 ml 1.00 ppm	100	99	100
	1.0 ml 10.0 ppm	84	96	98
	2.0 ml 10.0 ppm	-	94	-
	1.0 ml 100 ppm	56	96	60
	2.0 ml 100 ppm	-	94	-
Au(III)	1.0 ml 0.10 ppm	100	98	98
	1.0 ml 1.00 ppm	98	99	100
	1.0 ml 10.0 ppm	82	100	100
	0.5 ml 100 ppm	-	100	-
	1.0 ml 100 ppm	66	89	90
	2.0 ml 100 ppm	-	78	-
Hg(II)	0.5 ml 10.0 ppm	-	96	-
	1.0 ml 10.0 ppm	95	-	100
	0.5 ml 100 ppm	-	100	-
	1.0 ml 50 ppm	93	-	-
	1.0 ml 100 ppm	103	-	98
	0.5 ml 1000 ppm	-	100	-
	1.0 ml 1000 ppm	41	103	87
Tl(I)	0.5 ml 100 ppm	-	100	-
	0.5 ml 1000 ppm	-	100	-
	1.0 ml 1000 ppm	-	94	-

Table 12 summarizes the recoveries of germanium in the presence of various transition elements. Generally there is a very satisfactory recovery of germanium at concentrations of transition elements that would be encountered in the course of analysis. The sensitivity of the method is generally such that dilution of the sample solution will bring the concentration of the interfering element within the range where L-cysteine will reduce its interference to a negligible level.

Table 13 shows that the behaviour of hydride forming elements is different from that of transition elements. It appears that there is relatively little interference from these hydride-forming elements under the conditions of the reduction reaction, except for selenium. In fact, L-cysteine appears to inhibit the formation of germane at high concentrations of selenium. Surprisingly, tin shows essentially no interference, even though the conditions for the generation of stannane are essentially the same as for the generation of germane.

Table 13
Recoveries of Germanium from Solutions Containing Other Hydride-Forming Elements

Metal Ion Added	Amount Added		Germanium Recovery (%)	
			9.0 ml 1.00 ppb Ge in 0.04 M HNO_3 + 1.5 ml 6% m/V $NaBH_4$	9.0 ml 0.50 ppb Ge in 0.04 M HNO_3 and 0.4 % m/V L-cysteine + 2.0 ml 6% m/V $NaBH_4$
Sn(II)	0.5 ml	100 ppm	95	97
	1.0 ml	100 ppm	93	94
	0.5 ml	1000 ppm	98	103
	1.0 ml	1000 ppm	108	97
Pb(II)	1.0 ml	100 ppm	97	100
	0.5 ml	1000 ppm	-	100
	1.0 ml	1000 ppm	94	93
As(III)	0.5 ml	100 ppm	88	103
	1.0 ml	100 ppm	85	97
Sb(III)	0.5 ml	100 ppm	100	100
	1.0 ml	100 ppm	88	94
Se(IV)	0.5 ml	10 ppm	85	100
	1.0 ml	10 ppm	83	100
	0.5 ml	100 ppm	88	69
	1.0 ml	100 ppm	95	39
	0.5 ml	1000 ppm	48	26
	1.0 ml	1000 ppm	25	10
Te(IV)	0.5 ml	100 ppm	98	100
	1.0 ml	100 ppm	98	94

Interference effects from the sample matrix were also compared in the absence and presence of interference reducing agent. As shown in Figure 38, the signal of 1.8 ng ml^{-1} germanium in a solution of Open Hearth Iron 55E was severely suppressed by the sample matrix in the absence of interference reducing agent (B). However, with 0.4% L-cysteine dissolved in the sample solution, the matrix interferences were eliminated and thus a signal (A) corresponding to a recovery of 100% was obtained. Similar interference reduction by solid L-cystine was obtained in the determination of germanium in a copper matrix. Germanium in "Benchmark" Copper II was undetected as shown in Figure 39 (D), and therefore germanium standard was spiked into this sample solution so that it contained 1.0 ng ml^{-1} of germanium. The signals from germanium were compared in the presence (A) and absence (E) of L-cystine. With 0.4 g solid L-cystine, the suppressing effects due to the sample matrix were eliminated and the signal from 1.0 ng ml^{-1} germanium was completely recovered. Compared with the signal from 1.0 ng ml^{-1} germanium standard solution (B), the recovery of Ge from the sample was 105%.

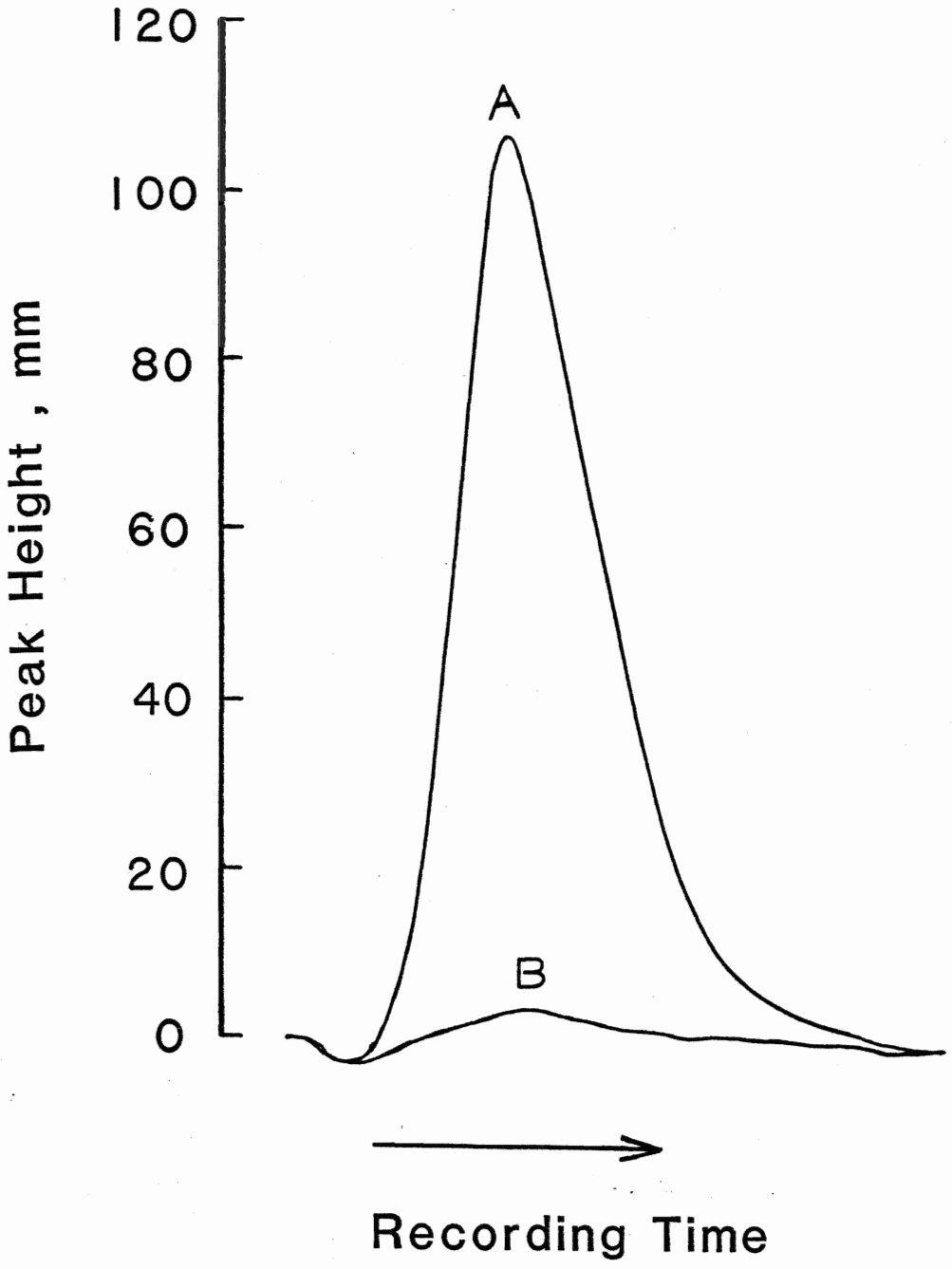

Figure 38. Comparison of the signals of 1.8 ng ml^{-1} Ge in a solution of Open Hearth Iron 55E in the presence (A) and absence (B) of L-cysteine

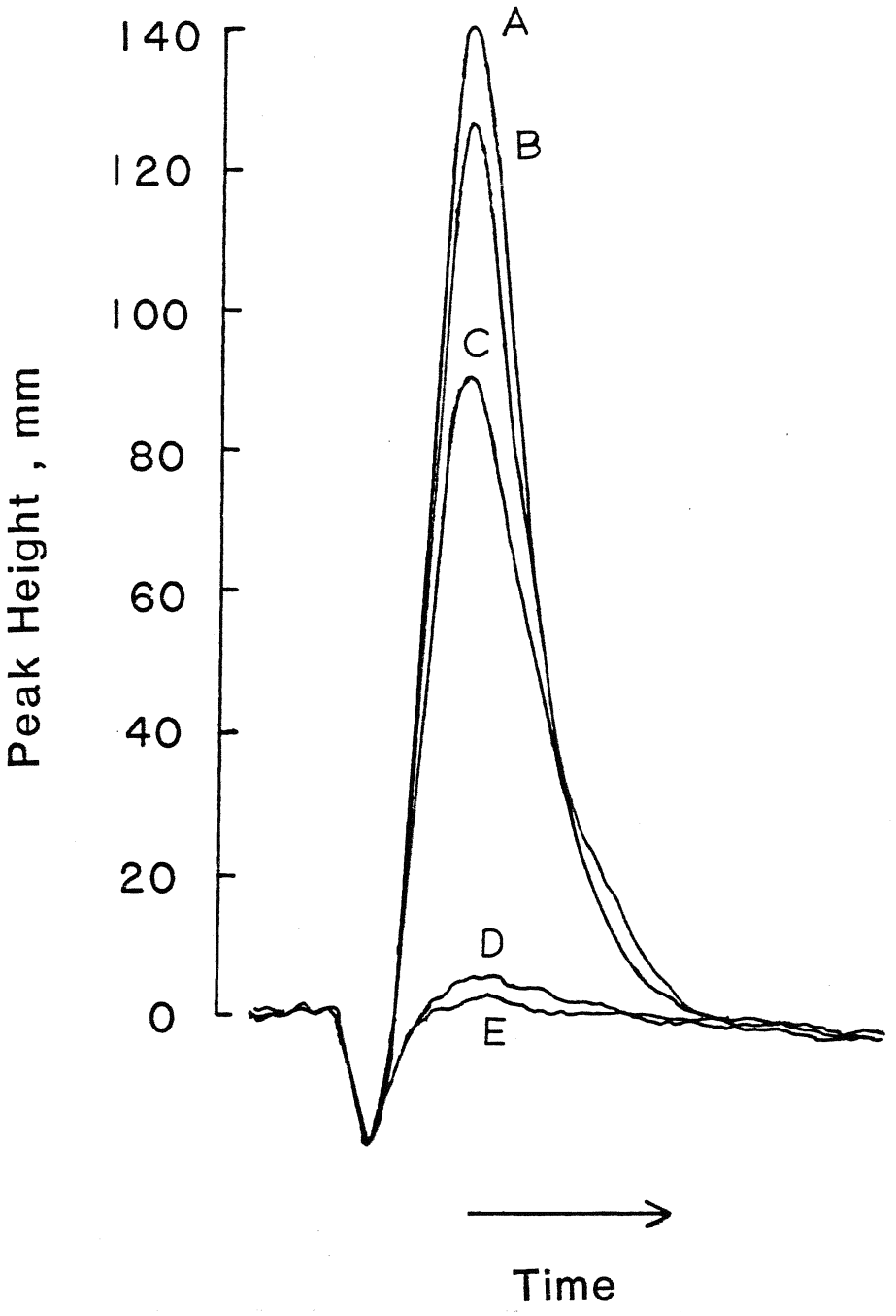

Figure 39. Reduction of interference from copper matrix by L-cystine
A-1.0 ng ml^{-1} Ge in " Benchmark " Copper II, with L-cystine. B-1.0 ng ml^{-1} Ge standard solution, with L-cystine. C-1.0 ng ml^{-1} G e standard solution, without L-cystine. D- " Benchmark " Copper II, with L-cystine. E-1.0 ng ml^{-1} Ge in " Benchmark " Copper II, without L-cystine.

Table 14. Effect of some sulphur and/or nitrogen containing compounds on germanium signals and interferences

Reagents Used	Relative Peak Height of Ge Signals	Recovery (%) of Ge Signals in the Presence of				
		1.0 ppm Ni	10 ppm Ni	100 ppm Cu	500 ppm Cu	100 ppm Co
none	100	8	0	10	0	0
thiourea	110	-	90	105	-	-
urea	90	-	0	14	-	-
$Na_2S_2O_3$	40-50	-	65-85	50-75	-	-
NH_2OHCl	65-75	-	60	55	-	-
penicillamine	170	100	65	-	70	65

Other possible interference reducing agents were also tried. These included thiourea, urea, $NH_2OH.HCl$, $Na_2S_2O_3$ and penicillamine. To save time, approximately 0.4 g solid reagents were directly added into the reaction vessel prior to the addition of germanium solution, interfering solution, and $NaBH_4$ solution. The effects on germanium signals and interference reduction are summarized in Table 14. It is interesting to point out the distinctive effects caused by thiourea and urea. Although the reducing property of thiourea could be thought to be part of the reason for interference reduction, a simple qualitative test indicated that this is unlikely to be true. Two mixture solutions, $Fe(NO_3)_3$ with thiourea and $Fe(NO_3)_3$ with urea, were tested by NH_4SCN solution. A red color appeared in both solutions, indicating that Fe(III) was not reduced to Fe(II). It is also important to note that there is also an acidity effect involved in the cases of $NH_2OH.HCl$ and $Na_2S_2O_3$. The pH values are shown in Table 15. The significant change of pH of the solution with the addition of $NH_2OH.HCl$ might cause the germanium signal to change. Therefore, to study the sole effect of interference reduction, adjustment of the pH of the solutions is recommended.

Table 15. pH of solutions with the addition of some reagents

Solution	pH values
1.0 ng ml^{-1} Ge in 0.04 M HNO_3	1.33
4% (m/V) $NaBH_4$ in 0.1 M NaOH	12.88
5.0 ml of 1.0 ng ml^{-1} Ge in 0.04 M HNO_3 (1) + 1.0 ml of 4% $NaBH_4$ in 0.1 M NaOH (2)	9.30
(1) + (2) + 0.1 g thiourea	9.31
(1) + (2) + 0.5 g thiourea	9.30
(1) + (2) + 0.05 g urea	9.34
(1) + (2) + 0.4 g urea	9.32
(1) + (2) + 0.05 g NH_2OHCl	8.26
(1) + (2) + 0.5 g NH_2OHCl	5.11
(1) + (2) + 0.1 g $Na_2S_2O_3$	9.16
(1) + (2) + 0.7 g $Na_2S_2O_3$	8.88
(1) + (2) + 0.1 g L-cystine	9.25
(1) + (2) + 0.5 g L-cystine	9.14
(1) + (2) + 0.05 g L-cysteine	8.81
(1) + (2) + 0.3 g L-cysteine	8.15
(1) + (2) + 0.3 g thiosemicarbazide ($NH_2CSNHNH_2$)	9.15

In addition to L-cystine and L-cysteine, other amino acids, such as glycine, alanine, valine, leucine, and histidine, were investigated in terms of their effects on sensitivity and interference reduction in the determination of germanium. Cobalt(II), copper(II), and nickel(II) were chosen as interfering ions, and approximately 0.4 g of the solid amino acid was used to reduce interference. The efficiencies of these amino acids in reducing the interferences are illustrated in Figures 40-42. As we can see from the figures, both peak heights of germanium signals and the interference reduction effect decreased from glycine to leucine, with the size of the alkyl group connected with the amino group (R-$CH(NH_2)$-COOH) (where R= -H, $-CH_3$, $(CH_3)_2CH$-, and $(CH_3)_2CHCH_2$-). Histidine (R=

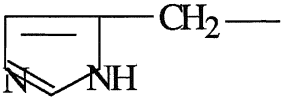

), on the other hand, proved very effective in reducing the interference effects, although it caused a decrease of germanium sensitivity by approximately 10%. In fact, histidine approved more efficient than L-cysteine and L-cystine in the reduction of interference from Ni(II) if we compare Figures 36 and 42. It should be noted that the optimum instrumental and hydride formation conditions for performing these experiments were obtained in the absence of amino acids. In the presence of amino acids, the optimum conditions may not be the same, and there may be potential to achieve better sensitivity and interference reduction effects. Nevertheless, the results indicated that appropriate amino acids, for example histidine, were promising interference reducing agent in germanium determinations by hydride generation.

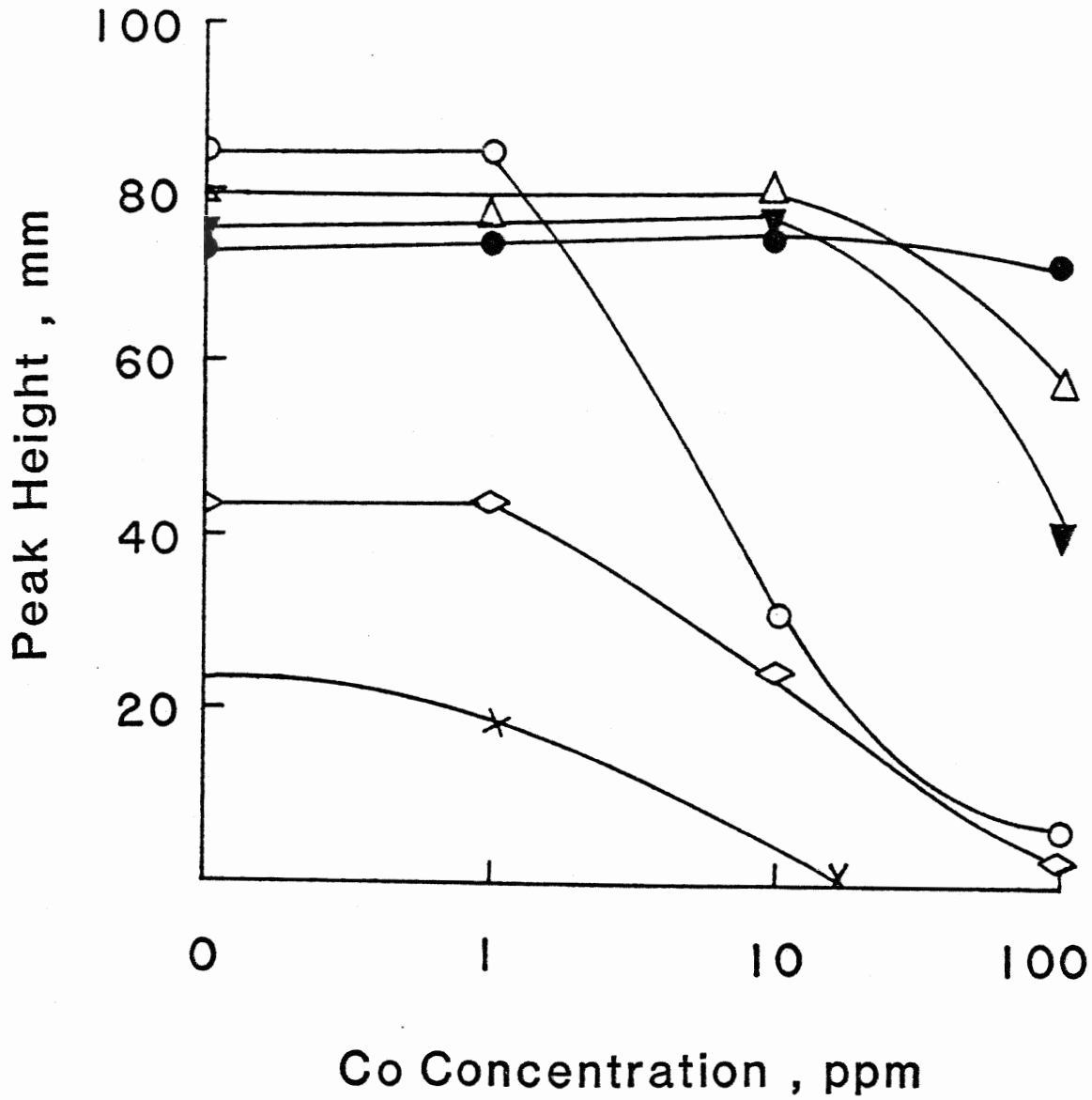

Figure 40. Effect of amino acids on signals from 5.0 ng ml^{-1} Ge in the presence of Co(II)
○ - without amino acid. ● - with 0.4 g histidine.
△ - with 0.4 g glycine. ▼ - with 0.4 g alanine.
◇ - with 0.4 g valine. × - with 0.4 g leucine.

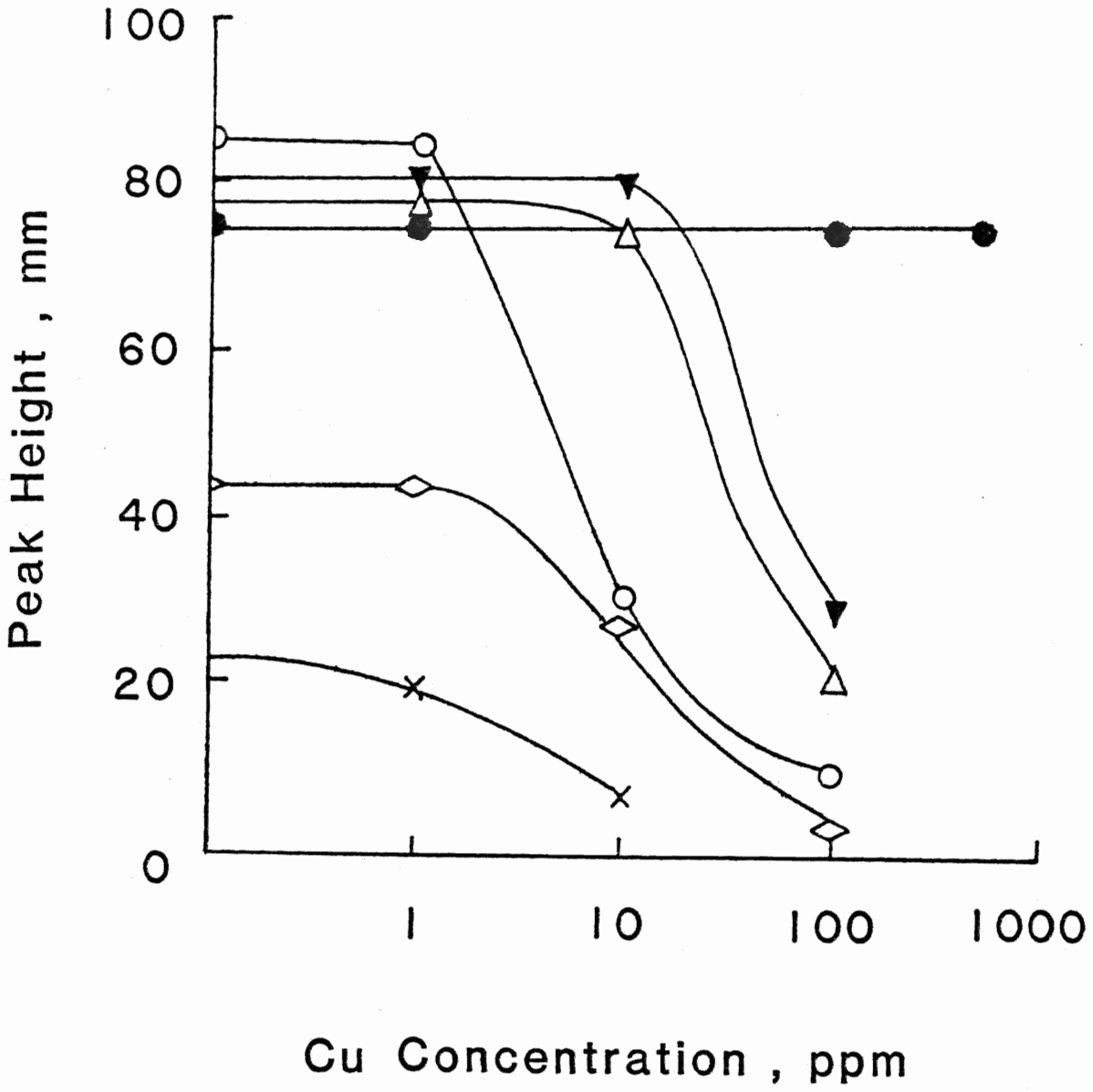

Figure 41. Effect of amino acids on signals from 5.0 ng ml^{-1} Ge in the presence of Cu(II)
○- without amino acid. ●- with 0.4 g histidine.
△- with 0.4 g glycine. ▼- with 0.4 g alanine.
◇- with 0.4 g valine. ×- with 0.4 g leucine.

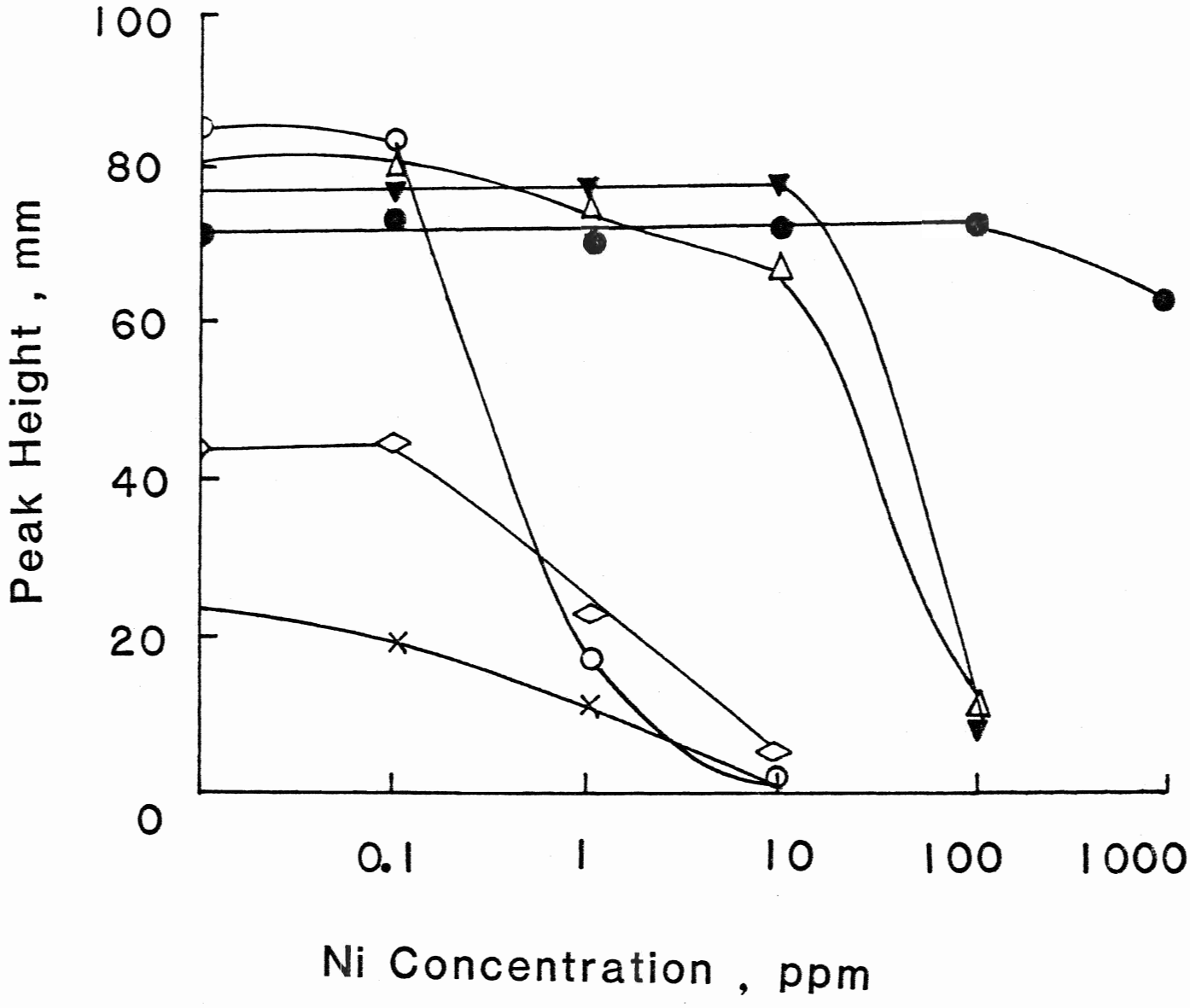

Figure 42. Effect of amino acids on signals from 5.0 ng ml^{-1} Ge in the presence of Ni(II)
○ - without amino acid. ● - with 0.4 g histidine.
△ - with 0.4 g glycine. ▼ - with 0.4 g alanine.
◇ - with 0.4 g valine. × - with 0.4 g leucine.

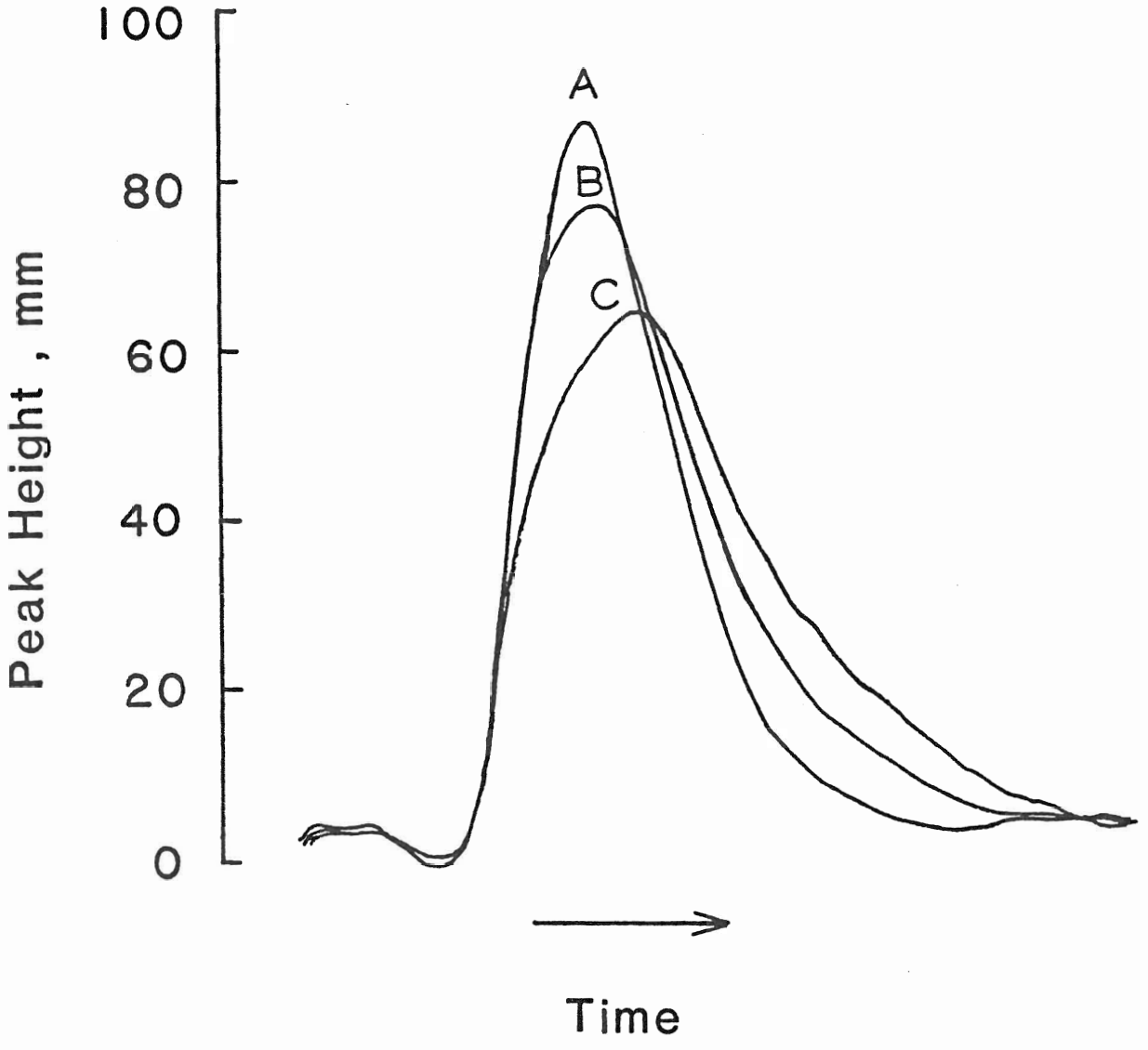

Figure 43. Comparison of peak profiles of 5.0 ng ml^{-1} G e in the presence of alanine(B), valine(C), and absence of amino acid(A)

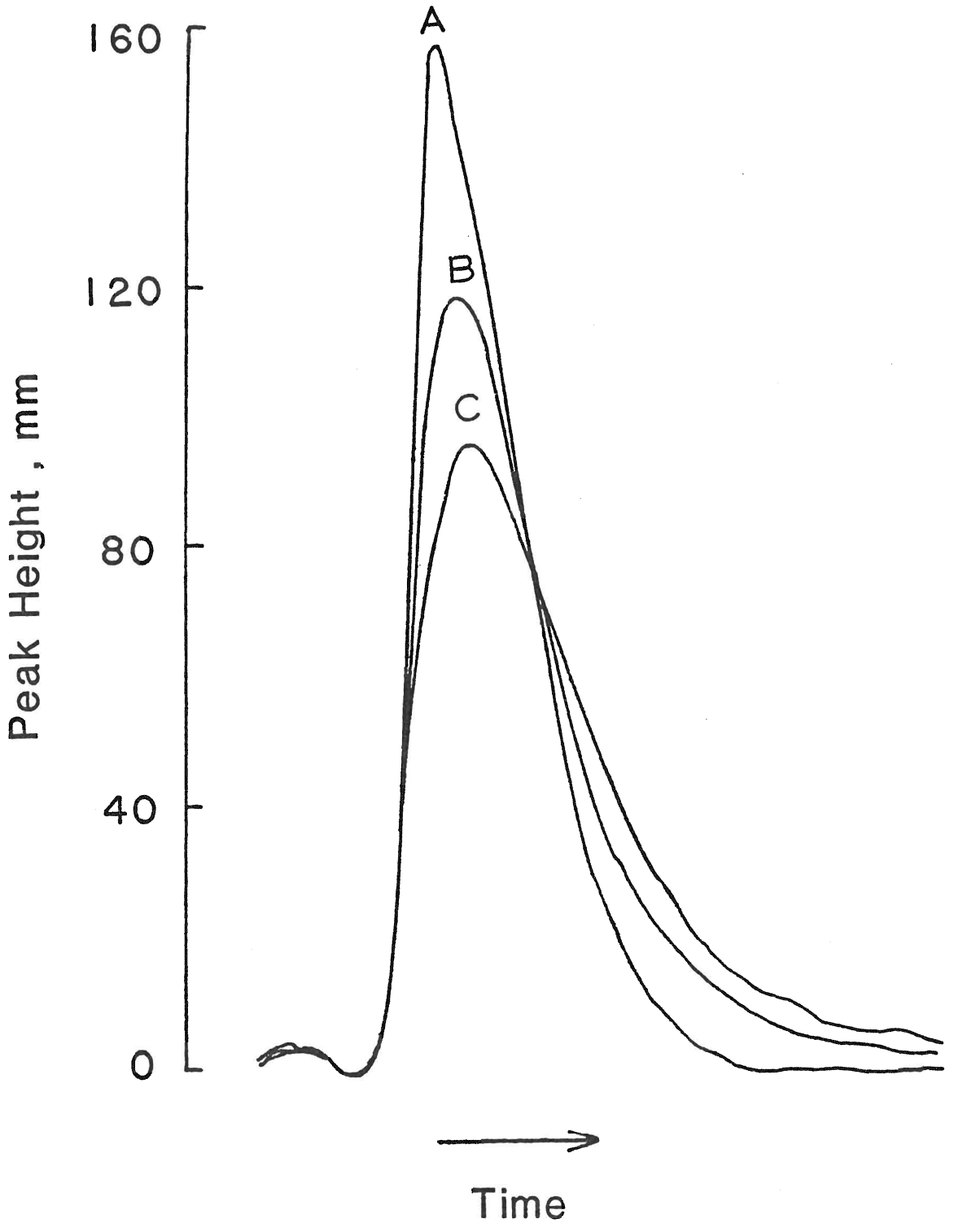

Figure 44. Comparison of peak profiles of 5.0 ng ml^{-1} Ge in the presence of L-cysteine(A), L-cystine(B), and absence of amino acid(C)

Table 16. Peak height and peak area of germanium signals

	Peak Height (cm)		Peak Area (cm^2)	
	Individual	Mean	Individual	Mean
Without	10.0		28.9	
Amino Acid	10.0		30.6	
	12.2	10.8	34.9	31.5
With	12.2		33.1	
Alanine	8.9	10.6	32.6	32.8
With	7.4		33.0	
Valine	7.4	7.4	32.4	32.7
With	16.8		41.2	
L-cysteine		16.8	38.7	40.0
With	12.2		40.8	
L-cystine		12.2	42.6	41.7
Without	10.1		36.5	
Addition		10.1	42.7	39.6

Figure 43 shows the peak profiles of germanium signal in the presence and absence of alanine and valine. In the presence of alanine (B) or valine (C), the peaks of germanium signals become lower and wider compared with that in the absence of amino acid (A). However, there was no significant difference in peak areas. Similar effects were obtained while comparing the absence (C) and presence of L-cystine (B) and L-cysteine (A) in germanium solution as shown in Figure 44. Peak height and peak area corresponding to the signals shown in Figures 43 and 44 are listed in Table 16. These results and the peak profiles have clearly shown the possible kinetic effect. Thus, the results imply that the effects of amino acids on germanium signals are probably not only dynamic, but also kinetic, during the hydride generation and transportation processes.

Qualitative Tests for Interference Studies

A series of qualitative reactions were performed in order to give a possible explanation of interference reduction mechanism. For simplicity, the reactions and the corresponding observations are tabulated in Table 17. As can be seen from the NH_4SCN test of iron, Fe(III) was reduced to Fe(II) in the presence of L-cysteine. Cu(II) was also possibly reduced to Cu(I). Ni(II) and Co(II), having no intermediate valency, were not reduced by L-cysteine.

Table 17. Some qualitative reactions and the observations

Reaction	Without cystine or cysteine	With L-cystine	With L-cysteine
1000 μg ml^{-1} $Fe(NO_3)_3$ (1)	yellow, clear	yellow, clear	intermediate blue quickly disappeared
(1) + NH_4SCN	red	red	colorless, clear
(1) + $NaBH_4$	black ppt	black ppt	no ppt, clear
(1) + $K_3Fe(CN)_6$	yellow, clear	green, clear	blue, suspension
1000 μg ml^{-1} $Cu(NO_3)_2$ (2)	blue	blue	pale-yellow, suspend
(2) + $NaBH_4$	black ppt	black ppt	clear yellow solution (disappeared after 30 min.), no ppt
1000 μg ml^{-1} $Ni(NO_3)_2$ (3)	green, clear	green, clear	green, clear
(3) + $NaBH_4$	black ppt	at first no ppt, ppt appeared with more $NaBH_4$ added	at first no ppt, twice amounts of $NaBH_4$ needed to cause black ppt
1000 μg ml^{-1} $Co(NO_3)_2$ (4)	red, clear	red, clear	red, clear
(4) + $NaBH_4$	black ppt	black ppt	about twice amounts of $NaBH_4$ to cause black ppt.

Note: ppt -- precipitation

This may not be relevant to the interference reduction. However, in the presence of L-cysteine, the absence of precipitation, while $NaBH_4$ was added to the transition metal ion solutions, may be an indication of complex reactions between L-cysteine and transition metal ions.

UV/Visible Spectroscopic Study of Interference

Since a conjugate system exists in amino acids, the UV/visible spectrum is usually available. If amino acids complex with metal ions, the UV/visible absorption wavelength should be shifted. Therefore, wavelength scans on the UV/visible spectrometer may give useful results for interference studies.

Figures 45 and 46 compare the wavelength scans of 200 $\mu g\ ml^{-1}$ $Cu(NO_3)_2$ (Figure 45) and 20 $\mu g\ ml^{-1}$ $Cu(NO_3)_2$ (Figure 46) in the presence and absence of L-cysteine in aqueous solutions. In the presence of L-cysteine, the absorbances of the Cu(II) solutions at 301.3 nm were significantly increased and the maximum absorbances were probably shifted to a lower wavelength. Slight effects of UV/visible absorption of $Fe(NO_3)_3$ in the absence and presence of L-cysteine were also observed. However, in the case of $Co(NO_3)_2$, the presence of L-cysteine did not change the wavelength for the maximum UV/visible absorption (Figure 47). The wavelength scans of germanium (Figure 48) and tin (Figure 49) solutions also indicated that the presence of L-cysteine had no significant effect on UV/visible absorption wavelengths.

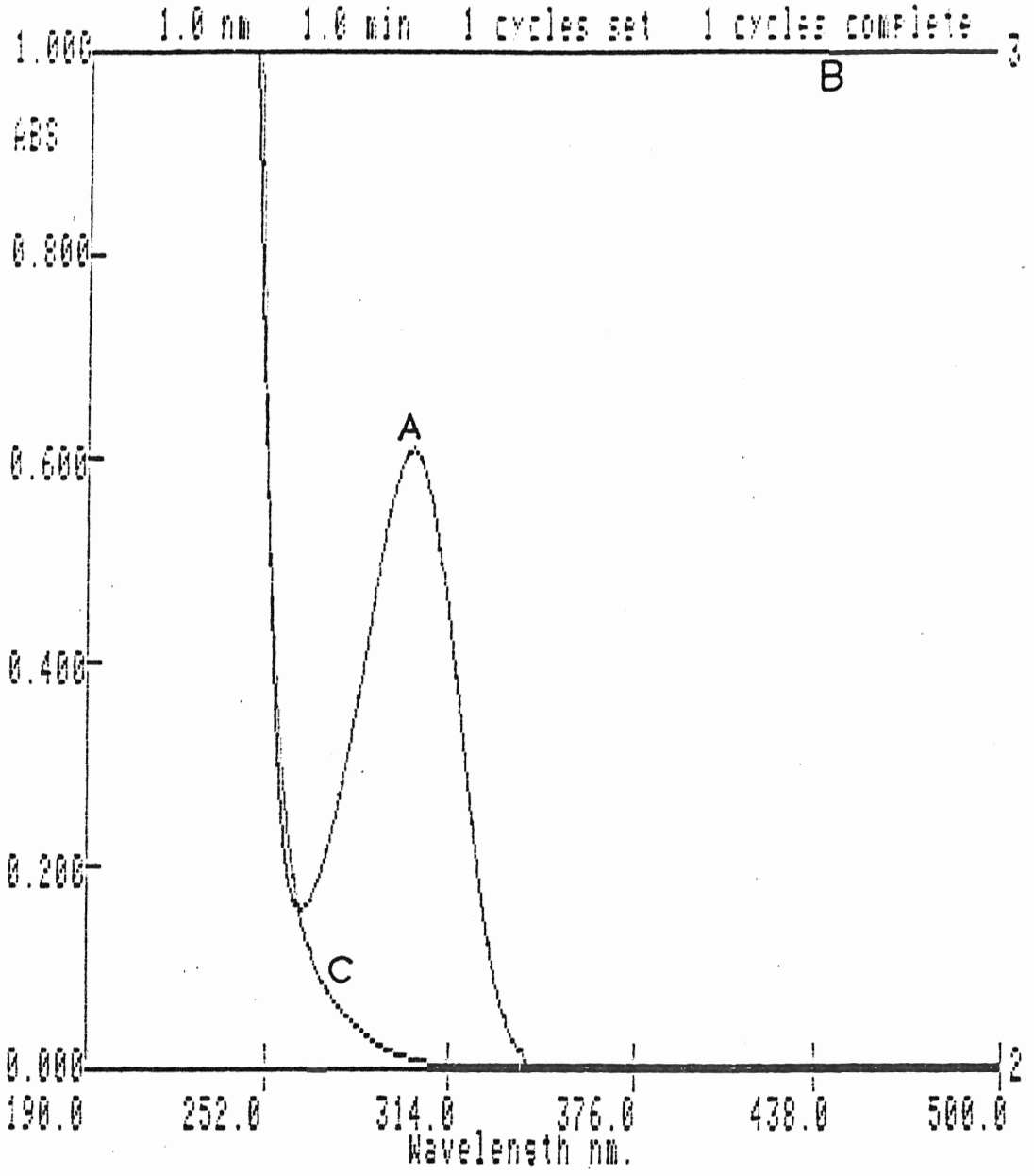

Figure 45. UV/Visible spectra
A-200 μg ml^{-1} Cu^{2+} in H_2O
B-200 μg ml^{-1} Cu^{2+} in 1.4% L-cysteine aqueous solution. C-1.4% L-cysteine aqueous solution.

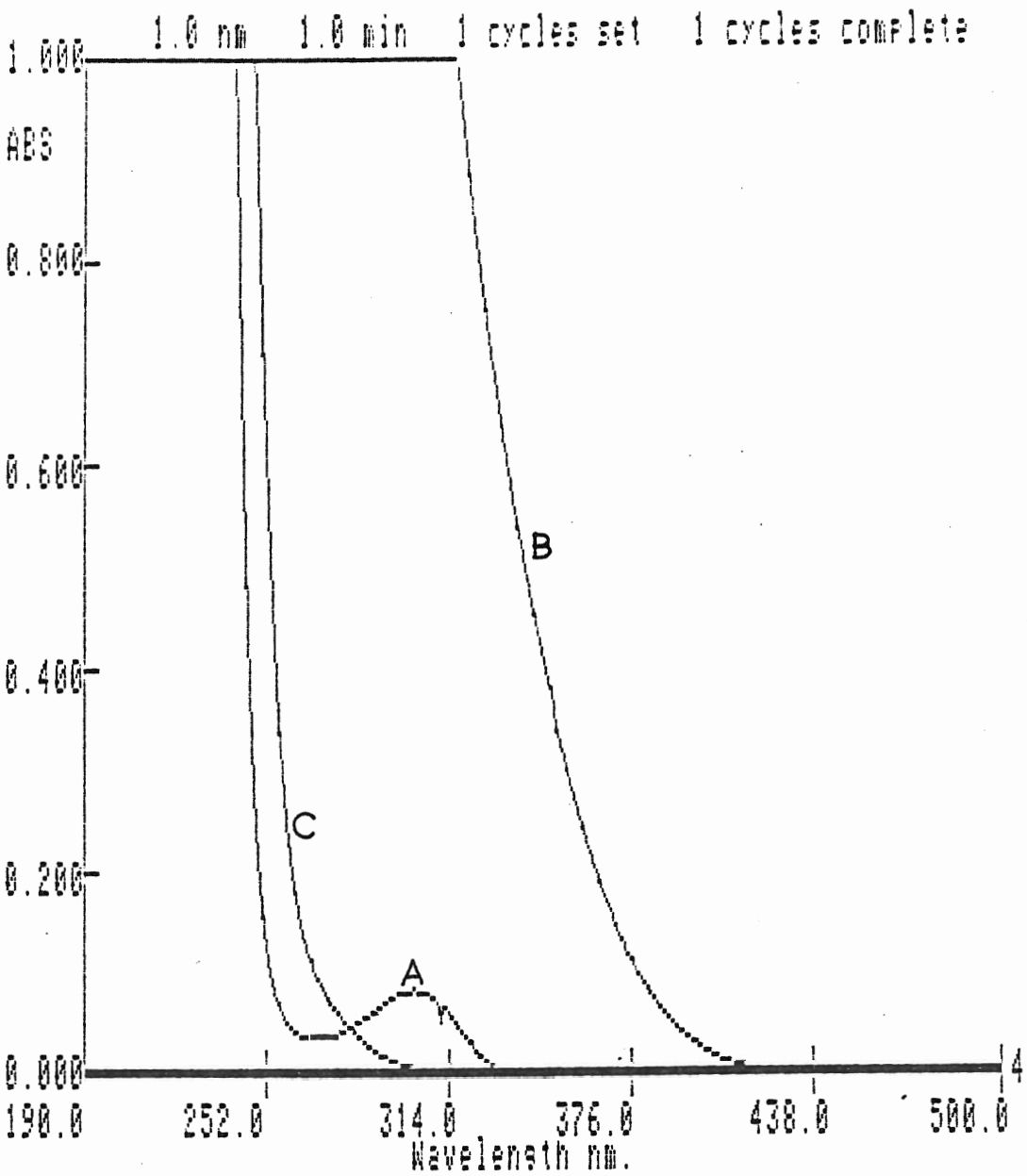

Figure 46. **UV/Visible spectra**
A-20 μg ml^{-1} Cu^{2+} in H_2O
B-20 μg ml^{-1} Cu^{2+} in 1.4% L-cysteine aqueous solution. C-1.4% L-cysteine aqueous solution.

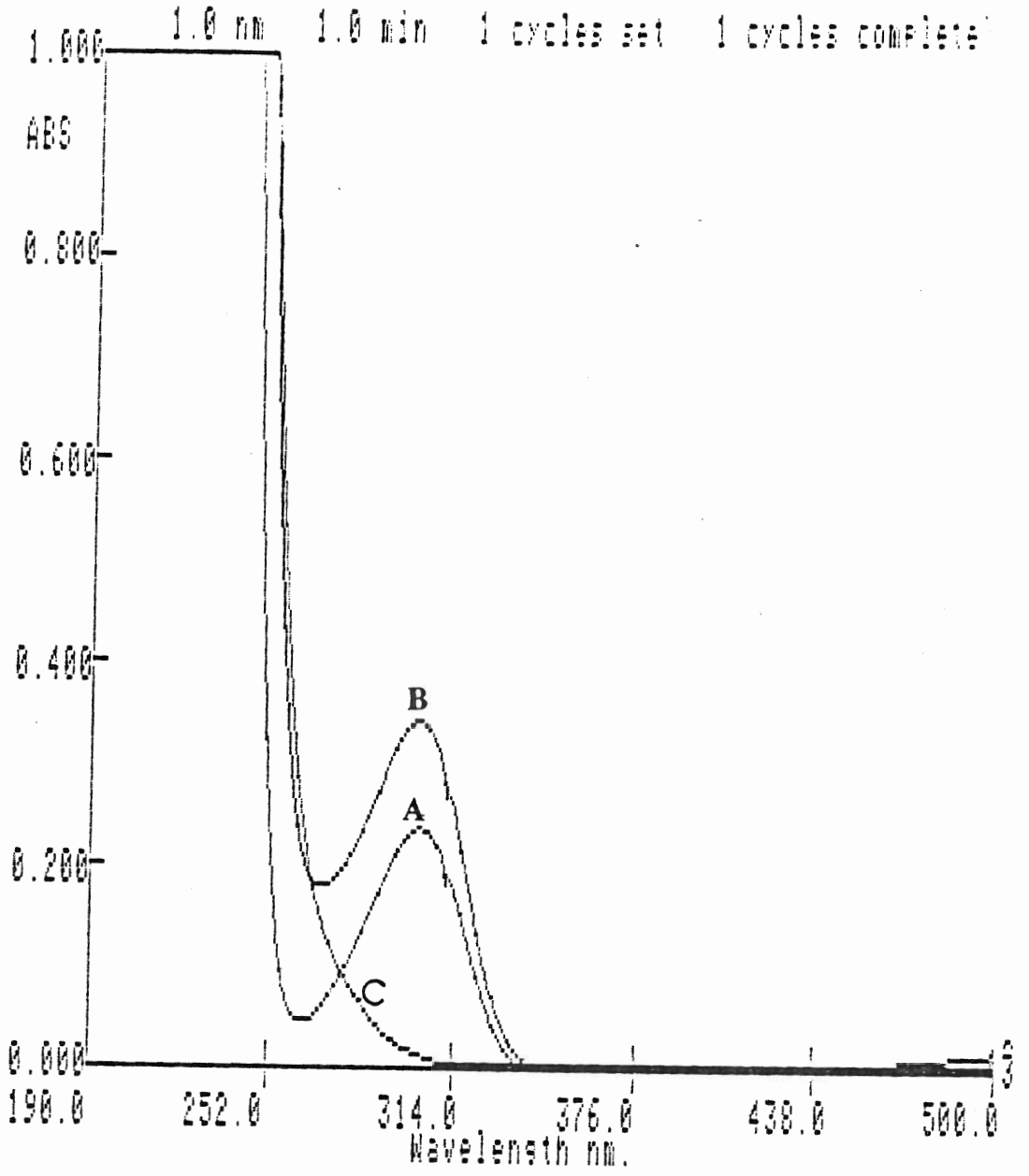

Figure 47. UV/Visible spectra.
A - 20 μg ml^{-1} Co^{2+} in H_2O.
B - 20 μg ml^{-1} Co^{2+} in L-cysteine aqueous solution.
C - 1.4% L-cysteine aqueous solution.

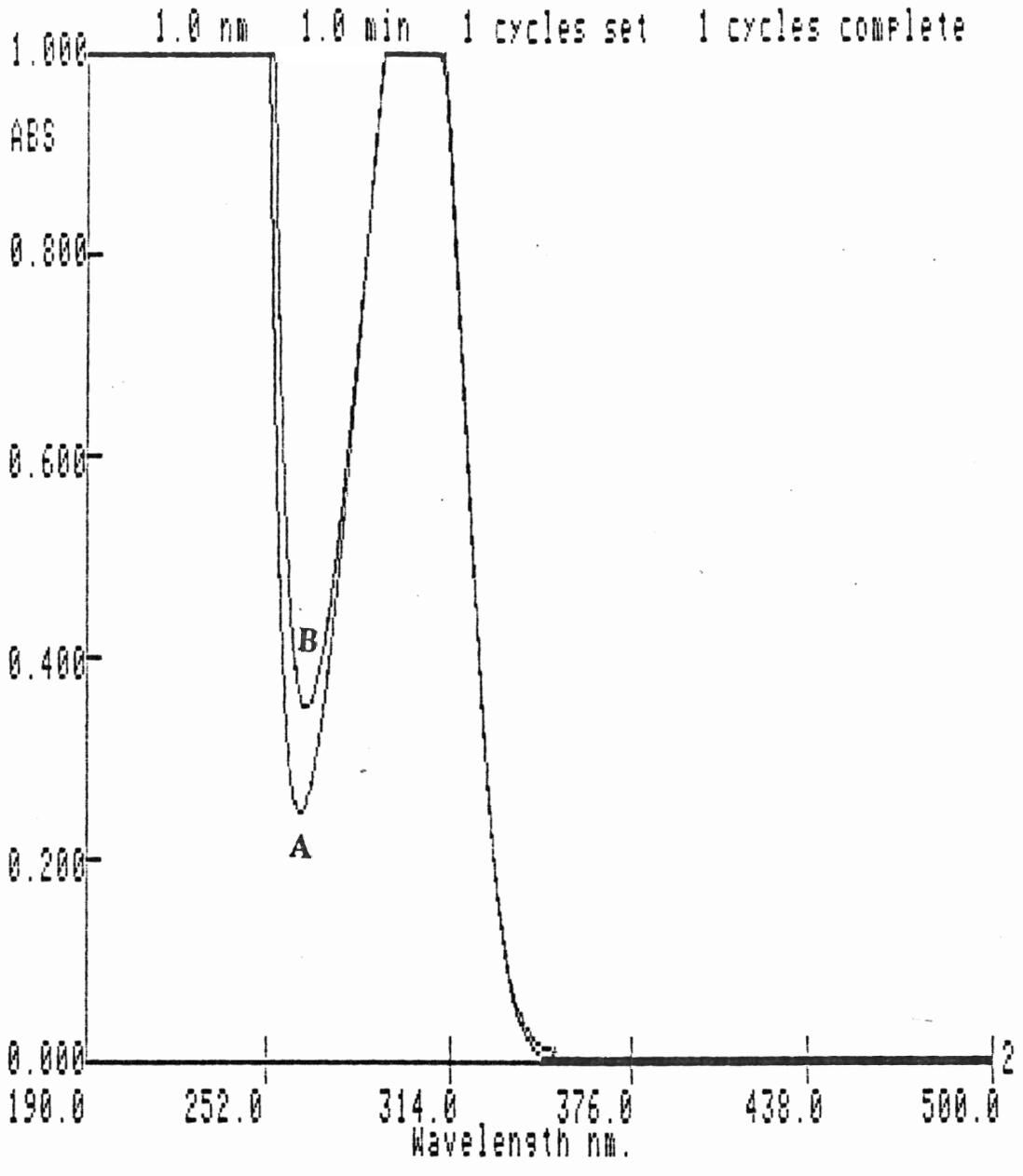

Figure 48. UV/Visible spectra.
A - 2 μg ml^{-1} Sn in H_2O.
B - 2 μg ml^{-1} Sn in L-cysteine aqueous solution.

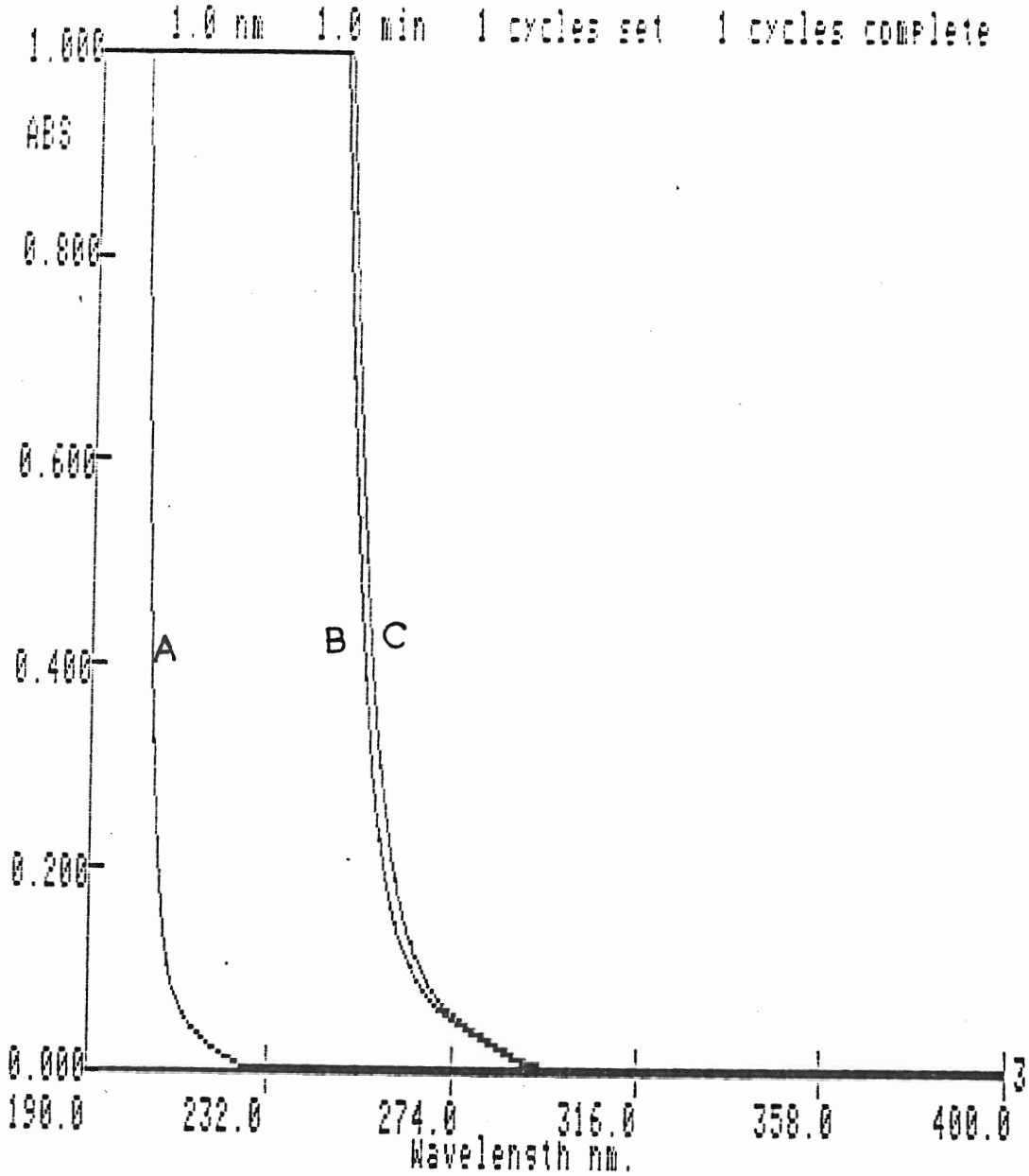

Figure 49. UV/Visible spectra
A-1 μg ml^{-1} Ge in H_2O.
B-1 μg ml^{-1} Ge in 1.4% L-cysteine aqueous solution. C-1.4% L-cysteine aqueous solution.

These results may not explain the interference effect and its reduction by L-cysteine. However, they imply that the interaction among analyte, interfering ions, and interference reducing agents are not significant before the hydride reduction process. This led us to concentrate on the interference reduction during the hydride formation and transportation periods.

Determination of Germanium in Standard Reference Materials

Determination of germanium in the "Benchmark" Copper I by the standard addition method (5 points) revealed that the germanium concentration was below the detection limit which, at the dilution employed in this determination, was 0.07 $\mu g\ g^{-1}$ (in the solid sample). The sample spiked with 0.5 μg of germanium was determined to have a concentration of $0.52\pm0.02\ \mu g\ g^{-1}$ by standard additions (5 points). This determination is consistent with a germanium concentration of less than $0.07\ \mu g\ g^{-1}$. Figure 50 illustrates the calibration and standard addition curves for the determination of germanium in the Open Hearth Iron 55E. The germanium content in the sample determined by standard addition (5 points), was $18.3\pm0.7\ \mu g\ g^{-1}$ and from a calibration curve (5 points) was $18.6\pm0.6\ \mu g\ g^{-1}$. The sample spiked with 20 μg of germanium gave a recovery of 103% based on a 5 point standard addition determination. The standard and sample solutions were made up to 0.4% (m/V) L-cysteine.

RSD

A series of determinations of a solution containing 0.10 ng ml^{-1} of germanium is shown in Figure 51. A relative standard deviation of 3.1 % was calculated based on the peak heights of these seven replicate determinations.

Detection Limit

With a 9.0 ml sample, the detection limit for the determination of germanium, defined as three times the noise, is 20 pg ml^{-1} or 180 pg for a 9.0 ml sample of the analyte in the presence of 0.4% (m/V) L-cysteine.

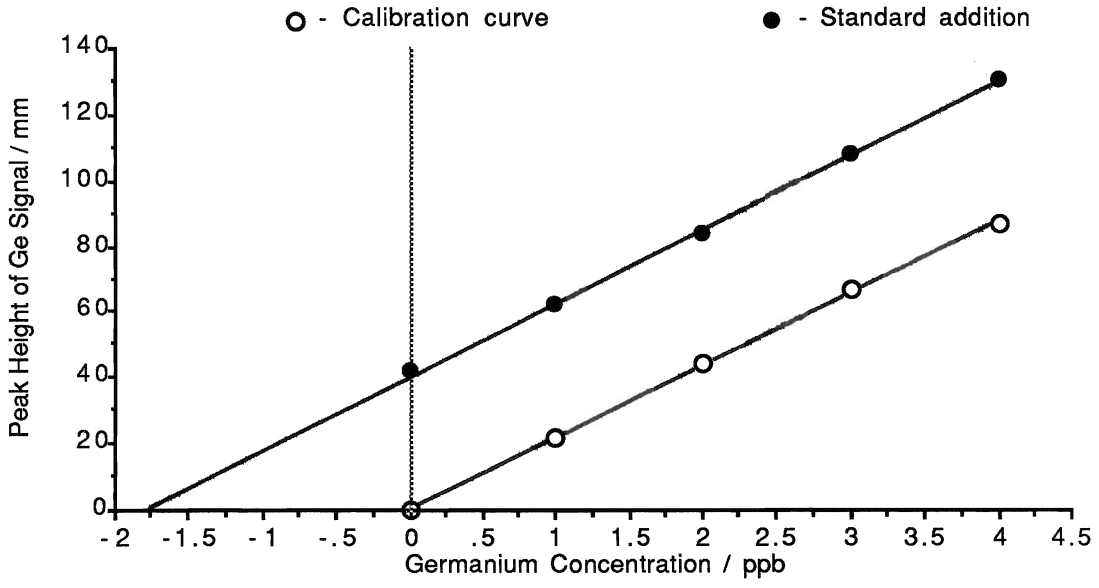

Figure 50. Comparison of calibration and standard addition curves in the determination of germanium in Open Hearth Iron 55E

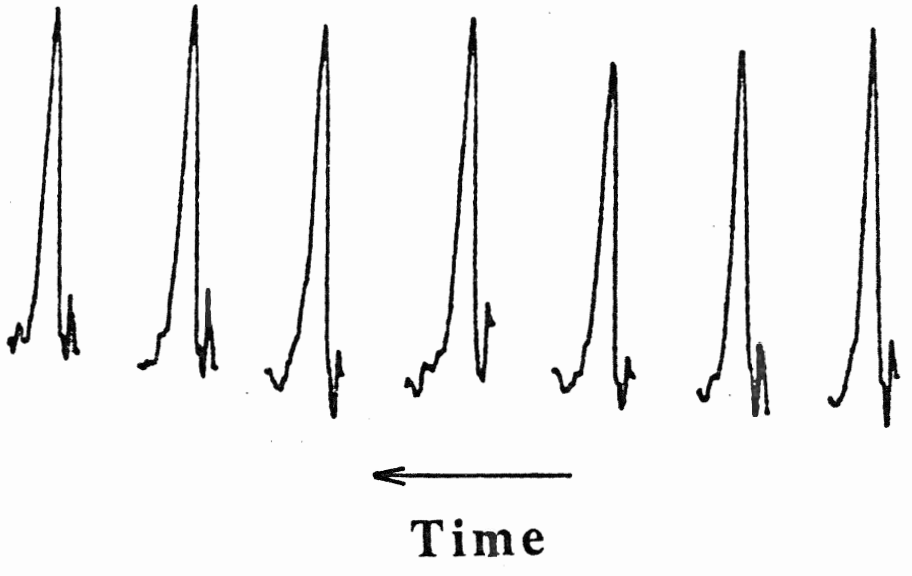

Figure 51. Seven replicate determinations of 0.10 ng ml^{-1} Ge in 0.015 M HNO_3 and 0.4% L-cysteine

IV. Determination of Lead

Comparison of Reaction Media

The optimum conditions for plumbane generation were studied with the gas flowing system. Choosing reaction media is one of the most important and critical steps. Reaction media containing acid and oxidizing agents were investigated as shown to be necessary by Jin and Taga (260), who studied reaction media for plumbane formation by using a continuous-flow hydride generator coupled with an AAS system.

HNO_3-H_2O_2, HNO_3-$(NH_4)_2S_2O_8$, and malic acid-$K_2Cr_2O_7$ systems were compared as hydride formation reaction media. In the HNO_3-H_2O_2 reaction system, the concentrations of both nitric acid and hydrogen peroxide had very critical effects on lead signals. Reproducible signals were difficult to obtain unless critical controls of HNO3 and H_2O_2 concentrations were employed. This appeared impractical in terms of simplicity, accuracy and speed of sample analysis.

The HNO_3-$(NH_4)_2S_2O_8$ reaction system was studied next in which the concentrations of HNO_3, $(NH_4)_2S_2O_8$, and $NaBH_4$ were varied. As shown in Figures 52 and 53, both nitric acid and ammonium persulphate concentrations affect the lead signal dramatically. Concentrations of 0.1 M HNO_3 and 5% (m/V) $(NH_4)_2S_2O_8$ were chosen as reaction media since the highest lead signals were achieved under these conditions. The response of lead signals with increasing sodium tetrahydroborate concentration is shown in Figure 54. Solutions of 5.0 ml of 10.0 ng ml^{-1} lead and 1.0 ml $NaBH_4$ in 0.1 M NaOH were used to carry out these experiments.

Maximum and identical lead signals were obtained at $NaBH_4$ concentration between 8% to 12% (m/V). Thus, 10% $NaBH_4$, stabilized with 0.1 M NaOH, was applied as the reducing agent for plumbane production from the reaction solutions of 0.1 M HNO_3 and 5% $(NH_4)_2S_2O_8$.

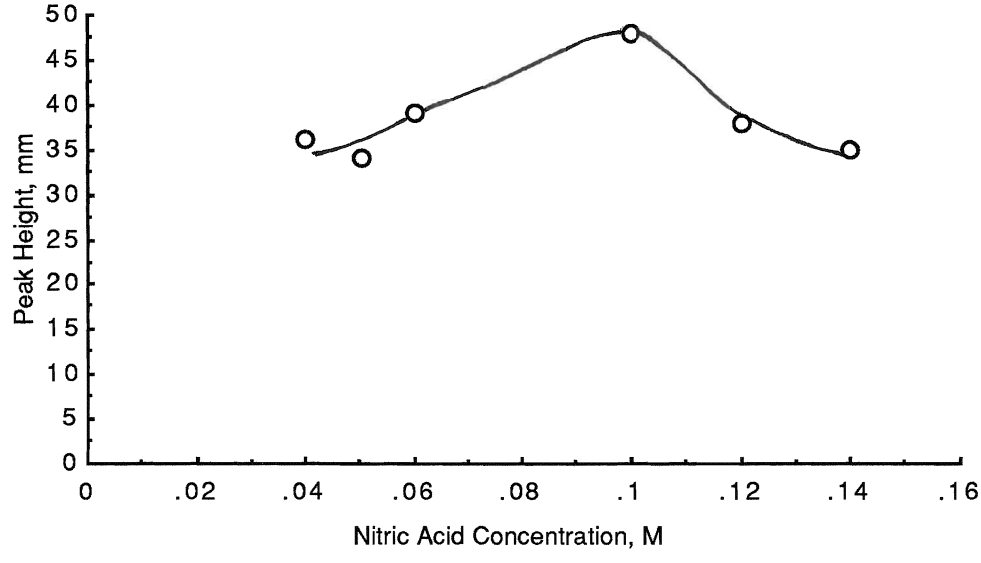

Figure 52. Effect of HNO_3 on lead signal

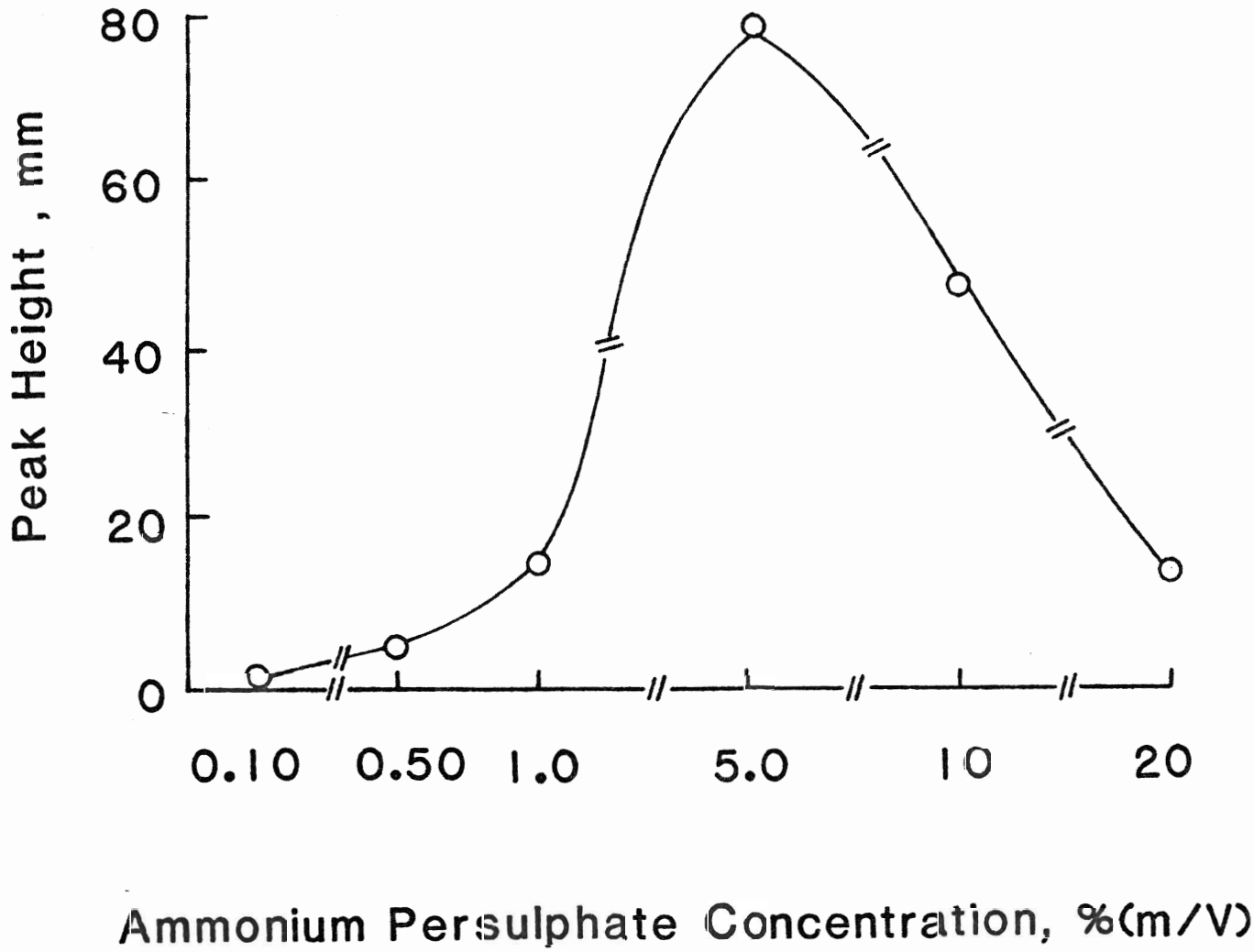

Figure 53. Effect of ammonium persulphate concentration on lead signal (5.0 ml 10.0 ng ml^{-1} Pb)

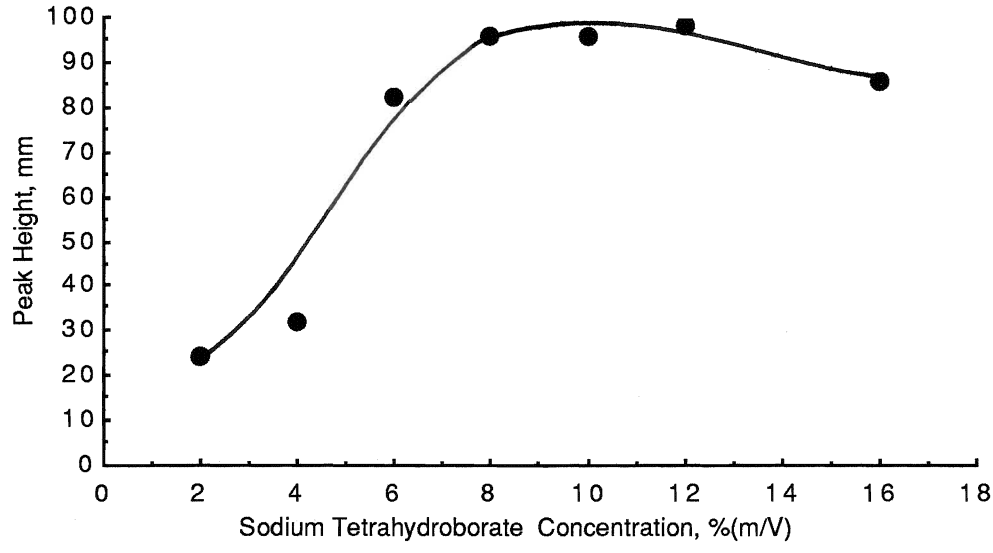

Figure 54. Effect of $NaBH_4$ concentration on lead signals.

The malic acid-potassium dichromate reaction system was found to give better reproducibility. The concentrations of the reagents involved, malic acid, $K_2Cr_2O_7$, and $NaBH_4$, were also investigated. Figure 55 illustrates the effect of malic acid concentration on lead signals. The highest lead signals appeared at malic acid concentrations within the range of 0.05 M to 0.07 M. Lead signals decreased beyond this range. Concentration of potassium dichromate, however, showed more critical effects on lead signals. As can be seen from Figure 56, the highest lead signal was obtained at $K_2Cr_2O_7$ concentration of 0.30% (m/V). A rapid decrease on lead signal appeared either above or below this level. Therefore, a 0.30% $K_2Cr_2O_7$ concentration was selected and analyte solutions were made up to this concentration in $K_2C_{r2}O_7$ so that the highest sensitivity was achieved and the uncertainty caused by $K_2Cr_2O_7$ concentration was avoided. While the increase in the concentration of malic acid, from 0.01 M to 0.10 M, had little effect on the pH of 0.2% $K_2Cr_2O_7$ solutions, the increase of $K_2Cr_2O_7$ concentration, from 0.05% to 2.0% (m/V), caused the pH continuously to increase as indicated in Table 18. At the given conditions, i.e., 0.060 M malic acid and 0.30% $K_2Cr_2O_7$, the initial pH of the solution, before the addition of $NaBH_4$, was 3.06. The effects of varying concentrations of reducing agent, $NaBH_4$, are shown in Figure 57. With the increase of $NaBH_4$ concentration from 2% to 12% (m/V), the signals from lead gradually increased and became identical at $NaBH_4$ concentration from 12% to 14%. A concentration of $NaBH_4$ of12% was thus chosen for all determinations with the malic acid-potassium dichromate system. Replacement of malic acid by tartaric acid gave similar results.

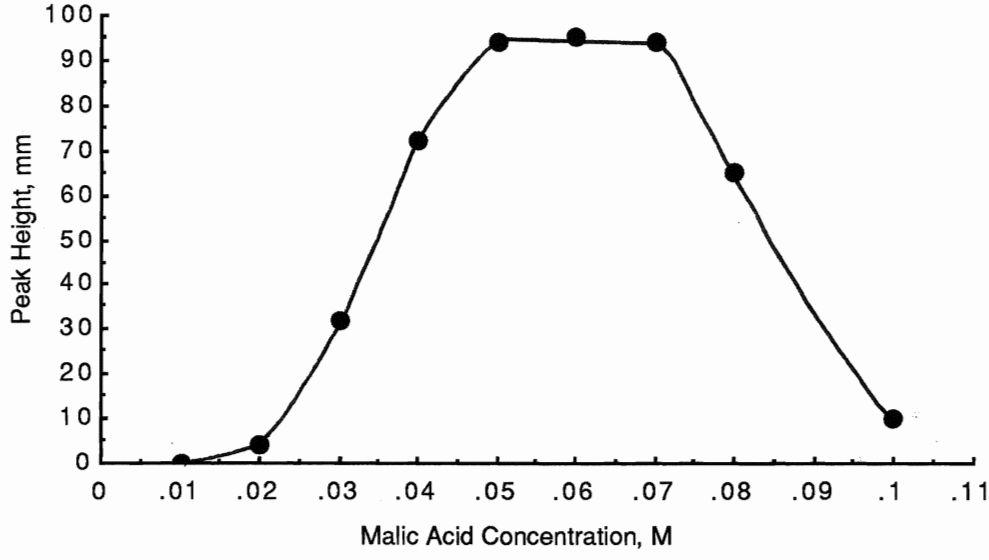

Figure 55. Effect of malic acid concentration on lead signals.
(0.3% (m/V) $K_2Cr_2O_7$ and 9% (m/V) $NaBH_4$)

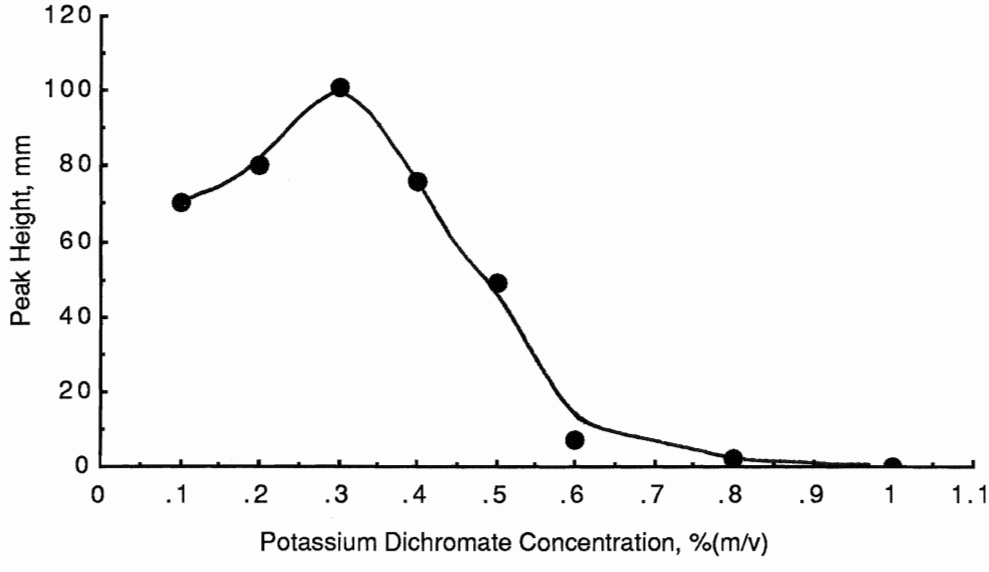

Figure 56. Effect of $K_2Cr_2O_7$ concentration on lead signals.
(0.06 M malic acid and 9% (m/V) $NaBH_4$)

Table 18. The pH values of lead containing solutions with increasing $K_2Cr_2O_7$ concentration in 0.06 M malic acid

$K_2Cr_2O_7$ Concentration, %(m/V)	pH Value
0.05	2.28
0.1	2.47
0.2	2.66
0.3	3.06
0.4	3.21
0.5	3.29
0.6	3.42
0.8	3.63
1.0	3.73
2.0	4.25

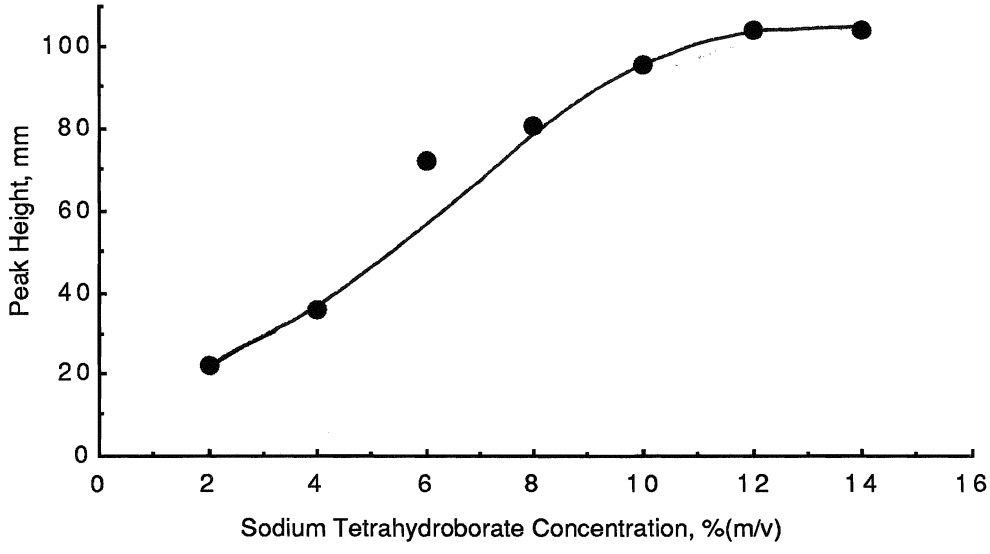

Figure 57. Effect of $NaBH_4$ concentration on lead signals.
(5.0 ml of 50.0 ng ml^{-1} Pb in 0.3% (m/V) $K_2Cr_2O_7$ and 0.06 M malic acid + 1.5 ml of $NaBH_4$ in 0.1 M NaOH)

Interference Studies

Interference effects from transition metal ions have proven very serious in the determination of lead as its hydride (260, 369-370, 380, 382, 386). However, no reference has been found that suggests a way to overcome the problem by using interference reducing agents until very recently (286). The extremely toxic reagent, NaCN, was reported to reduce the interference from Cu (II) to a level of 0.5 $\mu g\ ml^{-1}$. In an attempt to find a more efficient and less toxic interference reducing agent, a number of possible masking agents, chelating agents, or reducing agents were studied for interference reduction. Cu(II), Fe(II) and Ni(II) were chosen as interfering ions. The reaction media applied were 0.10 M HNO_3 and 0.50% $(NH_4)_2S_2O_8$. The results showed that many interference reducing agents used in the determination of most other hydride forming elements were not sufficient to reduce interference in lead determination. These reagents included EDTA, KI, KSCN, 1,10-phenanthroline, thiourea, sodium acetate, sodium oxalate, oxalic acid, salicylic acid, tartaric acid, semicarbazide, Na_3PO_4, NaH_2PO_4, and dibenzo-18-crown-6. It is interesting to note that amino acids, including L-cystine, L-cysteine, and histidine, did not reduce the interference from Ni, Cu, and Fe. Sodium citrate, ascorbic acid, penicillamine, dithizone, and thiosemicarbazide have been found to reduce interferences to a level where a 10-fold excess of interfering ions could be tolerated compared with those in the absence of interference reducing agents. The results of these reagents in reducing the interferences are summarized in Table 19. Although the interferences

from the transition metal ions studied were reduced, the effect was still severe, especially with Cu(II) solution.

With malic acid-potassium dichromate and tartaric acid-potassium dichromate, the interference effects from transition metal ions are also listed in Table 19. With these reaction media, the interferences were much less pronounced than with the nitric acid-ammonium persulphate reaction system. Interference from Cu(II) was the worst in all cases studied.

Determination of Lead in Tap Water

Since the interference from copper was problematic, a systematic decrease of lead signal in a copper-containing sample was studied. Figure 58 compares the calibration curve of lead standard solution and the standard addition curve of a water sample collected from copper pipes (with a dilution factor of four). Because of the signal suppression by copper, the two curves were not parallel. Therefore, a standard addition method is required for the analysis. From this method, the lead concentration was found to be 80.0 ng ml^{-1} in the tap water sample. The lead blank of the reagents corresponded to approximately 4.0 ng ml^{-1} in the solution. This blank value was subtracted from the sample result. The lead signal from a water sample collected from an iron tap (with a dilution factor of 4) was completely recovered, as shown in Figure 59, and both the standard addition method and calibration method can be used for the determination of lead.

Table 19. Interference of lead from transition elements

(5.0 ml of 10.0 ng ml^{-1} Pb)

Metal Ion	Amount Added (0.5 ml)	Recovery of Lead, %							
		0.1 M HNO_3 - 4% $(NH_4)_2S_2O_8$ System						0.3% $K_2Cr_2O_7$ 0.06 M tartaric acid	0.3% $K_2Cr_2O_7$ 0.06 M malic acid
		without addition	with sodium citrate	with ascorbic acid	with dithizone	with thiosemicarbazide	with penicillamine		
Fe (II)	10 ppm	30	100	112	112	-	45	-	96
	100 ppm	0	93	93	17	87	-	-	100
	1000 ppm	0	5	-	-	-	-	90	99
Co (II)	1.0 ppm	38	-	-	-	-	-	-	96
	10	-	-	-	-	-	-	-	100
	100	-	-	-	-	-	-	99	100
	1000	-	-	-	-	-	-	75	78
Ni(II)	1.0 ppm	0	85	107	77	90	100	-	98
	10	0	56	65	-	-	-	90	94
	50	0	0	-	-	-	-	-	98
	100	-	-	-	-	-	-	93	96
	1000	-	-	-	-	-	-	60	69

Discussion: Determination of Lead

Cu(II)	1.0 ppm	12	51	30	82	23	79	84	76
	10	0	0	-	-	-	18	32	34
Zn (II)	100 pm	-	-	7	-	-	-	87	98
	1000 ppm	-	-	-	-	-	-	-	18
Cd (II)	10 ppm	-	-	-	-	-	-	-	80
	100 ppm	-	-	-	-	-	-	27	49
Hg (II)	10	-	-	-	-	-	-	-	91
	100	-	-	-	-	-	-	-	100
	1000	-	-	-	-	-	-	-	106

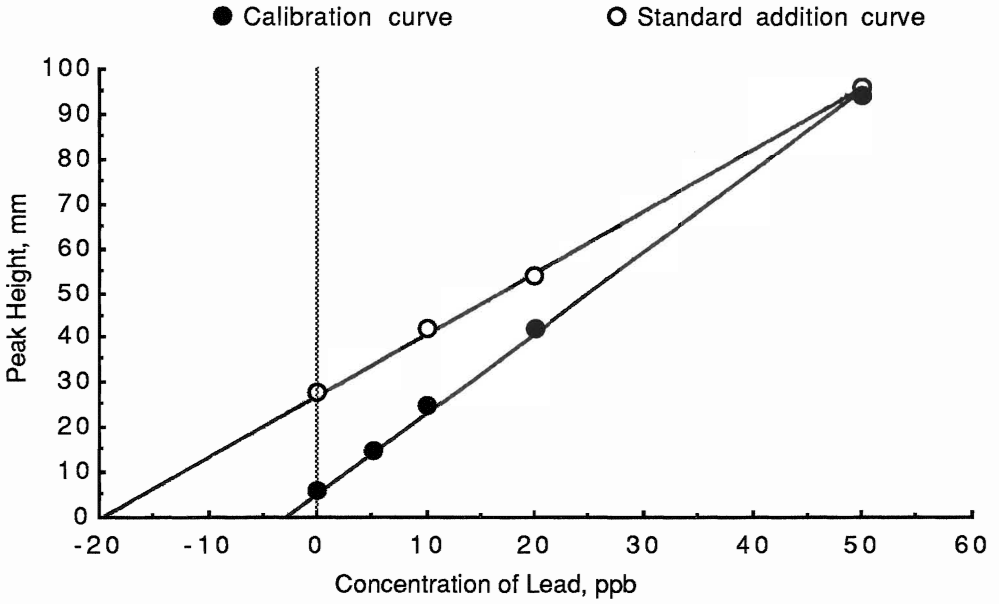

Figure 58. Comparison of calibration curve and standard addition curve of lead signal from tap water sample collected from a copper pipe.

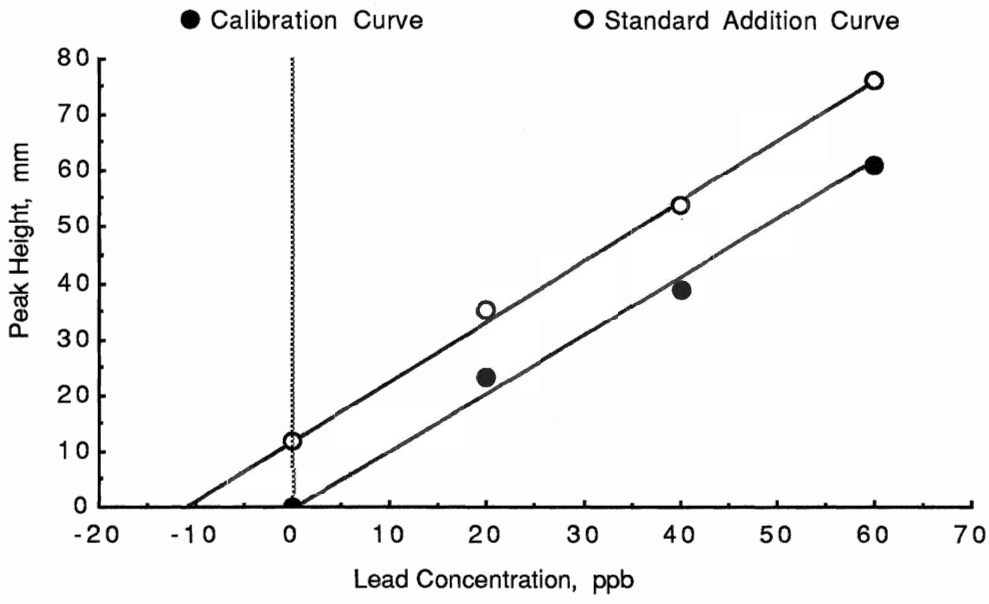

Figure 59. Comparison of calibration curve and standard addition curve of lead from tap water sample collected from an iron pipe.

V. Preliminary Investigations into the Determination of Antimony

Improvement of hydride generation method for antimony determinations

A gas flow system was also investigated for antimony determination by stibine formation. As a carrier gas, the argon flow rate was kept constantly between 760 to 970 ml min^{-1}. Unlike the other hydride forming elements studied, the production of stibine required only a very small amount of reducing agent, $NaBH_4$. In the normal procedures for the arsenic, germanium, tin and lead determinations as discussed in the previous sections, an analyte solution was injected into the reaction vessel and followed by the injection of $NaBH_4$ solution. However, in the determination of antimony, signals of antimony were recorded as the analyte solution was introduced into the reaction vessel, before the $NaBH_4$ solution was added. As shown in Figure 60, a sharp peak of Sb signal from 5.0 ml of 5.0 μg ml^{-1} Sb in 0.1 M HNO_3 was observed prior to the injection of $NaBH_4$ solution. After this peak, a further 1.5 ml solution of 10% $NaBH_4$ in 0.1 M NaOH was introduced into the reaction vessel containing the above solution. As indicated in Figure 60, no signal appeared at this stage (B). This meant that the stibine generation reaction was complete without the additional injection of $NaBH_4$ solution. After an injection of 1.5 ml of 10% $NaBH_4$ solution, six consecutive determinations of 5.0 ml of 5.0 μg ml^{-1} Sb gave the signals shown in Figure 61 without further introduction of reducing agent. This

may possibly be applied to rapid determination of antimony by using a high concentration of $NaBH_4$ solution for the first injection with no need to inject the $NaBH_4$ solution for each determination. This could be another project for research. The reproducibility had first to be improved. In order to avoid the uncertainty caused by any residual $NaBH_4$ present, a simple reversed order for the injection of sample and $NaBH_4$ solutions was employed, i.e., injection of the $NaBH_4$ solution prior to the sample solution to ensure that an excess of $NaBH_4$ was available. With this modification, the reproducibility of antimony signals was greatly improved. The antimony signal was observed instantaneously after the antimony solution was injected into the reaction vessel. Figure 62 shown five reproducible peaks (A) from 5.0 ml of 20.0 ng ml^{-1} antimony. Antimony blank (Figure 62 B) was undetected.

Nitric acid was used as the reaction medium for stibine production. The effect of nitric acid concentration on antimony signal is shown in Figure 63. Solutions of 5.0 ml of 0.20 μg ml^{-1} Sb and 1.0 ml of 4% $NaBH_4$ (m/V) in 0.03 M NaOH were used to perform these experiments. The highest signal of Sb was obtained at HNO_3 concentration of 0.040 M, and thus this was chosen for all determinations.

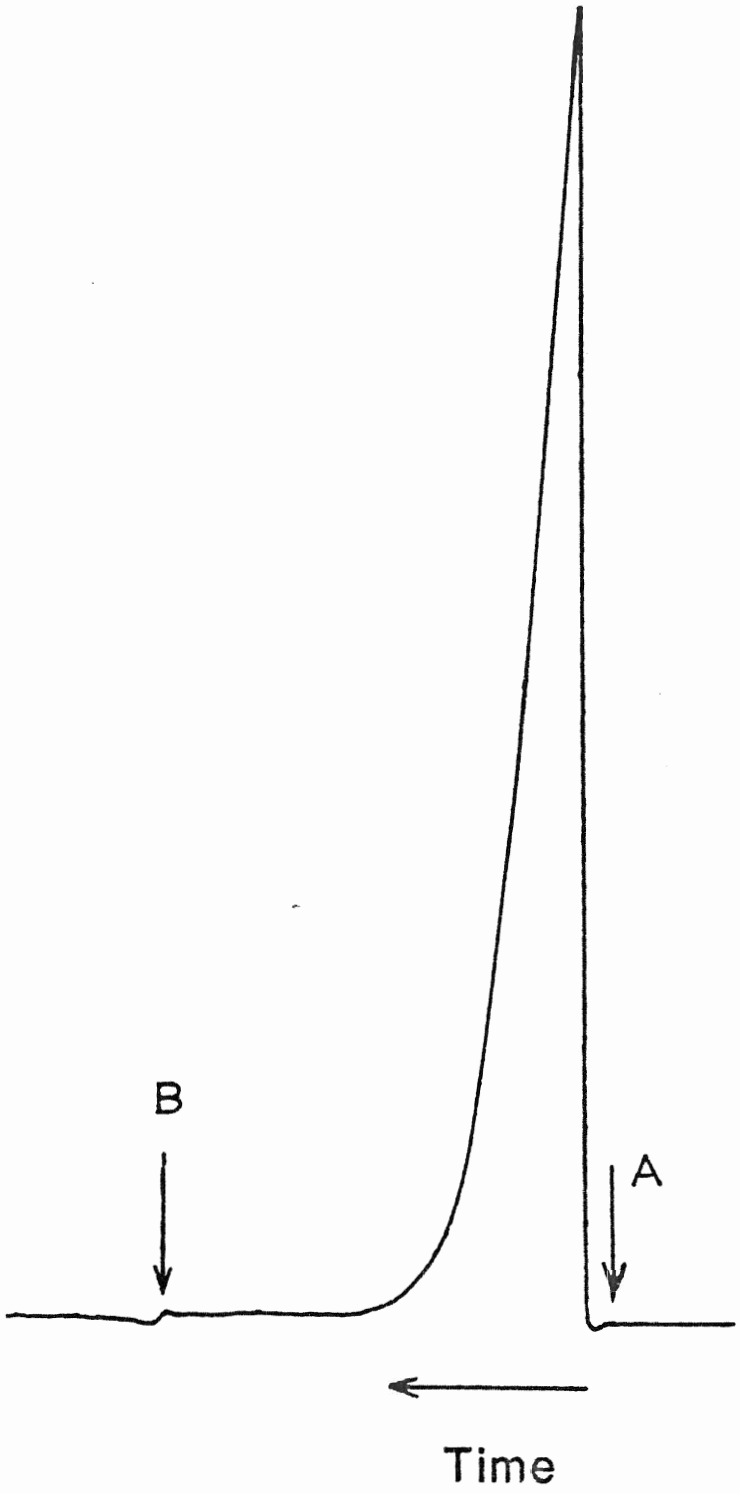

Figure 60. Peak profile of antimony signal.
A - Injection of 5.0 ml solution of 5.0 μg ml^{-1} Sb in 0.1 M HNO_3
B - Injection of 1.5 ml solution of 4% $NaBH_4$ in 0.1 M NaOH.

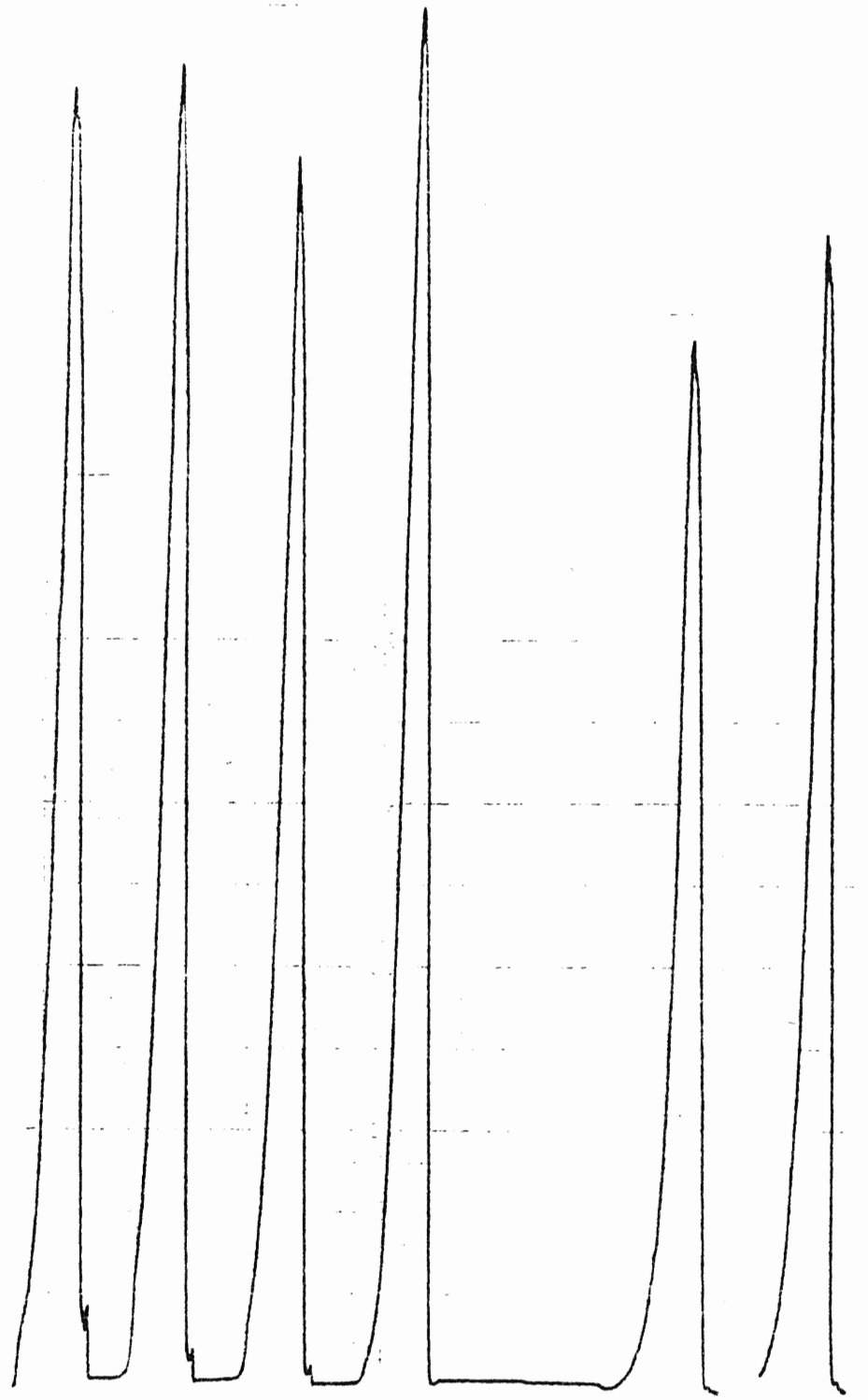

Figure 61. Six consecutive peaks of 5.0 ml of 5.0 µg ml^{-1} Sb after a single injection of 1.0 ml of 10% $NaBH_4$.

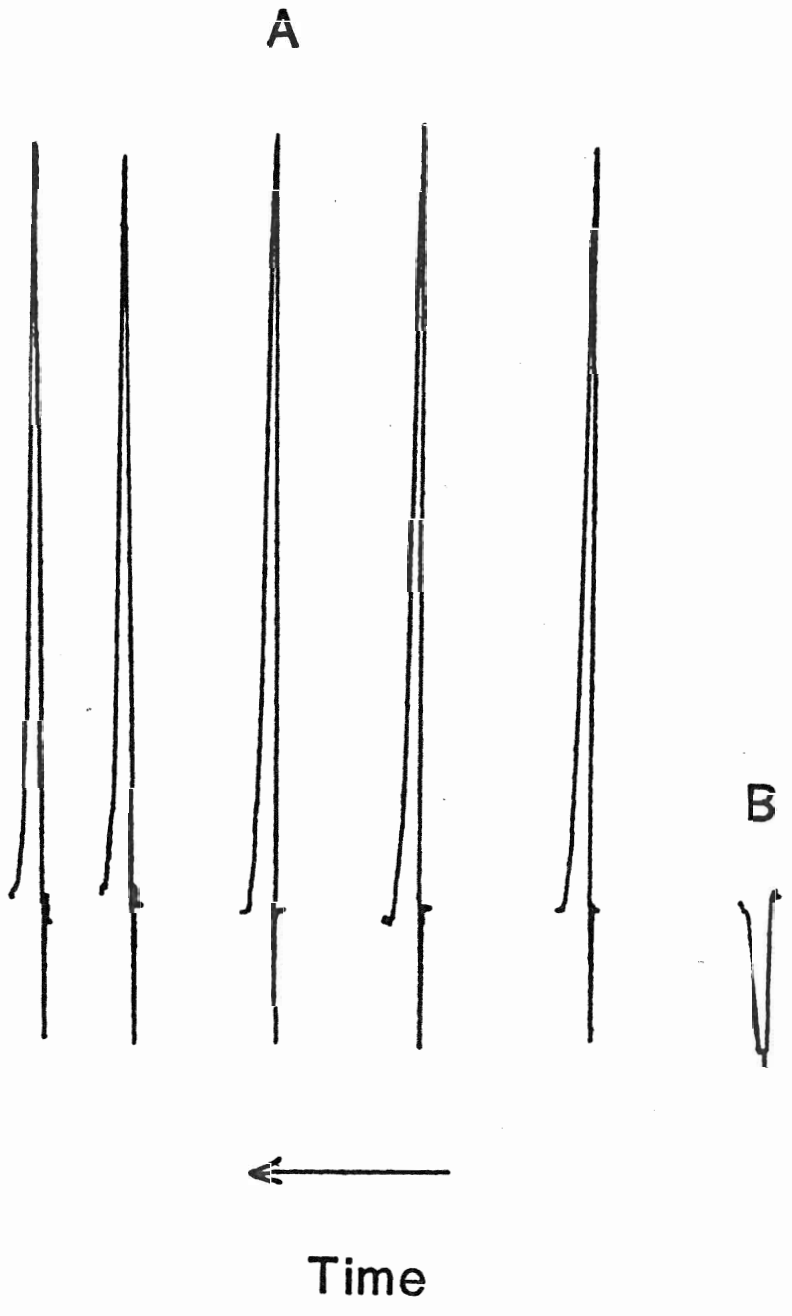

Figure 62. Reproducibility of peaks from 5.0 ml of 20.0 ng ml^{-1} Sb in 0.10 M HNO_3 (A) and blank (B).

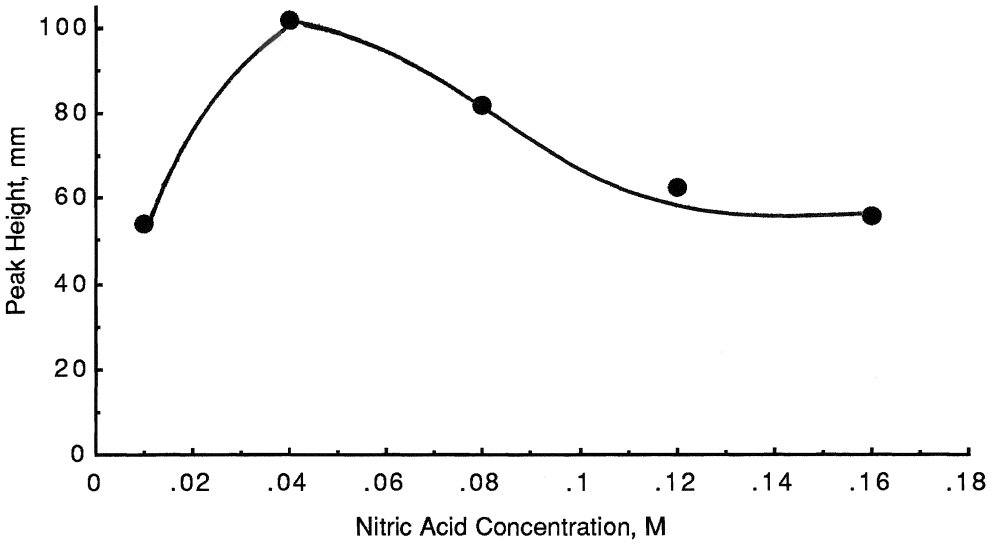

Figure 63. Effect of HNO_3 concentration on antimony signals.

Interference Reduction

Interference effects from a number of transition metal ions were studied. L-cysteine was demonstrated to be a suitable interference reducing agent. Solutions of 10.0 ng ml^{-1} Sb were made in either 0.040 M HNO_3 or 0.040 M HNO_3-0.4% (m/V) L-cysteine solution. In the presence and absence of L-cysteine, the recoveries of the Sb signal in the presence of Co(II), Cu(II), Ni(II), and Pt(IV), at a series of concentrations, were compared in Figures 5 and 6. As we can see from the figures, the interferences from Co(II), Cu(II), Ni(II), and Pt(IV) were significantly reduced with L-cysteine. These results, along with the others, are also summarized in Table 20. 1000 μg ml^{-1} of Cu(II) and Fe(II), 100 μg ml^{-1} of Co(II), 10 μg ml^{-1} of Ni(II) and Pt(IV), and 1 μg ml^{-1} or Pd(II) showed no significant interference on Sb determinations in the presence of 0.4% L-cysteine.

L-cysteine has shown promise in reducing interference in the determination of antimony. With more detailed studies, this method for the trace determination of antimony, by hydride formation in various matrices, could be improved.

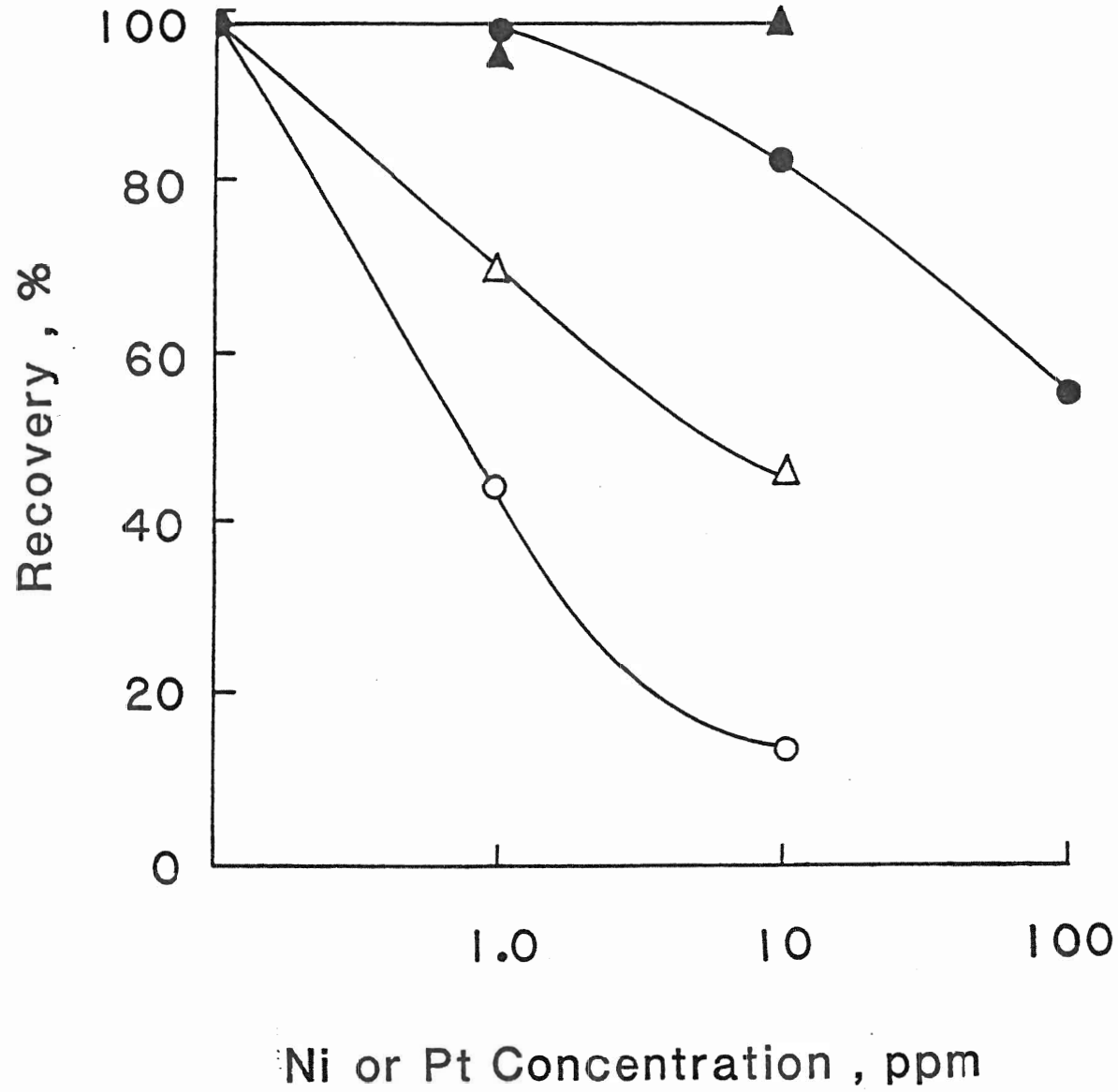

Figure 64. Recovery of 5.0 ml of 10.0 ng ml^{-1} Sb in the presence of Ni(II) and Pt(IV)

- ○ - in the presence of Ni(II)
- ● - in the presence of Ni(II), with L-cysteine
- △ - in the presence of Pt(IV)
- ▲ - in the presence of Pt(IV), with L-cysteine

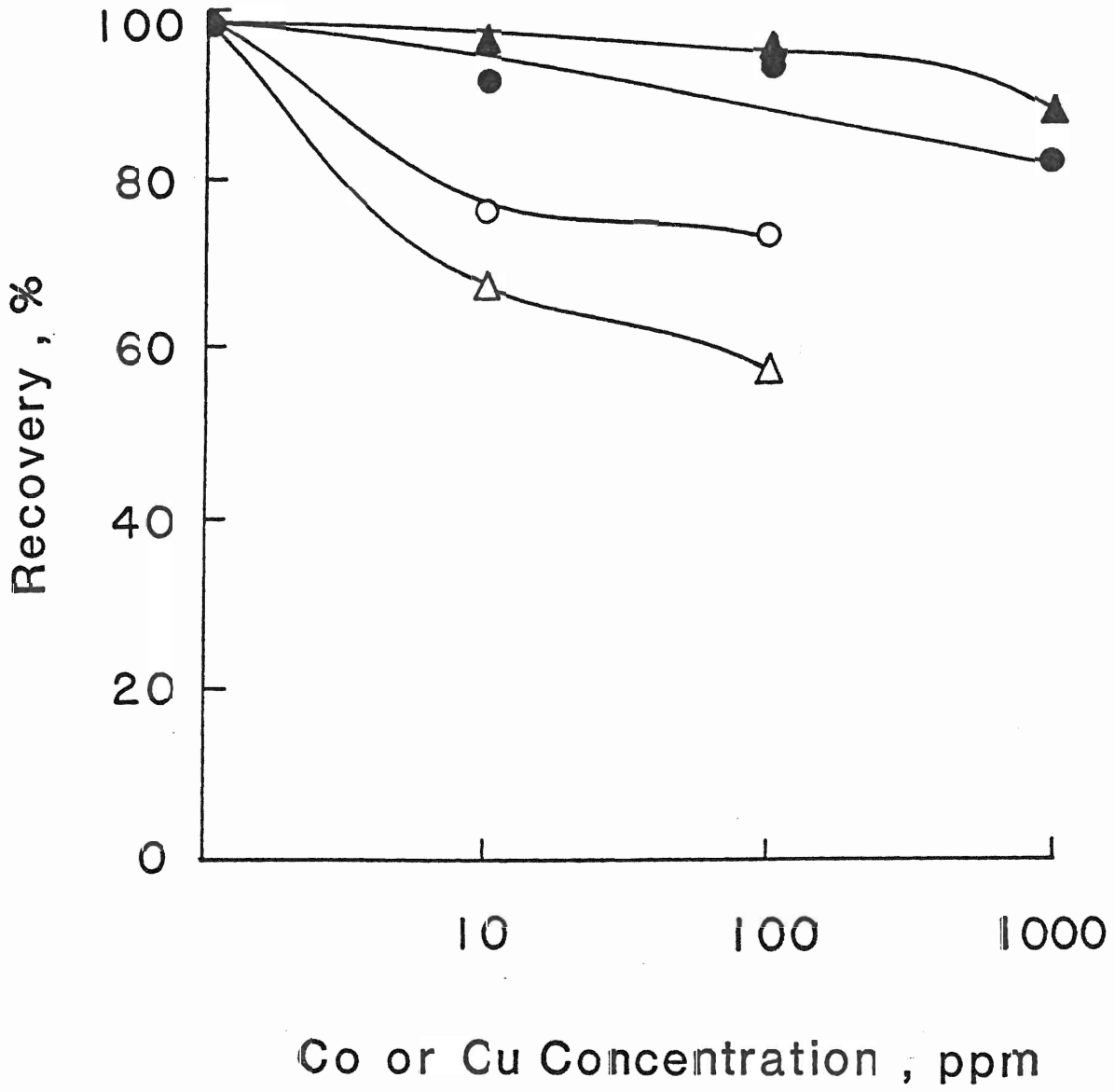

Figure 65. Recovery of 5.0 ml of 10.0 ng ml^{-1} Sb in the presence of Co(II) and Cu(II)

○ - in the presence of Co(II)
● - in the presence of Co(II), with L-cysteine
△ - in the presence of Cu(II)
▲ - in the presence of Cu(II), with L-cysteine

Table 20. Interference reduction by L-Cysteine in antimony determinations

Metal Ion	Amount Added (0.5 ml)	Recovery of 5 ml 10.0 ppb Sb (%) Without L-cysteine	With L-cysteine
Cu (II)	10 ppm	69	96
	100 ppm	60	95
	1000 ppm	-	89
Co (II)	10 ppm	77	90
	100 ppm	79	92
	1000 ppm	-	82
Ni (II)	1.0 ppm	44	96
	10 ppm	12	81
	100 ppm	0	55
Pt (IV)	1.0 ppm	70	95
	10 ppm	46	100
Pd (II)	1.0 ppm	-	94
	10 ppm	-	64
Fe (II)	10 ppm	-	101
	100 ppm	-	100
	1000 ppm	-	94

VI. Application of Signal Enhancement by Easily Ionized Elements in Hydride Generation DCP-AES Determination of Arsenic, Antimony, Germanium, Tin and Lead

Enhancement of Analyte Signal and Changes of Background

Signal enhancement by easily ionized elements (EIEs) is an important feature in DCP-AES. It depends on the EIE (139, 168), the concentration of EIE compounds (37, 143, 159-160), and the different elements determined (139, 141, 169). With the concern for these factors, this effect was studied by introducing each of the alkali and alkaline earth element-containing solutions at various concentrations in the determination of As, Sb, Ge, Sn and Pb by hydride generation DCP-AES. Distilled water, alkali, and alkaline earth element-containing solutions, with concentration ranging from 0.10M to 2.0M, were introduced to the d.c. plasma through a conventional peristaltic pump and a pneumatic nebulizer while the hydride, carried by argon, was introduced through the inner tube to the d.c. plasma. Atomic emission spectroscopic signals were then obtained with the spectrometer and recorded and measured with a chart recorder. Comparing the peak heights of the emission signals obtained in the presence of EIE solutions to those in the presence of distilled water, signal enhancement data and background results were calculated and shown in Table 21. The background increase(+) and reduction(-) values

indicate the background changes in the presence of EIEs compared to the background signal in the presence of distilled water, which was between 300 to 600, depending on the elements determined and the PMT and gain settings used, while the full scale of recording was 10,000 arbitrary units. The concentrations of As, Sb, Ge, Sn, and Pb solution used in performing this experiment were 20.0 ppb, 20.0 ppb, 2.0 ppb, 2.0 ppb, and 20.0 ppb, respectively.

As shown in Table 21, in all cases the As, Sb, Ge, Sn, and Pb, analytical signals were significantly enhanced with any of alkali element-containing compounds. Comparing the results obtained with aspiration of LiCl, LiOH with Li_2SO_4, and $MgCl_2$ with $MgSO_4$, we can see that the signal enhancement effect is essentially independent of anion, but dependent on the cation. With the increase of alkali metal concentration from 0.10M to 2.0M, the signal enhancement factor increases. Although a higher concentration of alkali elements may give a higher signal enhancement factor, a concentration of EIE of 1.0M is recommended since higher salt concentration may cause solid salt to appear on the top of the sample tube. It is worthy of note that, although the background level was changed with the introduction of alkali elements, no significant change of noise was observed.

With aspiration of alkaline earth element-containing solutions to the d.c. plasma, the signal and background results are more complicated and depend on the different analytes. As we can see in Table 21, in arsenic determinations, signals were enhanced and the background was decreased with all alkaline earth elements, whereas the opposite phenomenon was observed in the case of tin

determinations. In the determination of antimony and germanium, both signal and background were increased with increasing alkaline earth element concentration. For the determination of lead, Be, Ca, Sr, and Ba enhanced lead signal, whereas Mg suppressed the lead signal.

As a result of enhanced intensities of emission lines (142, 144), both peak height and peak area of emission signals were increased. There is no change in the peak width, however, as can be seen in the cases of lead (Figure 66a) and germanium (Figure 66b) signals when 1.0M KCl was introduced. Results of signal enhancement, measured by both peak height and peak area are summarized in Table 22.

It was also found that the enhancement effect of the EIE does not depend on the hydride generation procedure. As a trial, arsenic(III) and arsenic(V) were used as standards and they were made in solution with and without L-cysteine. The effect of EIEs on arsenic signals was then studied with the above reaction solutions. The results showed that same signal enhancement was observed by using either As(III) or As(V) as reaction solution. Also, similar enhancement effects were obtained in the presence and absence of L-cysteine, although L-cysteine speeded the hydride reaction and reduced the interference in the hydride generation process.

Table 21. Effect of EIEs on signal and background in the determination of As,Sb, Ge, Sn and Pb *

EIE Compound	EIE Conc. (M)	Signal Enhancement (%)					Background increase (+) or reduction (-) based on a background signal of 300 -- 600 (%)				
		As	Sb	Ge	Sn	Pb	As	Sb	Ge	Sn	Pb
LiCl	1.0	24	46	-	-	60	-19	-27	-	-	n.d.
	2.0	24	44	-	-	70	-20	-25	-	-	n.d.
LiOH	0.10	-	-	5	28	26	-	-	n.d.	+7	n.d.
	0.50	-	-	13	38	56	-	-	n.d.	+14	n.d.
	1.0	-	-	15	57	60	-	-	+6	+16	n.d.
	2.0	-	-	22	61	70	-	-	+16	+18	n.d.
Li_2SO_4	0.10	5	29	5	24	37	n.d.	n.d.	-	n.d.	-
	0.50	12	39	15	41	54	-10	n.d.	n.d.	+6	-
	1.0	21	42	20	45	61	-14	-6	-	+8	n.d.
	2.0	29	66	23	55	73	-17	-11	+10	+11	n.d.
NaCl	0.10	12	17	23	39	40	n.d.	+22	n.d.	+8	n.d.
	0.50	19	24	44	52	50	-12	+9	-	+16	n.d.
	1.0	21	46	44	65	60	-19	n.d.	-	+16	n.d.
	2.0	31	61	56	83	65	-18	-21	n.d.	+19	n.d.
KCl	0.10	5	12	40	28	30	n.d.	+36	-	+8	n.d.
	0.50	21	63	57	52	50	-19	n.d.	n.d.	+16	n.d.
	1.0	26	61	78	66	70	-26	-21	n.d.	+16	n.d.
	2.0	19	3	103	76	88	-26	-41	n.d.	+21	-6
RbCl	0.50	21	51	-	-	-	-18	+21	-	-	-
	1.0	36	61	56	46	90	-30	-20	+6	+31	+7
	2.0	36	10	103	68	90	-30	-31	+10	+63	-10
CsCl	0.50	31	39	64	-	85	-33	-37	n.d.	-	-10
	1.0	41	76	-	-	90	-34	-34	-	-	-14
	2.0	19	15	-	-	115	-33	-42	-	-	-18

EIE Compound	EIE Conc. (M)	Signal Enhancement (%)					Background increase (+) or reduction (-) based on a background signal of 300 -- 600(%)				
		As	Sb	Ge	Sn	Pb	As	Sb	Ge	Sn	Pb
$BeSO_4$	1.0	12	37	18	-25	14	n.d.	+71	+330	+86	+71
	2.0	-	-	24	-46	14	-	-	+450	+130	+100
$MgSO_4$	1.0	26	66	49	-100	-59	n.d.	+78	+150	+1400	+1500
	2.0	36	66	57	-	-	-6	+59	+260	-	-
$MgCl_2$	1.0	29	68	-	-	-69	n.d.	+70	-	-	+1500
	2.0	36	76	-	-	-	n.d.	+73	-	-	-
$CaCl_2$	1.0	38	56	43	-55	73	-10	+60	+110	+270	+140
	2.0	36	63	54	-	73	-11	+77	+360	-	+250
$SrCl_2$	1.0	38	42	49	-25	95	n.d.	+74	+130	+180	+130
	2.0	-	-	49	-55	73	-	-	+450	+300	+220
$BaCl_2$	0.50	19	37	29	0	77	-7	+110	+320	+150	+200
	1.0	19	39	43	-26	50	-9	+110	+580	+290	+340

*: "n.d." -- The change is not detectable.
"-" -- not determined.

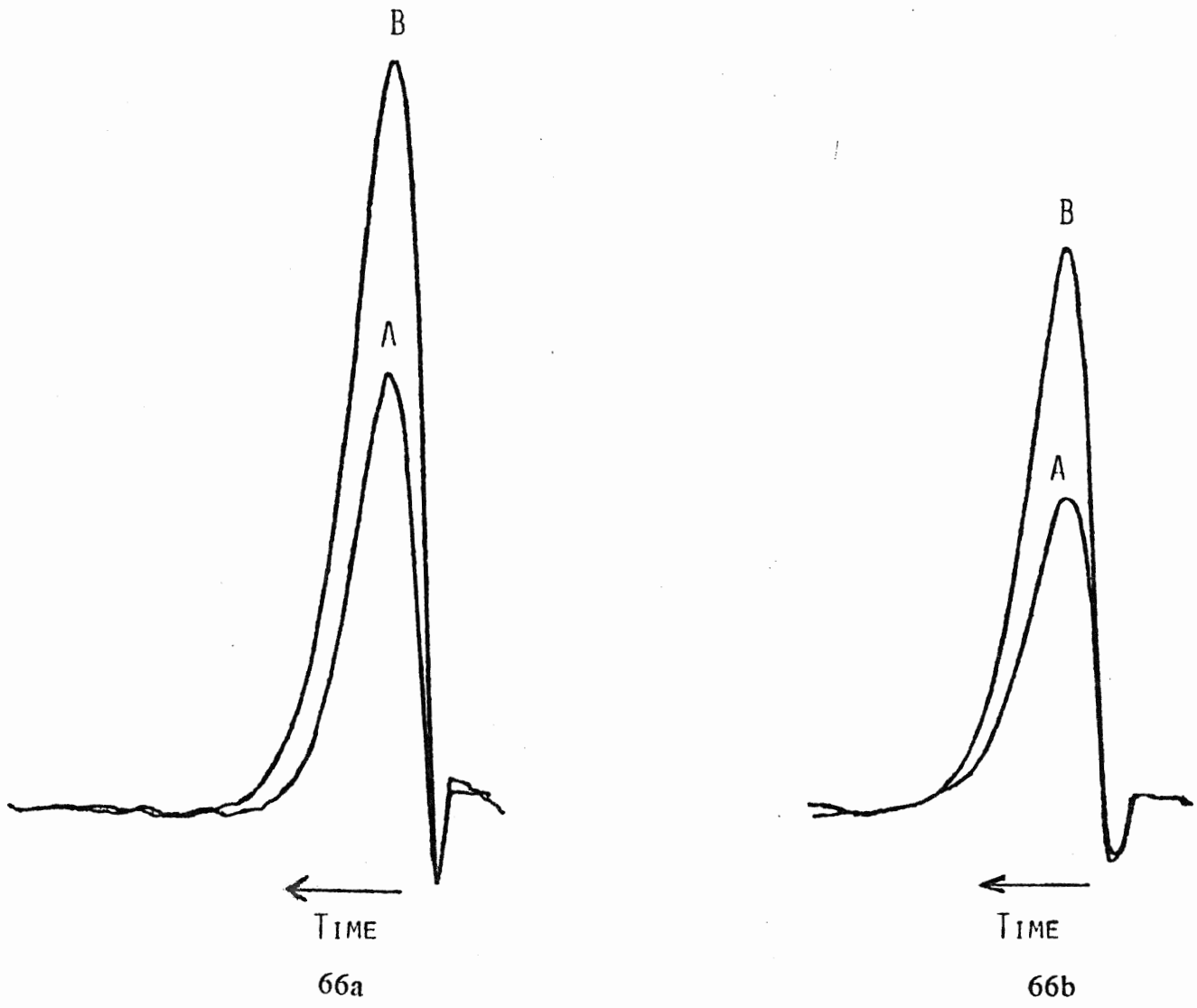

Figure 66. Comparison of signal profiles of 20.0 ppb Lead (66a) and 2.0 ppb Germanium (66b) in the presence of distilled water (A) and in the presence of 1.0 M KCl (B).

Table 22. Comparison of the enhancement by peak height and peak area

Element	EIE	Signal Enhancement (%)	
		Peak Height	Peak Area
Ge	1.0 M KCl	78	64
Pb	1.0 M KCl	70	75
As	1.0 M CsCl	50	78
Sb	1.0 M CsCl	74	77

Stability of the Enhanced Signals

In conventional DCP-AES, the uncertainty and nonreproducibility caused by EIEs is a severe problem due to variable or unknown EIE concentrations in different samples and to the difficulty in matching the matrix of sample and standard solutions. However, this problem is overcome in the hydride generation d.c. plasma system since the hydrides are separated from the sample matrix. Thus alkali or alkaline earth elements are not introduced to the plasma from the hydride generator along with the hydride even if they are present in the sample.

Since separate introduction of EIE solutions through the peristaltic pump and pneumatic nebulizer can be easily controlled, the concentration of EIE in the plasma can be kept constant. As shown in Figure 67, very reproducible germanium signals were obtained with and without EIE. Eleven replicate determinations of 0.50 ppb germanium gave a relative standard deviation (RSD) of 4.7% in the presence of distilled water and 4.1% in the presence of 1.0M KCl. Similar results were obtained for lead determinations, where eleven replicate determinations of 2.0 ppb lead gave a RSD of 6.0% in absence of EIE and 4.6% in the presence of 1.0M CsCl. We can also see from Figure 67 that there was no signal from the germanium blank even in the presence of 1.0 M KCl. The introduction of EIE reagents of analytical grade purity to the d.c. plasma did not increase the blank value because the concentrations of the analytes in these reagents are negligible compared to their detection limits by conventional DCP-AES.

Calibration

With EIEs, reproducible and enhanced signals were achieved, which is promising in improving sensitivity for trace analysis. In order to estimate the analytical applicability of signal enhancement by EIE, selective calibration and linear regression were performed. Figure 68 shows the calibration curves of lead, with concentrations from 0.0 ppb to 80.0 ppb. Linear calibration curves were obtained with or without EIE signal enhancement. Correlation coefficients of the two curves were 0.997 for water aspiration and 0.998 for 1.0M CsCl aspiration. The slopes of the line were 1.14 and 2.17 for the introduction of distilled water and 1.0M CsCl, respectively. Similar results were obtained for the determination of germanium. The correlation coefficients for concentration of germanium from 0.20 ppb to 2.0 ppb were 0.998 and 0.999 for the aspiration of distilled water and 1.0M KCl, respectively.

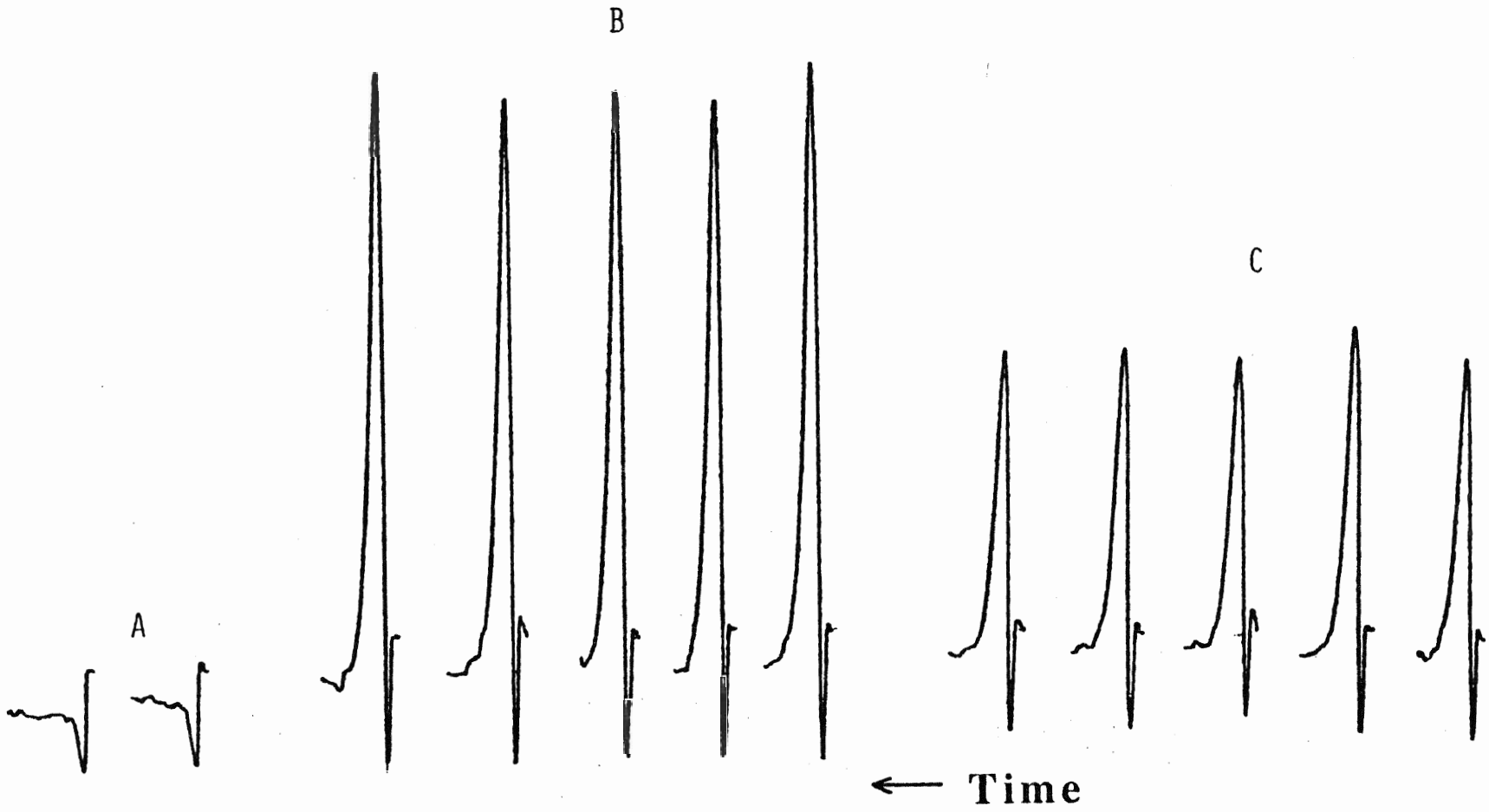

Figure 67. Comparison of signals of blank and germanium in the presence of 1.0 M KCl and distilled water.

A -- Blank, with introduction of 1.0 M KCl.

B -- 0.50 ppb Ge, with introduction of 1.0 M KCl

C -- 0.50 ppb Ge, with introduction of distilled water

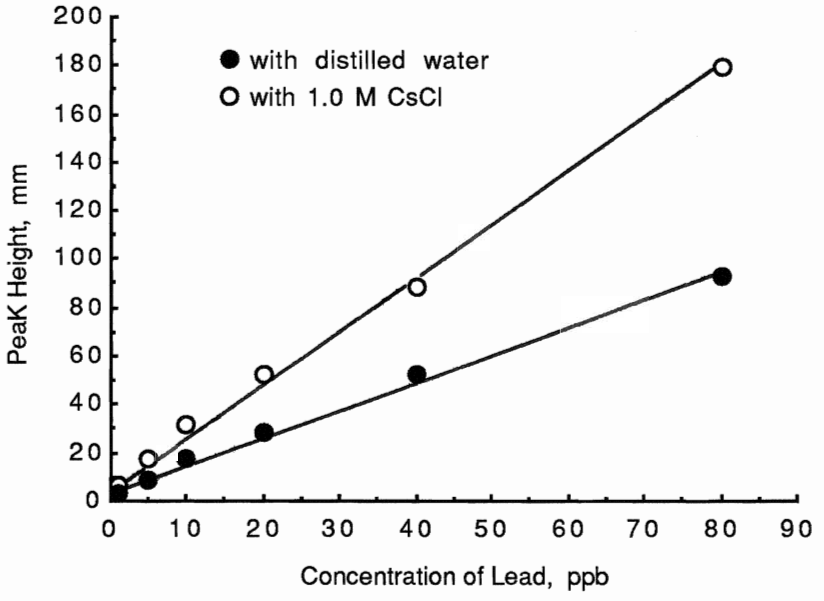

Figure 68. Comparison of lead calibration curves in the presence and absence of CsCl

Conclusion

Arsenic:

Matrix modification with 3% L-cystine in 5M HCl dramatically improves tolerance to transition elements by factors of 10-100. While interference by elements such as Ni(II) and Pt(IV) is greatly reduced, tolerance to the presence of Pd(II) and Au(III) is only slightly increased. Application of the method to the analysis of the NBS reference standards, Low Alloy Steel 363 and Open Hearth Iron 55E, yielded excellent results of 101 ± 7 μg g^{-1} As (certified value 100 μg g^{-1}) and 71 ± 7 μg g^{-1} (certified value 70 μg g^{-1}), respectively.

Preliminary studies with the gas flowing batch system of operation indicated that a 4-fold increase in the As emission signal was obtained in the presence of L-cysteine in a reaction medium of 0.1 M HNO_3. L-cystine, on the other hand, produced an enhancement factor of about 1.5.

Tin:

Studies of the production of stannane indicated that the effect of allowing argon to flow continuously through the reaction vessel was beneficial in decreasing the background noise and in improving reproducibility. The presence of 0.4 g L-cystine in a reaction medium of 0.05 M HNO_3 improved tolerance to transition elements by factors in the range 100-1000. However, interference by Pd(II), Pt(IV) and Au(III) was not eliminated by L-cystine.

The detection limit for Sn in solution was 20 pg ml^{-1}. The RSD at a concentration of 0.4 ng ml^{-1} Sn was found to be 2%. Excellent results were

obtained in application of the method to NBS standard reference materials highly concentrated in the otherwise problematic elements, Cu and Fe. Preliminary studies using 0.4% L-cysteine indicated that this would be an equally effective reagent in the reduction of interferences.

Germanium:

Optimum conditions for the determination of Ge in the presence of potential interferences were found to be 0.4% L-cysteine in a sample medium of 0.02-0.04 M HNO_3. A larger sample volume of 9 ml (rather than 5 ml) was employed by the use of L-cysteine in solution instead of the solid form of L-cystine; 2 ml of 6% $NaBH_4$ were employed for reduction. An increase in peak height signal of about 100% was seen in the presence of L-cysteine, while peak area was unchanged. Increased tolerance factors in the range 100-1000 were observed in the presence of transition elements (e.g. Cu, Ni, Co). L-cysteine(0.4%) and L-cystine(0.4g) behaved similarly in most cases with the clear exception of tolerance to Pd(II). L-cystine actually degraded results while L-cysteine allowed interference-free determination of Ge up to levels of about 10 $\mu g\ ml^{-1}$ Pd(II). In the study of mutual hydride-forming interferences, only Se was found to be problematic (suppression); this effect was actually enhanced in the presence of L-cysteine.

The detection limit for Ge was 20 $pg\ ml^{-1}$ in solution. An RSD of 3.1% was obtained at the 0.1 $\mu g\ ml^{-1}$ level of Ge. Germanium spiked in solutions of the NBS Copper I and Iron 55E standard reference materials were totally recovered.

Among other amino acids investigated, histidine appeared very

promising. While sensitivity (peak height) was not enhanced, tolerance to high concentrations of Ni(II) (> 100 μg ml^{-1}) was superior to that in the presence of L-cysteine.

Lead:

Conditions for the generation of plumbane were optimized for two oxidizing reaction media, HNO_3 - $(NH_4)S_2O_8$ and malic acid - $K_2Cr_2O_7$. The latter system not only resulted in better reproducibility, but also was much less susceptible to suppression of the Pb signal by transition elements.

Antimony:

Preliminary studies have indicated that the presence of L-cysteine has a beneficial effect in reducing interferences from Cu, C, Ni, and Pt in the determination of Sb in a reaction medium of 0.04 M HNO_3.

EIEs:

Advantage can be taken of the positive interference created by the presence of EIEs in analysis by DCP-AES. A constant amount of the EIE can be nebulized into the DCP separate from injection of the hydride. Signal enhancements in the range 40-90% (peak height or peak area) have been demonstrated in the determination of As, Ge, Pb, Sb, and Sn with nebulization of 1 M CsCl or 1 M KCl.

References

1. Greenfield, S.; Hieftje, G. M.; Omenetto, N.; Scheeline, A.; Slavin, W. *Anal. Chim. Acta* **1986**, 180, 69-98.
2. Pavlovic, B. V. *Fresenius Z. Anal. Chem.* **1986**, 324, 698-706.
3. Scheeline, A. *Prog. Anal. Atom. Spectrosc.* **1984,** 7, 21.
4. Greenfield, S.; McGeachin, H. McD.; Smith, P. B. *Talanta* **1975,** 22, 1-15.
5. Keirs, C. D.; Vickers, T. J. *Appl. Spectrosc.* **1977,** 31, 273-283.
6. Schrenk, W. G. *Appl. Spectrosc.* **1988,** 42, 4-11.
7. Broekaert, J. A. C. *Anal. Chim. Acta* **1987,** 196, 1-21.
8. Margoshes, M.; Scribaer, B. F. *Spectrochim. Acta* **1959,** 14, 138-145.
9. Korolev, V. V.; Vainshein, E. E. *J. Anal. Chem. USSR* **1959,** 14, 731.
10. Owen, L. E. *Appl. Spectrosc.* **1961,** 15, 150-152.
11. Margoshes, M.; Scribner, B. F. *J. Res. Nat. Bu. Stds.* **1963,** 674, 561.
12. Scribner, B. F.; Margoshes, M. *Proceeding IXth colloquium Spectroscopicum Internationale* (GAMS, Paris, 1962), pp. 309-324.
13. Korolev, F. A.; Kvaratskheli, Iu. K. *opt, Spectrosc.* **1961,** 10, 200.
14. Grechikhin, L. I.; Shimanovich, V. D. *Opt. Spectrosc.* **1962,** 13, 358.
15. Neeb, K. F.; Gebauhr, W. *Fresenius Z. Anal. Chem.* 1962, 190, 92.
16. Webb, M. S. W.; Wildy, P. C. *Nature* **1963,** 198, 1218.
17. Serin, P. A.; Ashton, K. H. *Appl. Spectrosc.* **1964,** 18, 166.
18. Lerner, R. *Spectrochim. Acta* **1964,** 20, 1619.
19. Sirois, E. H. *Anal. Chem.* **1964,** 36, 2389-2394.
20. Collins, A. G.; Pearson, C. A. *Anal. Chem.* **1964,** 36, 787-789.
21. McGinn, J. H. *Proc. 5th Int. Cong. Ionization Phenomena,* (Munich, 1961). **1962,** 1, 967.
22. Kranz, in *Emissionspektroskopie* (Akademie-Verlag, Berlin) **1964,** 160-172.
23. Kranz, E. in *Proceedings XIIth Colloquium Spectroscopicum Internationale* (Hilger, London), **1965,** 574-577.
24. Jahn, R. E. *Proc. 5th Int. Conf. Ionization Phenomena* (Munich, 1961), **1962,** 1, 955.
25. Yamamoto, M. *Jap. J. Appl. Phys.* **1962,** 1, 235.

26. Yamamoto, M. *Jap. J. Appl. Phys.* **1963,** 2, 62.
27. Goto, H.; Atsuya, I. *Fresenius Z. Anal. Chem.* **1967,** 225, 121. and **1968**, 240, 102.
28. Atsuya, I.; Goto, H. *Spectrochim. Acta* **1971,** 26B, 359-367.
29. Valente, S. E.; Schrenk, W, G. *Appl. Spectrosc.* **1970,**24, 197-205.
30. Elliott, W. G. *Amer. Lab.* **1970,** 2(3), 67-69, 71-72, CA 72: 128295d.
31. Elliott, W, G. *Amer. Lab.* **1971,** 3(8), 45-52, CA 77: 96504f.
32. Elliott, W, G. *1974 Pittsburgh Conference on Analytical Chemistry and Applied Spectroscopy,* Cleveland, Ohio, USA. paper No. 75.
33. Zander, A. T. *ind. Res. Devel.* **1982,** Feb, 146-150.
34. Miller, M. H.; Zander, A. T. *Spectrochim. Acta* **1986,** 41B, 453-467.
35. Johnson, G. W.; Taylor, H. E.; Skogerboe, R. K. *Spectrochim. Acta* **1979,**34B, 197-212.
36. Reednick, J. *Amer. Lab.* **1979,** 11(3), 53-54, 56-58, 60, 62.
37. Decker, R. J. *Spectrochim. Acta* **1980,** 35B, 19-31.
38. Mattoon, T. R.; Piepmeier, E. H. *Anal. Chem.* **1983,** 55, 1045-1050.
39. Masters, R. A.; Piepmeier, E. H. *Spectrochim. Acta* **1985,** 40B, 85-91.
40. Rippetoe, W. E.; Vickers, T. J. *Anal. Chem.* **1975,** 47, 2082-2086.
41. Hara, L. Y.; Parsons, M. L. *Anal. Chem.* **1985,** 57, 841-845.
42. Meyer, G. A. *Spectrochim. Acta* **1987,** 42B, 333-339.
43. Goliber, P. A.; Hendrick, M. S.; Michel, R. G. *Anal. Chem.* **1985,** 57, 2520-2526.
44. Hendrick, M. S.; Goliber, P. A.; Michel, R. G. *J. Anal. At. Spectrom.* **1986,** 1, 45-50.
45. Messman, J. D.; O'Haver, T. C.; Epstein, M. S. *Anal. Chem.* **1985,** 57, 416-420.
46. Wirz, P.; Gross, M.; Ganz, S.; Xcharmann, A. *Spectrochim. Acta* **1983,** 38B, 1217-1225.
47. Gray, A. L. *Anal. Chem.* **1975,** 47, 600-601.
48. Gray, A. L. *Analyst* **1975,** 100, 289-299.
49. Kovacic, N.; Ikonomov, N.; Simic, M. *Adv. Mass Spectrom.* **1980,** 8A, 414-419.
50. Todorovic, M.; Ikonomov, N.; Kovacic, N.; Rekalic, M.; Peric, M. *Fresenius Z. Anal. Chem.* **1981,** 306, 362-364.
51. Reednick, J. *Amer. Lab.* **1979,** March, 127.

52. Zander, A. T. *Anal. Chem.* **1986,** 58, 1139A-1149A.
53. Harrison, G. R. *J. Opt. Soc. Amer.* **1949,** 39, 522.
54. Cresser, M. S.; Keliher, P. N.; Wohlers, C. C. *Anal. Chem.* **1973,** 45, 111-117.
55. Keliher, P. N.; Wohlers, C. C. *Anal. Chem.* **1974,** 46, 682-687.
56. Keliher, P. N.; Wohlers, C. C. *Anal. Chem.* **1976,** 48, 333A-340A.
57. Keliher, P. N. *Res. Devel.* **1976,** 27(6), 26-30.
58. Richardson, D. *Spectrochim. Acta* **1953,** 6, 61-65.
59. Kirchgessner, W. G.; Finkelstein, N. A. *Anal. Chem.* **1953,** 25, 1034-1038.
60. Matz, G. J. *Amer. Lab.* **1973,** 5(3), 75.
61. Zander, A. T. *Ind. Res. Devel.* **1982,** March, 142-147.
62. Browner, R. F.; Boorn, A. W. *Anal. Chem.* **1984,** 56, 786A-798A.
63. Browner, R. F.; Boorn, A. W. *Anal. Chem.* **1984,** 56, 875A-888A.
64. Skogerboe, R. K..; Urasa, I. T.; Coleman, G. N. *Appl. Spectrosc.* **1976,** 30, 500.
65. Keirs, C. D.; Vickers, T. J. *Appl. Spectrosc.* **1977,** 31, 273.
66. Boyko, W, J.; Keliher, P. N. *Can. J. Spectrosc.* **1982,** 27, 51.
67. Sparkes, S.; Ebdon, L. *ICP Inform. Newsl.* **1986,** 12(1), 1-6.
68. Mazzo, D. J.; Elliott, W. G.; Uden, P. C.; Barnes, R. M. *Appl. Spectrosc.* **1984,**38, 585-590.
69. Mohamed, W.; Brown, R. M.; Fry, R. C. *Appl. Spectrosc.* **1981,** 35, 153-164.
70. Gilbert, T. R.; Penney, B. A. *Spectrochim. Acta* **1983,** 38B, 297-302.
71. Ng, K. C.; Caruso, J. A. *Appl. Spectrosc.* **1985,** 39, 719-726.
72. Gunn, A. M.; Kirkbright, G. F.; Millard, D. L. *Analyst* **1979,** 103, 1066.
73. Aziz, A.; Broekaert, J. A. C.; Leis, F. *Spectrochim. Acta* **1982,** 37B, 369-379.
74. Zimnik, P. R.; Sneddon, J. *Amer. Lab.* **1987,** 19(8), 86-90.
75. Elliott, W, G.; Matusiewicz, H.; Barnes, R. M. *Anal. Chem.* **1986,** 58, 1264-1265.
76. Mitchell, P. G.; Sneddon, J. *Talanta* **1987,**
77. Kirkbright, G. F.; Snook, R. D. *Anal. Chem.* **1979,** 51, 1938-1941.
78. Barnes, R. M.; Fodor, P. *Spectrochim. Acta* **1983,** 38B, 1191-
79. Ng, K. C.; Caruso, J. A. *Anal. Chem.* **1983,** 55, 2032-2036.

80. Mithcell, P. G.; Greene, B.; Sneddon, J. *Midrochim. Acta* **1986,** 1, 249-258.
81. Sparkes, S. T.; Ebdon, L. *J. Anal. At. Spectrom.* **1988,** 3, 563-569.
82. Ebdon, L.; Collier, A. R. *J. Anal. At. Spectrom.* **1988,** 4, 557.
83. McCurdy, D. L.; Wickman, M. D.; Fry, R. C. *Appl. Spectrosc.* **1985,** 39, 984-988.
84. Derie, R. *Anal. Chim. Acta* **1984,** 166, 61-69.
85. Madrid, Y.; Bonilla, M.; Camara, C. *4th Biennial National Atomic Spectroscopy Symposium(4th BNASS),* York, U.K. **1988,** June 29-July 1. Paper No. W31.
86. Armstrong, J. A.; Ebdon, L. *4th BNASS* Paper No. T3.
87. Wickman, M. D.; Fry, R. C.; Hoffman, M. K. *Appl. Spectrosc.* **1986,** 40, 351-355.
88. Comtois, R. R.; Kinsey, W. T. *Pittsburgh Conference on Anal. Chem. and Appl. Spectrosc.* 1982, Atlantic City, NJ.
89. Brown, J. R.; Saba, C. S.; Rhine, W. E.; Eisentraut, K. J. *Anal. Chem.* **1980,** 52, 2365-2370.
90. Kauffman, R. E.; Saba, C. S.; Rhine, W. E.; Eisentraut, K. J. *Anal. Chem.* **1982,** 54, 975-979.
91. Eisentraut, K. J.; Newman, R. W.; Saba, C. S.; Kauffman, R. E.; Rhine, W. E. *Anal. Chem.* **1984,** 56, 1086A-1094A.
92. Robbins, W. B.; Caruso, J. A. *Anal. Chem.* **1979,** 51, 889A-899A.
93. Nakahara, T. *Prog. Anal. At. Spectrosc.* **1983,** 6, 163.
94. Welz, B. *Chem. Brit.* **1986,** 22, 130-133.
95. Holak, W. *Anal. Chem.* **1969,** 41, 1712-1713.
96. Thompson, M.; Pahlavanpour, B.; Walton, S. J.; Kirkbright, G. F. *Analyst* **1978,** 103, 568-579, and 705-713.
97. Miyazaki, A.; Kimura, A.; Umezaki, Y. *Anal. Chim. Acta* **1970,** 90, 119-125.
98. Panaro, K. W.; Krull, I. S. *Anal. Lett.* **1984,** 17(A2)157-172.
99. Boampong, C.; Brindle, I. D.; Ceccarelli Ponzoni, C. M. *J. Anal. At. Spectrom.* **1987,** 2, 197-200.
100. Ebdon, L.; Sparkes, S. T. *Microchem. J.* **1987,** 36, 198-206.
101. Ek, P.; Hulden, S. G. *Talanta* **1987,** 34, 495-502.

102. Hayrynen, H.; Lajunen, L. H. J.; Peramak, P. *At. Spectrosc.* **1985,** 6, 88-90.
103. Brindle, I. D.; Ceccarelli Ponzoni, C. M. *Analyst* **1987,** 112, 1547-1550
104. Krull, I. S.; Panaro, K. W. *Appl. Spectrosc.* **1985,** 39, 960-968.
105. Lajunen, L. H. J.; Kinnunen, A.; Yrjanheikki, E. *At. Spectrosc.* **1985,** 6, 49-52.
106. Miyazake, A.; Kimura, A.; Umezaki, Y. *Anal. Chim. Acta* **1979,** 107, 395-398.
107. Van Loon, J. C. *Anal. Chem.* **1979,** 51, 1139A-1150A.
108. Carnahan, J. W.; Mulligan, K. T.; Caruso, J. A. *Anal. Chim. Acta* **1981,** 130, 227.
109. Lloyd, R. J.; Barnes, R. M.; Uden, P. C.; Elliot, W, G. *Anal. Chem.* **1978,** 50, 2025-2029.
110. Uden, P. C.; Barnes, R. M.; Disanzo, F. P. *Anal. Chem.* **1978,** 50, 852-855.
111. Uden, P. C.; Henderson, D. E.; Disanzo, F. P.; Lloyd, R. J.; Tetu, T. *J. Chromatogr.* **1980,** 196, 403.
112. Estes, S. A.; Poirier, C. A.; Uden, P.; Barnes, R. M. *J. Chromatogr.* **1980,** 196, 265-277.
113. Riska, G. D.; Estes, S. A.; Beyer, J. O.; Uden, P. C. *Spectrochim. Acta* **1983,** 38B, 407-417.
114. Treybig, D. S.; Ellebracht, S. R. *Anal. Chem.* **1980,** 52, 1633-1636.
115. Parano, K. W.; Erickson, D.; Krull, I. S. *Analyst* **1987,** 112, 1097-1105.
116. Ebdon, L.; Hill, S.; Ward, R. W. *Analyst* **1987,** 112, 1-16.
117. Uden, P. C.; Bigley, I. E. *Anal. Chim. Acta* **1977,** 94, 29-34.
118. Uden, P. C.; Quimby, B. D.; Barnes, R. M.; Elliot, W, G. *Anal. Chim. Acta* **1978,** 101, 99-109.
119. Uden, P. C.; Bigley, I. E.; Waters, F. H. *Anal. Chim. Acta* **1978,** 100, 555-561.
120. Koropchak, J. A.; Coleman, G. N. in Barnes, R. M. Editer, "Developments in Atomic Plasma Spectrochemical Analysis", Heyden and sons: London, 1981, pp. 345-350.

121. Krull, I. S.; Bushee, D.; Savage, R. N.; Scheicher, R. G. Smith, S. B. *Anal. Lett.* **1982,** 15, 267.
122. Krull, I. S.; Panaro, K. W. *J. Chromatogr. Sci.* **1983,** 21, 460-472.
123. Krull, I. S. Panaro, K. W. *Appl. Spectrosc.* **1985,** 39, 960-968.
124. Ebdon, L.; Hill, S. J.; Hones, P *Analyst* **1985,** 110, 515-517.
125. Biggs, W. R.; Gano, J. T.; Brown, R. J. *Anal. Chem.* **1984,** 56, 2653-2657.
126. Bardiner, P. E.; Bratter, P.; Negretti, V. E.; Schulze, G. *Spectrochim. Acta* **1983,** 38B, 427-436.
127. Bratter, P.; Gardiner, P. E.; Negretti, V. E.; Schulze, G. *Trace Element Anal. Chem. Med. Biol. Proc. Intl Workshop* (2nd), 1982, publ., 1983, Berlin, pp. 45-59.
128. Esptein, M. S.; Koch, W, F.; Epler, K. S.; O'Haver, T. C. *Anal. Chem.* **1987,** 59, 2872-2876.
129. Mitchell, P. G.; Ruggles, J. A.; Sneddon, J.; Radziemske, L. J. *Anal. Lett.* **1985,** 18, 1723-1732.
130. Sneddon, J.; Mitchell, P. G. *Amer. Lab.* **1986,** 18(11), 21.
131. Mitchell, P. G.; Sneddon, J.; Radziemski, L. J. *Appl. Spectrosc.* **1986,** 40, 274-275.
132. Mitchell, P. G.; Sneddon, J.; Radziemski, L. J. *Appl. Spectrosc.* **1987,** 41, 141-148.
133. Sneddon, J. *Spectrosc. Lett.* **1987,** 20, 423-430.
134. Fassel, V. A. *Science,* **1978,** 202, 183-191.
135. Greenfield, S.; McGeachin, H. McD.; Smith, P. B. *Talanta* **1976,** 23, 1-14.
136. "Inductively Coupled Plasmas in Analytical Atomic Spectrometry"; Montaser, A.; Golightly, D. W., Eds.; VCH Publishers: New York, 1987.
137. "Inductively Coupled Plasma Emission Spectroscopy", Parts I and II, Boumans, P. W. J. M., Ed.; Wiley: New York, 1987.
138. MaHard, J. A.; Twigg, K. M.; Bach, D. T.; Winefordner, J. D. *Spectrosc. Lett.* **1984,** 17, 285-294.
139. Skogerboe, R. K.; Urasa, I. T. *Appl. Spectrosc.* **1978,** 32, 527-532.
140. Fujiwara, K.; McHard, J. A.; Foulk, S. J.; Bayer, S.; Winefordner, J. D. *Can. J. Spectrosc.* **1980,** 25, 18-24.

141. Johnson, G. W.; Taylor, H. E.; Skogerboe, R. K. *Appl. Spectrosc.* **1980,** 34, 19-24.
142. Nygaard, D. D.; Gilbert, T. R. *Appl. Spectrosc.* **1981,** 35, 52.
143. Fox, R. L. *Appl. Spectrosc.* **1984,** 38, 644-647.
144. Miller, M. H.; Eastwood, D.; Hendrick, M. S. *Spectrochim. Acta* **1984,** 39B, 13-56. and references cited therein
145. "*Anal. Chem.* " Application Reviews, **1987, 1985, 1983, 1981, 1979.**
146. Collins, A. G. *Appl. Spectrosc.* **1967,** 21, 16-19.
.147. Szivek, J.; Jones, C.; Paulson, E. J.; Valberg, L. S. *Appl. Spctrosc.*, **1968,** 22, 195-197.
148. Schirrmeister, H. *Spectrochim. Acta* **1968,** 23B, 709-724.
149. Nygaard, D. D. *Anal. Chem.*, **1979,** 51, 881-884.
150. Eastwood, D.; Hendrick, M. S.; Sogliero, G. *Spectrochim. Acta* **1980,** 35B, 421-430.
151. Coleman, G. N.; Braun, W. P.; Allen, A. M. *Appl. Spectrosc.* **1980,** 34, 24-30.
152. Williams, R. R.; Coleman, G. N. *Spectrochim. Acta* **1983,** 38B, 1171-1178.
153. Rippetoe, W. E.; Johnson, E. R.; Vickers, T. J. *Anal. Chem.* **1975,** 47, 436-440.
154. Cantillo, A. Y.; Sinex, S. A.; Helz, G. R. *Anal. Chem.* **1984,** 56, 33-37.
155. Golightly, D. W.; Harris, J. T. *Appl. Spectrosc.* **1975,** 29, 233-240.
156. Bankston, D. C.; Humphris, S. E.; Thompson, G. *Anal. Chem.* **1979,** 51, 1218-1225.
157. Frank, A.; Petersson, L. R.; *Spectrochim. Acta* **1983,** 38B, 207-220.
158. Urasa, I. T. *Anal. Chem.* **1984,** 56, 904-908.
159. Rodriguez, M.; Sneddon, J. *At. Spectrosc.* **1986,** 7, 64-67.
160. Johnson, G. W.; Taylor, H. E.; Skogerboe, R. K. *Anal. Chem.* **1979,** 51, 2403-2405.
161. Eastwood, D.; Hendrick, M. S.; Miller, M. H. *Spectrochim. Acta* **1982,** 37B, 293-302.
162. Biggs, W. R.; Fetzer, J. C.; Brown, R. J. *Anal. Chem.* **1987,** 59, 2798-2802.

163. Lajunen, L. H. J.; Kurikka, A.; Ojaniemi, E. *At. Spectrosc.* **1987,** 8, 142-144. CA 107: 228003t
164. Williams, R. R.; Coleman, G. N. *Appl. Spectrosc.* **1981,** 35, 312-317.
165. Felkel, Jr. H. L.; Pardue, H. L. *Anal. Chem.*, **1978,** 50, 602-610.
166. Blades, M. W.; Lee, N. *Spectrochim. Acta* **1984,** 39B, 879-890.
167. Zander, A. T.; Miller, M. H. *Spectrochim. Acta* **1985,** 40B, 1023-1037.
168. Miller, M. H.; Keating, E.; Eastwood, D.; Hendrick, M. S. *Spectrochim. Acta* **1985,** 40B, 593-616.
169. Hendrick, M. S.; Seltzer, M. D.; Michel, R. G. *Spectrochim. Acta* **1986,** 41B, 335-348.
170. Fox, R. L. *Spectrochim. Acta* **1985,** 40B, 287-291.
171. Geigenson, M. D.; Carr, M. T. *Chem. Geol.* **1985,** 51, 19-27.
172. Norman, J. D.; Stumpe, L. A.; Trimm, J. R.; Johnson, F. J. *Assoc. Off. Anal. Chem.* **1983,** 66, 949-951. CA 99: 81712c.
173. Shen, R.; Zhen, C.; Qian, Q. *Fenxi Huaxue,* **1983,** 11(8), 599-604. CA 100: 5191f.
174. Yudelevich, I. G.; Cherevko, A. S.; Engelsht, V. S.; Pikalov, V. V.; Tagiltsev, A. P.; zheenbajev, Zh. Zh. *Spectrochim. Acta* **1984,** 39B, 777-785.
175. Govindaraju, K.; Mevelle, G. *Spectrochim. Acta* **1983,** 38B, 1447-1456.
176. Johnson, G. W.; Sisneros, T. E. *Rare Earth Mod. Sci. Technol.* **1982,** 3, 525-529.
177. Kanlipuly, C. J.; Westlank, A. D. *Talanta* **1988,** 35, 1-13.
178. Schucker, G. D.; Magliocca, T. S.; Su, Y. *Anal. Chim. Acta* **1975,** 75, 95.
179. Bowker, P. E.; Manheim, F. T. *Appl. Spectrosc.* **1982,** 36, 378-382.
180. Sinex, S. A.; Cantillo, A. Y.; Helz, G. R. *Anal. Chem.* **1980,** 52, 2342-2346.
181. Greene, B.; Mitchell, P. G.; Sneddon, J. *Spectrosc. Lett.* **1986,** 19, 101-111.
182. Grogan, W. C. *Spectrochim. Acta* **1983,** 38B, 357-369.
183. Greene, B.; Uranga, A.; Sneddon, J. *Spectrosc. Lett.* **1985,** 18, 425-436.

184. Pyy, L.; Lajunen, L. H. J.; Hakalas, E. *Am. Ind. Hyg. Assoc. J.* **1983,** 44, 609-614. CA 99: 92942d.
185. Chang, A. E..; Morse, R.; Harley, N. H.; Lippmann, M.; Cohan, B. S. *Am. Ind. Hyg. Assoc. J.* **1982,** 43, 117-119. CA 96: 90810y.
186. Lajunen, L. H.; Kubin, A. *Talanta* **1986,** 33, 265-270.
187. Debolt, D. C. *J. Assoc. Off. Anal. Chem.* **1980,** 63, 802-805. CA 93: 128234s.
188. Melton, J. R.; Hoover, W. T.; Morris, P. A. *J. Assoc. Off. Anal. Chem.* **1977,** 60, 873-875. CA 87: 132827f.
189. Wookis, T. C.; Hunter, G. B.; Holmes, J. H.; Johnson, F. J. *J. Assoc. Off. Anal. Chem.* **1980,** 63, 5-6. CA 92: 145565x.
190. Sutton, D. C.; Rusa, W. C.; Legotte, P. A. *Trace Subst. Environ. Health* **1981,** 15, 270-278. CA 97: 123310m.
191. Tempini, G.; Pugleise, F.; Franco, G.; Riganti, V.; Specchiarello, M. *G. Ital. Med. Lav.* **1982,** 4, 83-87. CA 98: 103756d.
192. Berndt, H.; Messerschmidt, J. *Fresenius Z. Anal. Chem.* **1980,** 301, 104-105. CA 93L 40775h.
193. Mifune, M. *Okayama Daiagaku Onsen Kenkyusho Hokoku.* **1980,** 50, 43-48. CA 93: 110016n.
194. Pyy, L.; Hakala, E.; Lajunen, L. H. J. *Anal. Chim. Acta* **1984,** 158, 297-303. CA 101: 34141r.
195. Hall, G. S.; Carr, M. J.; Cummings, E.; Lee, M. *Clin. Chem.* **1983,** 29, 1318. CA 99: 35544b.
196. Chandola, L. C.; Lordello, A. R. *Microchem. J.* **1983,** 28, 87-90. CA 98: 66582w.
197. Belliveau, J. F.; Griffin, H.; Salvolainen, A. *ASTM Spec. Tech. Publ.* **1981,** 747m 77-90. CA 98: 10784w.
198. Fernando, L. A. *Anal. Chem.* **1984,** 56, 1970-1973.
199. Gruffubm, H. *Environ. Meas. Lab. Environ. Q. (U. S. Dept. Energy)* **1979,** EML-356, 479-507. CA 91: 82533s.
200. Worthington, M. A. *ASTM Spec. Tech. Publ.* **1981,** 747, 91-105. CA 98: 10785x.
201. Czech, N. Wunsch, C. *Spectrochim. Acta* **1981,** 36B, 553-561.
202. Anttila, R.; Lajunen, L. H. *J. Finn. Chem. Lett.* **1985,** 5, 186-189. CA 104: 161116y.

203. Potter, N. M.; Vergosen, III. H. E. *Talanta* **1985,** 32, 545-548.
204. Fernando, L. A.; Heavner, W. D.; Gabrielli, C. C. *Anal. Chem.* **1986,** 58, 511-512.
205. Natanslon, S.; Czupryna, G. *Spectrochim. Acta* **1983,** 38B, 317-322.
206. Brown, J. R.; Saba, C. S.; Rhine, W. E.; Eisentraut, K. J. *Anal. Chem.* **1980,** 52, 2365-2370.
207. Kauffman, R. E.; Saba, C. S.; Rhine, W. E.; Eisentraut, K. J. *Anal. Chem.* **1982,** 54, 975-979.
208. Smith, M. R. *Anal. Chem.* **1980,** 52, 583-585.
209. Burdo, R. A.; Snyder, M. *Anal. Chem.* **1979,** 51, 1502-1508.
210. Hunter, G. B.; Woodis, T. C.; Johnson, F. J. *J. Assoc. off. Anal. Chem.* **1981,** 64, 25-27. CA 94: 64294x.
211. Same as 205
212. Czupryna, G.; Natansohn, S. *Mater. Sci. Res.* **1983,** 15, 491-497. CA 99: 15728m.
213. Urasa, I. T.; Ferede, F. *Anal. Chem.* **1987,** 59, 1563-1568.
214. Mchard, J. A.; Foulk, S. J.; Nikdel, S.; Ullman, A. H.; Pollard, B. D.; Winefordner, J. D. *Anal. Chem.* **1979,** 51, 1613-1616.
215. Kingsley, G. R.; Schaffert, R. R. *Anal. Chem.* **1951,** 23, 914-919.
216. Erdey, L.; Gergus, E.; Kocsis, E.; *Acta Chim. Hung.* **1955,** 7, 343.
217. Hahn, M. H.; Wolnik, K. A.; Fricke, F. L.; Caruso, J. A. *Anal. Chem.* **1982,** 54, 1048-1052.
218. Browner, R. F.; Boorn, A. W. *Anal. Chem.,* **1984,** 56, 875A-888A.
219. Manning, D. C. *At. Absorpt. Newsl.* **1971,** 10, 123.
220. Lichte, F. E.; Skogerboe, R. K. *Anal. Chem.* **1972,** 44, 1480-1482.
221. Fernandez, F. J.; Manning, D. C. *At. Absorpt. Newsl.* **1971,** 10, 86-92.
222. Pollock, E. M.; West, S. T. *At. Absorpt. Newsl.* **1972,** 11, 104.
223. Goulden, P. D.; Brooksbank, P. A. *Anal. Chem.* **1974,** 46, 1431-1436.
224. Chu, R. C.; Barron, G. P.; Baumgarner, P. A. W. *Anal. Chem.* **1972,** 44, 1476-1479.
225. Terashima, S. *Anal. Chim. Acta.* **1976,** 86, 43-51.
226. Maruta, T.; Sudoh, G. *Anal. Chim. Acta* **1975,** 77, 34-42.
227. Schaeffer, G. W.; Emilius, M., *J. Am. Chem. Soc.* **1954,** 76, 1203.
228. Macklen, E. D. *J. Chem. Soc.***1959,** 1989.

229. Braman, R. S.; Justen, L. L.; Foreback, C. C.*Anal. Chem.* **1972,** 44, 2195-2199.
230. Fernandez, F. J. *At. Absorpt. Newsl.* **1973,** 12, 93.
231. Bedard, M.; Kerbyson, J. D., *Anal. Chem.* **1975,** 47, 1441- 1444.
232. Chapman, J.F.; Dale, L. S. *Anal. Chim. Acta* **1979,** 111, 137-144.
233. Narasaki, H.; *F. Z. Anal. Chem.* **1985,** 321, 464-466.
234. Matsumoto, K.; Fuwa, K. *Anal. Chem.* **1982,** 54, 2012-2015.
235. McDaniel, M.; Shendrikar, A. D.; Reiszner, K. D.; West, P. W.; *Anal. Chem.* **1976,** 48, 2240-2243.
236. Siemer, D. D.; Koteel, P.*Anal. Chem.* **1977,** 49, 1096-1099.
237. Andreae, M. O. *Anal. Chem.* **1977,** 49, 820-823.
238. Fricke, F. L.; Robbins, W. B.; Caruso, J. A. *J. Assoc. off. Anal. Chem.* **1978,** 61, 1118.
239. Nakahara, T.; Wasa, T. *Chem. Express, **1986,*** 1 (9), 527-530. CA 105: 213869p.
240. Thompaon, M.; Pahlavanpour, B.; Qalton, S. J.; Kirkbright, G. F. *Analyst* **1978,** 103, 568-579.
241. Andreae, M.; Byrd, J. T.; *Anal. Chim. Acta* **1984,** 156, 147-157.
242. Donard, O. F. X.; Randall, L.; Rapsomanikis, S.; Weber, J. H. Intern. *J. Environ. Anal. Chem.* **1986,** 27, 55-67.
243. Braman, R. S.; Tompkins, M. A. *Anal. Chem.* **1979,** 51, 12-19.
244. Randall, L.; Donard, O. F. X.; Weber, J. H.*Anal. Chim. Acta* **1986,** 184, 197-203.
245. Vijan, P. N.; Wood, G. R. *At. Absorpt. Newsl.* **1974,** 13, 33.
246. Pierce, F. D.; Lamoreaux, T. C.; Brown, H. R.; Fraser, R. S. *Appl. Spectrosc.* 1976, 30, 38.
247. Fiorino, J. A.; Jones, J. W.; Capar, S. G. *Anal. Chem.* **1976,** 48, 120-125.
248. Thompson, K. C.; Thomerson, D. R. *Analyst* **1974,** 99, 575-595.
249. Orheim, R. M.; Bovee, H> H. *Anal. Chem.* **1974,** 46, 921-922.
250. Kang, H. K.; Valentine, J. L. *Anal. Chem.* **1977,** 49, 1829-1832.
251. May, I.; Greenland, L. P. *Anal. Chem.* **1977,** 49, 2376-2377.
252. Jin, K.; Terada, H.; Taga, M. *Bull. Chem. Soc. Jpn.* **1981,** 54, 2934.
253. Castillo, J. R.; Mir, J. M.; Martinez, C.; Gomez, M. T. *Fresenius' Z. Anal. Chem.* **1986,** 325, 171-174. CA 106: 11969f.

254. Tsunoda, A.; Matsumoto, K.; Fuwa, K. *Anal. Sci.* **1986,** 2, 119-123.
255. Greenland, L. P.; Campbell, E. Y. *Anal. Chim. Acta* **1976,** 87, 323.
256. Brown, A. A.; Ottaway, J. M.; Fell, G. S. *Anal. Chim. Acta* **1985,** 172, 329-333.
257. Hatfield, D. B. *Anal. Chem.* **1987,** 59, 1887-1888.
258. Knudson, E. J.; Christian, G. D. *Anal. Lett.* **1973,** 6, 1039.
259. Siemer, D. D.; Koteel, P.; Jariwala, V. *Anal. Chem.* **1976,** 48, 836-840.
260. Jin, K.; Taga, M. *Anal. Chim. Acta* **1982,** 142, 229-236.
261. Subramanian, K. S. *Fresenius' Z. Anal. Chem.* **1981,** 305, 382.
262. Subramanian, K. S.; Meranger, J. C. *Analyst* **1982,** 107, 157.
263. Welz, B.; Mecher, M. *Analyst* **1983,** 108, 213.
264. Julshamm, K.; Ringdal, D.; Slinning, K. E.; Braekkan, O. R. *Spectrochim. Acta,* **1983,** 37B, 473.
265. Lee, D. S. *Anal. Chem.* **1982,** 54, 1682-1686.
266. Drasch, G.; Meyer, L. V.; Kauert, G. *Fresenius' Z. Anal. Chem.* **1980,** 304, 141-142.
267. Lindahl, P. C. *At. Spectrosc.* **1985,** 6, 123-124.
268. Sturgeon, R. E.; Willie, S. N.; Berman, S. S. *Anal. Chem.* **1987,** 59, 2441-2444.
269. Sturgeon, R. E.; Willie, S. N.; Berman, S. S. *Anal. Chem.* **1985,** 57, 2311-2314.
270. Sturgeon, R. E.; Willie, S. N.; Berman, S. S. *Fresenius' Z. Anal. Chem.* **1986,** 3243, 788-792.
271. Thompson, M.; Pahlavanpour, B.; Walton, S. J.; Kirkbright, G. F. *Analyst* **1978,** 103, 705-713
272. Fry, R. C.; Denton, M. B.; Windsor, D. L.; Northway, S. J. *Appl. Spectrosc.* **1979,** 33, 399-404.
273. Eckhoff, M. A.; McCarthy, J. P.; Caruso, J. A. *Anal. Chem.* **1982,** 54, 165-168.
274. Nakahara, T. *Appl. Spectrosc.* **1983,** 37, 539-545.
275. Wolnik, K. A.; Fricke, F. L.; Hahn, M. H.; Caruso, J. A. *Anal. Chem.* **1981**, 53, 1030-1035.
276. Goulden, P. D.; Anthony, D. H. J.; Austen, K. D. *Anal. Chem.* **1981,** 53, 2027-2029.

277. Stieg, S.; Dennis, A. *Anal. Chem.* **1982,** 54, 605-607.
278. Broekaert, J. A. C.; Leis, F. *Fresenius' Z. Anal. Chem.* **1980,** 300, 22.
279. Sommer, D.; Ohls, K.; Koch, A. *Fresenius' Z. Anal. Chem.* **1981,** 306, 372.
280. Date, A. R. *Trac. Trends Anal. Chem.* **1983,** 2, 225-230.
281. Dougles, D. J.; Houk, R. S.; *Prog. Anal. At. Spectrosc.* **1985,** 8, 1-18.
282. Gray, A. L. *Spectrochim. Acta* **1985,** 40B, 1525-1537.
283. Houk, R. S. *Anal. Chem.* **1986,** 58, 97A-105A.
284. Wilson, D. A.; Vickers, G. H.; Hieftje, G. M.; Zander, A. T. *Spectrochim. Acta* **1987,** 42B, 29-38.
285. Powell, M. J.; Boomer, D. W.; McVicars, R. J. *Anal. Chem.* **1986,** 58, 2864-2867.
286. Wang, X.; Viczian, M.; Lasztity, A.; Barnes, R. M. *J. Anal. At. Spectrom.* **1988,** 3, 821-827.
287. Barnett, N. W.; Chen, L. S.; Kirkbright, G. F. *Spectrochim. Acta* **1984,** 39B, 1141-1147.
288. Barnett, N. W. *Spectrochim. Acta* **1987,** 42B, 859-864.
289. Tsujii, K.; Kuga, K. *Anal. Chim. Acta* **1974,** 72, 85.
290. Braun, K.; Slavin, W.; Walsh, A. *Spectrochim. Acta* **1982,** 37B, 721-726.
291. D'Ulivo, A.; Fuoco, R.; Papoff, P. *Talanta* **1985**, 32, 103-109.
292. Nakahara, T.; Wasa, T. *J. Anal. At. Spectrosc.* **1986,** 1, 473-477.
293. Kadeg, R. D.; Chistian, *Anal. Chim. Acta* **1977,** 88, 117.
294. Vien, S. H.; Fry, R. C. *Anal. Chem.* **1988,** 60, 465-472.
295. Skogerboe, R. K.; Bejmuk, A. P. *Anal. Chim. Acta* **1977,** 94, 297.
296. Lussi-Schlatter, B.; Brandenberger, H. *Adv. Mass Spectrom. Biochem. Med.* **1977**, 2, 231.
297. Belcher, R.; Bogdanski, S. L.; Henden, E.; Townshend, A. *Anal. Chim. Acta* **1977,** 92, 33.
298. Burguera, M.; Burguera, J. L. *Analyst* **1986,** 111, 171-174.
299. Henden, E. *Anal. Chim. Acta* **1985,** 173, 89-95.
300. Dedina, J. *Anal. Chem.* **1982,** 54, 2097-2102.
301. Smith, A. E. *Analyst* **1975,** 100, 300-306.

302. Petrick, K.; Krivan, V. *Anal. Chem.* **1987,** 59, 2476-2479.
303. Petrick, K.; Krivan, V. *Fresenius Z. Anal. Chem.* **1987,** 327, 338-342.
304. Pierce, F. D.; Brown, H. R. *Anal. Chem.* **1976,** 48, 693-695.
305. Pierce, F. D.; Brown, H. R. *Anal. Chem.* **1977,** 49, 1417-1422.
306. Hershey, J.W. ; Keliher, P. N. *Spectrochim. Acta* **1986,** 41B, 713-723.
307. Brown, Fr, R. M.; Fry, R. C.; Moyers, J. L.; Northway, S. J.; Denton, M. B.; Wilson, G. S. *Anal. Chem.* **1981,** 53, 1560-1566.
308. Evans, W. H.; Jackson, F. J.; Dellar, D. *Analyst* **1979,** 104, 16.
309. Dittrich, K.; Vorberg, B.; Wolthers, H. *Talanta* ***1979,*** 26, 747.
310. Welz, B.; Schubert-Jacobs, M. *J. Anal. Atom. Spectrom.* **1986,** 1, 23-27.
311. Astrom, O. *Anal. Chem.* ***1982,*** 54, 190-193.
312. Welz, B.; Melcher, M. *Analyst* **1984,** 109, 569-572.
313. Welz, B.; Melcher, M. *Analyst* **1984,** 109, 573-575.
314. Welz, B.; Melcher, M. *Analyst* **1984,** 109, 577-579.
315. Yamamoto, M.; Yamamoto, Y.; Yamashige, T. *Analyst* **1984,** 109, 1461.
316. Bye, R. *Talanta* **1986,** 33, 705-706.
317. Schlesinger, H. I.; Brown, H. C.; Finholt, A. E.; Gilbreath, J. R.; Hoekstra, H. R.; Hyde, E. K. *J. Am. Chem. Soc.* **1953,** 75, 215.
318. Aggett, J.; Hayashi, Y. *Analyst* (London) **1987,** 112, 277-282.
319. Vijan, P. N.; Chan, L. Y. *Anal. Chem.* **1976,** 48, 1788-1792.
320. Halicz, L.; Russell, G. M. *Analyst* **1986,** 111, 15-18.
321. Ebdon, L.; Wilkinson, J. R. *Anal. Chim. Acta* **1987,** 194, 177-187. CA 107: 118062c.
322. Aznarea, J.; Rabadan, J. M.; Ferrer, A.; Cipres, P. *Talanta* **1986,** 33, 458-460.
323. Narasaki, H. *Anal. Sci.* **1986,** 2 (4), 371-374. CA 106: 23000w.
324. Narasaki, H. *Anal. Sci.* **1986,** 2, 141-144. CA 105: 53660h.
325. Nakahara, T.; Wakisaka, T.; Musha, S. *Spectrochim. Acta* **1981,** 36B, 661-670.
326. Belcher, R.; Bogdanski, S. L.; Henden, E.; Townshend, A. *Analyst* **1975,** 100, 522-523.
327. Jin, K.; Terada, H.; Taga, M. *Bull. Cheml Soc. Jpn.* **1981,** 54, 2934.

328. Heden, E. *Analyst* **1982,** 107, 872.
329. Aggett, J.; Aspell, A. C. *Analyst* (London) **1976,** 101, 341-347.
330. Guimont, J. ; Pichette, M.; Rhéume, N. *At. Abs. Newsl.* **1977,** 16, 53-57.
331. Dornemann, A.; Kleist, H. *Fresenius' Z. Anal. Chem.* **1981,** 305, 379-381.
332. Peacock, C. J.; Singh, S. J. *Analyst* (London) **1981,** 106, 931-938.
333. Bye, R. *Analyst* **1986,**111, 111-113.
334. Brindle, I. D.; Ceccarelli Ponzoni, C. M. *Analyst* **1987**, 112, 1547-1550.
335. Kirkbright, G. F.; Taddia, M. *Anal. Chim. Acta* **1978,** 100, 145-150.
336. Thompson, M.; Pahlavanpour, B. *Anal. Chim. Acta* **1979,** 109, 251-258.
337. Haring, B. J. A.; Van Delft, W.; Bom, C. M. *Fresenius Z. Anal. Chem.* **1982,** 310, 217.
338. Anderson, R. K.; Thompson, M.; Culbard, E. *Analyst* **1986,** 111, 1143-1152.
339. Matsumoto, K.; Fuwa, K. *Bunseki Kagaku* **1981,** 30, 188-190.
340. Matsumoto, K.; Fujiwara, K.; Fuwa, K. *Anal. Chem.* **1983,** 55, 1665-1668.
341. Tao, H.; Miyazaki, A.; Bansho, K. *Kogai* **1985,** 20, 137-144. CA 103: 200603f.
342. Hashimoto, S.; Fujimara, K.; Fuwa, K. *Limnol. Oceanogr.* **1987,** 32(2), 729-735. CA 107: 183131p.
343. Busheina, I. S.; Headridge, J. B. *Talanta* **1982,** 29, 519-520.
344. Yan, D.; Yan, Z.; Cheng, G. S.; Li, A. M. *Talanta* **1984,** 31, 133-134.
345. Alder, J. F.; Jin, Q.; Snook, R. D. *Anal. Chim. Acta* **1981,** 123, 329.
346. Barnett, N. W. *J. Anal. At. Spectrom.* **1988,** 3, 969-972.
347. Michlewicz, K. G.; Carnahan, J. W. *Anal. Chim. Acta* **1986,** 183, 275.
348. Hatch, W. R.; Ott, W. L. *Anal. Chem.* **1968,** 40, 2085-2087.
349. Oda, C. E.; Ingle, Jr. J. D. *Anal. Chem.* **1981,** 53, 2030-2033.
350. DeAndrade, J. C.; Pasquini, C.; Bauan, N.; Ban Loon, J. C. *Spectrochim. Acta***1983,** 1329-1338.
351. Tesfalidet, S.; Irgum, K. *Anal. Chem.* **1988,** 60, 2031-2035.
352. Brueggemeyer, T. W.; Caruso, J. A. *Anal. Chem.* **1982,** 54, 872-875.

353. Sturgeon, R. E.; Willie, S. N.; Berman, S. S. *The third Chemical Congress of North America,* Toronto, June 5-10, **1988.** Analytical Chemistry Section, Paper No. 234. and *35th. Canadian Spectroscopy Conference,* Ottawa, August 8-10, **1988**. paper No. 40.
354. Tao, H.; Miyazaki, A.; Bansho, K. *Anal. Chem.* **1988,** 60, 1762-1765.
355. Halicz, L. *Analyst* **1985,** 110, 943-946.
356. Nakata, F.; Sunahara, H.; Fujimoto, H.; Yamamoto, M.; Kumenaru, T. *J. Anal. At. Spectrom.* **1988,** 3, 579-582.
357. Hambrick III, G. A.; Froelich Jr., P. N.; Andreae, M. O.; Lewis, B. L.; *Anal. Chem.* **1984,** 56, 421-424.
358. Andreae, M. O.; Froelin Jr, P. N. *Anal. Chem.* **1981,** 53, 287-291.
359. DeDoncker, K.; Dumarey, R.; Dams, R.; Hoste, J.; *Anal. Chim. Acta* **1986,** 187, 163-169.
360. Donard, O. F. X.; Rapsomanikis, S.; Weber, J. H.; *Anal. Chem.* **1986,** 58, 772-777.
361. Hodge, V. F.; Seidel, S.; Tompkins, M. A. *Anal. Chem.* **1979,** 51, 1256-1259.
362. Balls, P. W. *Anal. Chim. Acta,* **1987,** 197, 309-313. CA 107: 222802e.
363. Valkirs, A. L.; Seligman, P. F.; Olson, G. J.; Brinckman, F. E.; Matthias, C. L; Bellama, J. M. *Analyst* **1987,** 112, 17-22.
364. Sullivan, J. J. et al. *Anal. Chem.* **1988,** 60, 626-630.
365. Han, J. S.; Weber, J. H. *Anal. Chem.* **1988,** 60, 316-319.
366. Alvarez, G. H.; Capar, S. G. *Anal. Chem.* **1987,** 59, 530-533.
367. Molinari, G. P.; Trevisan, M.; Natali, P.; Del Re, A. A. M. *J. Agric. Food Chem.* **1987,** 35, 727-731. CA 107: 132485a.
368. Tsujii, K.; Kuga, K.; *Anal. Chim. Acta* **1978,** 101, 199-201.
369. Jin, K.; Taga, M.; Yoshida, H.; Hikime, S.; *Bunseki Kagaku* **1978,** 27, 759-764. CA 90: 132232v.

370. Vijan, P. N.; Sadena, R. S; *Talanta* **1980,** 27, 321-326.

371. Ng, K. C.; Shen, W. *Spectroscopy* **1987,** 2, 50-53. CA 106: 77916t.

372. Nakahara, T.; Wasa, T. *Anal. Sci.* **1985,** 1, 291-292. CA 104: 101549g.

373. Smith, R. *At. Spectrosc.* **1981,** 2, 155-158. CA 95: 209272w.

374. Ikeda, M.; Nishibe, J.; Hamada, S.; Tujino, R. *Anal. Chim. Acta* **1981,** 125, 109-115. CA 94: 202161e.

375. Vijan, P. N.; Wood, G. R. *Analyst* **1976,** 101, 966-973. CA 86: 182500u.

376. Castillo, J. R.; Mir, J. M.; Martinez, C.; Val, J.; Colon, M. P. *Microchim. Acta* **1985,** I, 253-263

377. Dulivo, A.; Fuoco, R.; Papoff, P. *Talanta,* **1986,** 33, 401-405.

378. Duvivo, A.; Papoff, P. *Talanta* **1985,** 32, 383-386.

379. Yamauchi, H.; Arai, F.; Yamamura, Y. *Ind. Health* **1981,** 19, 115-124. CA 95: 91768g

380. Aznarez, J.; Palacios, F.; Vidal, J. C.; Galban, J. *Analyst* **1984,** 109, 713-715. CA 101: 203414q.

381. Bomlla, M.; Rodriguez, L.; Camara, C. *J. Anal. At. Spectrom.* **1987,** 2, 157-161.

382. Nerlin, C.; Olavide, S.; Cacho, J.; *Anal. Chem.* **1987,** 59, 1918-1921.

383. Tsalev, D. L.; Mandjukov, P. B. *J. Anal. At. Spectrom.* **1987,** 2, 135-141.

384. Anderson, R. K.; Thompson, M.; Culbard, E. *Analyst* **1986,** 111, 1153-1158.

385. Lee, C. K.; Low, K. S.; *Pertanika* **1987,** 10, 69-73. CA 107: 234941n.

386. Maitain, T.; Uchiyama, S.; Saito, Y. *J. Chromatogr.* **1987,** 391, 161-168. CA 106: 190462e.

387. Yamamoto, Y.; Takada, K.; Kumamaru, T.; Yasuda, M.; Yokoyama, S.; Yamemoto, Y. *Anal. Chem.* **1987,** 59, 2446-2448.

388. Braman, R. S.; Johnson, D. L.; Foreback, C. C.; Ammons, J. M.; Bricker, J. L. *Anal. Chem.* **1977,** 49, 621-625.

389. Yamamoto, M.; Fujishige, K.; Tsubota, H. Yamamoto, Y. *Anal. Sci.* **1985,** 1, 47-50. CA 104: 135711u.

390. Sturgeon, R. E.; Willie, S. N.; Berman, S. S. *J. Anal. At. Spectrom.* **1986,** 1, 115-118.

391. Tioh, N. H.; Israel, Y.; Barnes, R. M. *Anal. Chim. Acta* **1986,** 184, 205-212. CA 105: 218104v.

392. Wang, W. J.; Hanamura, S.; Winefordner, J. D. *Anal. Chim. acta* **1986,** 184, 213-218. CA 105: 164087w.

393. Van der Veen, N. G.; Keukens, H. J.; Vos, G. *Anal. Chim. Acta* **1985,** 175, 325-328. CA 103: 66180k.

394. Vanloo, B.; Dams, R.; Hoste, J. *Anal. Chim. Acta* **1985,** 175, 325-328. CA 104: 28117h.

395. Apt, S. C.; Howard, A. G. *J. Anal. At. Spectrom.* **1986**, 1, 221-225.

396. Peramaki, P.; Lajunen, L. H. J. *Analyst* **1988**, 113, 1567-1570.

397. Sanz, J.; Gallarta, F.; Galban, J.; Castillo, J. R. *Fresenius' Z. Anal. Chem.* **1988**, 330, 510-515.

398. Aznarez, J.; Vidal, J.; Gascon, J. M. *At. Spectrosc.* **1986,** 7, 59-60. CA 105: 43691e.

399. Nakaharn, T.; Nakanishi, K.; Wasa, T. *Spectrochim. Acta* **1987**, 42B, 119-128.

400. Ohyama, J.; Marayama, F.; Dokiya, Y. *Anal. Sci.* **1987,** 3, 413-416. CA 107: 249152e.

401. Crock, J. G. *Anal. Lett.* **1986,** 19, 1367-1385. CA 105: 218024u.

402. Welz, B.; Wolynetz, M. S.; Verlinden, M. *Pure Appl. Chem.* **1987,** 59, 927-936.

403. Pettersson, J.; Hansson, L.; Olin, A. *Talanta* **1986,** 33, 249-254.

404. Agterdenbos, J.; Van Elteren, J. T.; Ter Heege, J. P. *Spectrochim. Acta* **1986,** 41B, 303-316.

405. Willie, S. N.; sturgeon, R. E.; Berman, S. S. *Anal. Chem.* **1986,** 58, 1140-1143.

406. Sanzolone, R. F.; Chao, T. T. *Geostand. Newsl.* **1987,** 11, 81-85. CA 106: 226575k.

407. Bye, R.; *Fresenius' Z. Anal. Chem.* **1984,** 317, 27-28.

408. Apte, S. C.; Howard, A. G. *J. Anal. At. Spectrom.* **1986,** 1, 379-382.

409. Wang, X.; Fang, Z. *Kexue Tongbao* (Foreign Lang. Ed.) **1986,** 31 (11), 791-792. CA 105: 75295v.

410. Piwonka, J.; Kaiser, G.; Toelg, G.*Fresenius' Z. Anal. Chem.* **1985,** 321, 225-234. CA 103: 67745k.

411. Ikeda, M. *Anal. Chim. Acta* **1985,** 170, 217-224. CA 103: 81031f.

412. Nakata, F.; Yasui, Y.; Matsuo, H.; Kumamaru, T. *Anal. Sci.* **1985,** 1 (5), 417-421. CA 104: 65205f.

413. Jin, K.; Taga, M.; Yoshida, H.; Hikime, S. *Bull. Chem. Soc. Jpn.* **1979,** 52, 2276-2280. CA 91: 133506v.

414. Fleming, H. D.; Ide, R. G. *Anal. Chim. Acta* **1976,** 83, 67-82.

415. Yamamoto, M.; Yasllda, M.; Yamamoto, Y. *Anal. Chem.* **1985,** 57, 1382-1385.

416. Yamamoto, M.; Urata, K.; Murashge, K.; Yamamoto, Y. *Spectrochim. Acta* **1981**, 36B, 671-677.

417. Walton, S. J. *Analyst* 1986, 111, 225-226.

418. Tsalev, D.; Mandzhukov, P. *Microchem. J.* **1987,** 35, 83-93. CA 106: 168006n. CA 106: 169006n.

419. Vanloo, B.; Dams, R.; Hoste, J. *Anal. Chim. Acta* **1983,** 151, 391-400. CA 99: 98465x.

420. Vanloo, B.; Dams, R.; Hoste, J. *Fonderie Belge* **1983**, 53, 7-16. CA 99: 81713d.

421 Hon, P. K.; Lau, O. W.; Cheung, W. C.; Wong, M. C. *Anal. Chim. Acta* **1980,** 115, 355-359. CA 92: 190756w.

422. Brodie, K. G.; Rowland, J. J. *Eur. Spectrosc. News* **1981,** 36, 41-42, 44. CA 96: 79070m.

423. Braman, R. S.; Tompkins, M. A. *Anal. Chem.* **1978,** 50, 1088-1093.

424. DeDoncker, K.; Bumarey, R.; Dams, R. *Stud. Environ. Sci.* **1986,** 29, 749-757. CA 106: 89387j.

425. Terashima, S. *Geostand. Newsl.* **1986,** 10(2), 127-130. CA 105: 202402e.

426. Hon, P. K.; Lau, O. W.; Tsui, S. K. *J. Anal. At. Spectrom.* **1986,** 1, 125-130.

427. DeDonker, K.; Dumarey, R.; Dams, R.; Hoste, J. *Anal. Chim. Acta* **1985,** 169, 339-341. CA 103: 31678b.

428. "Spectraspan V Emission Spectrometer, Operator's Manual," Spectrametrics, Andover, MA, 1983.

429. Boampong, C. M.Sc. Thesis, Brock University, 1983

430. Boampong, C.; Brindle, I. D.; Le, X-c.; Pidwerbesky, L.; Ceccarelli Ponzoni, C. M. *Anal. Chem.* **1988,** 60, 1185-1188.

431. Miller, J. C.; Miller, J. N. *Statistics for Analytical Chemistry;* Wiley: New York, **1984**; pp 82-107 and pp 56-57.

432. Brindle, I. D.; Le, X-c. *Analyst* **1988,** 113, 1377-1381.

433. Brindle, I. D.; Le, X-c.; Li, X-f. Presented at the*4th. BNASS* York, UK. June 29-July 2, 1988. *J. Anal. At. Spectrom.* **1989,** 4, March, in the press.

434. Fazakas, J. *Talanta* **1984**, 31, 573-577.

435. Ebdon, L.; Norman, P.; Sparkes, S. T. *Spectrochim. Acta* **1987,** 42B, 619.